

A Practical Guide for Pediatric Nuclear Medicine

Zvi Bar-Sever
Francesco Giammarile
Ora Israel
Helen Nadel
Editors

OPEN ACCESS

 Springer

A Practical Guide for Pediatric Nuclear Medicine

Zvi Bar-Sever • Francesco Giammarile
Ora Israel • Helen Nadel
Editors

A Practical Guide for Pediatric Nuclear Medicine

 Springer

Editors

Zvi Bar-Sever
Nuclear Medicine
Schneider Children's Medical Center
Petah-Tikva, Israel

Francesco Giammarile
Nuclear Medicine and Diagnostic
Imaging
International Atomic Energy Agency
Vienna, Austria

Ora Israel
Rappaport School of Medicine
Technion – Israel Institute
of Technol
Haifa, Israel

Helen Nadel
Pediatric Nuclear Medicine
Lucile Packard Children's Hospital
Palo Alto, CA, USA



ISBN 978-3-662-67630-1 ISBN 978-3-662-67631-8 (eBook)

<https://doi.org/10.1007/978-3-662-67631-8>

Open Access provided by a grant from the International Atomic Energy Agency.

International Atomic Energy Agency

© IAEA: International Atomic Energy Agency 2023

The opinions expressed in this publication are those of the authors/editors and do not necessarily reflect the views of the IAEA: International Atomic Energy Agency, its Board of Directors, or the countries they represent.

Open Access This book is licensed under the terms of the Creative Commons Attribution 3.0 IGO license (<http://creativecommons.org/licenses/by/3.0/igo/>), which permits use, sharing, adaptation, distribution and reproduction in any medium or format, as long as you give appropriate credit to the IAEA: International Atomic Energy Agency, provide a link to the Creative Commons license and indicate if changes were made.

Any dispute related to the use of the works of the IAEA: International Atomic Energy Agency that cannot be settled amicably shall be submitted to arbitration pursuant to the UNCITRAL rules. The use of the IAEA: International Atomic Energy Agency's name for any purpose other than for attribution, and the use of the IAEA: International Atomic Energy Agency's logo, shall be subject to a separate written license agreement between the IAEA: International Atomic Energy Agency and the user and is not authorized as part of this CC-IGO license. Note that the link provided above includes additional terms and conditions of the license.

The images or other third party material in this book are included in the book's Creative Commons license, unless indicated otherwise in a credit line to the material. If material is not included in the book's Creative Commons license and your intended use is not permitted by statutory regulation or exceeds the permitted use, you will need to obtain permission directly from the copyright holder.

The use of general descriptive names, registered names, trademarks, service marks, etc. in this publication does not imply, even in the absence of a specific statement, that such names are exempt from the relevant protective laws and regulations and therefore free for general use.

The publisher, the authors, and the editors are safe to assume that the advice and information in this book are believed to be true and accurate at the date of publication. Neither the publisher nor the authors or the editors give a warranty, expressed or implied, with respect to the material contained herein or for any errors or omissions that may have been made. The publisher remains neutral with regard to jurisdictional claims in published maps and institutional affiliations.

This Springer imprint is published by the registered company Springer-Verlag GmbH, DE, part of Springer Nature.

The registered company address is: Heidelberger Platz 3, 14197 Berlin, Germany

*This book is dedicated to the pioneers of this very special field,
to our patients and their families, and to our hard-working,
loyal teams and colleagues.*

Foreword

In the past few decades, Pediatric Nuclear Medicine and Molecular Imaging has become a rapidly growing area that includes diagnostic imaging, research, as well as therapeutic applications.

This publication highlights important aspects of the Nuclear Medicine practice in children as well as the differences with the approaches in adult patients.

Obtaining images of high diagnostic quality in infants and small children can be technically and medically challenging and often require special attention. It has been often stated that “Children are not small adults” and this is quite applicable to the practice of Nuclear Medicine in these small patients.

In children, administered activities are often significantly lower than in adults, requiring prolonged imaging acquisition times. Techniques for keeping the child still, sometimes for extended acquisition periods will be discussed. Such techniques include immobilization, sedation and exceptionally, general anesthesia.

Correct interpretation of pediatric images requires an awareness of the effects of normal growth and development on tracer pharmacokinetics and biodistribution as well as familiarity with pediatric diseases.

The introduction of technologies such as hybrid imaging, and new radiopharmaceuticals, are described in detail, underscoring the fact that these developments are aimed at improving diagnostic, structural and functional assessment of pediatric diseases.

This book provides a practical approach to the successful routine use of Nuclear Medicine procedures in children. It is based on the extensive expertise of dedicated pediatric nuclear medicine facilities and clinicians worldwide.

The IAEA has significantly enhanced the capabilities of many Member States in the field of Nuclear Medicine, highlighting functional and metabolic imaging as indispensable tools for the diagnosis, treatment planning, and management of diseases. In this project, Nuclear Medicine and Molecular Imaging are driven one step forward, advancing towards the challenging but also very rewarding work with pediatric patients.

I hope that referring physicians, pediatricians, clinicians, and other specialists involved in the care of children will find in this a valuable, detailed, and practical resource of Pediatric Nuclear Medicine as well as “tips and tricks” that should be of value in the management of their clinical practice.

I also hope that medical professionals throughout the world will benefit from this publication, that readers of this book will achieve further familiarization with the many unique characteristics of Pediatric Nuclear Medicine and Molecular Imaging and that it will inspire deeper learning as well as innovation in this wonderful field of medicine.

Radiology
Harvard Medical School
Boston, MA, USA, Divisions of Nuclear Medicine
and Molecular Imaging, Boston Children's
and Brigham and Women's Hospitals
Boston, MA, USA

Ted Treves

Preface

This publication on clinical Nuclear Medicine dedicated to pediatric patients is directed at Nuclear Medicine physicians, radiologists, oncologists, and clinicians in various specialties, medical physicists, medical technologists, radiopharmacists, laboratory medicine scientists, and researchers.

New technologies and radiotracers have been developed and introduced into the clinical Nuclear Medicine arena over the last decades, in some parts of the world more rapidly than in others. This publication describes Nuclear Medicine imaging modalities in the specific context of the management of pediatric patients. It provides a comprehensive overview of the current state-of-the-art in pediatric Nuclear Medicine, in addition to readdressing known tests, their protocols, clinical indications, and performance indices.

Training in using an accurate imaging methodology, in understanding and interpreting complex studies with potentially different tracer biodistribution, pitfalls and clinical relevance when used in children, are imperative for a successful implementation of present-day diagnostic and therapeutic capabilities. This publication aims to provide an answer to the need created for such training. It includes theoretical and practical aspects, as well as case-based presentations for each of the main indications for pediatric Nuclear Medicine tests that will ensure their use in an accurate and valuable clinical practice.

The authors are members of an international group of experts at the forefront of this field and their contributions represent a culmination of their professional efforts defining a global perspective on the subject. The authors have provided representative teaching cases in addition to their own clinical expertise and to an in-depth review of the literature. The reader is provided with age-dependent, commonly encountered clinical cases. The publication contains 12 chapters, takes a systems approach, and provides reference-based practical information that will be useful in the routine clinical setting. Chapters are organized in a similar structure starting with an overview as to the clinical value of a specific study and the most relevant clinical indications, methods to correctly request the study and prepare the patient. This is followed by description of the steps required to perform the study according to the most appropriate imaging protocol, based on those used by the expert authors in their home centers and presented in a “flash-card” format. The main normal biodistribution imaging patterns are presented, as well as useful calculations and settings when appropriate. Correlative imaging, review of variants, and possible drawbacks are detailed when deemed necessary. Each chapter discusses the Nuclear Medicine procedures that can and should be

used in the specific clinical pediatric arena. The length of the chapters varies according to the clinical significance of a particular test, the complexity of the methodology, and the number of cases included. Some longer chapters dedicated to the most common tests reflect the more extensive use of a procedure in the pediatric population presenting more cases and extensive overviews.

In addition to the 11 chapters presenting specific systems and/or diseases, the first chapter provides general information detailing the advantages and limitations for performing Nuclear Medicine tests in children, as well as suggestions on how to approach, analyze, and provide relevant data to the patients, and to their parents or caregivers. Doses of radiopharmaceuticals follow, whenever possible, the most recent version of the EANM pediatric dosage card calculator and/or the North American consensus guidelines for administered radiopharmaceutical activities in children and adolescents. Minimizing a child's exposure to ionizing radiation is an important consideration, thoroughly discussed in this section which addresses the appropriateness of pediatric nuclear imaging. Well-known and widely accepted acronyms such as PET/CT, SPECT/CT, SPECT, CT, MRI as well as activity units (e.g., mCi, MBq) have always been used as abbreviations with the intent not to burden the reader.

The design and content of this publication will hopefully promote essential debates and feedback with the goal of having Nuclear Medicine as a useful tool in the process of diagnosing and treating diseases in children and provides a good setting for an evidence-based collaboration between Nuclear Medicine physicians and pediatricians working in various fields. It is also intended to assist professionals as well as institutions in making decisions regarding the frameworks for effective management of pediatric patients.

The authors gratefully acknowledge the IAEA for technical support. A special thanks to M. Felipe Mendez for continuous assistance in preparing the manuscript.

Petah-Tikva, Israel
Vienna, Austria
Haifa, Israel
Palo Alto, CA, USA

Zvi Bar-Sever
Francesco Giammarile
Ora Israel
Helen Nadel

Contents

1	General Principles in Pediatric Nuclear Medicine	1
	Helen Nadel, Diana Paez, Zvi Bar-Sever, Ora Israel, and Francesco Giammarile	
2	Central Nervous System: The Brain and Cerebro-Spinal Fluid	15
	Lorenzo Biassoni, Helen Nadel, and Zvi Bar-Sever	
3	Cardiovascular System	33
	Pietro Zucchetta and Ora Israel	
4	Pulmonary System	47
	Zvi Bar-Sever and Pietro Zucchetta	
5	Thyroid	57
	Barry Shulkin and Thomas Neil Pascual	
6	Digestive Tract	75
	Anita Brink, Lorenzo Biassoni, and Zvi Bar-Sever	
7	Liver and Spleen	101
	Anita Brink, Zvi Bar-Sever, and Lorenzo Biassoni	
8	Genitourinary Tract	121
	Diego De Palma and Thomas Neil Pascual	
9	Lymphoscintigraphy	157
	Thomas Neil Pascual, Pietro Zucchetta, Kevin London, and Robert Howman-Giles	
10	Musculoskeletal System (Non-Oncologic Indications)	167
	Gopinath Gnanasegaran, Sharjeel Usmani, and Helen Nadel	
11	Infection and Inflammation Imaging	183
	Ora Israel, Enrique Estrada-Lobato, and Thomas Neil Pascual	
12	Pediatric Malignancies	199
	Helen Nadel, Barry Shulkin, Zvi Bar-Sever, and Francesco Giammarile	

List of Contributors

Zvi Bar-Sever Schneider Children's Medical Center, Tel Aviv University, Petah Tiqva, Israel

Institute of Nuclear Medicine, Schneider Children's Medical Center, Tel Aviv University, Petah Tiqva, Israel

Lorenzo Biassoni Department of Radiology, Great Ormond Street Hospital for Children NHS Foundation Trust, London, UK

Anita Brink Nuclear Medicine Service, Division of Pediatric Medicine, University of Cape Town, Cape Town, South Africa

Nuclear Medicine and Diagnostic Imaging Section, Division of Human Health, Department of Nuclear Sciences and Applications, International Atomic Energy Agency, Vienna, Austria

Diego De Palma Nuclear Medicine Unit, ASST Settelaghi, Varese, Italy

Enrique Estrada-Lobato Nuclear Medicine and Diagnostic Imaging Section, Division of Human Health, Department of Nuclear Sciences and Applications, International Atomic Energy Agency, Vienna, Austria

Francesco Giammarile Nuclear Medicine and Diagnostic Imaging Section, Division of Human Health, Department of Nuclear Sciences and Applications, International Atomic Energy Agency, Vienna, Austria

Gopinath Gnanasegaran Nuclear Medicine department, Royal Free London NHS Foundation Trust, London, UK

Robert Howman-Giles Nuclear Medicine Department, Children's Hospital at Westmead, University of Sydney, Sydney, NSW, Australia

Ora Israel Rappaport Faculty of Medicine, Technion, Haifa, Israel

Kevin London Nuclear Medicine Department, Children's Hospital at Westmead, University of Sydney, Sydney, NSW, Australia

Helen Nadel Lucile Packard Children's Hospital Stanford University, Palo Alto, CA, USA

Diana Paez Nuclear Medicine and Diagnostic Imaging Section, Division of Human Health, Department of Nuclear Sciences and Applications, International Atomic Energy Agency, Vienna, Austria

Thomas Neil Pascual Department of Science and Technology, Manila, Philippines

Barry Shulkin Department of Diagnostic Imaging, St. Jude Children's Research Hospital, Memphis, TN, USA

Sharjeel Usmani Department of Radiology and Nuclear Medicine, Sultan Qaboos Comprehensive Cancer CARE and Research Centre (SQCCCRC), Muscat, Oman

Pietro Zucchetta Nuclear Medicine Unit, Department of Medicine, Padova University Hospital, Padova, Italy

Abbreviations

AADC	Amino acid decarboxylase
ACD	Acid citrate dextrose
ACR	American College of Radiology
ALARA	As low as reasonably achievable
ALTE	Apparent life-threatening events
ASL	Arterial spin labeling
ATA	American Thyroid Association
AUC	Area under the curve
AV	Arterio-venous
BERA	Brainstem-evoked response audiometry
BSA	Body surface area
CBC	Complete blood count
CCK	Cholecystokinin
Ce	Contrast enhanced
CHT	Congenital hypothyroidism
CIC	Clean intermittent catheterization
CMV	Cytomegalovirus
CNS	Central nervous system
COMT	Catechol-O-methyltransferase
CRP	C-reactive protein
CRPS	Complex regional pain syndrome
CSF	Cerebro-spinal fluid
CT	Computed tomography
CTA	CT angiography
CTDI	CT dose index
CTPA	CT pulmonary angiography
CTT	Cortical transit time
CZT	Cadmium zinc telluride
DLP	Dose length product
DMSA	Dimercaptosuccinic acid
DRBC	Damaged red blood cell
DRC	Direct radionuclide cystography
DRF	Differential renal function
DTPA	Diethylene-triamine-pentaacetic acid
EANM	European Association of Nuclear Medicine
EC	Ethylene cysteine
ECD	Ethylene cysteinyl dimer

ECG	Electrocardiography
EDE	Effective dose equivalent
EDTA	Ethylene-diamine-tetraacetic acid
EEG	Electro-encephalography
EF	Ejection fraction
ESR	Erythrocytes sedimentation rate
F	Furosemide
FDG	Fluoro-deoxyglucose
FDOPA	Fluoro-dihydroxyphenyl-alanine
FOV	Field of view
FUO	Fever of unknown origin
FT4	Thyroxine
FWHM	Full width half maximum
GE	Gastric emptying
GEJ	Gastro-esophageal junction
GER	Gastro-esophageal reflux
GERD	Gastro-esophageal reflux disease
GFR	Glomerular filtration rate
GI	Gastrointestinal
GIB	Gastrointestinal bleeding
GIST	Gastrointestinal stromal tumor
GIT	Gastrointestinal tract
HBS	Hepato-biliary scintigraphy
HL	Hodgkin's lymphoma
HMPAO	Hexamethyl-propylene amine oxime
IAEA	International Atomic Energy Agency
IBD	Inflammatory bowel disease
ICU	Intensive care unit
IDA	Imino-diacetic acid
IRC	Indirect radionuclide cystogram
ITP	Idiopathic thrombocytopenic purpura
IV	Intravenous
KI	Potassium iodate
LAO	Left anterior oblique
LCH	Langerhans cell histiocytosis
LN	Lymph node
LPO	Left posterior oblique
L – R	Left-to-right
LV	Left ventricle
MAA	Macroaggregated albumin
MAO	Monoamine oxidase
MDP	Methylene-diphosphonate
MFO	Multifocal osteomyelitis
MIBI	Sestamibi
MIBG	Meta-iodo-benzyl guanidine
MIP	Maximum Intensity projection
MPS	Myocardial perfusion scintigraphy
MRA	Magnetic resonance angiography

MRCP	Magnetic resonance cholangiopancreatography
MRI	Magnetic resonance imaging
MSK	Musculo-skeletal
MUGA	Multigated acquisition
NaF	Sodium fluoride
NAI	Non-accidental injury
NE	Norepinephrine
NET	Neuroendocrine tumor
NG	Naso-gastric
NHL	Non-Hodgkin's lymphoma
NORA	Normalized residual activity
NSAIDs	Non-steroidal anti-inflammatory drugs
PE	Pulmonary embolism
PET/CT	Positron emission tomography/CT
PET/MRI	Positron emission tomography/MRI
PGL	Paraganglioma
PPGL	Pheochromocytoma and paraganglioma
PRRT	Peptide receptor radionuclide therapy
PTLD	Post-transplant lymphoproliferative disorder
PTU	Propylthiouracil
QC	Quality control
Qp	Pulmonary flow
Qs	Systemic flow
RAI	Radioactive iodine
RAIU	Radioactive iodine uptake
RAO	Right anterior oblique
RBCs	Red blood cells
RES	Reticulo-endothelial system
rhTSH	Recombinant human thyroid-stimulating hormone
R – L	Right-to-left
RPO	Right posterior oblique
ROI	Region of interest
RV	Right ventricle
SC	Sulfur colloid
SDH	Succinate dehydrogenase
SLN	Sentinel lymph node
SNMMI	Society of nuclear medicine and molecular imaging
SPECT	Single photon emission computed tomography
SPECT/CT	SPECT/computed tomography
SSKI	Supersaturated potassium iodide
SSTR	Somatostatin receptor
ST	Soft tissue
SUV	Standardized uptake value
T3	Tri-iodothyronine
T1/2	Half-life
TAC	Time activity curve
Tg	Thyroglobulin
TSH	Thyroid-stimulating hormone

UDCA	Urso-deoxycholic acid
UPJ	Uretero-pelvic junction
US	Ultrasound
UTI	Urinary tract infection
UVJ	Uretero-vesicular junction
VCUG	Voiding cysto-urethrography
VOD	Volume of distribution
V-Q	Ventilation-perfusion
VUR	Vesico-ureteral reflux
WBC	White blood cell



General Principles in Pediatric Nuclear Medicine

1

Helen Nadel, Diana Paez, Zvi Bar-Sever, Ora Israel, and Francesco Giammarile

1.1 General Information for Referring Physician, Parents, and NM Team [1–5]

Multidisciplinary Care Team

- The care team in nuclear medicine may include the nuclear medicine technologist(s), nuclear medicine nurse, child life specialist, anesthesiologist and anesthesia team, nuclear medicine physician, nuclear medicine/ radiology trainee, and referring physician.
- Close communication with referring specialists through multidisciplinary meetings is often utilized that can improve the impact of the nuclear medicine exam findings.

H. Nadel (✉)
Lucile Packard Children's Hospital Stanford
University, Palo Alto, CA, USA

D. Paez · F. Giammarile
Nuclear Medicine and Diagnostic Imaging Section,
Division of Human Health, Department of Nuclear
Sciences and Applications, International Atomic
Energy Agency, Vienna, Austria

Z. Bar-Sever
Schneider Children's Medical Center, Tel Aviv
University, Petah Tiqva, Israel

O. Israel
B&R Rappaport Faculty of Medicine, Technion,
Haifa, Israel

Departmental Workflow—Scheduling the Study

- Studies on children take longer than adults. Clear time on the schedule when studies in pediatric patients are scheduled.
- Book studies where the child needs to be fasting for prolonged periods of time as the first study of the day.

Information to Be Requested at Booking the Study

- Age.
- Weight and height.
- Gender identity of the patient.
- Contact information of parents/caregivers.
- Specific medical, developmental, or behavioral problems the patient may have.
- In cases that may require potential contrast material injection (SPECT/CT, PET/CT, PET/MRI) request information about:
 - Allergies.
 - Renal function.
 - History of previous contrast reaction.
- Parent's/caregiver's CONSENT: requirement for consent must follow national and institutional guidelines.

Information to Be Provided to Parent/Caregiver

- Whether the child should be fasting or can eat and or drink before the study.
- Duration of the study and whether there is a need for a hospital stay.
- How the study is done and what is required. For example, let the parent/caregiver know in advance if an intravenous (IV) line or urinary catheter will be placed.
- Explanation of radiation risk.
- Parents/caregivers should be informed about the application of topical anesthetic cream to possible injection sites prior to the procedure.
 - If this is planned, up to an hour is required for it to work so the patient should arrive an hour before the booking time of the study.
 - As an alternative, the parent/caregiver can put it on beforehand, outside of the department.
- Request a spare change of clothes for infants and small children.
- Parents/caregivers should bring the milk formula or any specific food that the child may need (more details in the respective chapters).
- Parents and referring physicians should be aware that certain studies require medical pre-medication preceding the scan (More details in the respective chapters).
- If the patient is close by when the study is booked it may be useful to invite the patient and caregivers into the camera room so that they know what to expect on the day of the study.

Prior to the Study

- Phone the parents on the day before the study to confirm date and time and to remind them of above-mentioned preparation.
- Arrange for an appropriate health care professional to arrive at the department for cannulation, if necessary.
- Since patient age in this category is defined as up to 18 years, when dealing with adolescents,

it is important to consider pregnancy and breastfeeding.

- Depending on institutional protocols, urine or serum pregnancy tests may be required.
- Inquire if an accompanying person is pregnant. This does not preclude her visit but appropriate radiation safety instructions should be provided.

On the Day of the Study

On arrival explain to the parent/caregiver and child what is going to happen during the study. Knowing what to expect, reduces anxiety and improves cooperation. This translates to higher-quality diagnostic images

- If available and/or necessary, as discussed above, place a local topical anesthetic on possible sites for injection.
- Do not let the child wait too long before starting the procedure.
- DO NOT LIE. Lying to your patient diminishes trust and greatly reduces cooperation.
- Tell your patient “I am going to give you an injection, it will be a bit sore, this is the only painful thing that will happen today”.
- Explain every step you execute to your patient in child friendly language: “I am going to move the bed under the camera now” etc. This leads to a marked reduction in patient anxiety.

Radiation Risks [6–9]

- Radiation-induced risk of adverse health effects is greater in children than in adults.
- There is no clear evidence regarding potential adverse health effects for the levels of exposure associated with medical imaging. However, the international health physics consensus is to optimize exposure to patients receiving these studies.
- Radiation-induced cancer risk is a function of effective dose administered, age, and gender.

- Females and younger patients are more susceptible to radiation-induced cancers.
- The optimal dose is typically understood as the lowest dose that still provides the diagnostic information necessary for proper care and therefore, on occasion, exposures higher than guideline recommendations may be necessary.
- It is recommended to weigh each request for imaging procedures that expose a patient to ionizing radiation, nuclear medicine tests in particular, with respect to their risk vs. potential clinical benefit and availability of nonionizing radiation imaging tests that can provide similar diagnostic information.
- Always be sure that the patient receives the lowest acceptable radiation exposure that allows for the highest quality diagnostic study. Modern cameras are more sensitive than older models and can produce high quality images with administered activities that are lower than the published recommendations.

Communicating Radiation Risks [10, 11]

- All parties should be mindful that the use of radiation is associated with theoretical risks that are, as a rule, significantly smaller than the risk of deciding not to perform an indicated scan.
- Care should be taken to communicate risks without raising undue alarm in patients or their families.
- Fear of radiation risk is detrimental to patients, in particular children, as well as their parents/caregivers. It can induce stress and lead to less than optimal studies or to the decision to avoid imaging. This may increase the rate of misdiagnoses with subsequent harm with no associated benefits.
- Communicating the risk associated with radiation dose can be very difficult as published articles on the topic use higher reference values than what is used in many parts of the world.
- A simple way of explaining the radiation risk from a nuclear medicine procedure is to compare it to everyday activities relative risk or to

the exposure individuals receive from natural background radiation in 1 year.

- The image gently website (<https://www.imagegently.org/Procedures/Nuclear-Medicine>) has more information on explaining radiation risk from imaging procedures.

Calculating the Administered Activity

- Use the latest versions of EANM pediatric dose card (Fig. 1.1) [12], or the North American Consensus Guidelines for Administered Radiopharmaceutical Activities in Children and Adolescents (Fig. 1.2,) [13].
- Both the EANM and SNMMI have dose calculators available online (Fig. 1.3):
- http://EANM.org/publications/dosage_calculator.php
- <http://www.snmmi.org/ClinicalPractice/PediatricTool.aspx>
- In addition, the PedDose App provided by the EANM proves to be a useful tool.
- If a radiopharmaceutical does not appear on the dose cards it is best to consult with an expert pediatric nuclear medicine center.

Sedation [14–16]

Suggestions for Avoiding Sedation

- In small babies and infants: tracer injection should be timed as close to the next breast/milk feeding as possible. A feed may be given from 30 min after tracer injection in infants not having anesthesia or sedation.
- Encourage the parent/caregiver to bring the child's own food, a pacifier and soothing toy or story books to the department.
- Infants: wrapping them snugly in a blanket increases the likelihood of a baby falling asleep.
- Toddlers: entertaining them reduces movement artifacts.
- School-age child, above the age of 6 years: is usually able to follow instructions.

BIO-MEDICAL IMAGING AND DOSIMETRY FOR PERSONALIZED HEALTH CARE

Dosage Card (Version 5.7.2016)

Multiple of Baseline Activity

Weight kg	Class A	Class B	Class C	Weight kg	Class A	Class B	Class C
3	1	1	1	32	3.77	7.29	14.00
4	1.12	1.14	1.33	34	3.88	7.72	15.00
6	1.47	1.71	2.00	36	4.00	8.00	16.00
8	1.71	2.14	3.00	38	4.18	8.43	17.00
10	1.94	2.71	3.67	40	4.29	8.86	18.00
12	2.18	3.14	4.67	42	4.41	9.14	19.00
14	2.35	3.57	5.67	44	4.53	9.57	20.00
16	2.53	4.00	6.33	46	4.65	10.00	21.00
18	2.71	4.43	7.33	48	4.77	10.29	22.00
20	2.88	4.86	8.33	50	4.88	10.71	23.00
22	3.06	5.29	9.33	52-54	5.00	11.29	24.67
24	3.18	5.71	10.00	56-58	5.24	12.00	26.67
26	3.35	6.14	11.00	60-62	5.47	12.71	28.67
28	3.47	6.43	12.00	64-66	5.65	13.43	31.00
30	3.65	6.86	13.00	68	5.77	14.00	32.33

$A[\text{MBq}]_{\text{administered}} = \text{Baseline Activity} \times \text{Multiple}$


- For a calculation of the administered activity, the baseline activity value has to be multiplied by the multiples given above for the recommended radiopharmaceutical class (see reverse).
- If the resulting activity is smaller than the minimum recommended activity, the minimum activity should be administered.
- The national diagnostic reference levels should not be exceeded!

Examples:


- ^{18}F FDP-PET Brain, activity to be administered [MBq] = 14.0×10.71 [MBq] = 150 MBq
50 kg:
- ^{123}I mIBG, activity to be administered [MBq] = 28.0×1 [MBq] = 28 MBq < 37 MBq (Minimum Recommended Activity)
3 kg:
→ activity to be administered: 37 MBq

This card is based upon the publication by Jacobs F, Thierens H, Plepaz A, Bacher K, Van de Wiele C, Ham H, Dierckx RA. Optimized tracer-dependent dosage cards to obtain weight-independent effective doses. Eur J Nucl Med Mol Imaging. 2005 May; 32(5):581-8.

This card summarizes the views of the Paediatric and Dosimetry Committees of the EANM and reflects recommendations for which the EANM cannot be held responsible. The dosage recommendations should be taken in context of „good practice“ of nuclear medicine and do not substitute for national and international legal or regulatory provisions.



Android App



iPhone App

EANM Executive Office
Schmalzhofgasse 26 · 1060 Vienna, Austria
Phone: +43 (0) 1 890 44 27, fax: +43 (0) 1 890 44 27-9
office@eanm.org · www.eanm.org · fb.com/officialEANM

Recommended Amounts in MBq

Radiopharmaceutical	Class	Baseline Activity (for calculation purposes only) MBq	Minimum Recommended Activity ¹ MBq
^{123}I (Thyroid)	C	0.6	3
^{123}I Amphetamine (Brain)	B	13.0	18
^{123}I HIPURAN (Abnormal renal function)	B	5.3	10
^{123}I HIPURAN (Normal renal function)	A	12.8	10
^{123}I mIBG	B	28.0	37
^{131}I mIBG	B	5.6	35
^{18}F FDG-PET torso	B	25.9	26
^{18}F FDG-PET brain	B	14.0	14
^{18}F Sodium fluoride	B	10.5	14
^{67}Ga Citrate	B	5.6	10
^{67}Ga -labelled peptides	B	12.8	14
$^{99\text{m}}\text{Tc}$ ALBUMIN (Cardiac)	B	56.0	80
$^{99\text{m}}\text{Tc}$ COLLOID (Gastric Reflux)	B	2.8	10
$^{99\text{m}}\text{Tc}$ COLLOID (Liver/Spleen)	B	5.6	15
$^{99\text{m}}\text{Tc}$ COLLOID (Marrow)	B	21.0	20
$^{99\text{m}}\text{Tc}$ DMSA	B	6.8	18.5
$^{99\text{m}}\text{Tc}$ DTPA (Abnormal renal function)	B	14.0	20
$^{99\text{m}}\text{Tc}$ DTPA (Normal renal function)	A	34.0	20
$^{99\text{m}}\text{Tc}$ ECD	B	51.8	100
$^{99\text{m}}\text{Tc}$ HMPAO (Brain)	B	51.8	100
$^{99\text{m}}\text{Tc}$ HMPAO (WBC)	B	35.0	40
$^{99\text{m}}\text{Tc}$ IDA (Biliary)	B	10.5	20
$^{99\text{m}}\text{Tc}$ MAA / Microspheres	B	5.6	10
$^{99\text{m}}\text{Tc}$ MAG3	A	11.9	15
$^{99\text{m}}\text{Tc}$ MDP	B	35.0	40
$^{99\text{m}}\text{Tc}$ Pertechnate (Cystography)	B	1.4	20
$^{99\text{m}}\text{Tc}$ Pertechnate (Ectopic Gastric Mucosa)	B	10.5	20
$^{99\text{m}}\text{Tc}$ Pertechnate (Cardiac First Pass)	B	35.0	80
$^{99\text{m}}\text{Tc}$ Pertechnate (Thyroid)	B	5.6	10
$^{99\text{m}}\text{Tc}$ RBC (Blood Pool)	B	56.0	80
$^{99\text{m}}\text{Tc}$ SestaMIBI/Tetrofosmin (Cancer seeking agent)	B	63.0	80
$^{99\text{m}}\text{Tc}$ SestaMIBI/Tetrofosmin ² (Cardiac rest scan 2-day protocol min)	B	42.0	80
$^{99\text{m}}\text{Tc}$ SestaMIBI/Tetrofosmin ² (Cardiac rest scan 2-day protocol max)	B	63.0	80
$^{99\text{m}}\text{Tc}$ SestaMIBI/Tetrofosmin ² (Cardiac stress scan 2-day protocol min)	B	42.0	80
$^{99\text{m}}\text{Tc}$ SestaMIBI/Tetrofosmin ² (Cardiac stress scan 2-day protocol max)	B	63.0	80
$^{99\text{m}}\text{Tc}$ SestaMIBI/Tetrofosmin ² (Cardiac rest scan 1-day protocol)	B	28.0	80
$^{99\text{m}}\text{Tc}$ SestaMIBI/Tetrofosmin ² (Cardiac stress scan 1-day protocol)	B	84.0	80
$^{99\text{m}}\text{Tc}$ Spleen (Denatured RBC)	B	2.8	20
^{99}Tc TECHNEGAS (Lung ventilation) ³	B	49.0	100

¹ The minimum recommended activities are calculated for commonly used gamma cameras or positron emission tomographs. Lower activities could be administered when using systems with higher counting efficiency.

² The minimum and maximum values correspond to the recommended administered activities in the EANM/ESCC procedural guidelines (Hesse B, Tagli K, Cuocolo A, et al). EANM/ESCC procedural guidelines for myocardial perfusion imaging in nuclear Cardiology. Eur J Nucl Med Mol Imaging. 2005 Jul;32(7):855-97.

³ This is the activity load needed to prepare the Technegas device. The amount of inhaled activity will be lower.

Fig. 1.1 The EANM calculator screen shot. Reproduced with permission from https://www.eanm.org/content-eanm/uploads/2017/01/EANM_Dosage_Card_040214.pdf. “This card summarises the views of the Paediatrics and Dosimetry Committees of the EANM and reflects recommendations for which the EANM cannot be held

responsible. The dosage recommendations should be taken in the context of “good practice” of nuclear medicine and do not substitute for national and international legal or regulatory provisions.” It is based upon work published in references [12, 30, 31]

- Patients in pain may be uncooperative. Proper pain relief given in consultation with the referring physician is beneficial and reduces movement artifacts on scans.
- If possible, have the parent/caregiver close by and let them help. For example, letting

- the patient sit on their lap during an esophageal transit study or milk scan is less intimidating than sitting on the technologist’s lap.
- When necessary parents/caregivers can assist the technologists in preventing motion during

Follow the new North American Guidelines for Pediatric Nuclear Medicine for high-quality images at low radiation dose.



2016 Update: North American Consensus Guidelines for Pediatric Administered Radiopharmaceutical Activities¹

Radiopharmaceutical	Notes	Administered Activity	Minimum Administered Activity	Maximum Administered Activity
¹²³ I-MIBG	[A]	5.2 MBq/kg (0.14 mCi/kg)	37 MBq (1.0 mCi)	370 MBq (10.0 mCi)
^{99m} Tc-MDP	[A]	9.3 MBq/kg (0.25 mCi/kg)	37 MBq (1.0 mCi)	
¹⁸ F-FDG	[A, B]	Body: 3.7-5.2 MBq/kg (0.10-0.14 mCi/kg) Brain: 3.7 MBq/kg (0.10 mCi/kg)	26 MBq (0.7 mCi) 14 MBq (0.37 mCi)	
^{99m} Tc-DMSA	[A]	1.85 MBq/kg (0.05 mCi/kg)	18.5 MBq (0.5 mCi)	100 MBq (2.7 mCi)
^{99m} Tc-MAG3	[A, C]	Without flow study: 3.7 MBq/kg (0.10 mCi/kg) With flow study: 5.55 MBq/kg (0.15 mCi/kg)	37 MBq (1.0 mCi)	148 MBq (4.0 mCi)
^{99m} Tc-IDA	[A, D]	1.85 MBq/kg (0.05 mCi/kg)	18.5 MBq (0.5 mCi)	
^{99m} Tc-MAA	[A]	If ^{99m} Tc used for ventilation: 2.59 MBq/kg (0.07 mCi/kg) No ^{99m} Tc ventilation study: 1.11 MBq/kg (0.03 mCi/kg)	14.8 MBq (0.4 mCi)	
^{99m} Tc-pertechnetate (Meckel diverticulum imaging)	[A]	1.85 MBq/kg (0.05 mCi/kg)	9.25 MBq (0.25 mCi)	
¹⁸ F-sodium fluoride	[A]	2.22 MBq/kg (0.06 mCi/kg)	14 MBq (0.38 mCi)	
^{99m} Tc (for cystography)	[E]	No weight-based dose	No more than 37 MBq (1.0 mCi) for each bladder filling cycle	
^{99m} Tc-sulfur colloid (for oral liquid gastric emptying)	[F]	No weight-based dose	9.25 MBq (0.25 mCi)	37 MBq (1.0 mCi)
^{99m} Tc-sulfur colloid (for solid gastric emptying)	[F]	No weight-based dose	9.25 MBq (0.25 mCi)	18.5 MBq (0.5 mCi)
^{99m} Tc-HMPAO (Cerectec)/ ^{99m} Tc-ECD (NeuroLite) for brain perfusion		11.1 MBq/kg (0.3 mCi/kg)	185 MBq (5 mCi)	740 MBq (20 mCi)
^{99m} Tc-sestamibi (Cardiolite)/ ^{99m} Tc-tetrofosmin (Myoview) for myocardial perfusion (single scan or first of 2 scans, same day)		5.55 MBq/kg (0.15 mCi/kg)	74 MBq (2 mCi)	370 MBq (10 mCi)
^{99m} Tc-sestamibi (Cardiolite)/ ^{99m} Tc-tetrofosmin (Myoview) for myocardial perfusion (second of 2 scans, same day)		16.7 MBq/kg (0.45 mCi/kg)	222 MBq (6 mCi)	1110 MBq (30 mCi)
^{Na} 123I for thyroid imaging		0.28 MBq/kg (0.0075 mCi)	1 MBq (0.027 mCi)	11 MBq (0.3 mCi)
^{99m} Tc-pertechnetate for thyroid imaging		1.1 MBq/kg (0.03 mCi/kg)	7 MBq (0.19 mCi)	93 MBq (2.5 mCi)
^{99m} Tc-RBC for blood pool imaging		11.8 MBq/kg (0.32 mCi/kg)	74 MBq (2 mCi)	740 MBq (20 mCi)
^{99m} Tc-WBC for infection imaging		7.4 MBq/kg (0.2 mCi/kg)	74 MBq (2 mCi)	555 MBq (15 mCi)
⁶⁸ Ge-DOTATOC or ⁶⁸ Ge-DOTATATE	[G]	2.7 MBq/kg (0.074 mCi/kg)	14 MBq (0.38 mCi)	185 MBq (5 mCi)

NOTES: This information is intended as a guideline only. Local practice may vary depending on patient population, choice of collimator, and the specific requirements of clinical protocols. Administered activity may be adjusted when appropriate by order of the nuclear medicine physician.

For patients who weigh more than 70 kg, it is recommended that the maximum administered activity not exceed the product of the patient's weight (kg) and the recommended weight-based administered activity. Some practitioners may choose to set a fixed maximum administered activity equal to 70 times the recommended weight-based administered activity, expressed as MBq/kg or mCi/kg, for example, approximately 10 mCi (370 MBq) for ¹⁸F-FDG body imaging. The administered activities assume use of a low energy high-resolution collimator for ¹²³I-iodine radiopharmaceutical and a medium energy collimator for ¹²³I-MIBG.

Individual practitioners may use lower administered activities if their equipment or software permits them to do so. Higher administered activities may be required in selected patients. No recommended dose is given for intravenous ⁶⁸Ge/rate. Intravenous ⁶⁸Ge/rate should be used very infrequently and only in low doses.

- The EANM Dosage Card 2014 version 2 administered activity may also be used.
- The low end of the dose range should be considered for smaller patients. Administered activity may take into account patient mass and time available on the PET scanner. The EANM Dosage Card 2014 version 2 administered activity may also be used.
- The administered activities assume that image data are reformed at 1 min/image. The administered activity may be reduced if image data are reformed at a longer time per image.
- A higher administered activity of 1 mCi may be considered for ascended pancreas.
- ^{99m}Tc-sulfur colloid, ^{99m}Tc-pertechnetate, ^{99m}Tc-DTPA or possibly other ^{99m}Tc radiopharmaceuticals may be used. There is a wide variety of acceptable administration and imaging techniques for ^{99m}Tc cystography, many of which will work well with lower administered activities. An example of appropriate lower administered activities is found in the 2014 revision of the EANM Pediatric Dose Card.
- The administered activity may be based on patient weight or on the age of the child.
- The administered activity is based on the EANM Dosage Card 2014 version 22 dosage for a 60 kg patient, using the minimum and maximum doses from the EANM Dosage Card. There was little experience with this radiopharmaceutical in children in North America at the time of preparation of this dosage table.

¹Gelbard ML, Parisi MJ, Teves ST. Pediatric Radiopharmaceutical Administered Doses: 2010 North American Consensus Guidelines. *J Nucl Med*. 2011; 52(2):318-322.
²Lossman AJ, Teves, ST. Pediatric Radiopharmaceutical Administration: Harmonization of the 2007 EANM Pediatric Dosage Card (Version 1.5.2008) and the 2010 North America Consensus guideline. *Eur J Nucl Med Mol Imaging* 2014; 41(8):1636 Epub Mar 6 2014



Fig. 1.2 North American Consensus Guidelines for Pediatric Administered Radiopharmaceutical Activities 2016. Reproduced with permission of imagegently.org

Dosage Calculator

Calculation of the administered activity in [MBq] and [mCi]

Weight

Radiopharmaceutical

Activity to be administered:
= 17 MBq or 0.46 mCi

This card is based upon the publication by Jacobs F, Thierens H, Piepsz A, Bacher K, Van de Wiele C, Ham H, Dierckx RA. Optimized tracer-dependent dosage cards to obtain weight independent effective doses. *Eur J Nucl Med Mol Imaging*. 2005 May; 32(5):581-8.

M. Lassmann, S.T.Treves. Pediatric Radiopharmaceutical Administration: Harmonization of the 2007 EANM Paediatric Dosage Card (Version 1.5.2008) and the 2010 North America Consensus guideline, *Eur J Nucl Med Mol Imaging*. 2014, DOI: 10.1007/s00259-014-2731-9.

Lassmann M, Biassoni L, Monsieurs M, Franzius C; EANM Dosimetry and Paediatrics Committees. The new EANM paediatric dosage card: additional notes with respect to F-18. *Eur J Nucl Med Mol Imaging*. 2008 Sep;35(9):1666-8. DOI: 10.1007/s00259-008-0799-9. Epub 2008 Jun 24. Erratum in: *Eur J Nucl Med Mol Imaging*. 2008 Nov;35(11):2141

This card summarises the views of the Paediatric and Dosimetry Committees of the EANM and reflects recommendations for which the EANM cannot be held responsible. The dosage recommendations should be taken in the context of "good practice" of nuclear medicine and do not substitute for national and international legal or regulatory provisions.

Fig. 1.3 Dose calculator snapshot. (based Reproduced with permission from <https://www.eanm.org/initiatives/dosage-calculator/>)

acquisition, for example, by gently securing the child's head when under the camera.

- Encourage the parent to hold the child's hand and talk to the patient during the study.
- Ensure that the accompanying caregiver is clear from the rotating camera heads.

Options for Distracting and Entertaining the Patient

- A TV screen mounted on one of the walls or ceiling above the gantry.
- A portable DVD player or one incorporated into the gamma camera.

- Stickers of popular cartoon characters or animals on the collimators.
- Smart phone to take pictures of the patient/ play games /play music on.
- Read a storybook.
- Crayons and paper to entertain the child during the waiting period.
- The toys in your department should be easy to clean, preferably plastic.
- Avoid soft and plush toys as they pose a significant infection and contamination risk.
- The patient is only allowed to leave the department once fully awake as determined by the nurse or physician in your department.
- Tell the parent/caregiver what to expect after sedation, and which warning signs to watch for.

1.2 Performing and Reporting the Study

Preparing and Administration of Radiopharmaceutical

Assessing the Need for Sedation

- Sedation and anesthesia carry risk, impose a logistical challenge requiring several hours of fasting prior to the procedure and need to be considered at the time of booking study.
- If conscious sedation is to be performed, the same preparation applies.
- For short studies sedation may not be necessary.
- Consult with institutional guidelines for recommended drugs to administer for sedation.

Principles and Protocols for Sedation/General Anesthesia

- Sedation should be performed by qualified, authorized personnel including your pediatric anesthesia service applying the standard sedation used in your institution.
- Sedation or general anesthesia should be used judiciously.
 - It can be indicated in young children beyond swaddling age and under 5 years of age or non-cooperative older children.
 - The need for sedation also depends on the study type, and should be considered in particular when performing SPECT/CT and PET/CT or PET/MRI.
- Do not sedate the patient if adequate resuscitation facilities are not available, including a correct size endotracheal tube.
- Document type, dose, and time of sedation.
- A qualified nurse or physician must be present with the child during the entire sedation Monitor continuously using a pulse oximeter (document pulse rate and oxygen saturation).

- If tracers are prepared in the Nuclear Medicine department, follow national regulations for radiopharmaceutical in-house preparation.
- If small amounts of activity have to be administered they may be difficult to draw up and the activity used to prepare the kit should be diluted.
- Use the smallest syringe available to draw up the dose. For pediatric doses a 1-ml syringe is ideal.
- A butterfly needle or venous cannula is recommended to administer the radiopharmaceutical. Direct large bore venipuncture needle should not be used.
- Post-injection saline flush is very important.

Setting up the Imaging Device

- Cover the collimator with absorbent material if the patient is positioned directly on the collimator. This protects your camera from contamination.
- Contamination can easily occur with studies such as milk scans or diuretic renography.

Positioning the Patient

- Wrap small babies tightly in a blanket (swaddle).
- To prevent patient motion, use restraining devices including papoose boards, sandbags, large saline bags, rolled towels, or vacuum immobilization bags, around the patient.

- Ensure the patient is firmly secured to the bed using Velcro straps (Fig. 1.4).
- When performing extremity imaging in a small child it is useful to bind the legs together (Fig. 1.5) and improve the position of the arms using splints.
- In older children, immobilize the feet together with the toes pointing inward, this improves the position of the hips and separates the tibia and fibula (Fig. 1.5).
- If the desired position cannot be obtained (due to pain or discomfort), care should be taken to place both limbs in similar positions.
- Patient should empty the bladder before starting the scan to be comfortable during the procedure.
- If SPECT/CT or PET/CT are performed, arms should be placed above the head if possible, to avoid beam-hardening artifacts on CT when the arms are in the field-of-view (FOV).
- For PET/MRI and other studies with longer sedation times arms should be placed down, by the side of the body.
- When the site of disease is in the head and neck, an additional image of head and neck is recommended with arms by the side of the body (Fig. 1.4).

Fig. 1.4 Firmly secured child using Velcro straps



Fig. 1.5 Immobilized legs to reduce motion and better visualization of pelvic and shin bones



Performing the Study

- Determine if all organs of interest are in the FOV, use a marker if needed.
- Zoom your images according to the patient size.
- A single FOV spot image of an infant is not acceptable for whole-body visualization.
- Long acquisition times increase the likelihood of motion artifacts degrading image quality.
- While it is important to follow pediatric imaging protocols, occasionally adjustments in the imaging sequence and duration are needed in order to tailor to the specific question at hand and to the degree of the child's cooperation.
- When the infant is asleep, start with imaging the region of concern rather than sequential images from head to toe.
- For some study types, e.g., bone scans, it is recommended to first image the pelvis while the urinary bladder is relatively empty.
- The technologist should note when there is possible radioactive urine contamination, clean the area and repeat the examination without contaminated clothing.

Reporting the Study

- Check the tracer biodistribution and quality of images before reporting the study.

The report should include:

- The indication for the study with pertinent medical history.
- Premedication and pharmacologic intervention, type, and duration.
- Any usage of sedation or general anesthesia.
- CT imaging dose report to include the CT dose index (CTDI) and dose length product (DLP) when required by national or local regulations.
- Presence of a urinary catheter.
- The radiopharmaceutical type, activity, route of administration and site.
- The imaging protocol: dynamic, planar, pin-hole, SPECT, SPECT/CT, PET/CT, or PET/MRI.
- A detailed study report of all findings.
- Comparison to a previous study (if performed and available) and/or, if indicated, with results of other imaging tests.

- Final impression.
- Suggestion for further evaluation as clinically indicated.
- Urgent or critical findings should be directly communicated by phone to the referring physician and this communication should be documented in the printed report, including the name of the physician, date and time of the communication.

1.3 Hybrid Imaging [17, 18]

- Hybrid imaging is now an important part of nuclear medicine, including pediatric patients.
- The power of the co-registered, cross-sectional capabilities of SPECT/CT, PET/CT, and PET/MRI provides more information than the sum of the parts standalone.
- With new techniques comes the added responsibility of optimizing the investigation.
- CT scan options for hybrid imaging studies (both PET/CT and SPECT/CT) include:
 - Attenuation correction and image optimization.
 - Study for anatomical localization.
 - Diagnostic CT with or without oral and/or IV contrast administration.
- CT settings for SPECT/CT or PET/CT should follow pediatric protocols for low-dose or diagnostic CT including:
 - Low-dose CT for anatomical localization, mainly if the patient had a diagnostic standalone CT within a short time interval prior to the hybrid imaging study.
 - Optimized study for diagnostic evaluation.
- Dose modulation should be applied for pediatric CT hybrid studies.
- CT images should be examined using bone, lung, and soft tissue windows.
- The choice of technique depends on local hospital protocols, team and clinician's preferences, and MRI availability.

SPECT/CT [19]

- Gamma camera imaging with single photon emitting radiotracers represents the majority

of procedures in a routine pediatric nuclear medicine practice.

- The optimization of technology for image acquisition, display, and analysis, as well as the emergence of new ^{99m}Tc -labelled agents are enhancing the value of SPECT/CT in terms of both clinical impact on patient care.
- In general, and specifically for non-oncological indications, the decision to perform the CT is made if clinically indicated or after the SPECT images are completed and reviewed and with the patient not having moved position [20].
- SPECT/CT has proven to be especially valuable by:
 - Precise localization of areas of abnormal and/or physiological SPECT tracer uptake.
 - Improving the sensitivity and specificity of nuclear medicine procedures.
 - Allowing for quantitation.
 - Optimized guide for interventional diagnostic procedures.
- When CT is acquired only to clarify SPECT findings, its FOV can be reduced to only cover the suspicious findings. This can significantly reduce the patient's dose.

PET/CT [21–24]

- True whole-body imaging from vertex to feet has been recommended to be performed in PET/CT studies of children as pediatric diseases may occur distal to elbows and knees.
- In general, pediatric CT scanning for PET/CT, even with optimized diagnostic techniques including IV contrast administration can be adequately performed with lower kVp and with dose modulation to lower mAs.
- By utilizing an optimized post-contrast CT examination with sufficient attenuation-correction, while staging a child presumed to have malignancy, one may possibly eliminate the 1–2 additional CT scan examinations that may have been performed.
- PET/CT can be also utilized for better delineation of target volumes for external beam radiation therapy.

PET/MRI [25, 26]

- This technology combines PET and MRI imaging with simultaneous acquisition.
- Potentially, any study that could be done with PET/CT could be performed with PET/MRI provided there are no contraindications for the child to have an MRI.
- As with CT, renal function should be known before study.
- Strengths of MRI as compared with CT:
 - Superior soft tissue contrast resolution.
 - It provides functional data, mainly for neurological cases.
 - Lack of ionizing radiation is highly appealing, particularly in pediatric, young adult, or pregnant patients.
 - With the development of full digital and total-body PET/CT and PET/MRI scanners, the administered activity can be significantly reduced.
- Limitations of PET/MRI:
 - Most children under 8 years of age will require sedation or general anesthesia for PET/MRI.
 - Non-sedated children may experience claustrophobia.
 - The technique and its evaluation are complex, the equipment is very costly and has limited availability in some countries.
 - PET/MRI has inferior performance (compared to CT) in detecting lung and cortical bone pathology.
 - There are more frequent artifacts on the attenuation correction maps.
 - A PET/MRI procedure can be of longer duration as compared to PET/CT, due to the prolonged MRI acquisition in cases of multiparametric sequences.

Adverse Reactions to Contrast Media [27]

- Various forms of contrast media have been used to improve medical imaging.
- Like any pharmaceutical, these agents are not completely devoid of risk. When used, it is

important to recognize and manage the small but real risks inherent in the use of contrast media.

- Adverse side effects from the administration of contrast media vary from minor physiological disturbances to rare but severe life-threatening situations.
- It is important to evaluate the likelihood of a patient to experience a subsequent reaction.
- The previous use of contrast media, and also presence of allergy and asthma are important parameters to evaluate prior to the scan.
- Renal insufficiency, cardiac status, and anxiety should also be evaluated.
- In some cases, premedication strategies such as steroid and antihistamine administration might be used.
- Being prepared for prompt treatment of the entire spectrum of contrast media reactions and potential adverse events includes prearranged response planning with the availability of appropriately trained personnel, equipment, and medications.
- The ACR manual's information on contrast reactions is a comprehensive resource for this topic. <https://www.acr.org/Clinical-Resources/Contrast-Manual>.

1.4 Correlative Imaging [27–29]

- Most radiologic correlative imaging modalities provide focused evaluation and not whole-body screening.
- Nuclear Medicine examinations in children often provide the capability for whole-body diagnostic imaging, occasionally revealing sites of disease that are outside the FOV of focused radiological investigations.
- Whole-body imaging is important because of the multifocal nature of certain oncologic and non-oncologic pediatric conditions.
- Referred pain, non-verbalization of infants, and difficulties in performing physical examination in non-cooperative children can result in directing focused radiologic examinations to the wrong sites.

- Nuclear Medicine examinations, however, must be correlated with history, physical, and correlative imaging.
- Correlative imaging can include radiographs, ultrasound (US), CT, and MRI.
- Plain radiographs are often utilized as initial imaging for children presenting with respiratory or gastrointestinal symptoms and may provide evidence of infectious, inflammatory, neoplastic, or traumatic diagnoses.
- Correlation with radiographs is particularly important for assessment of the musculoskeletal system.
- Conventional radiographs usually are followed by more specific imaging.
- In recent decades, radiation-free techniques such as US have unequivocally become the first choice modality for assessing pediatric patients.
- US is a readily available tool and is required for correlation when performing various nuclear medicine studies in children, such as renal studies.
- US should be the first study in a child with a palpable abdominal mass. It can detect the site of origin of the mass as well as involvement of solid organs. However, this is usually not the final diagnostic and/or staging test.
- Cross-sectional imaging with CT or MRI may be performed in a child presenting with a mass or with systemic symptoms.
- CT is more often utilized to assess lesions in the chest such as for pulmonary nodules that may not show activity on nuclear medicine studies either because of their size or lack of avidity.
- Because hybrid nuclear medicine studies are not able to be done as breath-hold studies, the sensitivity with a stand-alone breath-hold non-contrast CT of the lungs is often needed for correlation.
- CT studies may be performed as the first imaging test in particular in a child with trauma. Results of this CT may then be used to correlate with additionally performed functional nuclear medicine studies.
- MRI, where available, has become the procedure of choice in a variety, if not all, pediatric

clinical scenarios, in particular, in suspected oncologic diseases and cancer predisposition syndromes, acute osteomyelitis, and infection and inflammation in the brain and spine.

- The majority of MRI examinations are focused exams.
- One pitfall with MRI, as well as with CT or US, is the fact that these studies are most often primarily focused on the clinical site of concern and can therefore miss the site of disease in cases of referred pain or remote sites in the presence of multifocal disease, both common situations in children.

Acknowledgment The authors acknowledge the valuable contribution of John A. Kennedy, PhD, from the Rambam HealthCare Campus in Haifa, Israel.

References

1. Gordon I. Issues surrounding preparation, information and handling the child and parent in nuclear medicine. *J Nucl Med.* 1998;39(3):490–4.
2. Tyson ME, Bohl DD, Blickman JG. A randomized controlled trial: child life services in pediatric imaging. *Pediatr Radiol.* 2014;44(11):1426–32.
3. Biassoni L, Easty M. Paediatric nuclear medicine imaging. *Br Med Bull.* 2017;123(1):127–48.
4. Stunden C, et al. Comparing a virtual reality-based simulation app (VR-MRI) with a standard preparatory manual and child life program for improving success and reducing anxiety during pediatric medical imaging: randomized clinical trial. *J Med Internet Res.* 2021;23(9):e22942.
5. Djekidel M and Govindarajan KK, Nuclear medicine pediatric assessment, protocols, and interpretation, in *StatPearls*. 2022, StatPearls Publishing Copyright © 2022, StatPearls Publishing LLC.: Treasure Island (FL).
6. Fahey FH, et al. Standardization of administered activities in pediatric nuclear medicine: a report of the first nuclear medicine global initiative project, part 1-statement of the issue and a review of available resources. *J Nucl Med.* 2015;56(4):646–51.
7. Frush DP, Perez MDR. Children, medical radiation and the environment: an important dialogue. *Environ Res.* 2017;156:358–63.
8. Union E. European guidelines on diagnostic reference levels for paediatric imaging. 2018. 122 DOI: <https://doi.org/10.2833/003998>.
9. Poli GL, et al. Developing and implementing an imaging optimization study in pediatric nuclear medicine: experience and recommendations from an

- IAEA-Coordinated Research Project. *J Nucl Med.* 2021;62(4):570–6.
10. Fahey FH, Treves ST, Adelstein SJ. Minimizing and communicating radiation risk in pediatric nuclear medicine. *J Nucl Med.* 2011;52(8):1240–51.
 11. Siegel JA, et al. Dose optimization to minimize radiation risk for children undergoing CT and nuclear medicine imaging is misguided and detrimental. *J Nucl Med.* 2017;58(6):865–8.
 12. Lassmann M, Treves ST. Paediatric radiopharmaceutical administration: harmonization of the 2007 EANM paediatric dosage card (version 1.5.2008) and the 2010 North American consensus guidelines. *Eur J Nucl Med Mol Imaging.* 2014;41(5):1036–41.
 13. Treves ST, et al. 2016 update of the North American consensus guidelines for pediatric administered radiopharmaceutical activities. *J Nucl Med.* 2016;57(12):15N–8N.
 14. Krauss B, Green SM. Procedural sedation and analgesia in children. *Lancet.* 2006;367(9512):766–80.
 15. Wang X, Xu Z, Miao CH. Current clinical evidence on the effect of general anesthesia on neurodevelopment in children: an updated systematic review with meta-regression. *PLoS One.* 2014;9(1):e85760.
 16. Slovis TL. Sedation and anesthesia issues in pediatric imaging. *Pediatr Radiol.* 2011;41(Suppl 2):514–6.
 17. Goske MJ, et al. The 'Image Gently' campaign: increasing CT radiation dose awareness through a national education and awareness program. *Pediatr Radiol.* 2008;38(3):265–9.
 18. Fahey FH, et al. Dosimetry and adequacy of CT-based attenuation correction for pediatric PET: phantom study. *Radiology.* 2007;243(1):96–104.
 19. Nadel HR. SPECT/CT in pediatric patient management. *Eur J Nucl Med Mol Imaging.* 2014;41(Suppl 1):S104–14.
 20. Israel O, et al. Two decades of SPECT/CT - the coming of age of a technology: an updated review of literature evidence. *Eur J Nucl Med Mol Imaging.* 2019;46(10):1990–2012.
 21. Stauss J, et al. Guidelines for 18F-FDG PET and PET-CT imaging in paediatric oncology. *Eur J Nucl Med Mol Imaging.* 2008;35(8):1581–8.
 22. von Mehren M, et al. Soft tissue sarcoma, version 2.2018, NCCN Clinical Practice Guidelines in Oncology. *J Natl Compr Cancer Netw.* 2018;16(5):536–63.
 23. Magill D, Alavi A. Radiation safety concerns related to PET/computed tomography imaging for assessing pediatric diseases and disorders. *PET Clin.* 2020;15(3):293–8.
 24. Edwards KW. Preparation and logistic considerations in performing PET and PET/Computed Tomography in Pediatric Patients. *PET Clin.* 2020;15(3):285–92.
 25. Hirsch FW, et al. PET/MR in children. Initial clinical experience in paediatric oncology using an integrated PET/MR scanner. *Pediatr Radiol.* 2013;43(7):860–75.
 26. States LJ, Reid JR. Whole-body PET/MRI applications in Pediatric oncology. *AJR Am J Roentgenol.* 2020;215(3):713–25.
 27. Granata C, et al. Referral guidelines for medical imaging in children: an ESR-EuroSafe imaging survey on availability, awareness and use in clinical practice among European radiologists. *Eur Radiol.* 2021;31(10):7984–91.
 28. Strauss KJ, et al. Image gently: ten steps you can take to optimize image quality and lower CT dose for pediatric patients. *AJR Am J Roentgenol.* 2010;194(4):868–73.
 29. Frush DP, Sorantin E. Radiation use in diagnostic imaging in children: approaching the value of the pediatric radiology community. *Pediatr Radiol.* 2021;51(4):532–43.
 30. Jacobs F, et al. Optimized tracer-dependent dosage cards to obtain weight independent effective doses. *Eur J Nucl Med Mol Imaging.* 2005;32(5):581–8.
 31. Lassmann M, et al. EANM Dosimetry and Paediatrics Committees. The new EANM paediatric dosage card: additional notes with respect to F-18. *Eur J Nucl Med Mol Imaging.* 2008;35:1666–8. <https://doi.org/10.1007/s00259-008-0799-9>. Erratum in: *Eur J Nucl Med Mol Imaging.* 2008;35(11):2141

The opinions expressed in this chapter are those of the author(s) and do not necessarily reflect the views of the IAEA: International Atomic Energy Agency, its Board of Directors, or the countries they represent.

Open Access This chapter is licensed under the terms of the Creative Commons Attribution 3.0 IGO license (<http://creativecommons.org/licenses/by/3.0/igo/>), which permits use, sharing, adaptation, distribution and reproduction in any medium or format, as long as you give appropriate credit to the IAEA: International Atomic Energy Agency, provide a link to the Creative Commons license and indicate if changes were made.

Any dispute related to the use of the works of the IAEA: International Atomic Energy Agency that cannot be settled amicably shall be submitted to arbitration pursuant to the UNCITRAL rules. The use of the IAEA: International Atomic Energy Agency's name for any purpose other than for attribution, and the use of the IAEA: International Atomic Energy Agency's logo, shall be subject to a separate written license agreement between the IAEA: International Atomic Energy Agency and the user and is not authorized as part of this CC-IGO license. Note that the link provided above includes additional terms and conditions of the license.

The images or other third party material in this chapter are included in the chapter's Creative Commons license, unless indicated otherwise in a credit line to the material. If material is not included in the chapter's Creative Commons license and your intended use is not permitted by statutory regulation or exceeds the permitted use, you will need to obtain permission directly from the copyright holder.





Central Nervous System: The Brain and Cerebro-Spinal Fluid

2

Lorenzo Biassoni, Helen Nadel, and Zvi Bar-Sever

2.1 Brain Death Study

Clinical Indications

- Confirmation of brain death.

Pre-exam Information

- Is there a strong clinical suspicion of brain death?
- Did the patient sustain any recent injury to the head? If so, what is the location and severity of the injury?
- Does the patient have intracranial pressure monitors or drip sites on the scalp?
- What is the hemodynamic condition of the patient?

L. Biassoni (✉)
Department of Radiology, Great Ormond Street
Hospital for Children NHS Foundation Trust,
London, UK
e-mail: Lorenzo.Biassoni@gosh.nhs.uk

H. Nadel
Lucile Packard Children's Hospital Stanford
University, Palo Alto, CA, USA

Z. Bar-Sever
Schneider Children's Medical Center, Tel Aviv
University, Petah Tikva, Israel

Study Protocol for Brain Death Imaging [1, 2]

Patient Preparation

- In some institutions, when a non-specific radiopharmaceutical is used, a tourniquet is placed that encircles the head just above the eyebrows, ears, and around the posterior prominence of the skull. This reduces blood flow to the scalp and helps distinguish between cerebral and scalp activities.

Radiopharmaceutical, Administered Activity and Mode of Delivery

Radiopharmaceutical:

- Preferred: specific brain perfusion tracers $[^{99m}\text{Tc}]$ hexamethylpropyleneamine oxime (HMPAO) and $[^{99m}\text{Tc}]$ ethyl cysteinate dimer (ECD) have the advantage that allows for the evaluation of the posterior fossa.
- Alternative: brain non-specific perfusion tracers: $[^{99m}\text{Tc}]$ Pertechnetate (Pertechnetate) or $[^{99m}\text{Tc}]$ diethylenetriamine-pentaacetate (DTPA) have the advantage of low cost and availability.

Activity:

- Weight based, 370–740 MBq (10–20 mCi) or 18 MBq/Kg (0.5 mCi/kg).

Refer to the EANM pediatric dosage card and to the North American consensus guidelines on radiopharmaceutical administration in children in the respective EANM and Society of Nuclear Medicine and Molecular Imaging (SNMMI) and image gently web sites.

Note the slight discrepancy: for HMPAO and ECD, the EANM dosage card indicates a minimum dose of 100 MBq.

Reference to national regulation guidelines, if available, should be considered.

Acquisition Protocol

- Collimator: parallel-hole, low energy, high resolution.
- Position: supine.

Using a brain-specific perfusion tracer

- Dynamic study: anterior and posterior projections, 2 s/frame for a total of 2 min, matrix 128 x 128.
- Static images: start immediately after dynamic images; anterior, posterior, and two lateral planar views, duration of acquisition 300 s, matrix 256 × 256.
- SPECT: performed at 20–30 min after tracer injection, 25 s/step, 64 steps/head (for dual-head cameras), matrix 128 × 128.
- SPECT/CT is recommended in cases of skull and scalp trauma or deformities.

Using a non-specific cerebral perfusion tracer

- Dynamic study: anterior and posterior, 2 s/frame for a total of 2 min, matrix 128 × 128.
- Static images: starting immediately after dynamic images; anterior, posterior, and two lateral views, duration of acquisition 300 s, matrix 256 × 256.

Study Interpretation [3]

- Dynamic images are assessed while adjusting the window settings. Activity in the distribution of the anterior, middle, and posterior cerebral arteries and sagittal and lateral sinuses is evaluated.
- The study should be assessed for the presence or absence of:
 - Cerebral perfusion on dynamic images.
 - Filling of the cerebral sinuses on planar images.
 - Uptake of the tracer in cerebral structures on SPECT.

In cases of brain death:

- Arterial phase dynamic flow images show tracer distribution in the carotid arteries up to the base of the skull and no arterial blush over the cerebral hemispheres.
- Venous phase dynamic flow images show no activity in the venous sinuses although faint activity might be noted on late images.
- Static images confirm the absence of activity in the venous sinuses.
- SPECT images show the total absence of activity in any part of the brain.

Correlative Imaging

- Correlate with radiography for skull fracture.
- CT and MRI may show evidence of anoxic brain injury with/without uncal herniation.

Red Flags

- Use a line that is working well and try to give a good compact bolus.
- Central lines are often used for administration of vasoactive agents and electrolytes. Consult with the referring physician or nurse if it is safe to inject a bolus into that line.
- A peripheral line should be only used for tracer administration when a central line is unavailable.
- Do not inject through an intravenous (IV) line placed in the scalp.
- A tourniquet should not be placed prior to injection of non-specific tracers in cases of skull and scalp injuries.
- Make sure that the entire head is in the field-of-view (FOV). Use a marker to confirm before giving the injection.
- Static images must be performed immediately after the dynamic images. Diffusion of activity from the scalp through the epiploic veins into necrotic brain tissue and cerebral sinuses may occur.
- If the patient is hemodynamically unstable the SPECT may be performed earlier than the 20–30 min specified in the study protocol.
- If there is a history of traumatic brain injury with skull fractures and swelling, the study

may be difficult to interpret due to soft tissue accumulation of Pertechnetate. Using a brain-specific perfusion tracer and SPECT/CT will improve diagnostic certainty.

- Even the slightest tracer activity on SPECT in any part of the brain precludes the diagnosis of brain death. If noted, a repeat brain death scan should be performed within a few days. Most repeat scans will show disappearance of the residual tracer activity.

Take Home Messages

- The final impression of the study should state that either there is no evidence or that it shows evidence of brain perfusion.
- Brain-specific perfusion tracers can benefit from a SPECT or SPECT/CT acquisition which should be carefully evaluated.
- Careful inspection of SPECT images should ensure that there is no tracer uptake in cerebral structures, in particular, infratentorial activity.
- Brain death evaluation with non-specific tracers should only be used if brain-specific tracers are unavailable. DTPA is preferable to Pertechnetate.
- SPECT/CT can distinguish uptake in the brain from increased activity related to hyperemia in overlying structures.

Representative Case Examples

Case 2.1. Brain Death (Fig. 2.1)

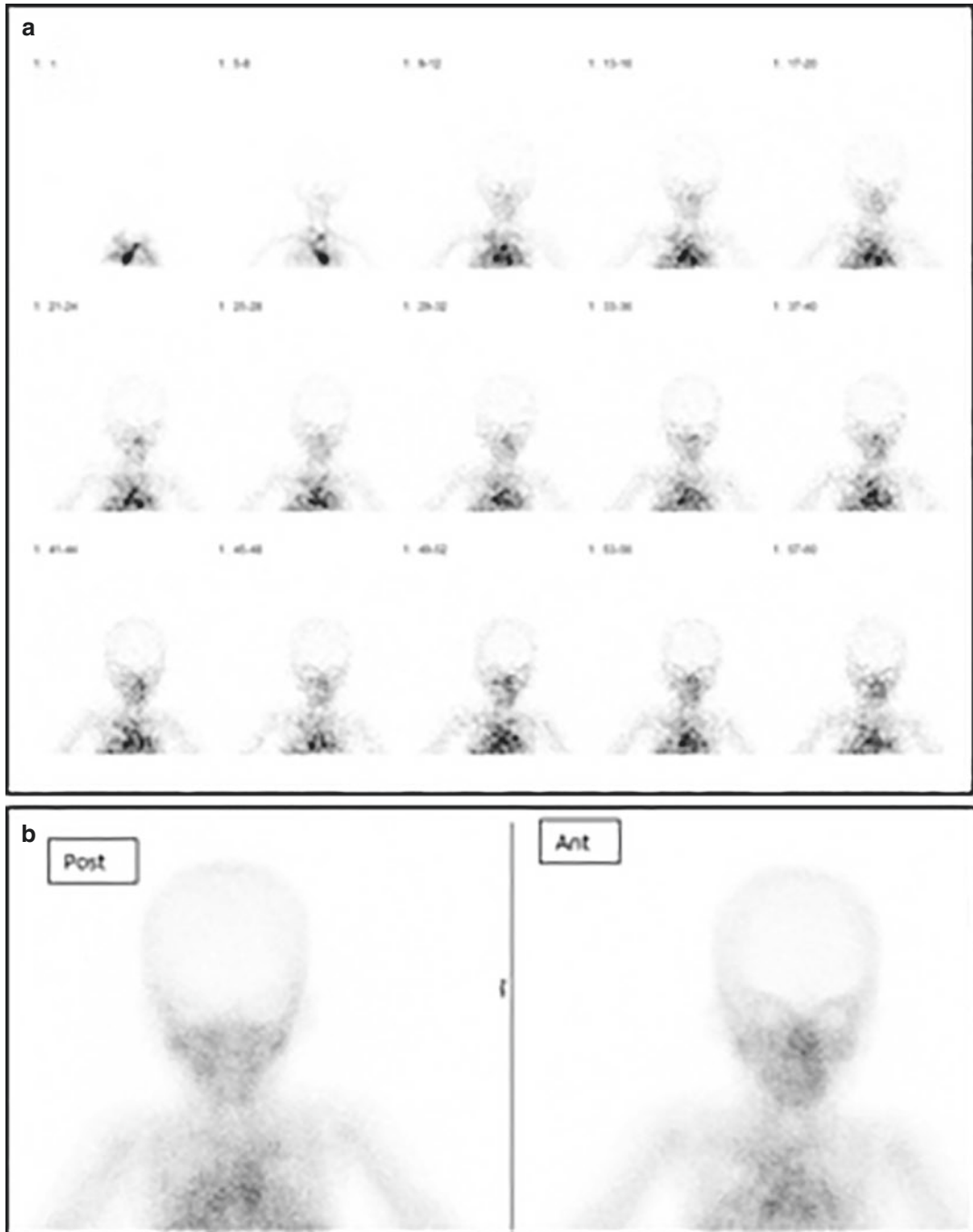


Fig. 2.1 History: A 9-month-old boy admitted to the hospital with hypovolemic shock due to gastroenteritis had a cardiopulmonary arrest 2 days before the study was requested. The brain death study was performed using Perthechnetate. Study report: There is no perfusion to the

cerebrum on the dynamic images (a). There is no filling of the cerebral sinuses on the static images (b). Impression: The study shows a lack of perfusion to the entire brain confirming the clinical diagnosis of brain death

Case 2.2. Equivocal Brain Scan in a Patient with Suspected Brain Death (Figs. 2.2 and 2.3)

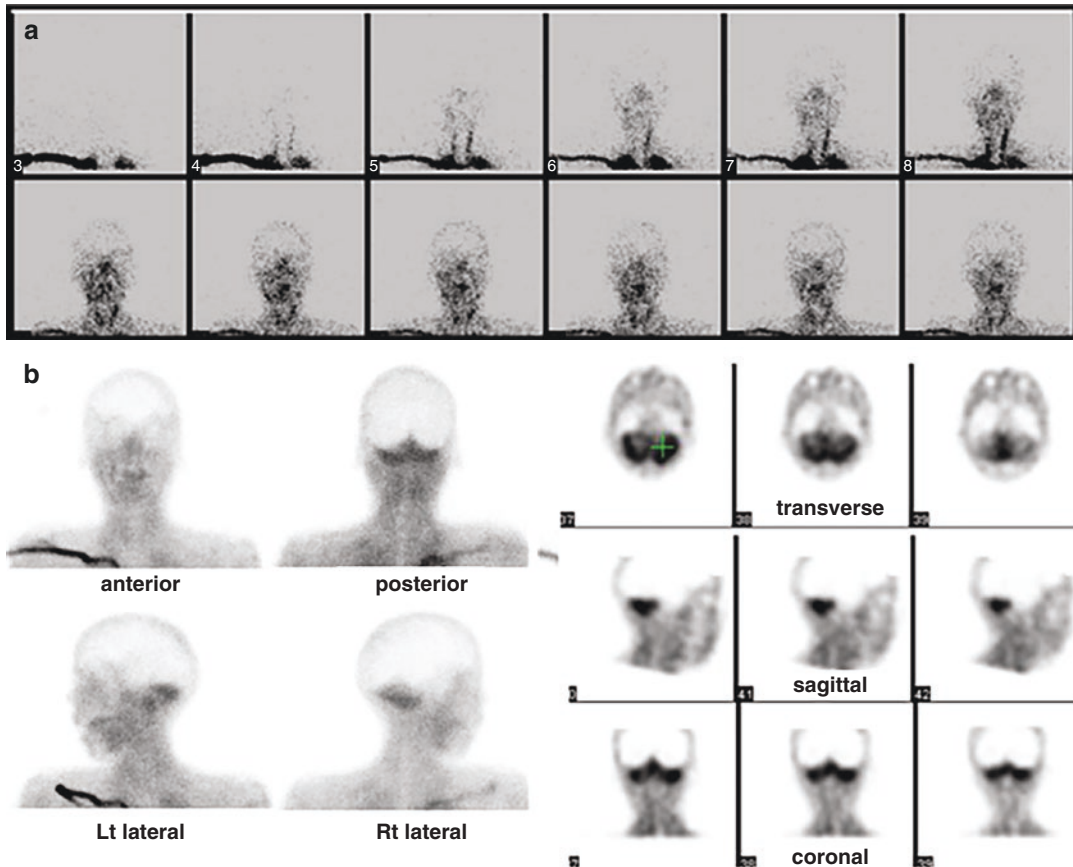


Fig. 2.2 History: A 14-year-old boy with congenital heart disease underwent cardiac surgery and had a sudden postoperative cardiovascular collapse. His pupils were dilated. He lost all brain stem reflexes. Brain CT demonstrated massive infarction of the entire left hemisphere and the right frontal lobe. His clinical status suggested brain death. A brain scan was performed following administration of ECD. Study report: Anterior radionuclide angiography (a) showed tracer distribution in the carotid arteries up to the base of the skull but no arterial blush in

the brain. Increased tracer uptake in the facial soft tissues was noted especially in the nasal area (“hot nose sign”). Early static images (b) showed no tracer localization in the brain parenchyma, but the posterior and lateral views showed uptake in the cerebellum, further confirmed on SPECT (c). Impression: Brain death could not be confirmed because of the residual perfusion visualized in the cerebellum. The patient’s neurological status did not change, and a repeat study was obtained 5 days later

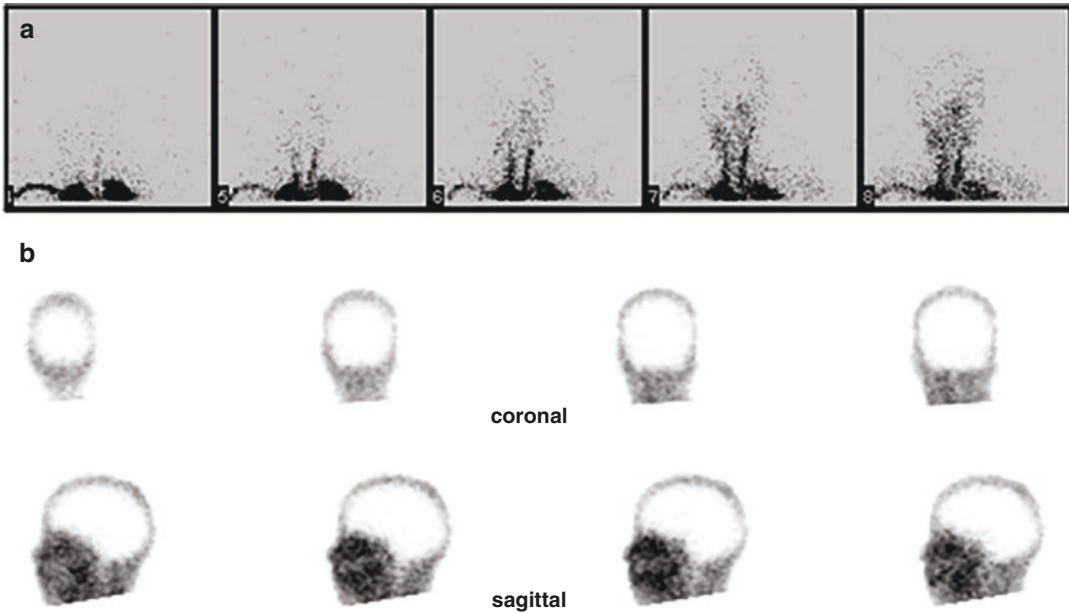


Fig. 2.3 History: Repeat brain scan in a 14-year-old boy with suspected brain death and an equivocal study performed 5 days before. Study report: Anterior dynamic study (a) showed no cerebral perfusion. SPECT (b)

showed no uptake in the cerebrum or cerebellum. Impression: The study confirms the clinical diagnosis of brain death

2.2 Drug-Resistant Epilepsy— Ictal and Interictal Brain Perfusion Spect

Clinical Indications

- To help localize the epileptogenic focus in children with drug-resistant epilepsy considered for surgical excision in patients who have a normal or inconclusive MRI or with discordant MRI findings as compared to the clinical and video-telemetry results.
 - There must be a good pre-test likelihood of unifocal seizures (or at least a dominant seizure).
 - The seizure should last long enough to be captured by the tracer injection (seizures lasting less than 20 s are unlikely to be captured

with an ictal SPECT, although the epileptogenic focus can still show prominent tracer uptake for some time after seizure ends).

Pre-exam Information

- The need for general anesthesia or sedation is evaluated for an individual patient.
- If general anesthesia is required, a slot should be available for both the morning and the afternoon scanning sessions, as the time when the patient fits is unknown.
- Some flexibility in the appointment bookings of the day is essential as the time when the child is going to fit is unknown and therefore the ictal scan may have to be slotted in between other pre-booked examinations.

Study Protocol for Brain Perfusion Imaging in Epilepsy [4–7]

Patient Preparation

- Ensure that the child has been admitted to the telemetry ward for at least 1–2 days to carefully study the EEG features of the seizures with the view to identify the characteristic seizure that has to be captured with the ictal tracer injection.
- Ensure that the neurologist looking after the child has decided whether it is necessary to reduce the dose of the anti-epileptic medications or to stop them altogether for one of 2 days prior to the ictal injection.
- Continuous EEG monitoring should start at least 2 h before the tracer injection and continue up to 15 min after the injection, to make sure that no seizures have occurred during the period of time leading up to tracer injection.
- If the child is going to be anesthetized for the interictal study, this will happen after the tracer injection.

Radiopharmaceuticals, Administered Activity, and Mode of Delivery

Radiopharmaceuticals

- [^{99m}Tc]ECD (ECD) is the radiopharmaceutical of choice if there is no radiopharmacy on site since it is more stable than the alternative [^{99m}Tc]HMPAO.
- [^{99m}Tc]HMPAO (HMPAO) can be safely used for the ictal perfusion SPECT if there is a radiopharmacy on site.
- [¹⁸F]Fluorodeoxyglucose (FDG) is often used for interictal studies.

Activity

- ECD and HMPAO: 7.4–11.1 MBq/kg (0.2–0.3 mCi/Kg), minimum 111–185 MBq (3–5 mCi).

- There are some differences between the North American consensus recommendations and the EANM dosage card as highlighted in the Image Gently website.
 - The North American consensus recommends 11.1 MBq (0.3 mCi/Kg), minimum dose of 185 MBq (5 mCi), and maximum of 740 MBq (20 mCi).
 - The EANM recommends a minimum dose of 100 MBq (2.7 mCi).
- FDG: 3.7 MBq/kg (0.10 mCi/kg), minimal dose: 14 MBq (0.37 mCi).

Refer to the EANM pediatric dosage card and to the North American consensus guidelines on radiopharmaceutical administration in children in the respective EANM and SNMMI and image gently web sites.

Reference to national regulation guidelines, if available, should be considered.

Mode of Delivery

For the ictal SPECT study

- When the characteristic seizure arises, the tracer has to be injected as soon as possible (within seconds) after seizure onset.
- After the seizure has come to an end, the nuclear medicine department must be notified as soon as possible, so that they can alert the anesthesiologists (if the scan requires general anesthesia) and prepare the gamma camera for the ictal SPECT scan.

For the interictal SPECT study

- There should be at least a 48-h interval after the ictal scan.
- The tracer should be injected in the Nuclear Medicine department in a quiet room with dim lights.
- A cannula must be placed at least 15 min prior to tracer injection.

- The child is instructed not to speak, read, or move for at least 5 min prior and up to 5 min after the injection.
- Acquisition should start at least 45 min after the injection of ECD or 40–90 min after the injection of HMPAO.

Acquisition Protocol

Patient positioning:

- Supine with head as far up into the headrest as possible and shoulders as low as possible.
- This could be aided by getting the patient to lay on a sheet that is pulled down over the shoulders and secured with a Velcro strap and the use of sponges or rolled-up pillowcases slotted on either side between the patient's head and the headrest.
- The patient needs to be as high as possible in the headrest to enable visualization of the back of the brain. Put the chin toward the chest to ensure that the entire cerebellum is included in the scan.

Acquisition parameters for SPECT:

- Collimator: low-energy, high or ultra-high resolution.
- Fan-beam collimator, if available, is preferred over a parallel-hole collimator.
- SPECT parameters:
 - For triple head camera: 120 steps, 40 steps/head, 20–25 secs/step.
 - For dual-head camera: 120 steps, 60 steps/head, 30 secs/step.
 - Acquisition mode: step-and-shoot is more frequently used. Continuous mode acquisition may provide shorter scan times and improve patient comfort.
 - Matrix 128 × 128.
 - Zoom: the acquisition pixel size should be one-third to one-half of the expected resolution.

Study Interpretation

- The clinical and EEG details must be known.
- A previously performed MRI using specific sequences for epilepsy should be available for comparison.
- The telemetry report of the SPECT seizure must be available.
- It is critical to have knowledge of the following information and record the timing (hh:mm:ss) where appropriate:
 - The exact time of EEG and clinical onset of the seizure.
 - The exact time of the tracer injection: start of the injection, end of the injection, end of flushing of the tracer with saline.
 - The exact time the seizure ends.
 - At least the time between flushing of tracer and seizure end (should be >15 secs).
 - EEG features at the time of seizure onset and immediately afterward.

Correlative Imaging [8–12]

- A previously performed MRI using specific sequences for epilepsy should be available for comparison and may show flair abnormality.
- Correlation with arterial spin labelling (ASL) sequences may be helpful to increase confidence in PET interpretation.

Red Flags

- It is of the utmost importance to administer the ictal tracer injection as early as possible after seizure onset. However, what seemed to be a seizure in its early onset may not evolve into a full seizure and, if the tracer has been injected too soon, it will capture an event that does not declare itself as a real seizure.
- The seizure ideally should not generalize into a tonic-clonic seizure shortly after tracer injection. If it does, when the tracer reaches the brain the electrical discharge will have propagated, resulting in several non-specific areas of hyperperfusion and therefore a lower likeli-

hood of identifying the epileptogenic focus as an area of predominant hyperperfusion.

- If the syringe with HMPAO (with stabilizer) has been in the telemetry ward for over 3 h without having been injected, it will be significantly dissociated between free Per technetate and HMPAO, with high uptake of free Per technetate in the salivary glands and with less uptake of HMPAO in the brain, resulting in poor quality images. If the child did not have a seizure within 3 h of the delivery of the syringe with HMPAO to the telemetry ward, another syringe with the tracer in it should be prepared and sent to the ward, and the previous unused syringe discarded.
- It is critical to have knowledge of the following pieces of information:
 - The time between the end of flushing and end of seizure: if this is shorter than 15 s the ictal SPECT may fail to capture the focus.
 - If the seizure lasts less than 15–20 s, it may be difficult to capture with an ictal SPECT injection, since it takes about 15 s for the tracer to reach the brain after flushing with saline.
 - If the EEG findings during/immediately after the seizure can lateralize and localize the seizure focus, identify the origin of the seizure and whether it generalized shortly after onset.
- If a fan-beam collimator is available, make sure that the whole head (including the cerebellum) is within the FOV.
- The ictal SPECT scan must be interpreted with the knowledge of the findings of an EEG performed before, during, and after the tracer injection. Ictal SPECT findings, considered in isolation, could be seriously misleading.
- The interictal SPECT study should also be performed always and correlated with the ictal study.
- If the patient is not under general anesthesia, communication with the patient via squeezing

the hand of an accompanying person may enable them to perform the study without risk of head movement during the scan.

Take Home Messages

- This test should be done in centers with a specialized epilepsy surgery program.
- The entire epilepsy team should be on site when the ictal study is performed; the results should be discussed during the multidisciplinary epilepsy team meeting.
- Medical personnel trained and authorized in injection of radiopharmaceuticals must be dedicated to the child on the day of the ictal SPECT scan (the injection of the radiotracer occurs on the ward in a dedicated EEG-video-telemetry room).
- The epilepsy team may reduce or stop anti-epilepsy medications prior to the ictal SPECT to induce the onset of the characteristic seizure.
- Within the telemetry ward, a single room for the child is necessary. This room becomes a controlled area once the radiopharmaceutical is brought in.
- Excellent communication between the telemetry ward, the nuclear medicine department, and the anesthesiologists is essential to coordinate the start of the SPECT images acquisition.
- An interictal SPECT scan in isolation is an insufficient test in the evaluation of a child with drug-resistant epilepsy. An FDG PET interictal study can be performed instead of an interictal SPECT study.
- Co-registration of the ictal SPECT and the interictal SPECT with the MRI is state-of-the-art and increases the diagnostic accuracy of each modality in the search for a much better of the epileptic focus. EEG monitoring during injection of FDG tracer is important to confirm an interictal state.

Representative Case Examples

Case 2.3. Right Epileptogenic Focus (Fig. 2.4)

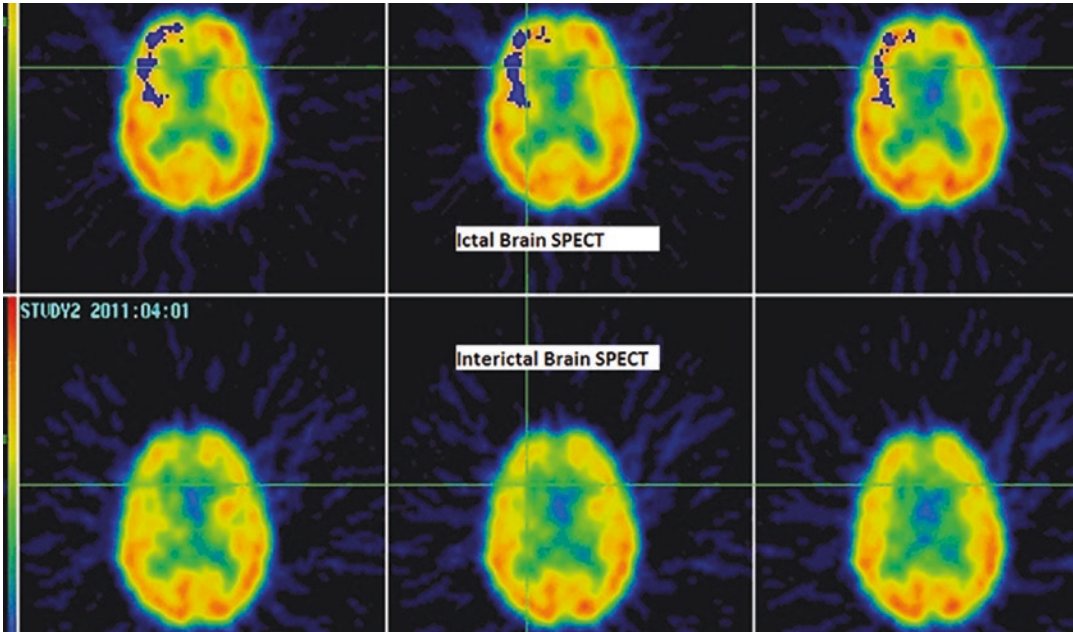


Fig. 2.4 History: A 1-year-old developmentally delayed boy, with asymmetric infantile spasms and focal seizures refractory to anti-epileptic medications, had a negative MRI. EEG showed continuous abnormalities in the right hemisphere, possibly the right anterior quadrant. For the ictal SPECT, ECD was administered during a typical cluster of spasms, with EEG changes lasting approximately 6 min. The injection was given 2:39 min after clinical seizure onset. The seizures continued for 79 s after flushing of the tracer. The EEG at the time of injection showed an extensive area of abnormality suggestive of seizures from the right hemisphere, possibly right anterior quadrant. Study report: On the ictal study (upper row) there is

increased tracer uptake in the right anterior frontal region. In the interictal study (lower row) performed 2 days later there is slightly reduced tracer uptake in the right anterior frontal region. Subtraction of interictal from ictal SPECT images (blue area upper row) shows a significant difference in radioactive counts in the anterior region of the right hemisphere, which correlates with EEG findings and clinical semiology. Impression: The findings suggest the presence of an epileptogenic focus in the anterior quadrant of the right hemisphere in the right frontal region. The patient was referred for invasive monitoring for further consideration of a possible right frontal resection

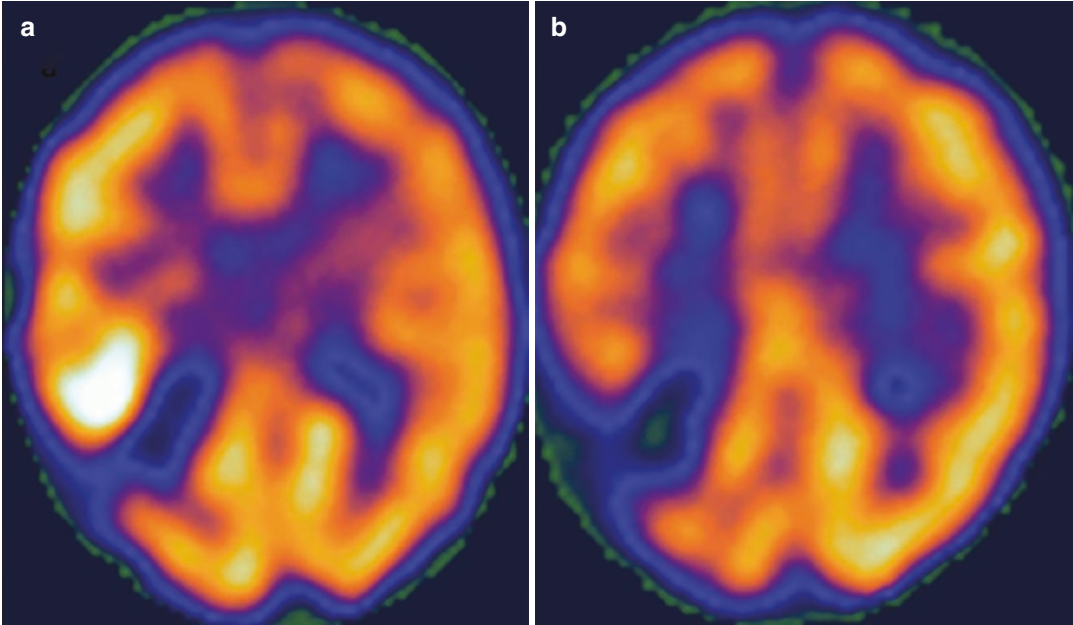
Case 2.4. Residual Right Epileptogenic Focus (Fig. 2.5)

Fig. 2.5 History: A child who had a right posterior parietal resection for focal cortical dysplasia continued to present with seizures after surgery. Study report: An ictal ECD SPECT (**a**) shows highly increased tracer uptake in the right parietal region, adjacent to the resection margin. This same area shows reduced uptake in the interictal

study (**b**). Impression: The findings suggest a residual epileptogenic focus after surgical resection. Review of MRI with specific sequences for epilepsy in this area showed changes compatible with residual focal cortical dysplasia. The child was referred for further surgery

Case 2.5. Right Focal Cortical Dysplasia
(Fig. 2.6)

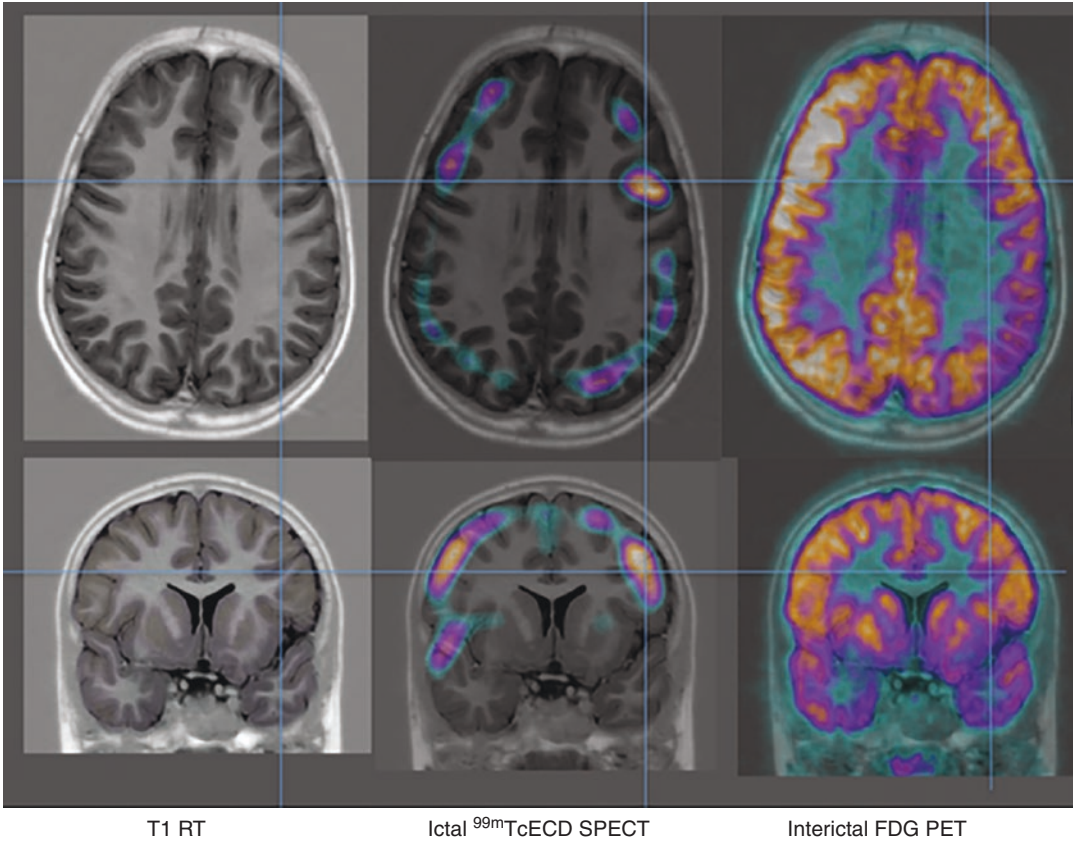


Fig. 2.6 History: An 11-year-old boy had refractory partial and complex partial seizures, localized on EEG to the left frontal lobe. Study report: MRI showed a possible area of focal cortical dysplasia in the left frontal lobe (crosshairs MRI, left column). Ictal SPECT co-registered with MRI (center column) following injection of ECD shows focally increased tracer uptake in the left frontal

area. This was confirmed in the interictal co-registered FDG PET/MRI study (right column). Impression: The study confirms an epileptogenic focus originating from the left focal frontal cortical dysplasia. Surgical resection was performed, and the patient is seizure-free at a 2-year follow-up

2.3 Cerebro-Spinal Shunt Patency Studies

Clinical Indications

- Patients with hydrocephalus with a CSF shunt who have clinical symptoms such as headache and vomiting, or an imaging suspicion of a malfunctioning shunt.

Study Protocol for CSF Shunt Patency Imaging [13–15]

Patient Preparation

- Review of medical history to determine the type of shunt (i.e., ventriculo-peritoneal, ventriculo-pleural, or lumbar-peritoneal).
- Review of the patient's CT and/or MRI to determine the site of the shunt reservoir.
- Shave the hair over the shunt reservoir.

Radiopharmaceutical, Administered Activity and Mode of Delivery

Radiopharmaceutical:

- [^{99m}Tc]DTPA (DTPA).

Activity:

- 20 MBq (0.55 mCi) in 0.1 ml volume drawn up in a tuberculin syringe. Refer to the EANM pediatric dosage card and to the North American consensus guidelines on radiopharmaceutical administration in children in the respec-

tive EANM and SNMMI and image gently web sites. Reference to national regulation guidelines, if available, should be considered.

Mode of delivery:

- Injected intrathecal or into the reservoir.

Acquisition Protocol

- Collimator: parallel-hole, low energy, high resolution.
- Position: supine.
- FOV: Head and shunt pathway (chest or abdomen depending on shunt type).
- Time of imaging: early, immediately, and at 40–90 min post-injection.
- Static image acquisition parameters: 300 s/view or 100 Kcounts, matrix 256 × 256.
- Posterior and lateral views of the head to detect reflux into the ventricles.
- Anterior static images of the entire distal length of shunt tubing following the head images (generally chest and/or abdomen). If there is no dispersion of the tracer in the abdomen, the patient is encouraged to stand up and, if possible, walk around.
- Additional, potentially required, delayed images up to 24 h of the head and chest/abdomen.
- SPECT/CT, when available can be performed to better define the presence and localization of the radiotracer uptake.
- For all images: note the time post-injection and label appropriately.

Study Interpretation

- Assess the location and type of shunt reservoir.
- Note whether CSF was readily withdrawn and sent for culture.
- Record the presence of ventricular reflux and tube activity, the time when the tracer reached the peritoneal cavity/pleura, and if there was free tracer distribution within the abdomen/pleural cavity.
- If free distribution of tracer is seen the distal end of the shunt is patent.
- If no CSF was taken from the reservoir and there is slow transit down the tube and no free distribution of activity, the shunt is most likely blocked at the ventricular end.

Correlative Imaging

- Radiography to confirm the type of shunt, i.e., ventriculo-atrial, ventriculo-pleural, or ventriculo-pelvic shunt.
- Radiographs for detection of shunt tube disruption and position of end of tube.

Red Flags

- A sterile technique should be used for drawing the dose and for the injection.
- The technologist/ radiographer of the nuclear medicine department should be trained to safely prepare the radiopharmaceutical to be injected.
- When performing intrathecal administration of radiopharmaceutical check for the purity of the compound and the activity to be injected.
- A surgeon or a specifically trained nuclear medicine physician should administer the tracer injection according to national and hospital regulations.

Take Home Messages

- The nurse/technologist assisting the doctor should press on the tube just below the injection site to induce reflux into the ventricles and thus test the patency of the proximal end.
- A sample of CSF should be taken, if possible, for cytology and culture.

Representative Case Examples

Case 2.6. Patent Shunt (Fig. 2.7)

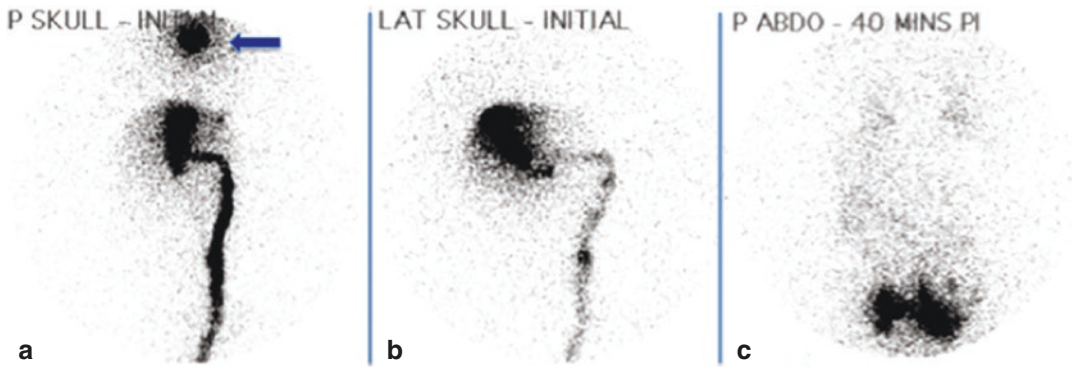


Fig. 2.7 History: A 4-year-old boy with a ventriculo-peritoneal CSF diversion shunt for congenital hydrocephalus presents with a recent headache and vomiting. MR showed mild dilatation of the ventricles with no change from the previous study. A Rickham reservoir was initially accessed aseptically, and CSF fluid was withdrawn for culture. Study report: The tracer was injected into the

Rickham reservoir (a, arrow) and passed rapidly from the ventricle into the shunt tube in the immediate post-injection images in posterior (a) and lateral (b) views. At 40 min post-injection (c) the tracer has distributed diffusely into the peritoneum. Impression: Patent ventriculo-peritoneal shunt

Case 2.7. Blocked Shunt (Fig. 2.8)

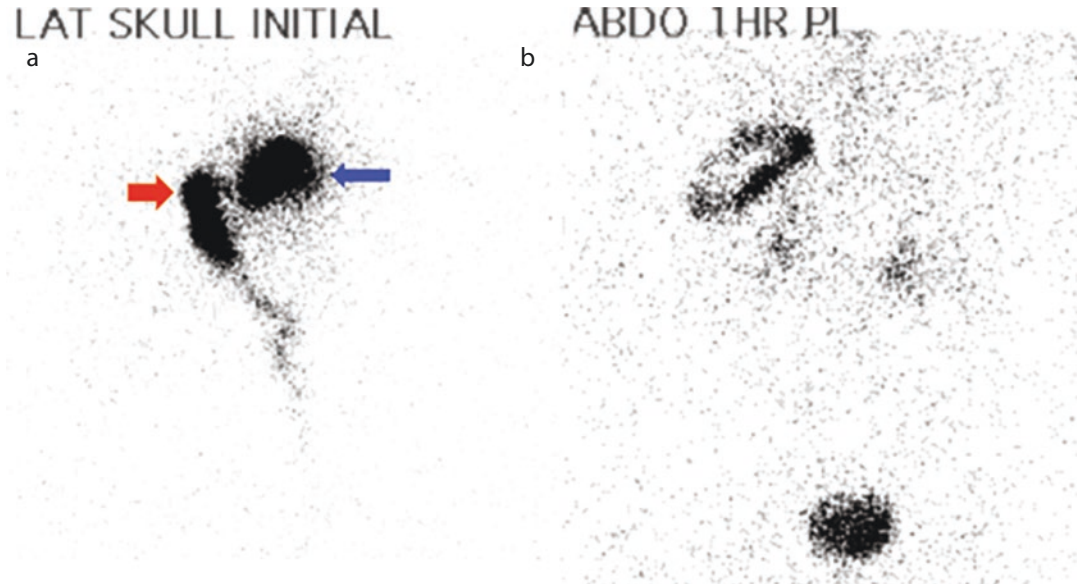


Fig. 2.8 History: A 7-year-old boy with a history of hydrocephalus secondary to a brain tumor, which had been successfully removed followed by insertion of a ventriculo-peritoneal shunt, developed lethargy and headache with occasional vomiting. MRI showed moderate dilatation of the ventricles. Study report: The tracer was injected via a Hakim reservoir (a, red arrow). The CSF appeared under increased pressure. On the immediate

post-injection image in lateral projection, the tracer flows back into the ventricle (a, blue arrow) indicating a patent proximal end. On images of the chest and abdomen performed 1 h post-injection (b) the tracer is shown to have passed slowly down the shunt tube and does not distribute into the peritoneal cavity. Mild renal excretion is seen. Impression: The findings indicate a blocked distal end of the ventriculo-peritoneal shunt

References

1. Donohoe KJ, et al. SNM practice guideline for brain death scintigraphy 2.0. *J Nucl Med Technol.* 2012;40(3):198–203.
2. American College of Radiology. ACR-ACNM-SNMMI-SPR Practice parameter for the performance of single-photon emission brain perfusion imaging (Including SPECT and SPECT/CT). 2021.
3. Zuckier LS, Kolano J. Radionuclide studies in the determination of brain death: criteria, concepts, and controversies. *Semin Nucl Med.* 2008;38(4):262–73.
4. Van Paesschen W, et al. The use of SPECT and PET in routine clinical practice in epilepsy. *Curr Opin Neurol.* 2007;20(2):194–202.
5. la Fougère C, et al. PET and SPECT in epilepsy: a critical review. *Epilepsy Behav.* 2009;15(1):50–5.
6. Juni JE, et al. Procedure guideline for brain perfusion SPECT using (99m)Tc radiopharmaceuticals 3.0. *J Nucl Med Technol.* 2009;37(3):191–5.
7. Kapucu OL, et al. EANM procedure guideline for brain perfusion SPECT using 99mTc-labelled radiopharmaceuticals, version 2. *Eur J Nucl Med Mol Imaging.* 2009;36(12):2093–102.
8. Patil S, Biassoni L, Borgwardt L. Nuclear medicine in pediatric neurology and neurosurgery: epilepsy and brain tumors. *Semin Nucl Med.* 2007;37(5):357–81.
9. Stanescu L, et al. FDG PET of the brain in pediatric patients: imaging spectrum with MR imaging correlation. *Radiographics.* 2013;33(5):1279–303.
10. Mountz JM, Patterson CM, Tamber MS. Pediatric epilepsy: neurology, functional imaging, and neurosurgery. *Semin Nucl Med.* 2017;47(2):170–87.
11. Tóth M, et al. The role of hybrid FDG-PET/MRI on decision-making in presurgical evaluation of drug-resistant epilepsy. *BMC Neurol.* 2021;21(1):363.

12. Khalaf AM, Nadel HR, Dahmouh HM. Simultaneously acquired MRI arterial spin-Labeling and interictal FDG-PET improves diagnosis of Pediatric temporal lobe epilepsy. *AJNR Am J Neuroradiol.* 2022;43(3):468–73.
13. Treves ST, et al. Central nervous system: the brain and cerebrospinal fluid. In: Treves ST, editor. *Pediatric nuclear medicine and molecular imaging.* Springer New York, New York, NY; 2014. p. 47–97.
14. Khalatbari H, Parisi MT. Complications of CSF shunts in Pediatrics: functional assessment with CSF shunt scintigraphy-performance and interpretation. *AJR Am J Roentgenol.* 2020;215(6):1474–89.
15. Kranz PG, et al. CSF-venous fistulas: anatomy and diagnostic imaging. *AJR Am J Roentgenol.* 2021;217(6):1418–29.

The opinions expressed in this chapter are those of the author(s) and do not necessarily reflect the views of the IAEA: International Atomic Energy Agency, its Board of Directors, or the countries they represent.

Open Access This chapter is licensed under the terms of the Creative Commons Attribution 3.0 IGO license (<http://creativecommons.org/licenses/by/3.0/igo/>), which permits use, sharing, adaptation, distribution and reproduction in any medium or format, as long as you give appropriate credit to the IAEA: International Atomic Energy Agency, provide a link to the Creative Commons license and indicate if changes were made.

Any dispute related to the use of the works of the IAEA: International Atomic Energy Agency that cannot be settled amicably shall be submitted to arbitration pursuant to the UNCITRAL rules. The use of the IAEA: International Atomic Energy Agency's name for any purpose other than for attribution, and the use of the IAEA: International Atomic Energy Agency's logo, shall be subject to a separate written license agreement between the IAEA: International Atomic Energy Agency and the user and is not authorized as part of this CC-IGO license. Note that the link provided above includes additional terms and conditions of the license.

The images or other third party material in this chapter are included in the chapter's Creative Commons license, unless indicated otherwise in a credit line to the material. If material is not included in the chapter's Creative Commons license and your intended use is not permitted by statutory regulation or exceeds the permitted use, you will need to obtain permission directly from the copyright holder.



Pietro Zucchetta and Ora Israel

3.1 First Pass Study

Clinical Indications [1, 2]

- Evaluation and quantification of cardiac left-to-right shunts
- To determine cardiac functional parameters such as LVEF in children with:
 - Atrial septal defect
 - Ventricular septal defect
 - Truncus arteriosus
 - Patent ductus arteriosus
 - Complete atrio-ventricular canal
 - Aorto-pulmonary collaterals

P. Zucchetta (✉)
Nuclear Medicine Unit, Department of Medicine,
Padova University Hospital, Padova, Italy
e-mail: pietro.zucchetta@unipd.it

O. Israel
Rappaport Faculty of Medicine, Technion, Haifa,
Israel

Study Protocol for First Pass Studies [3] Radiopharmaceutical, Activity and Mode of Delivery

Radiopharmaceuticals:

One of the following can be used:

- [^{99m}Tc]pertechnetate (Pertechnetate). In this case, premedication with perchlorate is advised to avoid unnecessary thyroid uptake.
- [^{99m}Tc]diethylene-triamine-pentaacetate (DTPA).
- [^{99m}Tc]sestamibi (MIBI) or [^{99m}Tc]Tetrofosmin. In this case, myocardial perfusion can be assessed after first pass acquisition.
- [^{99m}Tc]red blood cells (RBCs)—using the in vivo labelling kit has the additional benefit that an RVG can be performed after the first pass.

Activity:

- Weight-based; 9.6 MBq/kg (0.26 mCi/kg), range 80 MBq (2.16 mCi)—490 MBq (13.24 mCi).

Refer to the EANM paediatric dosage card and to the North American consensus guidelines on radiopharmaceutical

administration in children in the respective European Association of Nuclear Medicine (EANM) and Society of Nuclear Medicine and Molecular Imaging (SNMMI) and image gently web sites.

Reference to national regulation guidelines, if available, should be considered.

Delivery:

Injection technique:

- Arm used for injection is extended with a 90-degree angle from the body.
- Use of a central line is recommended, otherwise use the largest possible size intravenous (IV) cannula (not a butterfly needle!), placed and checked for patency before the study.
- The bolus should be small, less than 0.2 ml, with high specific activity.
- Rapid, uninterrupted, bolus injection should be followed by a rapid bolus of normal saline to flush the activity. This is best achieved using a three-way stopcock, connected to the radiotracer syringe and to a second syringe filled with saline (5–20 ml, depending on the calibre of the venous access).

Acquisition Protocol

- Collimator: low energy, high sensitivity
- Matrix 64 × 64
- Acquisition:
 - Dynamic study and anterior supine position.
 - Has to be gated if equilibrium LVEF measurements are performed in addition to evaluation of the shunt.
 - Should start a few seconds before injection, to avoid missing the first frames.
 - It is critical to center precisely the cardiac region in the field-of-view (FOV) before injecting the bolus.

FOV should extend from the supra-sternal notch to just below the xiphoid and include most lung parenchyma.

- Adequate zooming, considering the small dimensions of the cardiac cavities, particularly in younger children.
- For shunt evaluation a 2–4 frames/s rate is adequate.
- If LVEF measurements are required, a rate of at least 25 frames/s should be used for a total of 15–30 s, taking into account an early start of the acquisition.

Study Interpretation

Assessment of adequacy of bolus (Fig. 3.1)

- Quality control (QC) of the injected bolus should be the first step prior to processing.
- A ROI is placed over the superior vena cava (SVC) and a time activity curve (TAC) is generated.
- This TAC is used to check the adequacy of the bolus.
- If the bolus is adequate, the TAC shows a single peak with a full-width half maximum (FWHM) of less than 3 s.

Left-to-right shunt calculation (Fig. 3.1)

- A ROI is drawn over the lungs taking care to avoid the heart and large vessels and a TAC is generated.
- The normal pulmonary TAC shows a sharp peak, due to the transient tracer passage through the lungs followed by a smaller, wide-based peak representing the portion of the initial bolus returning to the lungs after recirculating through the systemic circulation.
- In case of a left-to-right shunt, there is persistence of tracer activity in the lungs due to premature pulmonary recirculation of the tracer through the shunt.

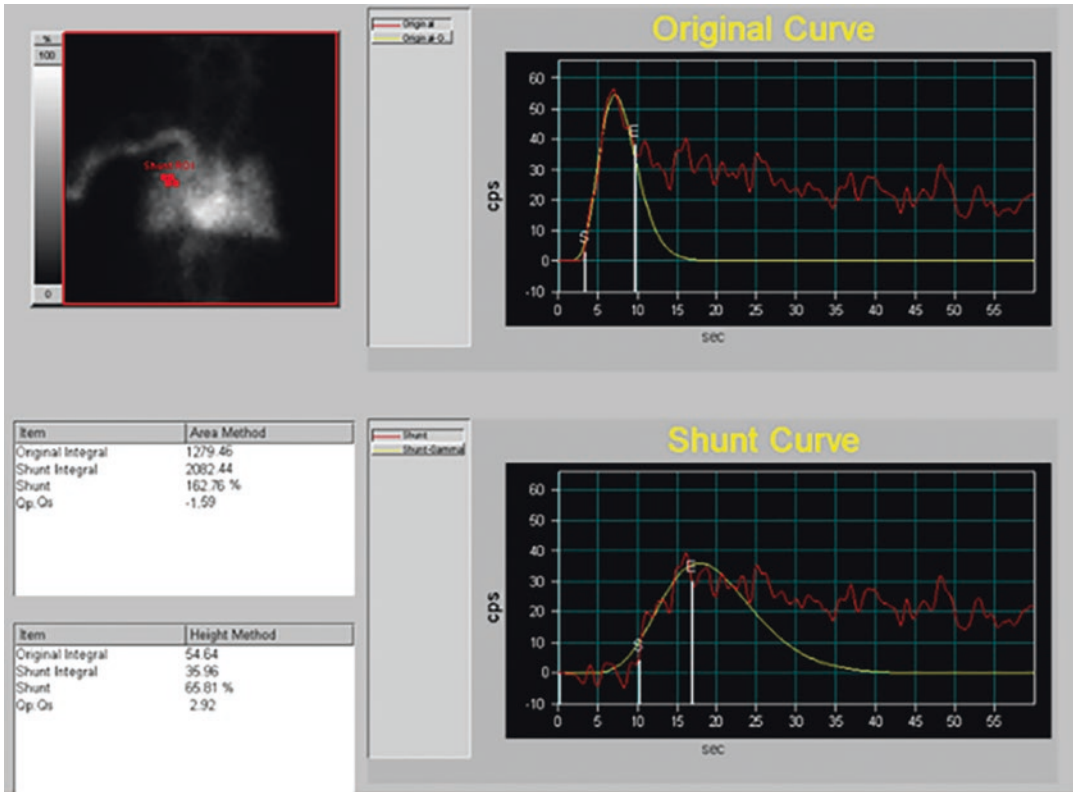


Fig. 3.1 Assessment of bolus adequacy and left-to-right shunt calculation. The square ROI depicts the SVC. The solid line represents the TAC obtained from counts measured in a ROI drawn over the lungs taking care to avoid the heart and large vessels. The broken line represents the area under the gamma-variate lung fitted curve. No addi-

tional curve is seen early after the lung curve to suggest premature recirculation related to a left-to-right shunt. The calculated Qp/Qs is 1.59. There is no evidence for a physiologically significant left-to-right shunt

- The magnitude of the persistent pulmonary activity is proportional to the size of the shunt.
- In moderate-to-severe shunts, there is poor visualization of the left side of the heart and the aorta.
- The TAC is further fitted with a gamma-variate curve. The area under the gamma-variate lung fitted curve is calculated. The value obtained is denoted as Qp.
- The gamma-variate fitted curve is then subtracted from the original lung curve in order to get the recirculation shunt curve.
- A second gamma-variate fit is performed on the recirculation curve and the area under the new fitted curve is denoted as Qshunt.
- The systemic flow denoted as Qs is calculated as the difference between Qp and Qshunt and is consistent with the recirculation after the first pass through the body.
- The ratio between the Qp/Qs is considered normal if below 1.4–1.6.
- The report should include a description of the passage of tracer through the cardiac right atrium, right ventricle, lungs, left atrium and ventricle and systemic circulation.

Correlative Imaging

- Trans-esophageal echocardiography and ultrasound (US) bubble study may be used to identify shunt.
- Magnetic resonance angiography (MRA) and CT angiography (CTA) may also show the presence of a left-to-right shunt.
- Echocardiography and MRI have replaced in most instances this modality for calculations of the left and right ventricular EF.

Red Flags

- Meticulous injection and imaging technique and data processing are mandatory to obtain reliable and reproducible results.
- Avoid injecting whilst the patient is crying because rapid changes in intrathoracic pressure will likely cause bolus fragmentation and render the study inadequate.
- QC of the injected bolus should be the first step prior to processing. A fragmented or spread bolus will introduce errors in the computation of the first pass study.
- If the bolus is inadequate, a second study can be performed with approximately twice the

initial activity. This applies only to studies performed with DTPA and Perchnetate. If both injections fail, the study should be postponed to another day.

- The ROI drawn over the lungs should avoid the heart and large vessels.

Take Home Messages

- Anterior supine position offers the best spatial resolution since the detector is at a minimum distance from the heart. Left anterior oblique (LAO) view gives the best separation between LV and right ventricle (RV) and is preferred if evaluation of ventricular function is required. Right anterior oblique (RAO) view offers the best separation between the right atrium and RV.
- Left-to-right shunts mostly involve the atrial and/or ventricular septa.
- The first pass study is a sensitive technique to detect the presence of a left-to-right shunt and to quantify the magnitude of the shunt by calculating the ratio between the pulmonary and systemic circulations (Q_p/Q_s).

Representative Case Examples

Case 3.1. Normal First Pass Study, Exclusion of Left-to-Right Shunt (Fig. 3.2)

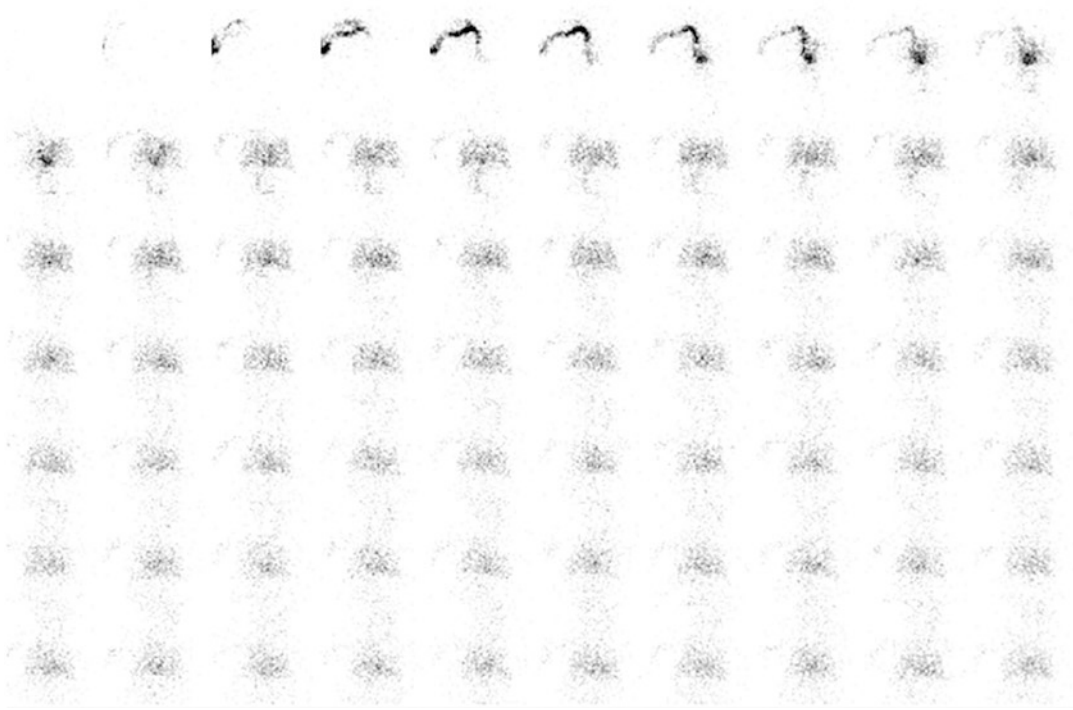


Fig. 3.2 History: The study was requested to exclude a left-to-right cardiac shunt. Study report: Dynamic images demonstrate sequential arrival of activity into the superior vena cava, the right side of heart, pulmonary arteries,

lungs, pulmonary veins and the left side of heart. Impression: Normal study. No left-to-right shunt was detected

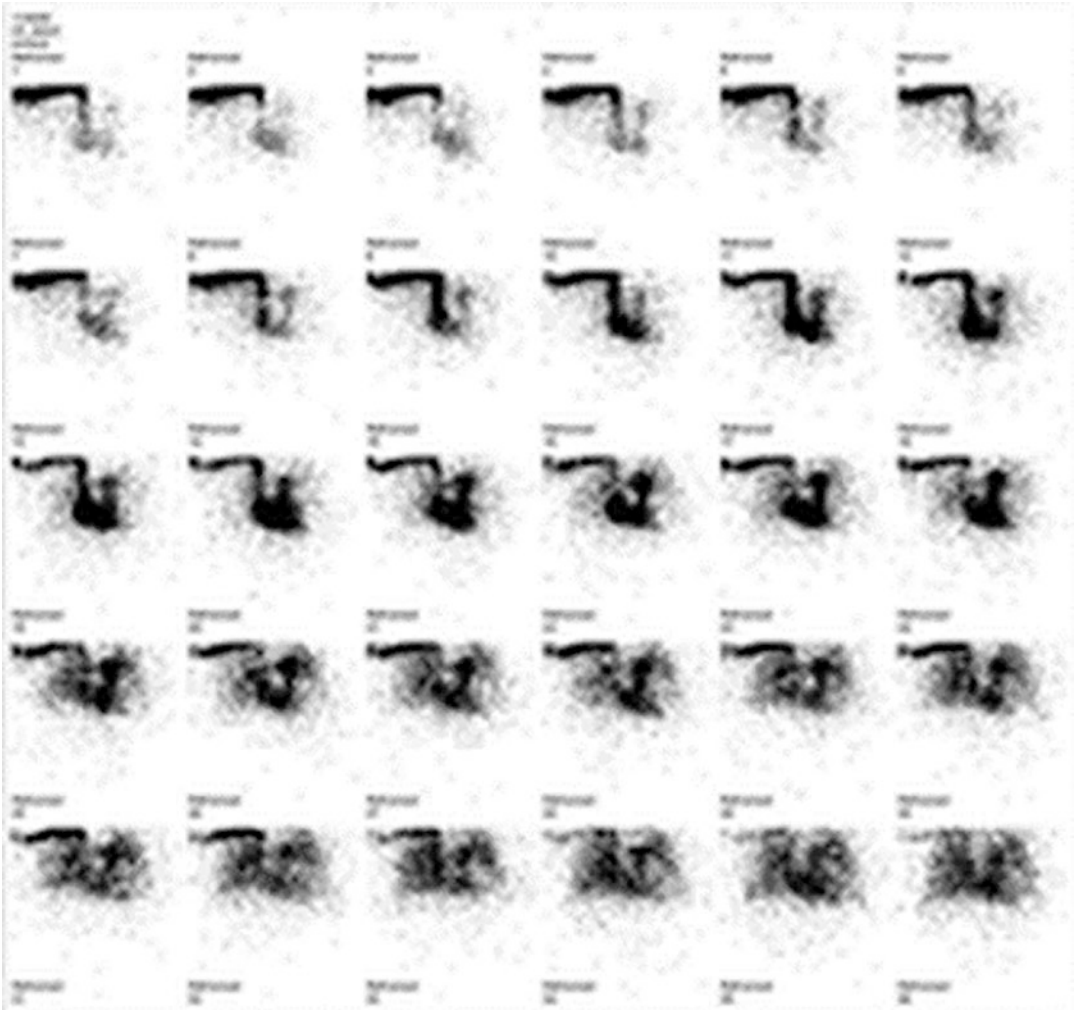
Case 3.2. Left-to-Right Shunt (Fig. 3.3)

Fig. 3.3 History: A child with a heart murmur was detected on routine stethoscope auscultation. Study report: Dynamic images show a sharp bolus travelling via the superior vena cava into the RV and the lungs. There is

persisting tracer activity within the lungs due to premature recirculation through the left-to-right shunt, as well as in the LV and systemic circulation. Impression: Left-to-right shunt

3.2 Myocardial Perfusion Scintigraphy

Clinical Indications [4]

- Coronary malformations.
- Post-surgical coronary abnormalities (i.e., arterial switch in transposition of great arteries).
- Kawasaki disease.
- Arteritis (Takayasu).
- Cardiomyopathy.
- Chest pain (not a common indication in pediatrics population).
- Chest trauma.

Study Protocol for Myocardial Perfusion Studies [5, 6]

Patient Preparation

- Knowledge of a number of factors that may influence the final interpretation of the study, such as the patient's cardiac and coronary anatomy and/or cardiac surgery history.
- Results of prior MPS studies.
- Medication—in case the patient is taking any of the below drugs and if clinically feasible stop.
 - Vasodilators for 24 h.
 - Calcium antagonists for 2 days.
 - Beta-blockers for 3 days.
 - Theophylline for 24 days (particularly for adenosine test).
- Avoid caffeine for 24 hours.
- Sedation is often required up to the age of 5–6 years.

Stress Testing [7]

- *Physical stress* (ergometer or treadmill): should be performed when possible.
- *Pharmacological stress*: is preferred in younger children and whenever patients

and/or parents/caregivers cannot offer the necessary compliance.

- Adenosine is preferred over dipyridamole because it has a shorter biological half-life (around 10 s).
- For the use of adenosine or dipyridamole as a cardiac stressor reference to national regulation guidelines, if available, should be considered.
- Pump infusion is desirable for adenosine intravenous administration (0.14 mg/kg/min for 6 min).
- Only scarce literature is available for the paediatric use of regadenoson, but data are promising [8].
- A second venous access should be used for the infusion of the tracer. If it is not feasible, a two-way stopcock positioned directly on the cannula is the best solution to inject quickly, stopping the adenosine infusion for a few seconds and avoiding an adenosine bolus.

Radiopharmaceutical, Administration Activity, Mode of Delivery

Radiopharmaceuticals:

- [^{99m}Tc]SestaMIBI (MIBI)
- [^{99m}Tc]Tetrofosmin.

Activity:

- Depends heavily on the sensitivity of the available camera.
- As a rule of thumb, a minimum recommended activity of 80 MBq (2.2 mCi) is considered acceptable, but lower activities are possible (and desirable).

Refer to the EANM paediatric dosage card and to the North American consensus guidelines on radiopharmaceutical administration in children in the respective European Association of Nuclear Medicine (EANM) and Society of

Nuclear Medicine and Molecular Imaging (SNMMI) and image gently web sites.

Reference to national regulation guidelines, if available, should be considered.

Acquisition Protocol

- Camera: a dual-heads camera in 90 degrees configuration is preferred.
- Collimators: low-energy high-resolution or dedicated cardiac collimators. Consider ultra-high resolution (UHR) collimators in newborns and younger infants.
- Position: supine, arms above head.
- Orbit: 180°, from RAO to left posterior oblique (LPO), keep the orbit as tight as possible.
- 60 projections, 128 × 128 matrix, 25–30 s/frame, depending on camera sensitivity.
- Adequate acquisition zooming.
- Gated SPECT should be acquired whenever possible.

Study Interpretation

- Evaluation of raw images in cine mode to determine the presence of potential sources of image artefact and the distribution of extracardiac tracer activity.
- Check proper orientation of the post-stress and rest images.
- Assess whether myocardial perfusion defects are present and if so determine their:
 - Extent/size: small, medium, large.
 - Severity: mild, moderate, severe.
 - Presence and extent of reversibility: reversible or irreversible.
 - Location: based on segment model [9, 10].

Red Flags

- Requirements for performing stress tests: continuous ECG monitoring, blood pressure measurements and pediatric resuscitation equipment.
- Physical stress is difficult to perform in younger children, for the lack of suitable equipment and because of the short attention span.
- When performing physical stress it can be difficult to reach the target heart rate in some congenital situations, due to sinus node dysfunction (e.g. Fontan circulation) or pharmacological interference.
- Adequate zooming during acquisition is essential to get enough detail in the images.
- Reconstruction parameters (e.g. filter) have to be adapted to the small size of the heart.
- Normal myocardial perfusion patterns may differ widely from normal distribution as seen in adult ischemic heart disease, such as visualization of the RV, a different ventricular septum morphology.
- Normalcy databases for quantitative perfusion scoring are not validated for pediatric patients.
- In order to avoid unnecessary sedation and reduce radiation exposure, it is advisable to perform stress testing first. In case of a negative stress study, the rest study is omitted.
- Reporting functional data obtained from the gated images can be helpful, but requires careful quality control before processing, because of the difficult delineation of the myocardial profile of the small heart chambers.

Take Home Messages

- Acquisition techniques must be adapted to the clinical and anatomical situation.
- Ergometer or treadmill stressing should be performed when possible. It is more physiologic and can offer useful additional information such as exercise capacity or symptoms.

- Pharmacological stress is often preferred in young children.
- Pump infusion is desirable for adenosine intravenous administration to achieve a constant infusion rate.
- Adenosine with a shorter biological half-life, around 10 s, is preferred over dipyridamole. Its side effects are easily managed,

usually without the need for the antidote (theophylline).

Representative Case Examples

Case 3.3. Normal Myocardial Perfusion Study (Fig. 3.4)

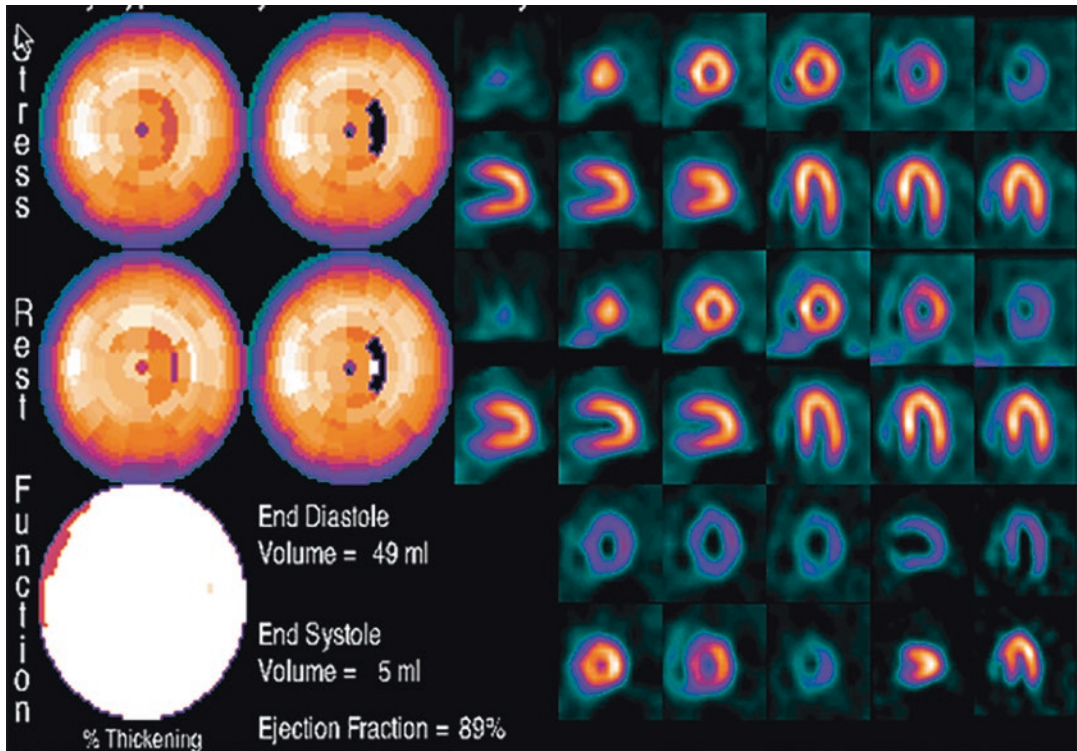


Fig. 3.4 History: Patient with Takayasu's arteritis. Study report: An exercise gated myocardial perfusion stress test was performed. Overall study quality is excellent. There is

normal myocardial perfusion at stress and rest. The LVEF is 89%. Conclusion: Normal myocardial perfusion scintigraphy

Case 3.4. Reversible Perfusion Defect in Anterior Wall (Fig. 3.5)

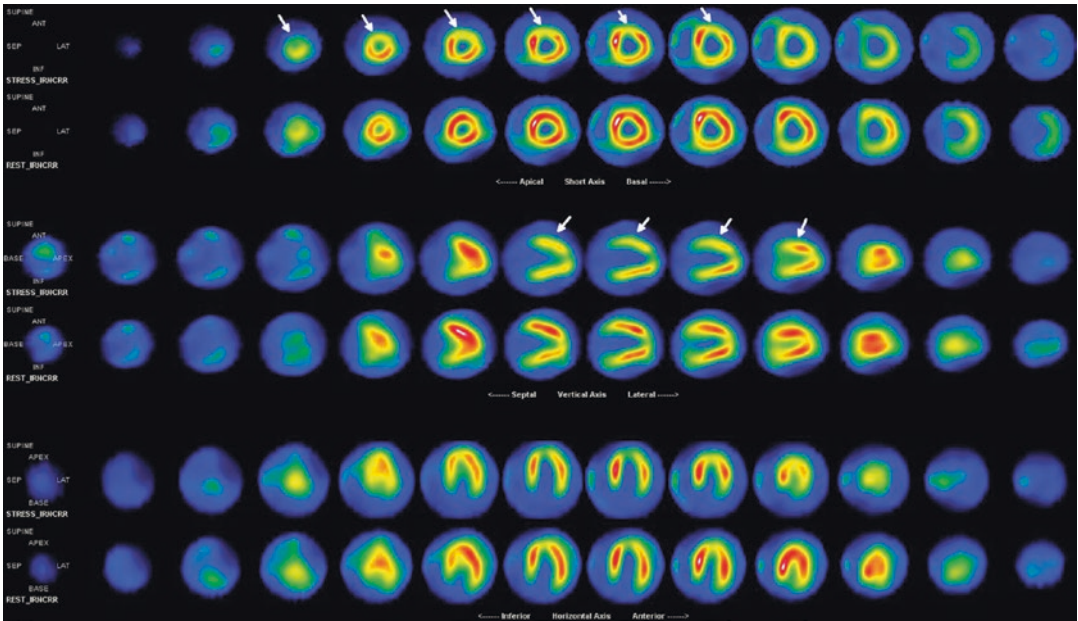


Fig. 3.5 History: A 11-year-old boy after arterial switch operation for transposition of the great arteries with left coronary malformation complained of mild chest discomfort during exercise. Exercise ischemia is suspected. Stress/rest test (ergometer) followed by MIBI injection

was performed. Study report: There is decreased perfusion in the anterior wall (apical and mid-planes, white arrows) improving at rest. Impression: Reversible hypoperfusion of the anterior wall

Case 3.5. Partially Reversible Perfusion Defects (Fig. 3.6)

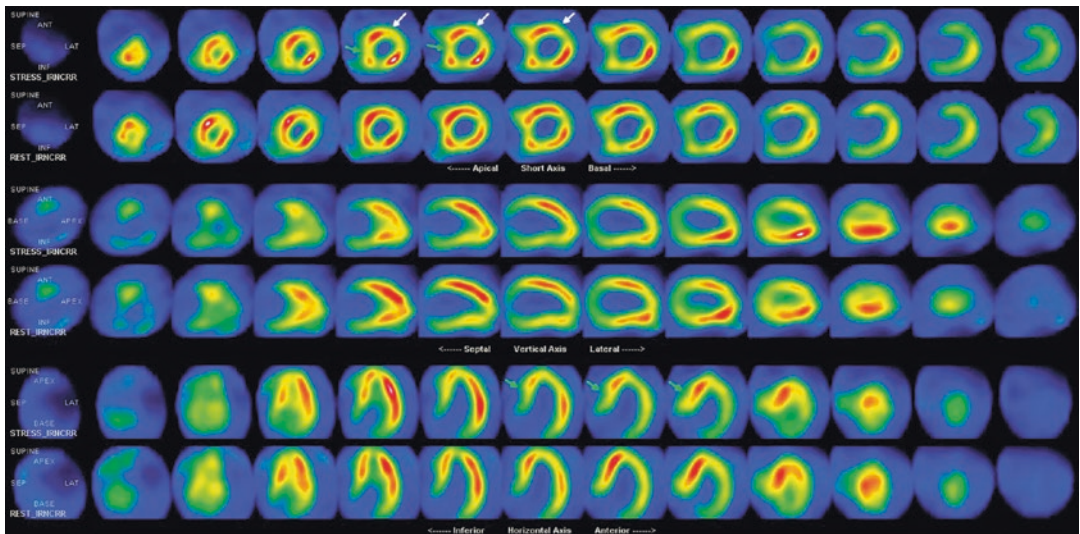


Fig. 3.6 History: A 14-year-old boy after arterial switch operation for transposition of the great arteries and anomalous origin of the coronary arteries. Stress/rest test (ergometer) followed by MIBI injection was performed. Study report: On the stress study (upper row) there is mild

hypoperfusion of the antero-lateral wall (white arrows) and the septum (green arrows) with partial improvement on the rest study (lower row). Impression: Partially reversible hypoperfusion in antero-lateral wall and septum

3.3 Blood Pool Scintigraphy of Vascular Structures

Clinical Indications [11, 12]

- Evaluation of hemangiomas or other vascular malformations.
- To rule out unsuspected additional lesions.
- In cases with high clinical suspicion but with inconclusive US, CT and/or MRI.

Pre-Exam Information

- Location and size of the lesion(s) suspected as hemangiomas.
- Findings on correlative radiologic imaging.

Study Protocol for RBC Scintigraphy [13]

Radiopharmaceutical, Activity and Mode of delivery.

Radiopharmaceutical:
[^{99m}Tc]RBCs (RBC) [14].

- In vitro labelling is the method of choice and should be employed when an adequate facility and proper radiopharmacy practices are available because of significantly higher labelling efficiency and a lower likelihood of artefacts related to free ^{99m}Tc.
 - 1–3 ml of the patient's blood are drawn anticoagulated with heparin or acid citrate dextrose (ACD).
 - RBCs are labelled with a commercially available preparation according to the manufacturer's instructions.
 - General blood manipulation/handling precautions should be implemented. The labelled blood should be slowly re-injected to the patient from whom it was drawn.

- In vivo labelling:
 - ¹²⁵I pyrophosphate is injected in appropriate, weight-based amount obtained from the package insert of the commercial cold kit.
 - Administration of [^{99m}Tc] Pertechnetate follows 20 minutes later.

Activity (Pertechnetate):

- 74 MBq/Kg (2 mCi/kg), a minimum dose of 74 MBq (2 mCi).

Refer to the EANM paediatric dosage card and to the North American consensus guidelines on radiopharmaceutical administration in children in the respective European Association of Nuclear Medicine (EANM) and Society of Nuclear Medicine and Molecular Imaging (SNMMI) and image gently web sites.

Reference to national regulation guidelines, if available, should be considered.

Acquisition Protocol

- Collimator: low energy, all purpose.
- Position: supine.
- FOV: according to the location of the lesion to be investigated, preferably whole body.
- Dynamic study: 1 s/frame, 60 s, matrix 128 × 128, zoom according to child's size.
- Static blood pool images: early, following the dynamic study and late, 2 h after tracer injection: 500 Kcounts, projections according to body region, matrix 256 × 256.
- SPECT following late static images: 25 s/step, 120 projections, matrix 128 × 128, size-appropriate zoom.
- When available SPECT/CT can clarify foci of uncertain origin.

Study Interpretation

- Vascular malformations may show an arterial blush on the dynamic phase when bolus injection is performed.
- Foci of increased tracer accumulation on the late blood pool planar or SPECT images are likely to represent haemangiomas.

Correlative Imaging

- US may be used to characterize the solid and cystic component of vascular lesions and with Doppler assessment may provide some information on vascularity.
- CTA or MRI/MRA may also identify and characterize vascular lesions.

Red Flags

- Injection of in vitro labelled RBC requires extreme caution to ensure that the blood is injected into the patient from whom it was drawn. To reduce the chance of misadministration, it is advised to avoid booking more than one in vitro labelled RBC study per day.
- In vivo RBC labelling allows optimal bolus injection.

- Inadequate RBC labelling may result in free Per technetate in circulation. Uptake in the thyroid gland and gastric mucosa will suggest improper labelling. Care should be taken not to confuse physiologic uptake and excretion of Per technetate with foci of increased blood pool activity.
- The ability to detect hemangiomas depends on their size and location. Those smaller than 1.5 cm in diameter may not be evident especially when situated in organs with high blood pool activity or when they are adjacent to large blood vessels.
- Small hemangiomas are better evaluated with contrast-enhanced CT or MRI.

Take Home Messages

- Hemangiomas and vascular malformations might be multifocal, especially in infants. It is advised to perform a whole-body scan to screen for additional findings throughout the body.
- SPECT/CT improves the accuracy and diagnostic confidence.

Representative Case Examples

Case 3.6. Facial Hemangioma (Fig. 3.7)

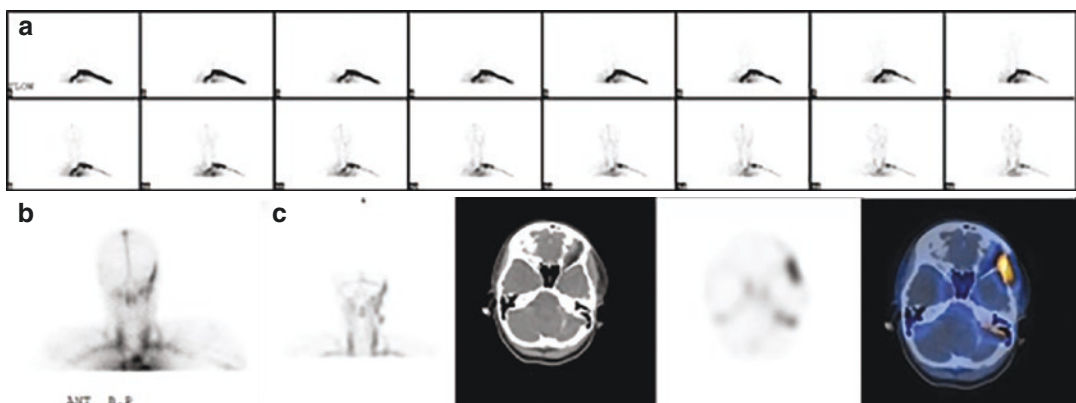


Fig. 3.7 History: A 17-year-old girl presented with a 15-mm pulsatile mass in left face, suspected to be of vascular origin. Study report: Dynamic study of the head (a) following the injection of Tc-RBC does not show areas of increased blood flow. Early planar anterior view of the head (b) shows a slightly increased blood pool in the lateral aspect of the left face. Transaxial slices of SPECT/CT

performed at 2 h after radiotracer administration (c) demonstrate an area of increased blood pool corresponding to swelling of soft tissues in the left temporal-zygomatic area. Impression: The findings are consistent with a vascular lesion with venous blood supply in the left face. US-guided fine needle aspiration confirmed the diagnosis of hemangioma

References

- Hesse B, et al. EANM/ESC guidelines for radionuclide imaging of cardiac function. *Eur J Nucl Med Mol Imaging*. 2008;35(4):851–85.
- Treves, S.T. and H. Schelbert, Cardiovascular system, in *Pediatric nuclear medicine and molecular imaging*, S.T. Treves., 2014, Springer New York: New York, NY. p. 147–188.
- Partington SL, et al. Clinical applications of radionuclide imaging in the evaluation and management of patients with congenital heart disease. *J Nucl Cardiol*. 2016;23(1):45–63.
- Milanesi O, Stellin G, Zucchetta P. Nuclear medicine in pediatric cardiology. *Semin Nucl Med*. 2017;47(2):158–69.
- Kondo C. Myocardial perfusion imaging in pediatric cardiology. *Ann Nucl Med*. 2004;18(7):551–61.
- Sundaram PS, Padma S. Role of myocardial perfusion single photon emission computed tomography in pediatric cardiology practice. *Ann Pediatr Cardiol*. 2009;2(2):127–39.
- Robinson B, et al. Usefulness of myocardial perfusion imaging with exercise testing in children. *Pediatr Cardiol*. 2012;33(7):1061–8.
- Noel CV, et al. Myocardial stress perfusion MRI: experience in pediatric and young-adult patients following arterial switch operation utilizing Regadenoson. *Pediatr Cardiol*. 2018;39(6):1249–57.
- Weindling SN, et al. Myocardial perfusion, function and exercise tolerance after the arterial switch operation. *J Am Coll Cardiol*. 1994;23(2):424–33.
- Hernandez-Pampaloni M, et al. Myocardial perfusion and viability by positron emission tomography in infants and children with coronary abnormalities: correlation with echocardiography, coronary angiography, and histopathology. *J Am Coll Cardiol*. 2003;41(4):618–26.
- Burroni L, et al. Preoperative diagnosis of orbital cavernous hemangioma: a ^{99m}Tc-RBC SPECT study. *Clin Nucl Med*. 2012;37(11):1041–6.
- Eivazi B, Werner JA. Extracranial vascular malformations (hemangiomas and vascular malformations) in children and adolescents—diagnosis, clinic, and therapy. *GMS Curr Top Otorhinolaryngol Head Neck Surg*. 2014;13:Doc02.
- Dong H, et al. The application of technetium-99m-red blood cell scintigraphy in the diagnosis of orbital cavernous hemangioma. *Nucl Med Commun*. 2017;38(9):744–7.
- INTERNATIONAL ATOMIC ENERGY AGENCY. Radiolabelled autologous cells: methods and standardization for clinical use. Vienna: INTERNATIONAL ATOMIC ENERGY AGENCY; 2015.

The opinions expressed in this chapter are those of the author(s) and do not necessarily reflect the views of the IAEA: International Atomic Energy Agency, its Board of Directors, or the countries they represent.

Open Access This chapter is licensed under the terms of the Creative Commons Attribution 3.0 IGO license (<http://creativecommons.org/licenses/by/3.0/igo/>), which permits use, sharing, adaptation, distribution and reproduction in any medium or format, as long as you give appropriate credit to the IAEA: International Atomic Energy Agency, provide a link to the Creative Commons license and indicate if changes were made.

Any dispute related to the use of the works of the IAEA: International Atomic Energy Agency that cannot be settled amicably shall be submitted to arbitration pursuant to the UNCITRAL rules. The use of the IAEA: International Atomic Energy Agency's name for any purpose other than for attribution, and the use of the IAEA: International Atomic Energy Agency's logo, shall be subject to a separate written license agreement between the IAEA: International Atomic Energy Agency and the user and is not authorized as part of this CC-IGO license. Note that the link provided above includes additional terms and conditions of the license.

The images or other third party material in this chapter are included in the chapter's Creative Commons license, unless indicated otherwise in a credit line to the material. If material is not included in the chapter's Creative Commons license and your intended use is not permitted by statutory regulation or exceeds the permitted use, you will need to obtain permission directly from the copyright holder.



Zvi Bar-Sever and Pietro Zucchetta

4.1 Clinical Indications [1–4]

- Assessment of differential perfusion to the lungs and/or regional, to lung zones (lobes) in children with congenital heart disease and associated stenosis of the pulmonary vessels, most commonly Tetralogy of Fallot, showing altered blood flow to the lungs.
- Assessment of lung perfusion following corrective surgery or cardiac catheterization with balloon dilatation of a pulmonary vessel, the most common indication for perfusion lung scintigraphy in children.
- Demonstration and quantitation of shunts between the right (pulmonary) and left (systemic) circulation, mainly in children with cyanotic heart disease.
- Evaluation of the hepato-pulmonary syndrome in patients with liver disease or after liver transplant.
- Assessment of lung function:
 - Before and after lung transplantation.
 - In congenital lung malformations (e.g. lobar emphysema, cystic adenomatoid malformation and pulmonary sequestration).

- In structural abnormalities of the chest (e.g. congenital diaphragmatic hernia, pectus excavatum and spinal scoliosis).
- In airway diseases (e.g. cystic fibrosis, foreign body aspiration and bronchopulmonary dysplasia).
- Diagnosis of pulmonary embolism (PE).

4.2 Pre-Exam Information

- Child's age and degree of cooperation, to determine the likelihood of obtaining a ventilation study when required and the type of ventilation scan when options are available.
- Exact anatomy of congenital cardiac malformations before or after corrective surgery.
- Presence of right-to-left shunt, of pulmonary hypertension or of solitary lung.

Study Protocol for Perfusion Lung Scan [2, 5, 6]

Radiopharmaceuticals, Activity and Mode of Delivery.

Radiopharmaceutical:

- [^{99m}Tc]macroaggregated albumin (MAA), typically 10–40 microns in size.

Z. Bar-Sever (✉)

Institute of Nuclear Medicine, Schneider Children's Medical Center, Tel Aviv University, Petah Tiqva, Israel

P. Zucchetta

Nuclear Medicine Unit, Department of Medicine, Padova University Hospital, Padova, Italy

© The Author(s) 2023

Z. Bar-Sever et al. (eds.), *A Practical Guide for Pediatric Nuclear Medicine*, https://doi.org/10.1007/978-3-662-67631-8_4

Activity:

- Should take into account whether a ventilation study is preceding or immediately following the perfusion scan (the order of exams depending on clinical indications and local preferences).
 - If no ventilation scan is performed: 1.11 MBq/kg (0.03 mCi/kg), minimum activity: 14.8 MBq (0.4 mCi).
 - If perfusion scan is performed immediately after ventilation scan: 2.6 MBq/kg (0.07 mCi/kg).
 - The typical number of MAA particles should not exceed 50,000 in newborns and 165,000 in 1-year-old infants. In cases of right-to-left shunt, of pulmonary hypertension or of a single functioning lung, the number of particles should be 10,000.

Refer to the EANM paediatric dosage card and to the North American consensus guidelines on radiopharmaceutical administration in children in the respective EANM and SNMMI and image gently web sites. Reference to national regulation guidelines, if available, should be considered.

Mode of delivery:

- The tracer should be injected with the patient supine.

Acquisition protocol

- Collimator: low energy, high or ultra-high resolution.
- Planar images: anterior, posterior, 4 obliques and occasionally 2 lateral views, 300,000–500,000 counts/view, 256 × 256 matrix.
- SPECT and SPECT/CT when available are recommended in selected clinical scenarios.

Study Protocol for Ventilation Lung Scan [2, 4, 7]**Radiopharmaceuticals, Activity and Mode of Delivery.***Radiopharmaceutical*

- ^{99m}Tc-labelled aerosols: [^{99m}Tc] diethylene-triamine-pentaacetate (DTPA) is the most common agent. The aerosol is created by a jet or ultrasonic nebulizer and introduced through a face mask.
- ^{99m}Tc-labelled carbon nanoparticles: *Technegas*®, an aerosol which consists of the ^{99m}Tc molecule cocooned by layers of graphite thus creating small particles (5–30 nm wide) that are suspended in Argon gas [8].

Radioactive gases:

- [¹³³Xe] Xenon (¹³³Xe), is at present unavailable in some countries and more expensive than aerosols.
- [^{81m}Kr] Krypton (^{81m}Kr) is an inert gas eluted with humidified air through a ⁸¹Rubidium/^{81m}Kr generator. Availability and high cost are limiting factors.

Activity:

- DTPA: scaled down according to the child's weight from DTPA aerosol adult dose of 900–1300 MBq (25–35 mCi) in the nebulizer, from which the lungs receive approximately 20–40 MBq (0.5–1.0 mCi).
- *Technegas*®: minimum dose 100 MBq.
- ¹³³Xe: 10–12 MBq/kg (0.3 mCi/kg), minimum 100–120 MBq (3 mCi).
- ^{81m}Kr: in adults, the dose is 40–400 MBq (1.1–10.1 mCi) which would result in an estimated effective dosage of 0.004–0.01 mSv in children.

Refer to the EANM paediatric dosage card and to the North American consensus guidelines on radiopharmaceutical administration in children in the respective EANM and SNMMI and image gently web sites.

Reference to national regulation guidelines, if available, should be considered.

Note that ^{133}Xe and $^{81\text{m}}\text{Kr}$ do not appear on the EANM dosage card.

Mode of delivery:

- DTPA: the child should take deep breaths for several minutes. Cooperation is important and prevents application of the study in infants and young uncooperative children.
- Technegas®: requires a special apparatus, generator, for preparation of the inhaled aerosol.
- ^{133}Xe : requires a dedicated administration and trapping systems to trap and exhaust the exhaled gas.
- $^{81\text{m}}\text{Kr}$: is inhaled via a face mask.

Acquisition protocol

- The ventilation scan is usually done first followed by the perfusion study.
- [^{133}Xe] scans: in supine position, posterior view dynamic imaging, 5 sec/frame. The dynamic nature of the ^{133}Xe study precludes multiple views acquisition.
- [$^{99\text{m}}\text{Tc}$] agents: static images at equilibrium, similar views as for the perfusion study, up to 100,000 counts/view.
- SPECT is recommended, allowing better comparison with perfusion scan.
- SPECT/CT, if available, may be also indicated, if not performed already as part of the perfusion scan.

4.3 Perfusion and Ventilation Study Interpretation

Visual patterns of perfusion and ventilation lung scans should be interpreted according to the requested clinical indication:

Congenital heart disease: [9, 10]

- Any tracer localization in the brain or kidneys should be reported as evidence of right-to-left shunt.
- In classic Glenn shunt (end-to-end pulmonary artery/superior vena cava anastomosis) upper extremity injection will result in tracer traveling through the superior vena cava into the right lung only. Tracers injected in the lower extremity will result in localization in the left lung only. In cases of a bidirectional Glenn shunt (end-to-side anastomosis), upper extremity injection will result in tracer accumulation in both lungs. Tracer injected into the lower extremity will travel from the inferior vena cava and enter the systemic circulation bypassing the lungs.

Hepato-pulmonary syndrome [11]:

- The shunt is intrapulmonary leading to the visualization of activity in the systemic circulation.

Congenital and acquired airway disease [4]:

- Global and regional distribution of pulmonary ventilation and perfusion are reported.

Pulmonary embolism [12, 13]:

- The hallmark of PE remains demonstrating a mismatch between absent or reduced perfusion in lung segments and preserved ventilation.

Specifically, dynamic [^{133}Xe] studies should be interpreted as follows:

- Initial images after a single breath reflect regional lung ventilation.

- Equilibrium phase images, after multiple breaths through a rebreathing inhalation system, reflect the distribution of aerated air space volume.
- Subsequent images after gas administration ceases reflect washout from the airspaces. Air trapping when present is typically evident during this phase.
- Alternatively, it is possible to calculate the shunt index by obtaining the ratio between brain counts from a brain ROI and lung counts from a ROI placed on both lungs on the posterior view, corrected by background:
Background corrected brain counts/background corrected lung counts $\times 100$
(Normal value 0.42 ± 0.30) [14].

4.4 Perfusion and Ventilation Differential Lung Function Analysis

- In addition to visual inspection of images, studies can be processed to provide a quantitative analysis.
- Quantification of lung perfusion is usually assessed on anterior and posterior planar projections, and more recently using quantitative SPECT or SPECT/CT segmentation methods.
 - Differential lung perfusion and/or ventilation is calculated by comparing left and right lung counts obtained from whole lung regions-of-interest (ROIs) and is expressed in percentages.
 - ROIs can be placed on the posterior view only or both the posterior and anterior view to obtain conjugate counts for calculating the geometric mean.
 - ROIs can be split into upper middle and lower zones for each lung for a crude assessment of regional lung perfusion and ventilation. Modern processing software allows determination of these values according to lung lobes and segments and should be preferred when available.
- In patients with shunting between the pulmonary and systemic circulations, MAA particles embolize pre-capillary arterioles in the systemic circulation. The brain and kidneys that receive a large portion of the cardiac output, are visualized.
- Right-to-left (R-L) shunt magnitude calculation can be obtained by drawing whole body and lung ROIs and using the following formula:
R-L shunt (%) = [(total body counts–lung counts)/total body counts] $\times 100$ [1].

4.5 Correlative Imaging

- Chest radiograph correlation is required when PE is suspected.
- CT pulmonary angiography (CTPA) correlation may increase the specificity of ventilation/perfusion (V/Q) scans.

Red Flags

- For perfusion studies, injection should be given in supine position to reduce the effect of gravity on the particle distribution between the upper and lower lung zones.
- In complex situations (e.g. cavo-pulmonary anastomosis, aka Glenn shunt and Fontan circulation) it is required to split the bolus administration to upper and lower limbs.
- Blood should not be drawn into the injection syringe since this may result in blood clots containing MAA particles that can affect the radio-tracer distribution in the pulmonary circulation.
- Images may appear inhomogeneous when using a small number of MAA particles but they can be sufficient for visual assessment and semi-quantitation of whole lung and regional perfusion. The number of MAA particles:
 - Should not exceed 50,000 in newborns and 165,000 in 1-year-old infants.
 - Should be around 10,000 cases of right-to-left shunt, of pulmonary hypertension or of a single functioning lung.
- Tracer localization in the thyroid gland, seen on the chest views, requires additional scans of the head to distinguish between free Pertechnetate due to improper MAA labelling and right-to-left shunt. Pertechnetate can be

seen in the thyroid, the gastric mucosa and renal collecting systems. In case of shunts the tracer will be seen in the brain.

- Inadequate ventilation can result in low radio-labelled aerosol concentration in the periphery of the lungs and accumulation in the trachea, large airways, oropharynx, oesophagus and stomach, limiting the diagnostic accuracy. These effects are accentuated in cases with an abundance of airway secretions.
- The ^{81}Rb generator/ $^{81\text{m}}\text{Kr}$ generator is expensive and not widely available [3, 15, 16].
- The original PIOPED and revised PIOPED criteria as well as the new European guidelines for lung scintigraphy in adults with suspected PE have not been validated in children [13].

4.6 Take Home Messages

- Plan the study carefully, keeping in mind that ventilation scans may be difficult to obtain in young children.
- When both ventilation and perfusion studies are performed sequentially, the activities of the administered doses should be adjusted so the count rate from the second study is 3 times higher than that from the first study.
- When both perfusion and ventilation SPECT studies are obtained, they should be aligned and displayed side by side [13].
- Comparison to previous studies, when present, is essential to determine temporal changes and to assess the effectiveness of therapeutic interventions. This requires meticulous standardization of the study, including patient positioning and ROI drawing.
- When a right-to-left shunt is suspected the field-of-view of the perfusion study should be extended to visualize the presence or absence of tracer in the brain or renal parenchyma.
- A meticulous technique is important during the inhalation phase of the ventilation studies to achieve good tracer penetrance into peripheral airways and to prevent environmental contamination.
- Semi-quantitation of differential and regional lung perfusion and ventilation can be easily calculated and is important for planning and monitoring therapeutic decisions, and for long-term follow-up.
- The diagnosis of PE in adults as well as, although less common, in children, shifted in recent years from scintigraphic techniques to CT angiography (CTA). There are a number of risk factors for PE in children, the most common being the presence of a central line catheter. There has been some resurgence of ventilation/perfusion scintigraphy not only as a solution for PE evaluation when CTA is contraindicated (contrast allergy, chronic renal failure), but also to reduce the radiation burden compared with CTA.
- Perfusion and ventilation SPECT and/or SPECT/CT processed with iterative reconstruction methods because of the low count rates have improved the diagnostic accuracy for diagnosis of PE.
- For certain indications such as PE, a normal perfusion study performed first may eliminate the need for a ventilation study if it is normal.
- The most common congenital cardiac malformation with associated pulmonary stenosis is Tetralogy of Fallot. Baseline perfusion studies assess the severity of the condition and follow-up studies can determine the impact of therapeutic measures (balloon dilatation, stent placement etc.).
- When interpreting perfusion lung scans, in cases of congenital heart disease, it is essential to know:
 - The anatomy of the malformations and the corrective surgery that was performed.
 - If tracer was injected in the upper or lower extremity veins.
- Technegas® behaves as a ‘pseudo-gas’ with good penetration into the peripheral airspaces. Inhalation of Technegas® requires less patient cooperation and produces high-quality ventilation images.
- ^{133}Xe ventilation can be applied successfully to children with limited cooperation. It is a dynamic study, allowing only one view, typically posterior. The study should be performed prior to the perfusion acquisition.
- $^{81\text{m}}\text{Kr}$ enters the alveolar spaces and pulmonary circulation by diffusing into the alveolar capil-

laries. It returns from the peripheral circulation to the lungs and is exhaled. Equilibrium is reached rapidly with a constant concentration in the lungs allowing static images.

- $^{81\text{m}}\text{Kr}$ ventilation requires little cooperation, has a very low radiation burden due to the short half-life of $^{81\text{m}}\text{Kr}$ of 13 seconds and can be applied in studies of infants and young children.

4.7 Representative Case Examples

Case 4.1. Assessment of Pulmonary Artery Stenosis (Fig. 4.1)

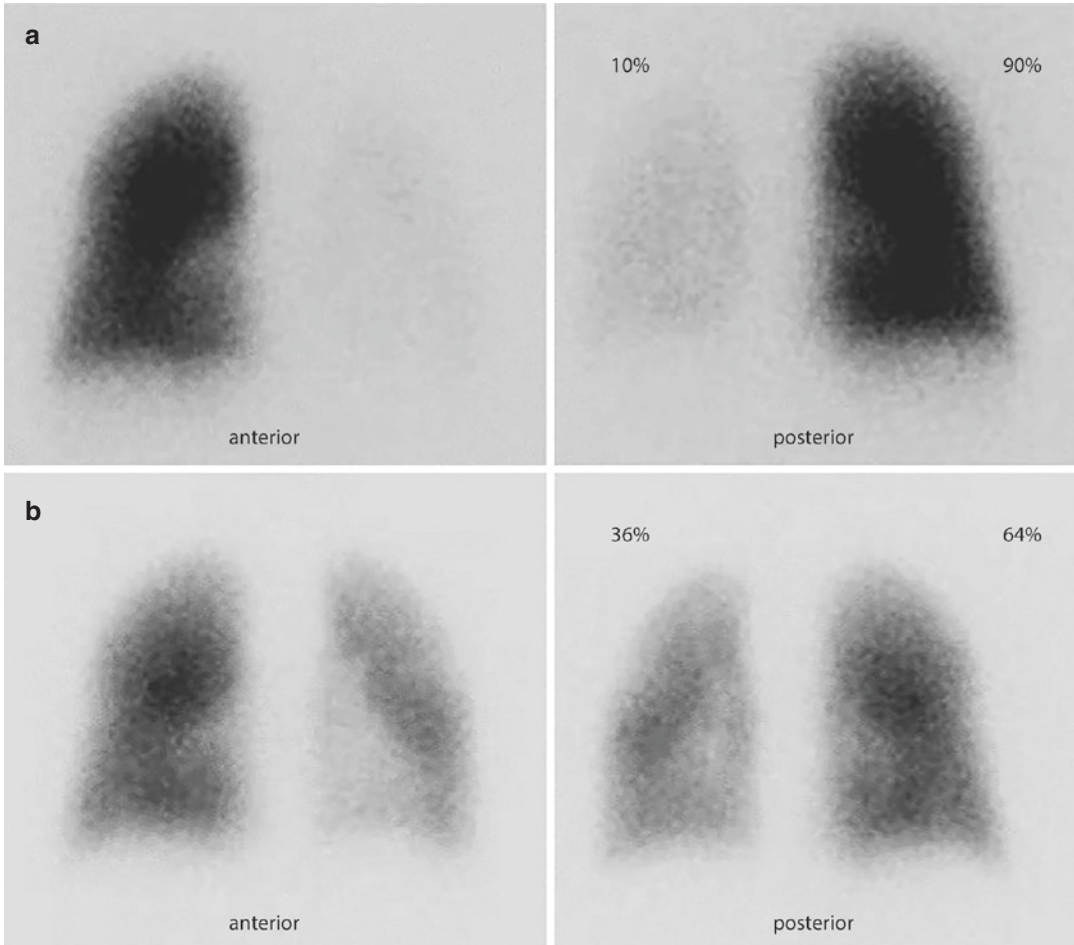
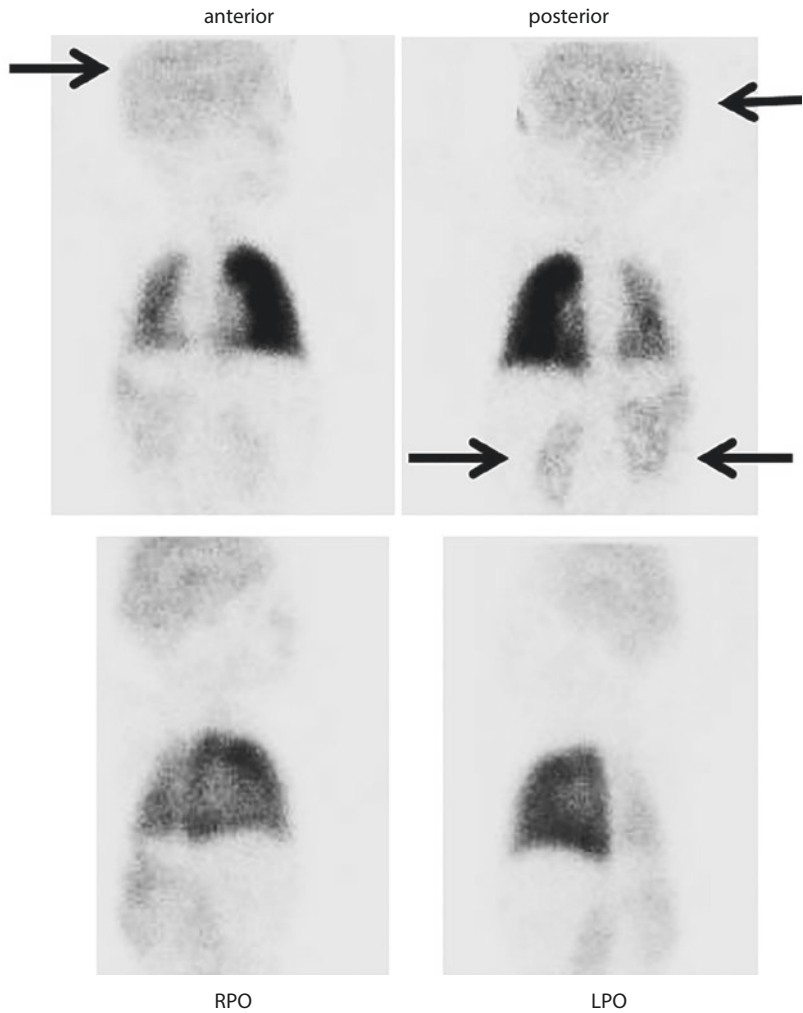


Fig. 4.1 History: A 4-year-old boy underwent perfusion lung scintigraphy to assess the impact of an isolated left pulmonary artery stenosis on the differential pulmonary perfusion. Anterior and posterior images (a) show a marked global reduction of the perfusion of the left lung. The differential perfusion was 90% and 10% to the right and left lungs, respectively. Based on these results he underwent cardiac catheterization with balloon dilatation

of the left main pulmonary artery. A follow-up lung scan performed 6 months later (b) demonstrates improved perfusion to the left lung. The differential perfusion to the left lung increased from 10% to 36%. Impression: Marked improvement in left lung perfusion due to the successful intervention. NB: This case demonstrates how a perfusion lung scan guides decisions on the need for therapeutic interventions and evaluates their success

Case 4.2. Right-to-Left Shunt (Fig. 4.2)

Fig. 4.2 History: A 10-month-old boy with complex congenital cardiac anomalies including situs inversus, corrected transposition of the great arteries and pulmonary atresia, underwent a left-sided modified Blalock Taussig shunt at the age of 1 month. Perfusion lung scan was performed to assess a stenosis of the right pulmonary artery. Study report: There is a reduction in the pulmonary perfusion of the right lung. In addition, there is diffuse tracer activity in the brain, in the parenchyma of both kidneys and in the spleen located in the right upper quadrant due to situs inversus (arrows). Impression: The findings suggest the presence of a shunt from the pulmonary to the systemic circulation, a right-to-left shunt



Case 4.3. Congenital Cystic Adenomatoid Malformation (Fig. 4.3)

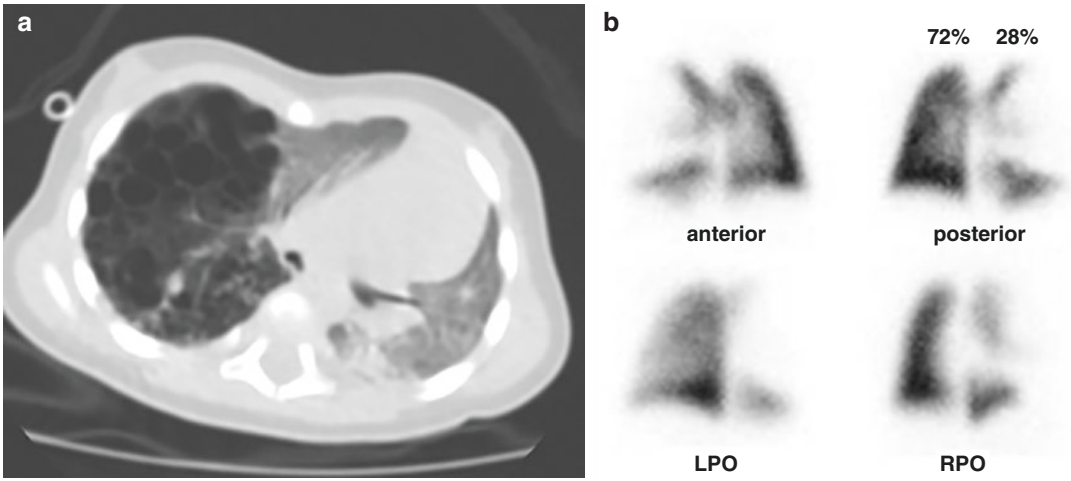


Fig. 4.3 History: A 4-month-old girl with a large congenital cystic adenomatoid malformation of the right lung as seen on chest CT (a). Study report: Baseline perfusion lung scintigraphy (b) shows a large perfusion defect in the right lung corresponding to the malformation. The differential perfusion was: right lung 28%, left lung 72%.

Impression: Decreased perfusion to right lung corresponding to the structural malformation seen on CT. Subsequently, the infant underwent surgery to resect the malformation and to reconstruct the right pulmonary artery

Case 4.4. Hypoplastic Left Lung (Fig. 4.4)

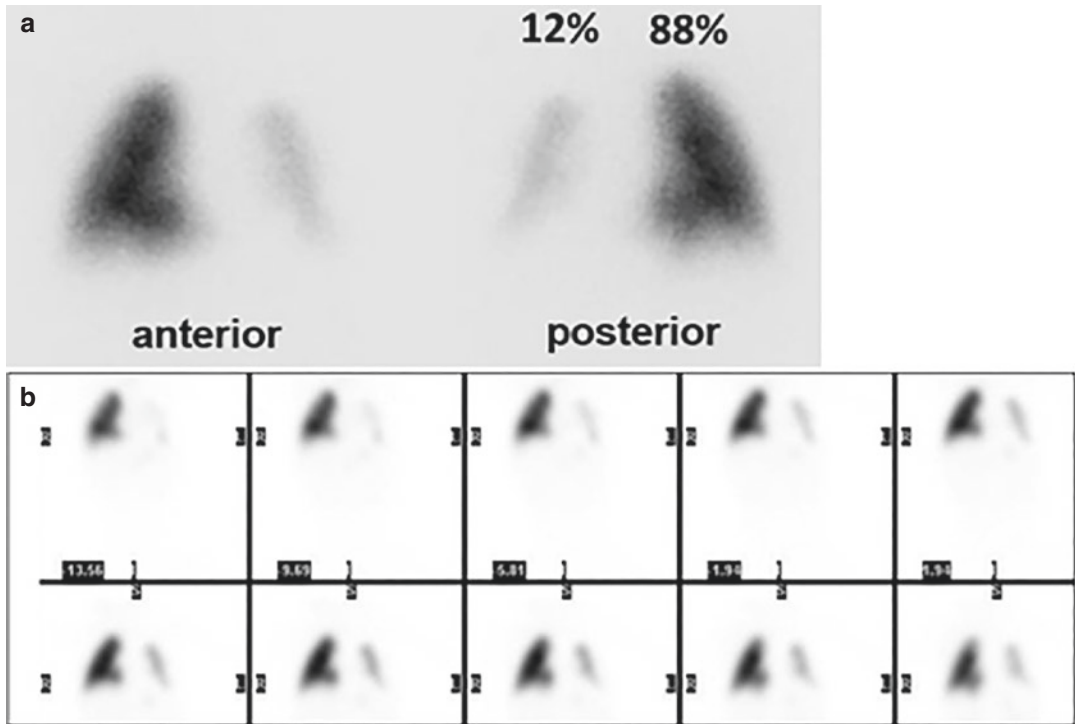


Fig. 4.4 History: A 7-month-old preterm infant with a hypoplastic left lung caused by congenital paralysis of the left hemi-diaphragm had lung perfusion scintigraphy to assess the differential pulmonary perfusion. Study report: Anterior and posterior perfusion images (a) and coronal

SPECT slices (b) show a small left lung with a marked reduction in pulmonary perfusion contributing only 12% to the total pulmonary perfusion. Impression: Hypoplastic left lung with a marked decrease in relative perfusion

References

1. Ciofetta G, et al. Guidelines for lung scintigraphy in children. *Eur J Nucl Med Mol Imaging*. 2007;34(9):1518–26.
2. Parker JA, et al. SNM practice guideline for lung scintigraphy 4.0. *J Nucl Med Technol*. 2012;40(1):57.
3. Grant FD, Treves ST. Lung Imaging. In: Treves ST, editor. *Pediatric nuclear medicine and molecular imaging*. New York, NY: Springer New York; 2014. p. 131–45.
4. Sanchez-Crespo A. Lung ventilation/perfusion single photon emission computed tomography (SPECT) in infants and children with nonembolic chronic pulmonary disorders. *Semin Nucl Med*. 2019;49(1):37–46.
5. Lassmann M, Treves ST. Paediatric radiopharmaceutical administration: harmonization of the 2007 EANM paediatric dosage card (version 1.5.2008) and the 2010 North American consensus guidelines. *Eur J Nucl Med Mol Imaging*. 2014;41(5):1036–41.
6. Treves ST, et al. 2016 update of the North American Consensus Guidelines for pediatric administered radiopharmaceutical activities. *J Nucl Med*. 2016;57(12):15n–8n.
7. ACR-SNM-SPR Practice Guideline for the performance of pulmonary scintigraphy in adults and children. 2009.
8. Burch WM, Sullivan PJ, McLaren CJ. Technegas—a new ventilation agent for lung scanning. *Nucl Med Commun*. 1986;7(12):865–71.
9. Chien KJ, et al. Assessment of branch pulmonary artery stenosis in children after repair of tetralogy of Fallot using lung perfusion scintigraphy comparison with echocardiography. *Ann Nucl Med*. 2016;30(1):49–59.
10. Milanesi O, Stellin G, Zucchetta P. Nuclear medicine in pediatric cardiology. *Semin Nucl Med*. 2017;47(2):158–69.
11. Grilo-Bensusan I, Pascasio-Acevedo JM. Hepatopulmonary syndrome: what we know and what we would like to know. *World J Gastroenterol*. 2016;22(25):5728–41.
12. Patocka C, Nemeth J. Pulmonary embolism in pediatrics. *J Emerg Med*. 2012;42(1):105–16.
13. Bajc M, et al. EANM guideline for ventilation/perfusion single-photon emission computed tomography (SPECT) for diagnosis of pulmonary embolism and beyond. *Eur J Nucl Med Mol Imaging*. 2019;46(12):2429–51.
14. Grimon G, et al. Early radionuclide detection of intrapulmonary shunts in children with liver disease. *J Nucl Med*. 1994;35(8):1328–32.
15. Li DK, et al. Krypton-81m: a better radiopharmaceutical for assessment of regional lung function in children. *Radiology*. 1979;130(3):741–7.
16. Pomet R, Therain F. The use of Kr-81m in ventilation imaging. *Clin Nucl Med*. 1982;7(3):122–30.

The opinions expressed in this chapter are those of the author(s) and do not necessarily reflect the views of the IAEA: International Atomic Energy Agency, its Board of Directors, or the countries they represent.

Open Access This chapter is licensed under the terms of the Creative Commons Attribution 3.0 IGO license (<http://creativecommons.org/licenses/by/3.0/igo/>), which permits use, sharing, adaptation, distribution and reproduction in any medium or format, as long as you give appropriate credit to the IAEA: International Atomic Energy Agency, provide a link to the Creative Commons license and indicate if changes were made.

Any dispute related to the use of the works of the IAEA: International Atomic Energy Agency that cannot be settled amicably shall be submitted to arbitration pursuant to the UNCITRAL rules. The use of the IAEA: International Atomic Energy Agency's name for any purpose other than for attribution, and the use of the IAEA: International Atomic Energy Agency's logo, shall be subject to a separate written license agreement between the IAEA: International Atomic Energy Agency and the user and is not authorized as part of this CC-IGO license. Note that the link provided above includes additional terms and conditions of the license.

The images or other third party material in this chapter are included in the chapter's Creative Commons license, unless indicated otherwise in a credit line to the material. If material is not included in the chapter's Creative Commons license and your intended use is not permitted by statutory regulation or exceeds the permitted use, you will need to obtain permission directly from the copyright holder.



5.1 Thyroid Scintigraphy in Congenital Hypothyroidism

Clinical Indications [1–4]

- To determine the etiology of CHT.
- To differentiate between permanent and transient forms of CHT.

Pre-Exam Information

- This is an urgent scan and should be booked within 3–4 days from birth.
- A thyroid function blood test may be performed following the positive screening result. If this confirms the diagnosis of hypothyroidism, the newborn is started on thyroxine.
- Is the infant receiving hormonal replacement therapy? If so, for how many days?
- Whether there has been maternal thyroid disease during pregnancy and/or antithyroid drug therapy.

- History of exposure of the newborn to iodine-containing antiseptics used in maternal (C-section) or newborn surgery or contrast media in radiologic procedures.

Study Protocol for Thyroid Scintigraphy in Neonates [5, 6]

Patient Preparation

- A cannula is placed for tracer injection and blood tests if required.
- No fasting is required for intravenous (IV) radiotracer administration.
- Oral ^{123}I administration requires 2 h of fasting before the scan to ensure rapid and complete absorption.

Radiopharmaceutical, Activity, and Mode of Delivery.

Radiopharmaceutical:

- [$^{99\text{m}}\text{Tc}$]Pertechnetate (Pertechnetate): is the preferred radiopharmaceutical in children because of its quick localization within thyroid tissue.
- [^{123}I]Na Iodine (^{123}I) is theoretically the most physiologic radiopharmaceutical and yields better images even with low uptake.

B. Shulkin (✉)
Department of Diagnostic Imaging, St. Jude
Children's Research Hospital, Memphis, TN, USA
e-mail: Barry.Shulkin@stjude.org

T. N. Pascual
Department of Science and Technology,
Manila, Philippines

Activity:

- **Pertechnetate:** the injected activity in a neonate is about 10 MBq (0.35 mCi).
- ¹²³I administered IV: the recommended activity is 3 MBq (0.08 mCi) but some centers use only 1.2 MBq (0.03 mCi).
- ¹²³I administered orally (following 2 hours fast): 0.2 MBq/Kg (0.005 mCi/Kg) with a minimum dose of 3 MBq (0.08 mCi).

Refer to the EANM pediatric dosage card and to the North American consensus guidelines on radiopharmaceutical administration in children in the respective EANM and SNMMI and image gently web sites.

Reference to national regulation guidelines, if available, should be considered.

Delivery:

- IV tracers are administered through a cannula, which should be adequately flushed with normal saline before and after the injection.

Acquisition Protocol.*Pertechnetate:*

- **Time of imaging:** 15–20 min post-injection.
- **Pinhole collimator** is recommended when available.
 - If a pinhole collimator is not available use general purpose, high or ultra-high resolution collimator.
- **Position:** supine with the neck extended. A folded towel under the neck helps achieve the desired extension.
 - The infant is secured to the camera bed, with the arms by the side of the body.
- **Projections:** standard anterior, right and left anterior oblique (RAO, LAO). A lat-

eral view of the neck indicated in cases of ectopy, is obtained with the infant lying on his side.

- ⁵⁷Co markers positioned on the supra-sternal notch and optionally on the chin to improve spatial orientation.
- **Acquisition parameters:**
 - **Duration:** 5–10 min/view.
 - Alternatively: 250 Kcounts; for images with markers 50 Kcounts.
 - **Pinhole:** 100–200 Kcounts.
 - **Zoom** of 1.5–2 (typical), matrix 128 × 128 or 256 × 256.

¹²³I

- **Time of imaging** 2–6 h if early imaging is desired. Otherwise 24 h after ingestion is standard.
- All other parameters are the same as for Pertechnetate (*see above*).

Study Interpretation

- **Normal scan:**
 - Symmetrical tracer uptake in both thyroid lobes, resembling a butterfly shape.
 - The gland is positioned at the base of the neck, the normal thyroid bed.
 - Faint uptake is seen in the salivary glands and the gastric mucosa.
- **Lack of tracer uptake** in the thyroid gland can be due to:
 - Agenesis.
 - Maternal antithyroid antibodies in the newborn's blood (preventing tracer uptake).
- **Ectopic focal uptake:**
 - In the upper neck midline, the region of the oropharynx, suggests a “lingual thyroid.”
 - One or, occasionally, two foci in the lower neck, above the normal thyroid bed, located along the thyroglossal duct.
- **Faint, ill-defined uptake** in thyroid bed can be due to:
 - Maternal antibodies.

- Exposure of the newborn to iodine.
- A hypoplastic gland.
- Treatment with replacement thyroid hormones for more than 7 days.
- Visualization of a single lobe is due to hemiagenesis.
- Intense uptake in both lobes of a normally positioned thyroid gland suggests dysmorphogenesis.

Perchlorate Discharge Test [7]

- Iodide is an essential substrate of thyroid hormones. It is normally trapped in thyroid cells and undergoes organification and incorporation into tyrosine residues in thyroglobulin (Tg). Organification defects in thyroid hormone synthesis cause accumulation of free iodide in the thyroid cells.
- Perchlorate is a drug that shares the same uptake mechanism as iodide and is also trapped in thyroid cells. This results in the discharge of excess non-organified iodide from the cells.

Perchlorate Test Protocol

- Following administration of ^{123}I a region of interest (ROI) is placed over the thyroid gland and a background ROI over the right lung.
- 90 mg of Perchlorate is administered orally.
- A repeat anterior view of the thyroid is obtained after 60 minutes and processed with the same ROI.
- A positive study indicating an organification defect requires a greater than 10% decay-corrected reduction in the net thyroid counts at 60 min after Perchlorate administration.

Correlative Imaging

- US of the neck may show the presence of the thyroid in the neck and can be used to screen for a possible mass at the base of the tongue. This assessment can however be difficult due to small size of infants and thus limited access to the neck area. When a normally situated gland is visualized, an ectopic gland can be excluded.
- Neck US can help determine the presence or absence of the thyroid that is not visualized on scintigraphy as well as to confirm the morphology and location of the gland.
- If struma ovarii is suspected US or other cross-sectional imaging of the pelvis may be warranted.

Red Flags

- It is best to perform the thyroid scan before the initiation of hormonal replacement therapy, but scheduling limitations should not postpone treatment.
- Some centers prefer to position the child directly on the collimator surface, lying in the prone position with the head gently cradled in the hands of a parent/caregiver or staff.
- In practice, the use of ^{123}I is not necessary unless a perchlorate discharge test is planned.
- Some centers use a reduced dose of ^{123}I administered IV by more than 50% of the recommended activity, 1.2 MBq (0.03 mCi) instead of 3 MBq (0.08 mCi) with satisfactory image quality while also achieving a significant decrease in the effective exposure dose.

Take Home Messages

- ^{123}I is not widely available, being expensive and having a higher radiation burden than Technetate.
- Thyroid scans for CHT are urgent studies and should be given priority in scheduling.
- Study results can still be informative after a few days of therapy.

- Positioning the child directly on the collimator surface in the prone position decreases the distance between the thyroid gland and the collimator, improving spatial resolution and shorter acquisition time.
- Pinhole collimators provide optical magnification and enhance the spatial resolution that may improve diagnostic accuracy. This is especially important given the small thyroid gland size in the newborn.
- In cases of dyshormonogenesis, when using ^{123}I , a perchlorate discharge test can substantiate the diagnosis. Perchlorate will not discharge iodide from normal thyroid glands.
- The normal uptake of Pertechnetate is 0.4–4% of the injected activity.
- Faint, ill-defined uptake in the thyroid bed is less specific than the other patterns of thyroid

visualization and can be due to a number of causes, as described above.

- Maternal antithyroid antibodies in the newborn's blood can severely impede tracer uptake by the gland due to transient hypothyroidism, a condition that subsides within a few weeks after the disappearance of the antibodies from the blood. Neck US can help distinguish between this option and agenesis of the gland.
- The best study interpretation is obtained when combining scintigraphy and results of neck US.

Representative Case Examples

Case 5.1. Non-visualization of Thyroid Gland (Fig. 5.1)

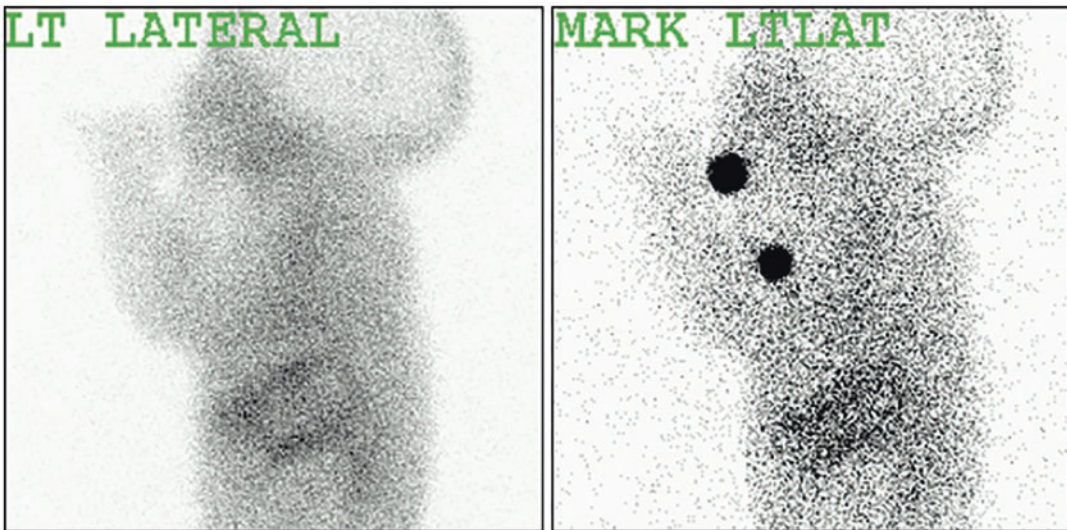


Fig. 5.1 History: Neonate with congenital hypothyroidism. Study report: In the left lateral view (right, with, and left, without markers), there is no evidence of functioning

thyroid tissue in the neck or elsewhere. Impression: The findings are compatible with thyroid agenesis or a severely dysplastic thyroid

Case 5.2. Sublingual Thyroid (Fig. 5.2)

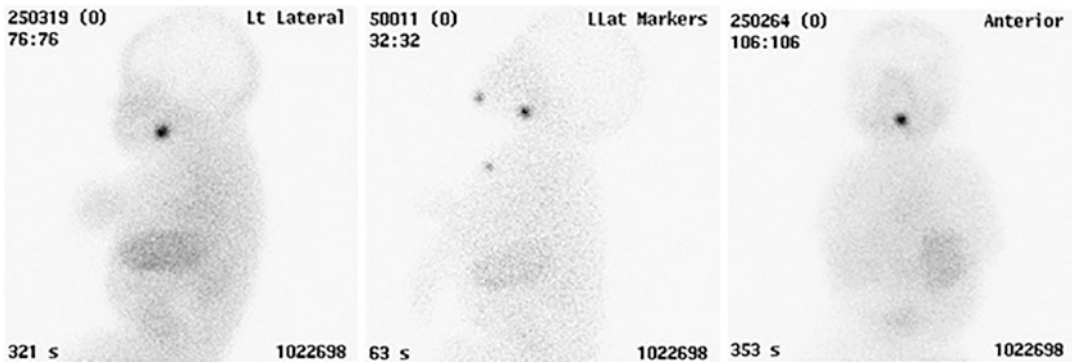


Fig. 5.2 History: Neonate with congenital hypothyroidism. Study report: On left lateral views (left without markers, center with markers) there is a focal area of Per technetate uptake in the sublingual position. In the anterior view (right) the focus appears round-shaped and

not in the typical butterfly shape of the normal thyroid gland. Impression: The findings are compatible with a sublingual thyroid. This child is likely to need thyroxine for life

Case 5.3. Ectopic Thyroid Tissue (Fig. 5.3)

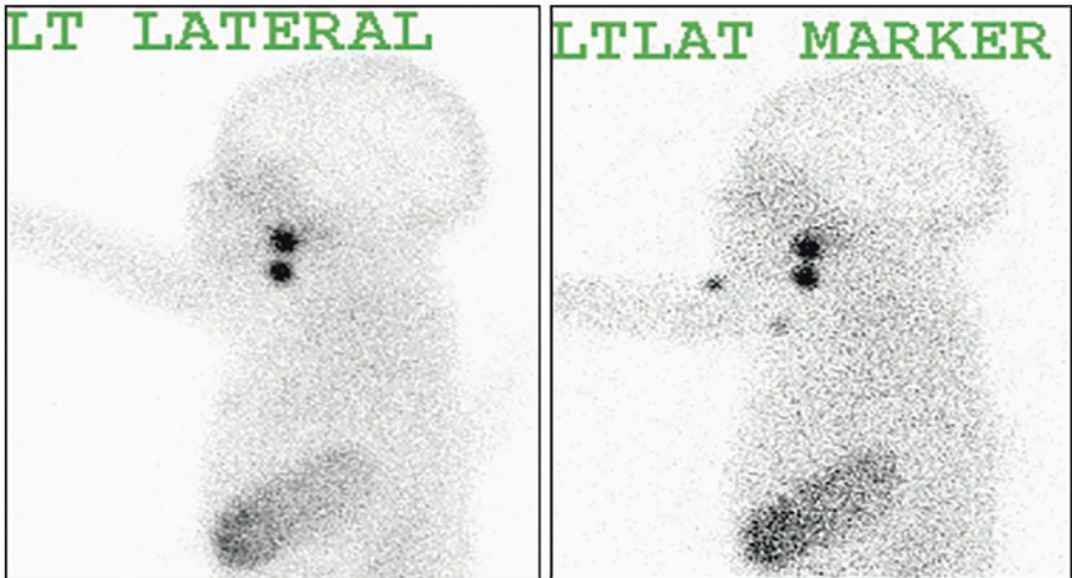


Fig. 5.3 History: Neonate with congenital hypothyroidism. Study report: Following administration of Per technetate, on the left lateral view (left, without markers) there are two foci of tracer uptake behind the tongue. No tracer uptake is seen in the physiologic thyroid loca-

tion in the neck (right, with markers). Impression: The findings are compatible with foci of functioning ectopic sublingual thyroid tissue. This child is likely to need thyroxine for life

Case 5.4. Dyshormonogenesis (Fig. 5.4)

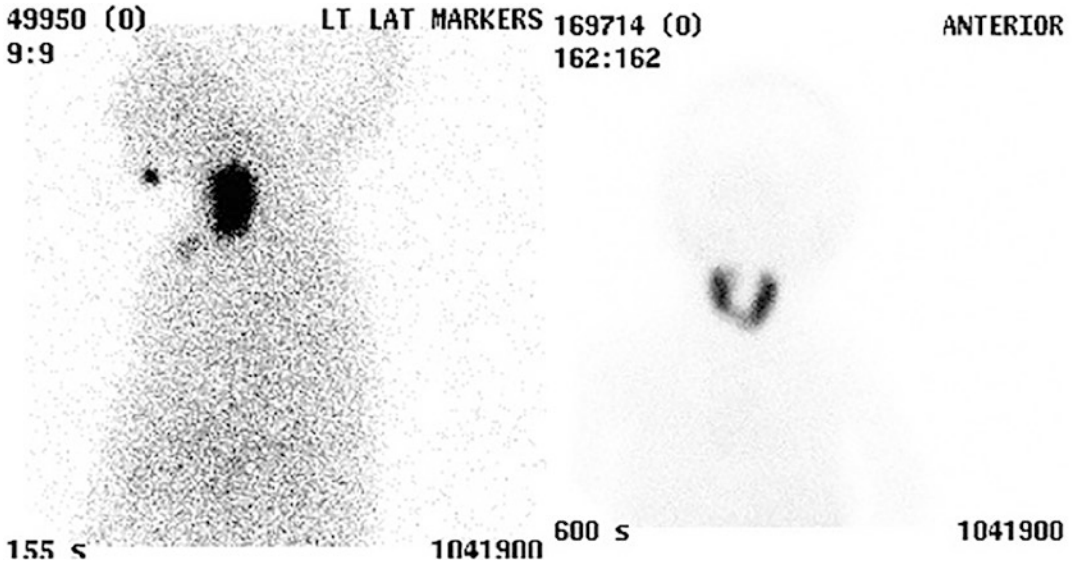


Fig. 5.4 History: Neonate with congenital hypothyroidism. Study report: There is high Pertechnetate uptake of 13.6% (normal range: 0.45–4%) in a normally located

thyroid gland (left-lateral, right-anterior view) showing the usual butterfly shape. Impression: The findings are compatible with dyshormonogenesis

5.2 Thyroid Scintigraphy in Acquired Benign Thyroid Disease

Clinical Indications [8]

- Determining the cause of abnormal thyroid function, both in hyper- and hypothyroidism.
- Evaluation of goiter.
- Evaluation of thyroid nodules.
- Determining the presence of functioning thyroid tissue in a suspected thyroglossal cyst.
- Suspected thyroiditis.
- In combination with radioiodine uptake (RAIU) measurement to calculate the dose for radioactive iodine (RAI) therapy.

Pre-Exam Information

- Recent values of thyroid function tests (thyroid hormones, TSH, antithyroid antibodies).
- History of thyroid disease in the family.
- Medications taken by the child with emphasis on thyroid hormones, antithyroid drugs [e.g., methimazole (mercaptizol®), propylthiouracil (PTU)], and iodine-containing medications (e.g., amiodarone)].
- History and date of exposure to iodine in IV contrast media and iodine-containing antiseptics (e.g., surgical preparation with betadine).
- History of previous thyroid surgery and RAI therapy.
- History of iodine-rich diets or intake of vitamins or nutritional support products.

Study Protocol for Thyroid Scintigraphy

Patient Preparation

- When possible, it is advised to withhold a thyroid scan until the effects of interfering factors diminish:
 - Discontinue iodine-containing drugs, diet, and supplements.
 - Iodine-rich foods and supplements (e.g., seaweed, kelp, and sushi): 1 week.

Lugol's solution, Saturated Solution of Potassium Iodide (SSKI), KI tablets, vitamin/minerals: 1–3 weeks.

Cough medications and skin cleansers containing iodine: 2–4 weeks.

IV iodinated contrast: 4–6 weeks.

Amiodarone: 3–6 months.

- Discontinue drugs that interfere with RAI uptake.

Methimazole, PTU: 3 days.

Lithium carbonate: 1 year (rarely used in children).

- In cases of oral RAI administration: fast for 1–2 hours prior to and 30 minutes after the administration to ensure adequate absorption.

Radiopharmaceutical, Activity, and Mode of Delivery.

Radiopharmaceuticals:

- [^{99m}Tc]Pertechnetate (Pertechnetate): readily available.
- [¹²³I]Na Iodine (¹²³I): theoretically the best tracer.
- [¹³¹I]Na Iodine (¹³¹I): as a rule, it should not be used for the evaluation of benign thyroid diseases, especially in children.

Activity and mode of delivery:

- Pertechnetate: 1.1 MBq/Kg (0.03 mCi/Kg), minimum 7 MBq (0.19 mCi), maximum 93 MBq (2.5 mCi).
- ¹²³I:
 - Administered orally: 3.7–7.4 MBq (0.1–0.2 mCi) after a fast of 1 h.
 - Administered IV: 0.28 MBq/kg (0.0075 mCi/kg) minimum 1 MBq (0.027 mCi), maximum 11 MBq (0.3 mCi).
- ¹³¹I: 0.15–0.37 MBq (0.004–0.01 mCi).
 - Administered orally for RAIU measurements after a fast of 1–2 h.

Refer to the EANM pediatric dosage card and to the North American consensus guidelines on radiopharmaceutical administration in children in the respective EANM and SNMMI and image gently web sites.

Reference to national regulation guidelines, if available, should be considered.

Acquisition Protocol

- Collimator: general purpose, high- or ultrahigh resolution.
 - Pinhole collimator is recommended when available.
- Position: supine, a folded towel under the neck to achieve desired extension.
- The child should be secured to the camera bed. Arms are down by the side of the body.
- Time of imaging:
 - Perchnetate: 20 min after administration.
 - ^{123}I : 2–6 hours after oral and 1 hour after IV administration.
- Static scans: anterior, RAO, LAO, and anterior “bird’s eye” non-zoomed view.
- Duration of acquisition:
 - Perchnetate: 100–200 Kcounts/view.
 - ^{123}I : 50–100 Kcounts/view or 5–20 min.
- Matrix 128 x 128 or 256 x 256.
- ^{57}Co markers should be placed on the suprasternal notch, the chin, and any palpable thyroid nodule to improve spatial orientation.

RAIU Test

- Provides quantitative assessment of RAIU values as a diagnostic add-on to thyroid scan findings.
- It is required for dose calculation when RAI therapy is planned.

- Can be performed with either ^{123}I or ^{131}I .
- Typically RAIU is measured with a probe detector.
- A second dose with the same activity as the one administered to the patient is used as a standard.
- RAIU calculation: ratio between background-corrected counts in the thyroid and counts in the standard.
- Time of measurement: typically at 24 h. Earlier measurements at 4–6 h can be performed as well.
- Normal values: 3–16% at 4 h and 8–25% at 24 h.

Study Interpretation (for Thyroid Scan and RAIU) [9–14]

- The maximal length of each thyroid lobe should be measured serving as a tool to assess the size of the gland.

Suspected hyperthyroidism

- Graves’ disease: demonstrates diffuse thyroid enlargement, increased, homogenous tracer activity, high RAIU.
- “Toxic” autonomous nodule: intense focal uptake and faint, suppressed activity in the remainder of the gland.
- Multinodular goiter: appears as several foci of increased or decreased tracer activity in the thyroid. Some may have mild autonomous activity without suppression of uptake in the adjacent normal gland tissues.
- Thyroid inflammation such as subacute or Hashimoto thyroiditis: various degrees of reduced tracer uptake in the gland and reduced RAIU.

Hypothyroidism

- Autoimmune hypothyroidism or secondary to prior thyroid ablation: reduced tracer uptake and low RAIU.
- Chronic thyroiditis (e.g., Hashimoto): may appear as patchy tracer activity in some cases.
- Ectopic autonomous thyroid tissue (rare cases, e.g., struma ovarii): reduced tracer activity in the thyroid due to TSH suppression.

Correlative Imaging [15–17]

- Thyroid US should be correlated for assessment of gland appearance, presence of nodules, calcification, and vascularity.

Red Flags [18, 19]

- Discontinuation of medications in preparation for a thyroid scan should be decided in collaboration with the referring physician.
- ^{131}I should not be used, in particular, in children, because of the high radiation burden and inferior imaging properties related to its high-energy gamma emission of 364 keV and beta particle emission which adds to radiation burden and limits the amount that may be prescribed, and its relatively long physical half-life of approximately 8 days.
- When imaging with a pinhole collimator the thyroid should fit within the central two-thirds of the FOV to prevent distortion of the gland anatomy.
- Some scintigraphic and RAIU findings are characteristic of specific entities causing thyroid dysfunction, while others are non-specific.
- Small amounts of tracer are excreted in the saliva and accumulate in the oropharynx and esophagus, mimicking uptake in ectopic thyroid tissue or in a pyramidal lobe. Asking the patient to swallow a few sips of water before imaging will eliminate activity in the mouth and esophagus and help prevent misinterpretations.
- Normal RAIU value may depend on the prevalence of iodine in the diet and can vary among different geographical locations.
- Normal RAIU in the presence of very low TSH levels can still indicate Graves' disease.
- Thyroid inflammation may cause transient hyperthyroidism due to the uncontrolled release of thyroid hormones from damaged thyroid tissue.
- Inappropriate intake of thyroid hormones (thyrotoxicosis factitia) can also cause hyperthyroidism with reduced tracer uptake.
- Reduced uptake in euthyroid patients can be due to an iodine-rich diet, to iodine-containing

medications/supplements, to IV administered contrast agents, to antithyroid drugs and hormonal replacement therapy.

- Certain processing software can calculate the percent tracer uptake in the gland from the injected dose. This requires measuring the full and empty syringe counts, and placing thyroid and background regions of interest. The percent uptake from injected dose can aid visual assessment of the intensity of tracer uptake but has not been formally validated and cannot routinely replace RAIU with a dedicated probe.

Take Home Message

- Accurate pre-exam information is essential for the correct interpretation of thyroid scans.
- When available, findings on thyroid scans should always be interpreted in conjunction with thyroid function tests, pertinent clinical findings, and neck US results.
- The presence of a focal increased or decreased tracer uptake seen in the thyroid on a scan and suspected to represent a nodule should be verified by manual palpation and US of the neck.
- An anterior “bird’s eye” non-zoomed view provides a larger FOV that includes the head, neck, and chest, demonstrates the position of the thyroid relative to other structures and allows detection of an intrathoracic extension of the thyroid tissue such as a retrosternal goiter.
- Thyroid nodules are found in approximately 5–7% of children and young adults. They require further evaluation with US-guided fine needle aspiration (FNA) regardless of their appearance on scintigraphy to exclude malignancy.
- Pertechnetate is preferred in children because of the lower radiation burden than ^{123}I which is the most physiologic tracer but limited in availability and expensive.
- RAIU measurements and thyroid scan can be performed with an oral dose of ^{123}I .
- When early RAIU measurements show very low or no uptake, there is no need to recall the

patient for a 24-hour measurement the next day.

- A significant drop between the early and late measurements is characteristic of high iodine turnover in the thyroid.
- In practice, the use of ^{123}I is not a necessity unless a perchlorate discharge test is planned or when used orally for a combined thyroid scan and RAIU measurement.
- When available, ^{123}I is highly preferable to ^{131}I due to the lower radiation exposure and improved image quality.
- The study report should include:
 - Medical history, thyroid function tests, medications, dietary supplements, other

factors that could affect the scan and RAIU results.

- Size and structure of the gland, homogeneity and intensity of tracer activity, uptake in ectopic locations (e.g., pyramidal lobe and thyroglossal cyst).
- Presence and type of thyroid nodules (hot, cold, warm) their location and correlation with manual palpation findings and US results.

Representative Case Examples

Case 5.5. Graves' Disease (Fig. 5.5)

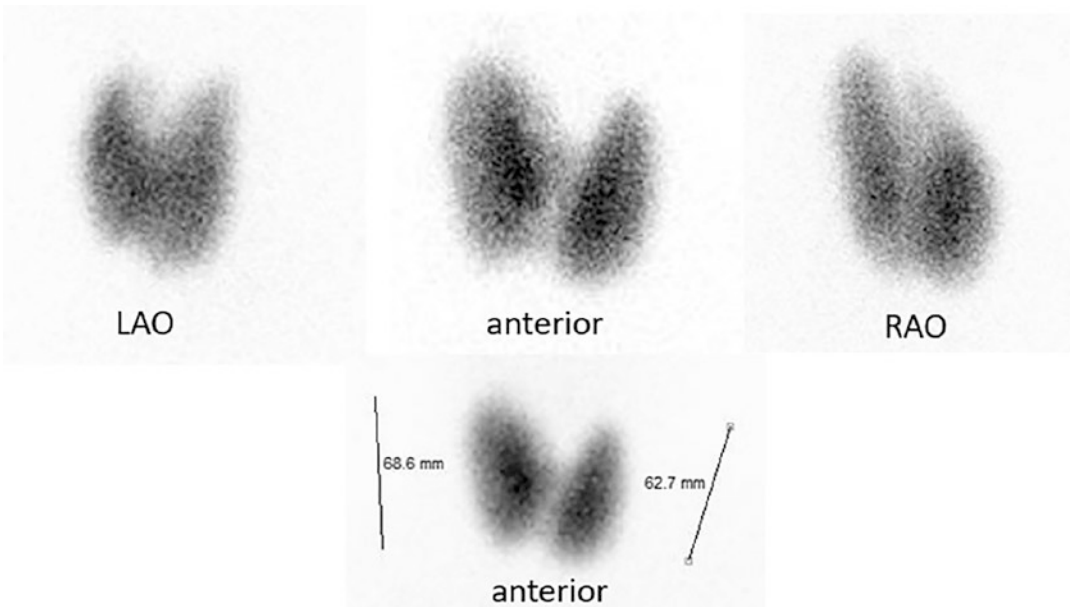


Fig. 5.5 History: A 13-year-old girl presented with heat intolerance, excessive perspiration, tachycardia, palpitations, increased appetite, and weight loss. Thyroid function tests showed a barely measurable plasma TSH of 0.008 mIU/L (normal range 0.51–4.0 mIU/L), highly elevated levels of FT4 70 pmol/L (normal range 10.7–18 pmol/L) and T3 > 30 pmol/L (normal levels 3.5–6.5 pmol/L). Physical examination revealed a large goiter. A Pertechnetate thyroid scan was requested to determine the cause of her overt hyperthyroidism. Study

report: Anterior, LAO and RAO pinhole views (top row) and anterior parallel-hole collimator “bird’s eye” view with size measurements (bottom row) show a markedly enlarged thyroid gland, right lobe larger than left, with intense, homogenous tracer activity. The percent tracer uptake from the injected dose of Pertechnetate is markedly elevated, 30%. Impression: The findings are consistent with Graves’ disease. The girl was treated with beta adrenergic antagonists and methimazole with gradual clinical and biochemical improvement

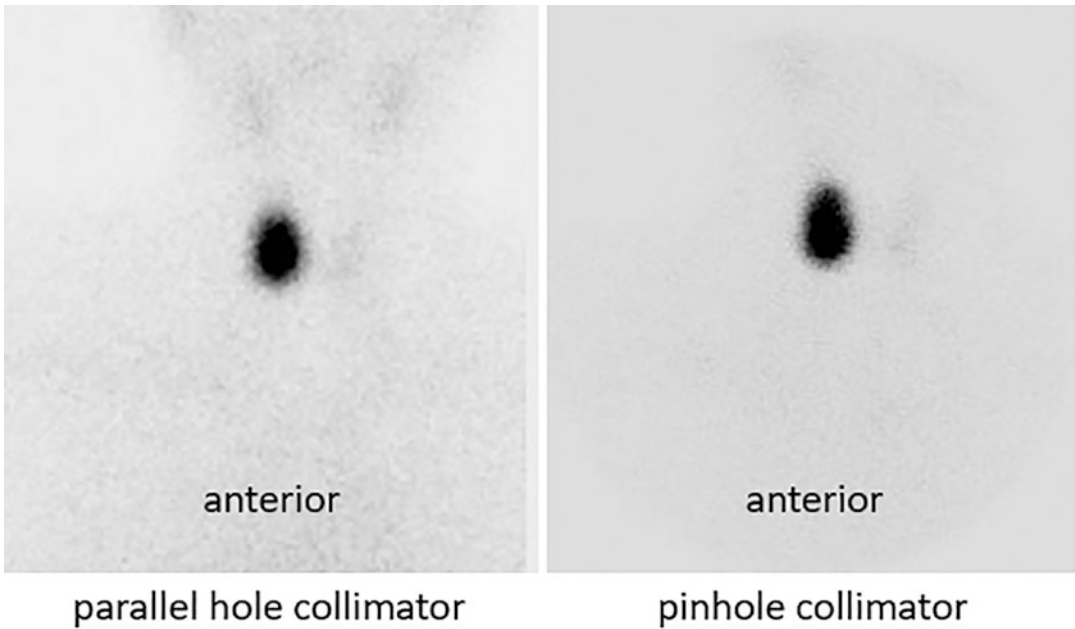
Case 5.6. Autonomous Adenoma (Fig. 5.6)

Fig. 5.6 History: A 16-year-old girl complained of fatigue, weakness and headaches for several months. Her lab results showed low TSH levels, normal FT4 and mildly elevated T3. Physical examination revealed a nodule in the right thyroid lobe. Neck US demonstrated a 2.7×1.5 cm solid nodule in the lower pole of the right thyroid lobe. Study report: A Pertechnetate thyroid scan, anterior view with a parallel-hole collimator (left) and anterior pinhole image (right) show intense tracer uptake

in the lower part of the right thyroid lobe, at the location of the known nodule. The remainder of the right lobe and the entire left lobe show only very faint tracer activity. Impression: The findings are consistent with an autonomous thyroid adenoma suppressing tracer uptake in the normal gland. FNA showed colloid, groups of follicular cells and scattered follicular and microfollicular structures with minor atypia. The patient underwent surgical resection of her right thyroid lobe

5.3 Thyroid Cancer Imaging

Clinical Indications [20–25]

- Post-thyroidectomy: using either ^{123}I or ^{131}I , depending on availability, diagnostic whole-body scan and 24-hour neck RAIU performed at 6–12 weeks post-surgery and Tg measurements. While the American Thyroid Association (ATA) guidelines suggest this for intermediate- and high-risk groups, many pediatric centers perform it in all risk groups [24]:
 - To determine the presence and extent of residual functioning thyroid tissue.
 - To determine the need and dose of RAI for ablation of remnant thyroid tissue.
 - To determine the need and dose of RAI for treatment of metastatic or recurrent disease.
- After RAI therapy: Using either ^{123}I or ^{131}I , depending on availability:
 - Surveillance.
 - To detect the presence and location of residual cancer, recurrence and/or metastases.
- FDG can be used in cases with suspected recurrence because of rising Tg and negative RAI imaging (for doses, acquisition protocol, and study interpretation, see Chap. 12).

Pre-Exam Information [26, 27]

- Discontinue iodine-containing drugs and diet:
 - Iodine-rich foods and supplements (e.g., seaweed, kelp, and sushi): 1 week.
 - Lugol's solution, SSKI, KI tablets, vitamin/minerals: 1–3 weeks.
 - Cough medications and skin cleansers containing iodine: 2–4 weeks.
 - IV iodinated contrast: 4–6 weeks.
 - Amiodarone: 3–6 months.
- Discontinue drugs that interfere with RAI uptake.
 - Lithium carbonate: 1 year (rarely used in children).

- Confirm adequate TSH levels: 30 mIU/L or higher (measured 1–3 days before RAI administration).

Study Protocol for Imaging Pediatric Thyroid Cancer [25, 27, 28]

Patient Preparation.

Methods to reach these TSH levels:

- Thyroid hormone withdrawal:
 - Levothyroxine (l-T4) deprivation for 4 weeks.
 - Alternative: change to triiodothyronine (T3) for 4 weeks, followed by T3 discontinuation for 2 weeks before RAI scintigraphy.
- Recombinant human TSH (rhTSH) stimulation.
 - No need to stop thyroid hormone treatment.
 - Day 1 and 2: intramuscular injection of 0.9 mg rhTSH.
 - Day 3: administration of RAI.
 - Day 4: imaging with ^{123}I .

On the day of the examination:

- Fast for 2 hours prior to tracer administration and continue for 1-h post-administration.
- Instruct the patient to drink water prior to imaging to clear physiologic activity remaining after RAI has been swallowed.

Radiopharmaceutical, Activity, and Mode of Delivery

Radiopharmaceuticals:

- [^{123}I]Na Iodine (^{123}I) oral solution/capsule
- [^{131}I]Na Iodine (^{131}I) oral solution capsule
- [^{18}F]-Fluorodeoxyglucose (FDG).

Activity:

- [¹²³I]Na Iodine in adults: 37–74 MBq (1–2 mCi).
- [¹³¹I]Na Iodine in adults: 37–148 MBq (1–4 mCi).
- [¹⁸F]FDG: 3.7–5.2 MBq/kg (0.1–0.14 mCi/kg) minimum 26 MBq (0.7 mCi).

There is no consensus regarding weight-based administration of these tracers in children.

Reference to national regulation guidelines, if available, should be considered.

Acquisition Protocol*Diagnostic scan:*¹²³I

- Collimator: low energy or medium energy.
- Time of imaging: 6–24 h after RAI administration.
- 15–20% window centered on 159 keV photopeak.

¹³¹I

- Collimator: high energy.
- 15–20% window centered on the 364-keV photopeak.
- Time of imaging: 24–72 h after RAI administration.
- The use of radioactive markers in the neck allows the differentiation between uptake in remnant thyroid tissue, salivary glands, or lymph node metastases.

*Post-therapy scan.*¹³¹I

- Time of imaging: 4–7 days post RAI therapy.

Acquisition parameters:

- Patient positioning: supine with neck in slight extension.
- Whole-body (vertex to mid-thigh) 8–10 cm/min, matrix 256 x 1024.
- Spot images (head, neck, chest, abdomen): 10 min/view, matrix 256 x 256 can replace or be added to whole-body imaging.
- SPECT or SPECT/CT with non-contrast CT, when available, can increase the accuracy and diagnostic confidence of the test.
 - FOV: skull base-to-upper abdomen to evaluate for cervical, upper mediastinal, and pulmonary metastatic disease.
 - 20 sec/step, 64 projections, matrix 128 x 128; iterative reconstruction.

Study Interpretation [29]

- Physiologic activity is seen in the stomach, large intestines, and bladder and of low intensity in the liver and salivary glands.
- False positives can occur due to pooling of excreted activity in sites including saliva in mouth or esophagus, uptake in salivary glands, thymus, ectopic thyroid, and inflammatory foci.
- False negatives can be caused by inadequate patient preparation.
- Star artifacts can be seen as marked streaks going in multiple directions from an area with intense tracer activity.

Correlative Imaging

- Correlation with US of the neck for assessment of remnant thyroid tissue as well as for diagnosis and localization of enlarged regional lymph nodes prior to FNA.
- Correlation with chest CT (without iodinated contrast if ¹³¹I therapy is considered) to evaluate for pulmonary metastases.

Red Flags

- Some centers use lower ^{131}I doses, 37–74 MBq (1–2 mCi), for diagnostic scans in order to reduce the risk of stunning if treatment is considered.
- Adjustment of brightness and contrast on the display monitor of the workstation is standard for appropriate interpretation of whole-body studies.
- Star artifacts can appear in areas with intense tracer activity. They occur because of penetration of photons through the collimator septae, due to a very large flux of photons and/or due to penetration of high-energy photons.
- External contamination can be due to spilled tracer activity onto clothes, skin, or collimator.
- Up to 7% of patients with thyroid cancer have remnant thyroid tissue, and 25% have metastases seen only on the ^{131}I scan performed 3 days post-therapy.
- Additional RAI-avid foci will be detected only on the seventh day of study in approximately 10% of remnant thyroid tissue foci and in 30% of metastatic lesions.

Take Home Messages

- Performing two post-therapy scans can be difficult. The decision for a repeat scan should be made after the initial scan, in cases it is negative, and the patient's Tg is "positive," or if there is clinical or other imaging evidence of metastases. The delayed scan should attempt

to identify the site of the elevated Tg or to define whether the structural abnormality is RAI-avid.

- For ^{123}I there is better lesion detectability on images at 24 hours since in early studies, performed after 6 h, there is still high blood pool and background activity.
- For ^{131}I there is better lesion detectability on diagnostic images performed at 48–72 h. In 24-h studies, images may not have clearly defined activity, and repeat acquisition may be needed to improve the target-to-background ratio.
- Static spot images are, as a rule, superior to computer integrated whole-body acquisitions obtained from moving detectors since they are often obtained following a longer acquisition time, thus resulting in better image quality. They also have the advantage of repeating only a shorter time acquisition if the child moves.
- Focal increased activity in the thyroid bed can be related to remnant thyroid tissue, to small tracer amounts excreted onto the floor of the mouth or esophagus, or malignant lesions such as metastatic lymph nodes. SPECT/CT can help distinguish between these options [30].

Representative Case Examples

Case 5.7. Post-Therapy ^{131}I Study (Fig. 5.7)

Case 5.8. Papillary Thyroid Cancer, Lung Metastasis (Fig. 5.8)

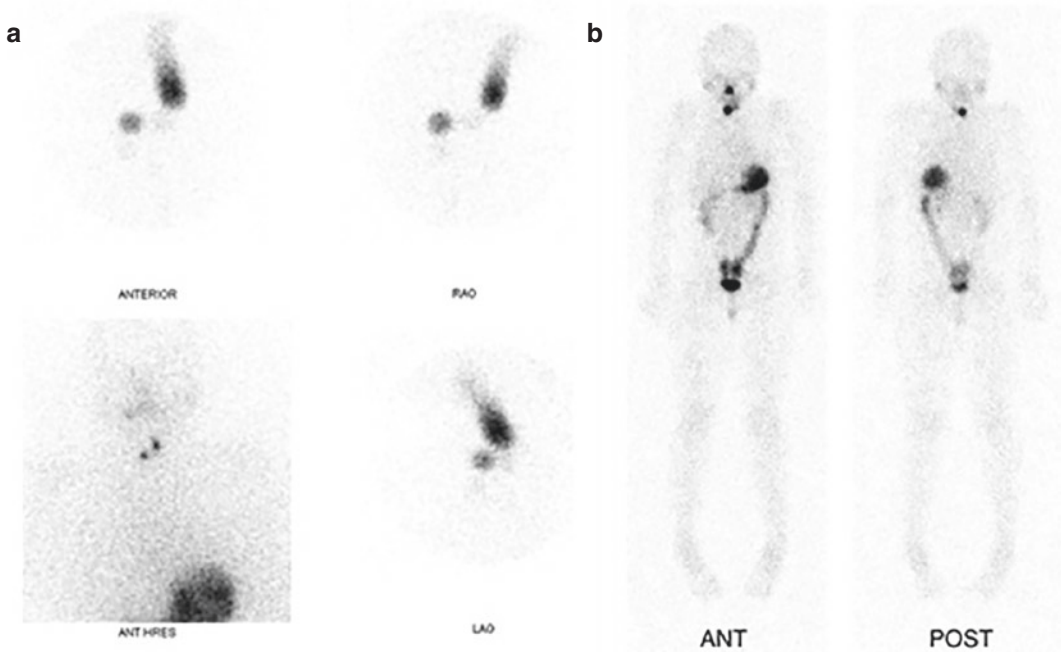


Fig. 5.7 History: A 9-year-old girl had a right thyroid lobe resection followed by complete thyroidectomy for follicular thyroid cancer. Study report: on the post-surgery ^{123}I thyroid scan (a) there are RAI-avid foci with 3% residual tracer uptake in the neck, more in the left lobe of the thyroid. Repeat surgery was performed only on the left side neck because of a significant amount of scar tissue on the right side. The patient then received a 1110 MBq

(30 mCi) ablative dose of ^{131}I and was referred for a post-therapy whole-body scan (b). This study shows a focus of increased tracer uptake in the right neck, corresponding to the known remnant thyroid tissue in the right lobe. No additional lesions are seen. Note also physiologic RAI activity in the GIT, mainly the stomach and bowel, and the urinary bladder, and salivary glands. Impression: No evidence of metastatic thyroid cancer

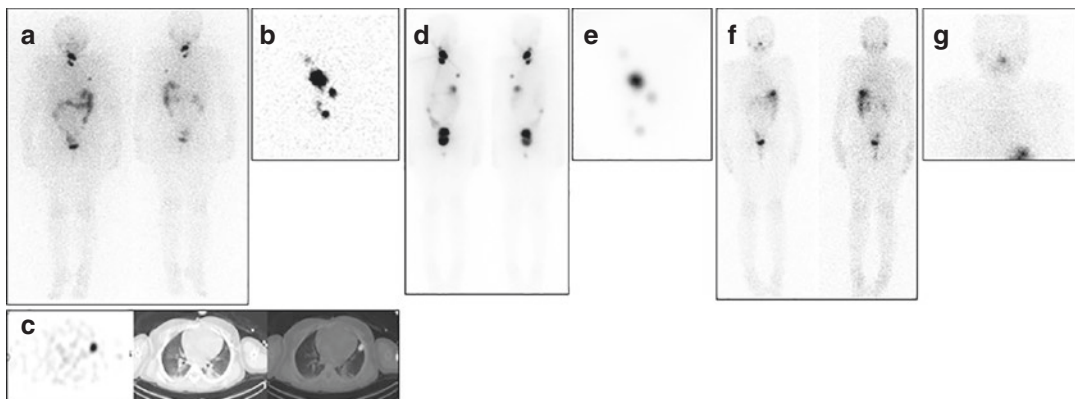


Fig. 5.8 History: A 6-year-old girl presented with a right-sided neck mass and underwent thyroidectomy. A 4-cm papillary carcinoma with extrathyroidal extension and lymph node involvement was found. Study report: The ^{123}I post-thyroidectomy scan (a, whole-body anterior and posterior views, b, pinhole images of the neck) revealed several foci of remnant thyroid tissue in the neck as well as a focal area of tracer uptake in a left lung nodule as demonstrated on SPECT/CT (c), consistent with a RAI-avid left lung metastasis. The patient received a therapeutic dose of

3663 MBq (99 mCi) ^{131}I . Post-therapy ^{131}I whole-body (d) and pinhole images of the neck (e) show the same findings seen on the pretreatment scan. Note also the large amount of physiological RAI excreted into the urinary bladder. A surveillance ^{123}I follow-up study including a whole-body (f) and pinhole neck scan (g) performed 1 year after RAI treatment shows resolution of the previously seen foci of increased RAI activity in the neck and in the left lung metastasis. There are no new areas of abnormal RAI uptake. Impression: No evidence of thyroid cancer

Case 5.9. Dedifferentiated Non-RAI-Avid, FDG-Avid Thyroid Cancer (Fig. 5.9)

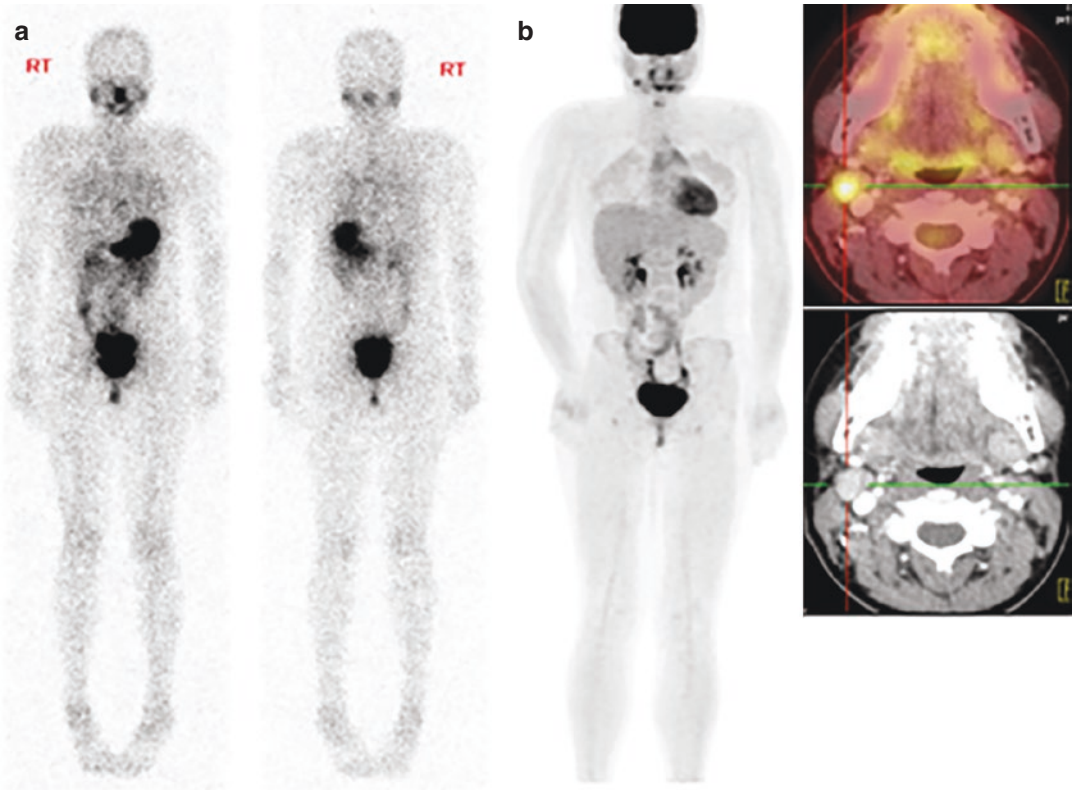


Fig. 5.9 History: A 14-year-old girl presented with a right thyroid nodule. US-guided FNA diagnosed papillary thyroid cancer. The patient underwent thyroidectomy and lymph node dissection. Right cervical lymph node metastases were found. Study report: A ^{123}I whole-body scan performed after surgery was negative (**a**). The patient received RAI treatment with 3440 MBq (93 mCi) ^{131}I . No sites of disease were found on a post-therapy scan (not

shown). Six months later, the patient presented with rising Tg levels and suspicious cervical nodes on US. Because of known non-RAI-avid disease, the patient was referred to FDG-PET/CT (**b**) which shows a focal area of tracer uptake in the right upper cervical region. Impression: The findings are consistent with right cervical lymph node metastasis, further confirmed following lymph node dissection

References

- American Academy of Pediatrics, et al. Update of newborn screening and therapy for congenital hypothyroidism. *Pediatrics*. 2006;117(6):2290–303.
- Grant FD, Treves ST. Thyroid. In: Treves ST, editor. *Pediatric nuclear medicine and molecular imaging*. New York, NY: Springer New York; 2014. p. 99–129.
- Leger J, et al. European Society for Paediatric Endocrinology consensus guidelines on screening, diagnosis, and management of congenital hypothyroidism. *J Clin Endocrinol Metab*. 2014;99(2):363–84.
- van Trotsenburg P, et al. Congenital Hypothyroidism: a 2020-2021 Consensus Guidelines Update-An ENDO-European Reference Network Initiative Endorsed by the European Society for Pediatric Endocrinology and the European Society for Endocrinology. *Thyroid*. 2021;31(3):387–419.
- Clerc J, et al. Scintigraphic imaging of paediatric thyroid dysfunction. *Horm Res*. 2008;70(1):1–13.
- Worth C, et al. Thyroid scintigraphy differentiates subtypes of congenital hypothyroidism. *Arch Dis Child*. 2021;106(1):77–9.
- Meller J, et al. Diagnostic value of 123iodine scintigraphy and perchlorate discharge test in the diagnosis of congenital hypothyroidism. *Exp Clin Endocrinol Diabetes*. 1997;105(Suppl 4):24–7.
- Volkan-Salanci B, Kiratlı P. Nuclear medicine in thyroid diseases in pediatric and adolescent patients. *Mol Imaging Radionucl Ther*. 2015;24(2):47–59.
- Williams JL, Paul DL, Bisset G 3rd. Thyroid disease in children: part 1: state-of-the-art imaging in pediatric hypothyroidism. *Pediatr Radiol*. 2013;43(10):1244–53.
- Williams JL, Paul D, Bisset G 3rd. Thyroid disease in children: part 2 : state-of-the-art imaging in pediatric hyperthyroidism. *Pediatr Radiol*. 2013;43(10):1254–64.
- Gupta A, et al. A standardized assessment of thyroid nodules in children confirms higher cancer prevalence than in adults. *J Clin Endocrinol Metab*. 2013;98(8):3238–45.
- Corrias A, Mussa A. Thyroid nodules in pediatrics: which ones can be left alone, which ones must be investigated, when and how. *J Clin Res Pediatr Endocrinol*. 2013;5(Suppl 1):57–69.
- Giovanella L, et al. EANM practice guideline/ SNMMI procedure standard for RAIU and thyroid scintigraphy. *Eur J Nucl Med Mol Imaging*. 2019;46(12):2514–25.
- Iakovou I, Giannoula E, Sachpekidis C. Imaging and imaging-based management of pediatric thyroid nodules. *J Clin Med*. 2020;9:2.
- Silva CT, Navarro OM. Pearls and pitfalls in pediatric thyroid imaging. *Semin Ultrasound CT MR*. 2020;41(5):421–32.
- Tritou I, et al. Pediatric thyroid ultrasound: a radiologist's checklist. *Pediatr Radiol*. 2020;50(4):563–74.
- Fornwalt B, et al. Pediatric thyroid nodules: ultrasound characteristics as indicators of malignancy. *OTO Open*. 2022;6(1):2473974x211073702.
- Mariani G, et al. The role of nuclear medicine in the clinical management of benign thyroid disorders, part 1: hyperthyroidism. *J Nucl Med*. 2021;62(3):304–12.
- Mariani G, et al. The role of nuclear medicine in the clinical management of benign thyroid disorders, part 2: nodular goiter, hypothyroidism, and subacute thyroiditis. *J Nucl Med*. 2021;62(7):886–95.
- Grigsby PW, et al. Childhood and adolescent thyroid carcinoma. *Cancer*. 2002;95(4):724–9.
- Newman KD, et al. Differentiated thyroid cancer: determinants of disease progression in patients <21 years of age at diagnosis: a report from the surgical discipline Committee of the Children's cancer group. *Ann Surg*. 1998;227(4):533–41.
- Luster M, et al. Thyroid cancer in childhood: management strategy, including dosimetry and long-term results. *Hormones (Athens)*. 2007;6(4):269–78.
- Franzius C, et al. Procedure guideline for radioiodine therapy and 131iodine whole-body scintigraphy in paediatric patients with differentiated thyroid cancer. *Nuklearmedizin*. 2007;46(5):224–31.
- Francis GL, et al. Management guidelines for children with thyroid nodules and differentiated thyroid cancer. *Thyroid*. 2015;25(7):716–59.
- Lebbink CA, et al. New national recommendations for the treatment of pediatric differentiated thyroid carcinoma in The Netherlands. *Eur J Endocrinol*. 2020;183(4):P11–8.
- Kuijt WJ, Huang SA. Children with differentiated thyroid cancer achieve adequate hyperthyrotropinemia within 14 days of levothyroxine withdrawal. *J Clin Endocrinol Metab*. 2005;90(11):6123–5.
- Luster M, et al. Recombinant thyrotropin use in children and adolescents with differentiated thyroid cancer: a multicenter retrospective study. *J Clin Endocrinol Metab*. 2009;94(10):3948–53.
- Bartel Chair TB, et al. SNMMI procedure standard for scintigraphy for differentiated thyroid cancer. *J Nucl Med Technol*. 2020;48(3):202–9.
- Mostafa M, et al. Variants and pitfalls on radioiodine scans in pediatric patients with differentiated thyroid carcinoma. *Pediatr Radiol*. 2016;46(11):1579–89.
- Nadel HR. SPECT/CT in pediatric patient management. *Eur J Nucl Med Mol Imaging*. 2014;41(Suppl 1):S104–14.

The opinions expressed in this chapter are those of the author(s) and do not necessarily reflect the views of the IAEA: International Atomic Energy Agency, its Board of Directors, or the countries they represent.

Open Access This chapter is licensed under the terms of the Creative Commons Attribution 3.0 IGO license (<http://creativecommons.org/licenses/by/3.0/igo/>), which permits use, sharing, adaptation, distribution and reproduction in any medium or format, as long as you give appropriate credit to the IAEA: International Atomic Energy Agency, provide a link to the Creative Commons license and indicate if changes were made.

Any dispute related to the use of the works of the IAEA: International Atomic Energy Agency that cannot be settled amicably shall be submitted to arbitration pursuant to the UNCITRAL rules. The use of the IAEA: International Atomic Energy Agency's name for any purpose other than for attribution, and the use of the IAEA: International Atomic Energy Agency's logo, shall be subject to a separate written license agreement between the IAEA: International Atomic Energy Agency and the user and is not authorized as part of this CC-IGO license. Note that the link provided above includes additional terms and conditions of the license.

The images or other third party material in this chapter are included in the chapter's Creative Commons license, unless indicated otherwise in a credit line to the material. If material is not included in the chapter's Creative Commons license and your intended use is not permitted by statutory regulation or exceeds the permitted use, you will need to obtain permission directly from the copyright holder.



Anita Brink, Lorenzo Biassoni, and Zvi Bar-Sever

6.1 Gastroesophageal Reflux Scintigraphy (“MILK SCAN”)

Clinical Indications [1, 2]

GER scintigraphy, is a sensitive, noninvasive, physiologic, direct technique indicated to detect GER and possible pulmonary aspiration in children with:

- Signs and symptoms suggesting gastroesophageal reflux disease (GERD).
- Recurrent lower respiratory tract infections.
- Recurrent vomiting.
- Failure to thrive.
- Apparent life-threatening events (ALTE).

A. Brink (✉)

Nuclear Medicine Department, Division of Radiation Medicine, University of Cape Town, Cape Town, South Africa

Nuclear Medicine and Diagnostic Imaging Section, Division of Human Health, Department of Nuclear Sciences and Applications, International Atomic Energy Agency, Vienna, Austria

L. Biassoni

Department of Radiology, Great Ormond Street Hospital for Children NHS Foundation Trust, London, UK
e-mail: Lorenzo.Biassoni@gosh.nhs.uk

Z. Bar-Sever

Schneider Children’s Medical Center, Tel Aviv University, Petah Tiqva, Israel

Pre-Exam Information

- Feeding route: Orally, through nasogastric (NG) or permanent gastric tube.
- Volume and composition of a regular meal.
- Does the child have a milk allergy?
- Barium study performed in the previous 48 h?

Study Protocol for GER Test (“Milk Scan”) [3]

Patient Preparation:

- Older children: 4–6 h fast
- Young infants: The study should be scheduled to replace a normal feeding, assuming the infant is fed every 3–4 h.
- Bring a feeding bottle with the child’s regular meal such as cow milk, expressed breast milk, milk-based formula, and an additional empty bottle.
- Children allergic or intolerant to milk: orange juice or other liquid meal substitutes can be used.

Radiopharmaceutical, Administered Activity, Mode of Delivery

Radiopharmaceutical:

- [^{99m}Tc]sulfur colloid (SC)—is recommended.
- Alternative: [^{99m}Tc]Sn colloid, [^{99m}Tc]phytate.

Activity:

- A fixed dose of 9.25 MBq (0.25 mCi) for SC is recommended by the SNMMI. The EANM pediatric dose card uses patient weight to calculate the dose.
- Refer to the EANM pediatric dosage card and to the North American consensus guidelines on radiopharmaceutical administration in children in the respective EANM and SNMMI and image gently web sites.

Reference to national regulation guidelines, if available, should be considered.

Mode of Delivery—Feeding the Child:

- Added to 1/3–1/2 of the normal milk or formula feeding volume.
- Introduce this labelled portion to the stomach by oral feeding or, in children with feeding difficulties, through a NG tube (to be removed after feeding) or through an existing gastric tube.
- Continue feeding from a separate bottle containing the remaining non-labelled portion of the meal.
- The total meal volume should be similar to the volume the child is given for regular meals.
- Ideally, feeding should be completed within 10–15 mins.
- When possible, young infants should be burped before imaging.
- Placing disposable absorbent sheets lined on one side with plastic material over the neck, chest, and abdomen can contain potential contamination.

Acquisition Protocol:

- Position: Supine.
- Posterior views with the detector behind the patient.

- Field-of-view (FOV): Chest and upper abdomen.
- *Acquisition parameters:*
 - Posterior dynamic images for 60 mins, 10–30 s/frame, matrix 128 × 128.
 - 1-h static anterior and posterior views of the chest, immediately after dynamic study, for an acquisition time of 3–5 mins, matrix 256 × 256.
 - 2–4 h static anterior and posterior views of the chest, after completion of the meal, for an acquisition time of 3–5 mins, matrix 256 × 256.
 - 24-h static images can be obtained as well.
 - Markers placed over suprasternal notch and xiphoid and/or ⁵⁷Co transmission image of the thorax can be used to improve orientation and help determine the reflux level and to adequately localize ectopic activity over the chest.

Study Interpretation

- New appearance of tracer activity in the esophagus indicates an episode of GER.
- If reflux is detected the following parameters should be recorded:
 - Number of episodes.
 - Level of reflux: proximal or distal esophagus, oropharynx.
 - Intensity of reflux: mild, moderate, severe.
 - Volume of reflux: can be calculated by drawing a region-of-interest (ROI) over the activity in the esophagus and over the activity in the esophagus and stomach.
- Estimate the residence time of the GER by dividing the number of frames showing tracer activity in the esophagus by the total number of frames.

- Tracer localization in the tracheobronchial tree or in the lung parenchyma can be suggestive of pulmonary aspiration.
- Including the stomach in the FOV allows calculation of “milk based” gastric emptying (GE) rates.
- Visual inspection can be aided by creating a time-activity curve (TAC) from a ROI placed over the esophagus.
- The continuation of feeding with the non-labelled portion of the meal plays an important role by clearing residual tracers from the oropharynx and esophagus prior to imaging.
- A child with feeding difficulties should be fed using a NG tube.
- If the child is fed through a naso-jejunal tube this should be replaced by a NG tube prior to the study.

Correlative Tests and Imaging

- Extended esophageal pH monitoring:
 - Requires placement of a transnasal pH catheter into the esophagus to measure the pH over 24 h.
 - Extended monitoring provides an accurate estimation of the residence time of gastric content in the esophagus.
 - A drop in esophageal pH below 4 is suggestive of an acid reflux episode.
 - Limitations: invasive nature; inability to detect episodes of nonacidic reflux which have been associated with several pulmonary manifestations of GERD.
 - Intraluminal esophageal electrical impedance electrodes placed on a NG tube detect both acidic and nonacidic retrograde flow in the esophagus and are often coupled with esophageal pH monitoring thus increasing the sensitivity of the study.
- Barium contrast radiography:
 - It is less sensitive in detecting reflux episodes and pulmonary aspiration.
 - It can show anatomical conditions that produce symptoms similar to GERD (pyloric stenosis, malrotation, etc.).
 - It can assess GER complications such as esophagitis and esophageal strictures.
- GER scintigraphy can also diagnose gastric dysmotility providing the stomach is included in the FOV.
- This study has a low detection yield for the detection of aspiration. Contamination artifacts over the lungs can be erroneously interpreted as pulmonary aspiration or prevent detection of such aspiration.
- GER scintigraphy can also diagnose gastric dysmotility providing the stomach is included in the FOV.

Take Home Messages

- GER scintigraphy is a low dose, simple, sensitive, and physiologic study that can diagnose all three related conditions: GER, pulmonary aspiration, and gastric dysmotility.
- SC is not absorbed by the GI or pulmonary mucosa and remains stable in the acidic medium of the stomach.
- Scintigraphy, with its long imaging time, can help diagnose GER, an intermittent phenomenon.
- Static images performed at 1 and 2 h, and potentially 24 h after administration of the radioactive meal aim to detect subtle pulmonary aspiration that was not evident in the early, dynamic images.

Red Flags

- Extra care should be taken to avoid external contamination due to spillage of labelled milk during feeding or due to vomiting or regurgitation.

Representative Case Examples

Case 6.1. Severe Gastroesophageal Reflux Disease (Fig. 6.1)

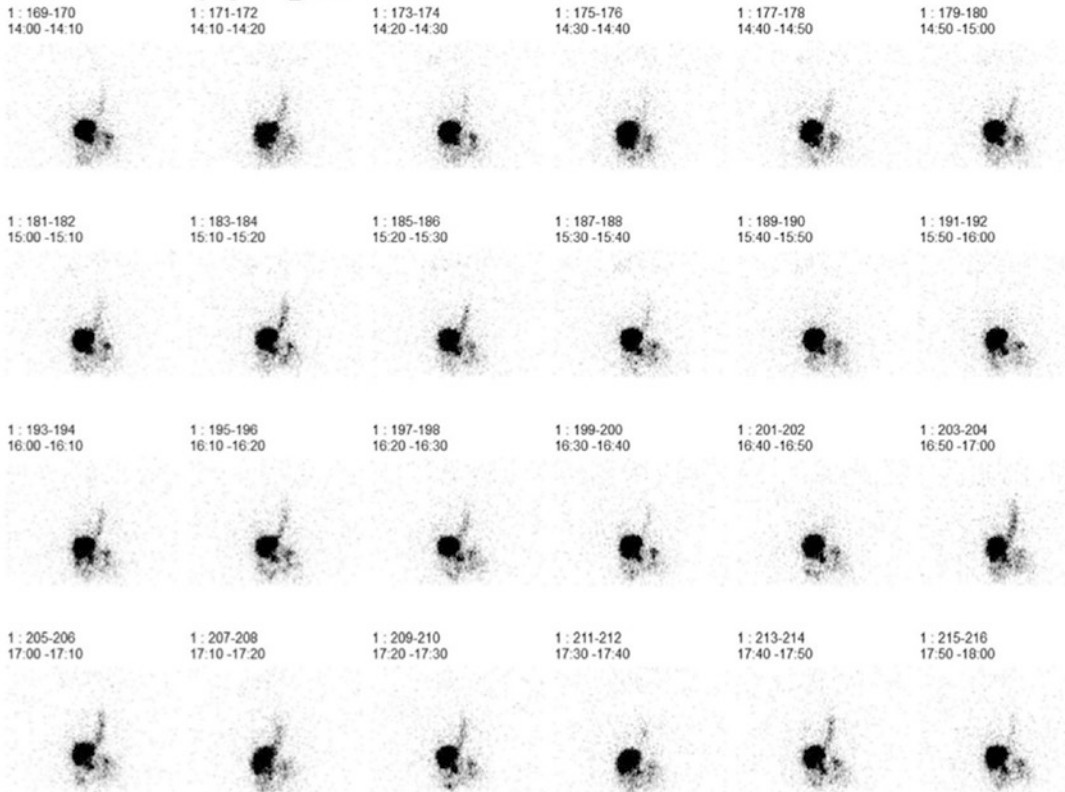


Fig. 6.1 History: An 8-year-old child with Trisomy 21 and Moya-Moya disease. Aspiration was noted on a recently modified barium swallow test. A milk scan was performed to assess for GER after administration of 18 MBq [Tc]Sn colloid in a volume of feed of 230 ml given through a nasogastric tube which was removed before the reflux search. Study report (only the frames

recorded from 14 to 18 mins are shown): Reflux reaching the proximal esophagus is seen on most of the 360 frames recorded during the observation period. The longest reflux lasts 170 s. The refluxes contain up to 9 and 11% of total activity. Impression: The findings are consistent with very severe GER

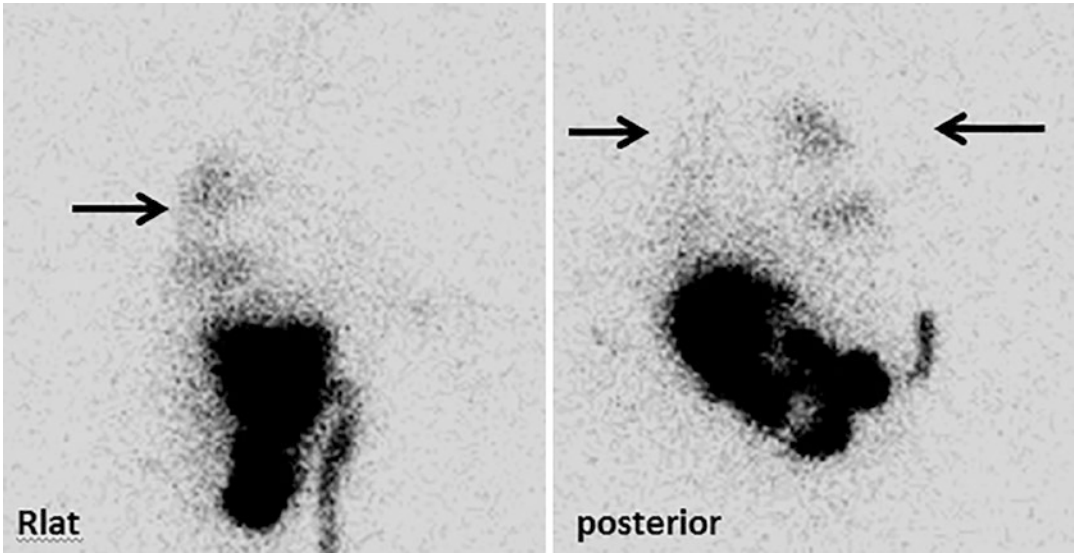
Case 6.2. Pulmonary Aspiration (Fig. 6.2)

Fig. 6.2 History: A 12-year-old boy with spastic cerebral palsy and failure to thrive presented with swallowing difficulties. A GER study was performed to assess if GERD was the cause for his failure to thrive. The tracer and a milk-based meal were given orally. Study report: Multiple refluxes were observed during the GER study that fre-

quently reach buccal level (not shown). Posterior static images recorded at the end of the reflux search (left) and at 2 h after tracer administration (right), demonstrate a large amount of tracer activity in the bronchial tree (arrows), more on the right. Impression: The findings are consistent with pulmonary aspiration

6.2 Gastric Emptying

Clinical Indications [4]

- Determination of the gastric emptying rate in children with suspected gastric dysmotility:
 - Solid GE is considered more reliable and is the preferred study in older children and adolescents.
 - Liquid GE (better referred to as a semisolid meal), mostly milk based, is the only study that can be performed in infants and young children.

Pre-Exam Information

- History of food allergies, especially to milk or eggs.
- Feeding route: orally, NG tube, permanent gastric tube.
- Medications: some drugs such as proton pump inhibitors can affect GE.
- The referring physician should be consulted on whether the gastric motility should be assessed with or without medication intake.

Study Protocol for Liquid Gastric Emptying Test [1, 4, 5]

Patient Preparation:

- Older children: 4–6 h fast.
- Infants and young children:
 - Plan the study to replace scheduled feeding (assuming the infant is fed every 3–4 h).
 - Bring the child's regular meal (cow milk, human milk, milk-based formula) in his/her regular feeding bottle and an additional empty bottle.

Radiopharmaceutical, Administered Activity, Mode of Delivery

Radiopharmaceutical:

- [^{99m}Tc]sulfur colloid (SC)—is recommended.
- Alternative: [^{99m}Tc]Sn colloid, [^{99m}Tc] phytate.

Activity:

- A fixed dose of 9.25 MBq (0.25 mCi) for SC is recommended by the SNMMI. The EANM pediatric dose card uses patient weight to calculate the dose.
- Refer to the pediatric dosage card and to the North American consensus guidelines on radiopharmaceutical administration in children in the respective EANM and SNMMI and image gently web sites. Reference to national regulation guidelines, if available, should be considered.

Mode of Delivery:

- Added to 1/3–1/2 of the normal milk or formula feeding volume.
- Introduce this labelled portion to the stomach by oral feeding or, in children with feeding difficulties, through a NG tube (to be removed after feeding) or through an existing gastric tube.
- Continue feeding from a separate bottle containing the remaining non-labelled portion of the meal.
- The total meal volume should be similar to the volume the child is given for regular meals.
- Ideally, feeding should be completed within 10–15 mins.
- When possible, young infants should be burped before imaging.
- Placing disposable absorbent sheets lined on one side with plastic material over the neck, chest, and abdomen can contain potential contamination.
- Older children allergic or intolerant to milk: orange juice or other liquid meal substitutes can be used.

Acquisition Protocol:

Liquid gastric emptying—GE with milk or formula is often performed simultaneously with evaluation of GER.

Acquisition Parameters:

- Position: supine, secured to the imaging bed.
- FOV: should include the abdomen. If possible, the chest should be in the FOV when the study is also performed to evaluate GER.
- Acquisition parameters:
- Posterior view.
- Dynamic images for 60 mins, 10–30 s/frame, matrix 128 × 128.
- Static images at 1 and 3 h, matrix 256 × 256.
- Older children: anterior and posterior 1-, 2-, and 4-h static images of the stomach and chest over 3–5 mins, matrix 256 × 256.
- Infants: posterior images only at 1 and 3 h.

Study Processing and Interpretation [6–8]

- Percent GE values are calculated by placing separate ROIs over the stomach and bowel activity and further dividing the bowel counts by the sum of the gastric and bowel counts.
- Normal reference values for liquid GE in infants and young children up to 5 years old are not defined but “pseudo”-normal values derived retrospectively from a large study group of children are currently used [8].
- Normal liquid GE was defined retrospectively as >50% at 1 h and > 80% at 3 h post-feeding.

Study Protocol for Solid Gastric Emptying Test [1, 4, 5]**Patient Preparation:**

- Older children: 4–6 h fast.
- Young children: plan the study to replace scheduled feeding (assuming the infant is fed every 3–4 h).

Radiopharmaceutical, Administered Activity, Mode of Delivery*Radiopharmaceutical:*

- [^{99m}Tc]sulfur colloid (SC)—is recommended.
- Alternative: [^{99m}Tc]Sn colloid, [^{99m}Tc] phytate.

Activity:

- A fixed dose of 9.25 MBq (0.25 mCi) for SC is recommended by the SNMMI. The EANM pediatric dose card uses patient weight to calculate the dose.

Refer to the pediatric dosage card and to the North American consensus guidelines on radiopharmaceutical administration in children in the respective EANM and SNMMI and image gently web sites.

Reference to national regulation guidelines, if available, should be considered.

Mode of Delivery:

- The standard meal used for adults can be adapted for pediatric studies:
 - 120 grams of egg white
 - 2 toasted slices of white bread
 - 30 grams of strawberry jam
 - 120 ml of water
- Alternative (in cases of egg allergy or intolerance): meal based on bran, pudding, chocolate crispy cake, yogurt, cheddar cheese.

Acquisition Protocol:

- The adult protocol for solid gastric emptying should be used when possible.
- Static upright anterior and posterior views of the upper abdomen are acquired for 1 min at: time 0 (immediately) and at 1, 2, 3, and 4 h after meal ingestion.

Study Processing and Interpretation [6–8]

- GE measurements are based on gastric counts derived from the geometric mean of anterior and posterior 1 min static images in the upright position.
- Normal values of residual stomach activity at 1, 2, 3, and 4 h with a standard solid meal are available for adults. These values were validated in a large group of pediatric patients, and it has been shown that these criteria can be applied to pediatric patients.
- These values are:
 - 37–90% at 1 h
 - 30–60% at 2 h
 - Less than 30% at 3 h.
 - Less than 10% at 4 h.

Correlative Imaging

- GE scintigraphy is the gold standard for the assessment of functional abnormalities in gastric motility.
- Upper GI endoscopy can assist in excluding other causes of motility disorders such as esophagitis, gastritis, or masses.
- Conventional radiologic imaging techniques are used for the evaluation of anatomical malformations that cause motility disorders.
- Barium contrast radiography specifically is used to exclude anatomical abnormalities which could mimic functional abnormalities such as malrotation, stenoses, etc.

Red Flags

- Meal standardization is essential for the scintigraphic evaluation of GE as well as for any meaningful comparison of follow-up studies.
- The most stable label is achieved by cooking the radiopharmaceutical with egg whites. Cooking with whole egg results in lower labelling stability.
- Alternative meals given to children with egg allergy or intolerance are less standardized and the labelling stability may be significantly lower.
- If vomiting occurs during the study, the calculated gastric residuals may be inaccurate.
- In infants posterior views are sufficient because of the small body habitus. They are more comfortable and allow easy access to technologists and caregivers.
- In older children, acquisition of both anterior and posterior views allows for a more precise assessment of gastric activity from the geometric mean of counts obtained in both images.
- The images should be scrutinized for patient motion. If present, the gastric ROI may be inaccurate and include activity originating from adjacent bowel loops. Applying motion correction can resolve this issue. For static images, it is advised to draw a separate gastric ROI for each image.

Take Home Messages

- GE with milk or formula is often performed simultaneously with an evaluation of GER.
- Meal standardization is essential.
- The most commonly used quantitative value is the gastric residual activity which can be easily calculated by dividing the decay corrected counts within a gastric ROI at specific time points by the initial gastric counts at the start of the acquisition.
- Solid GE is more standardized and reliable and should be used when possible.

- “Pseudo” normal reference values for liquid gastric emptying in children younger than 5 years were recently established, derived retrospectively from a selected group of over 2000 children without risk factors for gastric dysmotility who underwent GER scintigraphy.

Representative Case Examples

Case 6.3. Delayed Gastric Emptying (Fig. 6.3)

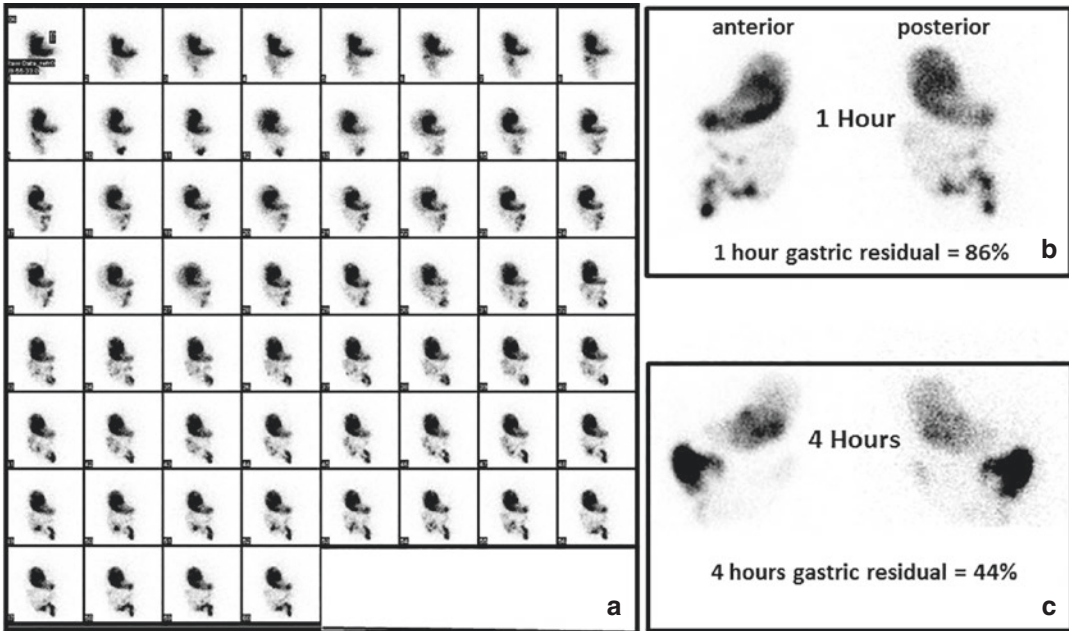


Fig. 6.3 History: A 22-month-old girl with repeat episodes of regurgitation and vomiting was referred for evaluation. The patient was fed orally with 230 cc of milk formula labelled with Tc-sulfur colloid. Study report: Posterior view dynamic images obtained for 60 mins (**a**) demonstrate marked retention of tracer in the stomach.

Static images obtained at 1 h (**b**) and 4 h (**c**) after completion of feeding show significant gastric residual activity. The gastric residue from the initial gastric activity was 86% at 60 mins and 44% at 4 h. Impression: These findings suggest delayed gastric emptying

6.3 Esophageal Transit Studies

Clinical Indications

Visual detection and quantitative evaluation of esophageal transit abnormalities.

Study Protocol for Esophageal Transit Studies [1]

Patient Preparation:

- Plan the study to replace scheduled feeding (assuming the infant is fed every 3–4 h).
- Bring the child's regular meal (cow milk, human milk, milk-based formula) in his/her regular feeding bottle and an additional empty bottle.

Radiopharmaceutical, Administered Activity, Mode of Delivery

Radiopharmaceutical:

- [^{99m}Tc]Sn-colloid or [^{99m}Tc]sulfur colloid.

Activity:

- A fixed dose of 9.25 MBq (0.25 mCi) for SC is recommended by the SNMMI. The EANM pediatric dose card uses patient weight to calculate the dose.

Refer to the pediatric dosage card and to the North American consensus guidelines on radiopharmaceutical administration in children in the respective EANM and SNMMI and image gently web sites.

Reference to national regulation guidelines, if available, should be considered.

Delivery:

- A small volume (2.5–5 ml) of the feed is labelled and given to the patient with a syringe.

Acquisition Protocol:

- The study is performed with the detector upright.
- The child drinks the activity on the parent's/caregiver's lap with the back against the camera, so the esophagus is viewed from the left posterior oblique position.
- Acquisition parameters: dynamic study, 0.5 s/frame, 120 frames, matrix 128 × 128.
- Take care to keep the child still during the acquisition.

Study Interpretation

- Review the raw data in planar and cine format.
- The raw data is then converted to a condensed image (Fig. 6.4).

Normal Transit Study

- The normal transit time of activity through the entire esophagus is less than 3 s.
- With most swallows, there is a transient hold-up of activity at the level of the gastroesophageal junction (GEJ) which should decrease from a maximum of 4 s for swallow initiated during the first 4 s of the study to less than 0.5 s after 12 s.
- A hold-up of less than 2 s is considered normal.

Common Pathological Patterns

- Hold-up in the proximal esophagus, at the cricopharyngeal level, with prolonged initiation of swallowing: can be found in children with neurological abnormalities.
- Hold-up high in the esophagus with slower transit distal to the stricture: can indicate esophagitis due to causes other than GER or to the presence of anatomical abnormalities (e.g., aberrant pulmonary artery, repaired tracheoesophageal fistula, esophageal stricture).

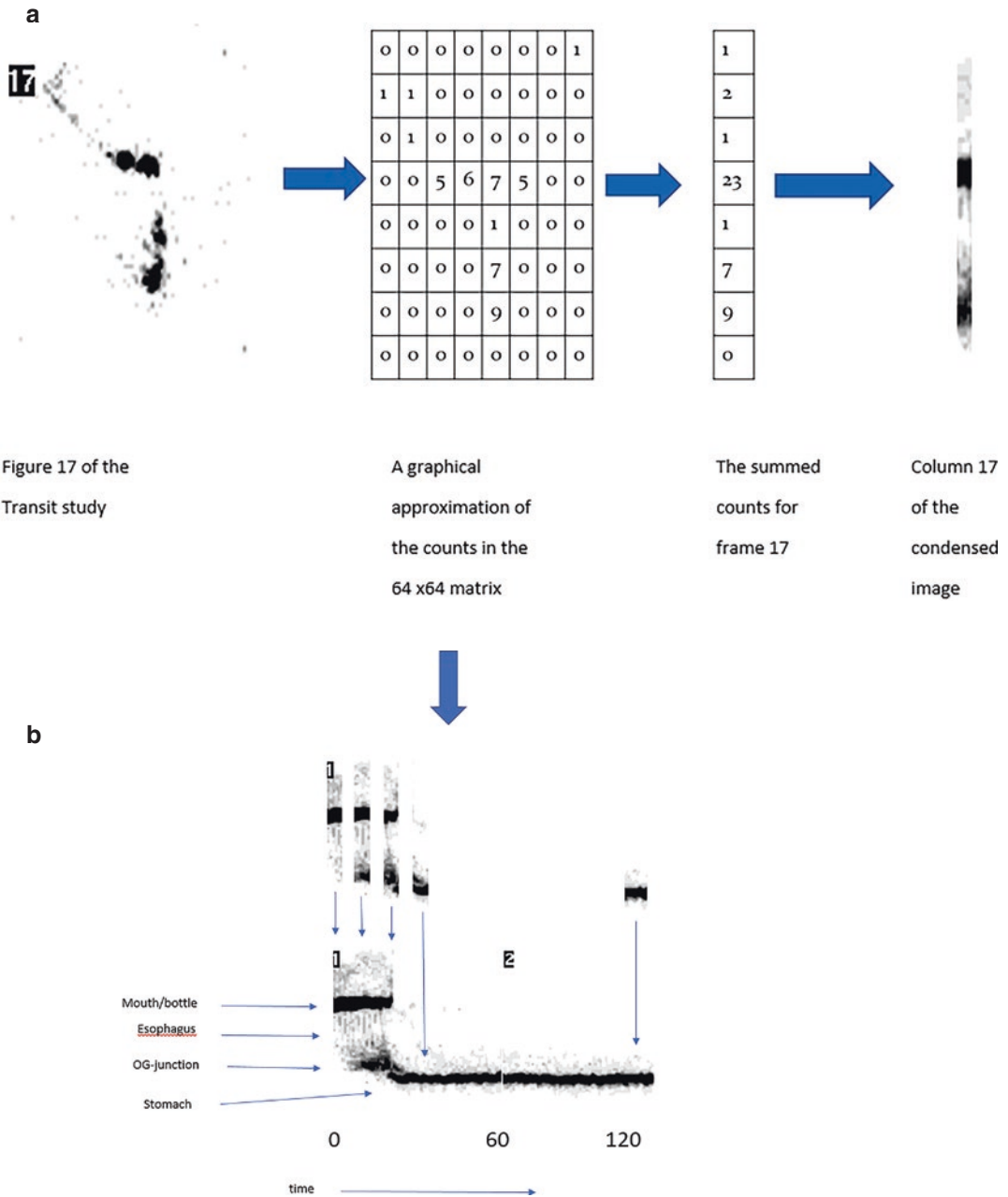


Figure 17 of the Transit study

A graphical approximation of the counts in the 64 x64 matrix

The summed counts for frame 17

Column 17 of the condensed image

Fig. 6.4 Condensed image in a study with normal esophageal transit. Image (a) illustrates how the raw data of a single image of the dynamic series are compressed into a single column of the condensed image. Image (b) illustrates how the summed columns of each of the dynamic

image frames are arranged sequentially to form the condensed image. The condensed image makes it easier to assess the transit of activity through the esophagus from the mouth to the stomach

- Hold-up at more distal esophageal levels with succeeding swallows or slowing of each successive swallow may be seen in:
- Prematurity.
- Transient over the first 3 months.
- In children who are developing cerebral palsy or those with low muscle tone such as in case of Trisomy 21 or myopathy.
- Severe “general” illnesses such as malnutrition, cardiac diseases with poor stamina, and respiratory distress.
- Hold-up at the same level with multiple swallows proximal to the GEJ: may be consistent with esophageal spasm secondary to reflux esophagitis.

Correlative Imaging

- Modified Barium swallow if available may provide useful additional information on the different phases of swallowing.

Red Flags

- Residual buccal activity in a child with a poor sucking reflex can make interpretation of a transit study very difficult.
- Contamination frequently occurs since children spit out the activity or drool during the study. Placing paper towels under the child’s chin allows the technologist to quickly remove contamination during study acquisition.
- Identifying contamination is crucial as it can be mistaken for “hold-up,” particularly on the condensed image.
- To prevent artifacts on the condensed image the technologist should ensure that the activity in the bottle/ syringe does not move in front of or below the child’s mouth or anterior to the patient’s neck or chest. Always move the activity vertically down to and up from the mouth.

Take Home Message

- The clinical differential diagnosis between a severe esophageal transit abnormality and GER is difficult.
- Esophageal transit studies are easy to perform and give valuable information regarding possible esophageal dysmotility or GER.
- If a child has been fed via a NG tube for a prolonged period, a transit study should be avoided, and the child should rather be given the feed for the reflux study via the NG tube.

Representative Case Examples

Case 6.4. Normal Esophageal Transit Study (Fig. 6.5)

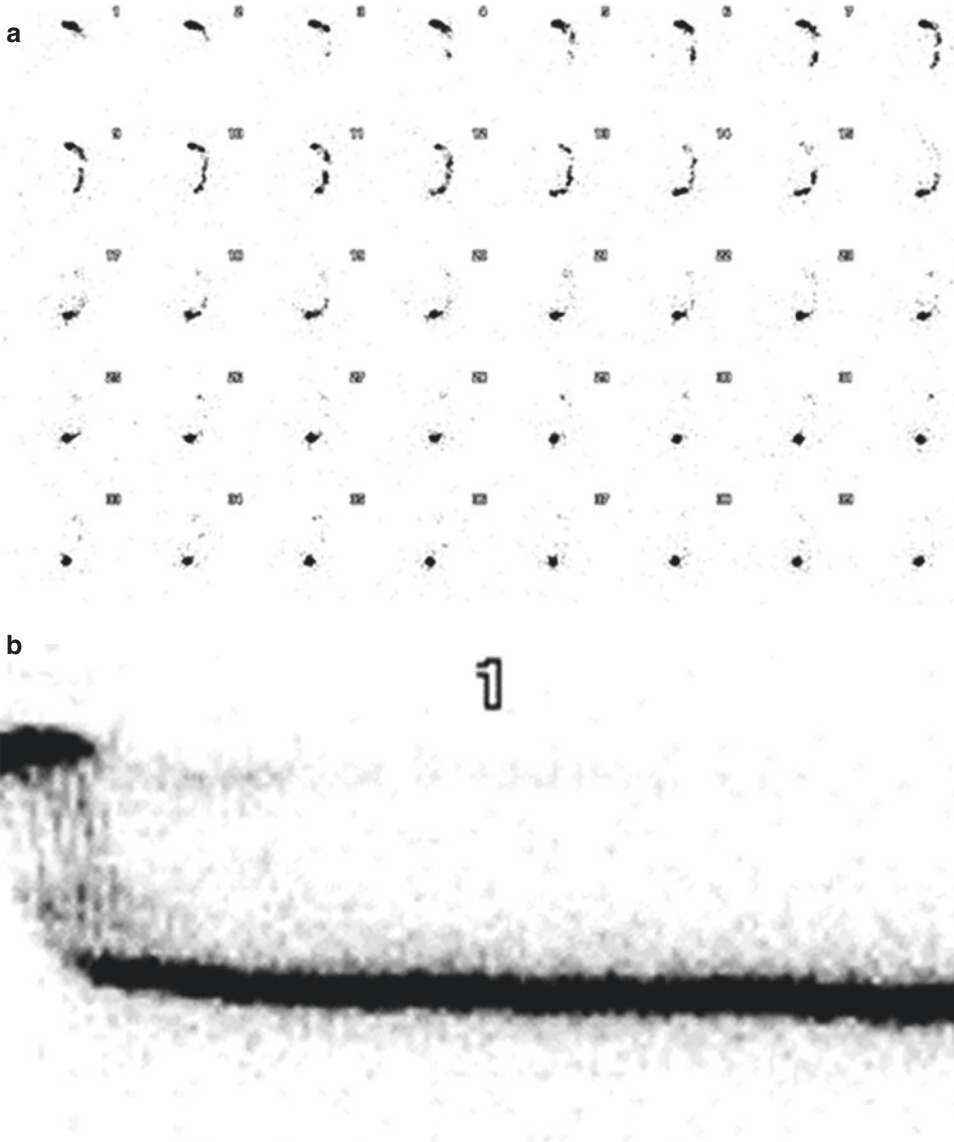


Fig. 6.5 History: A 9-month-old baby was repeatedly admitted to the hospital with recurrent chest infections and pneumonia over the last 5 months. The transit study was performed as a precursor to the GER study. Study report: There is rapid progression of tracer activity from the mouth to the stomach with all observed swallows (a). In condensed image (b), the black horizontal line at the top of the image represents the mouth and bottle, which both clear of activity after the first few frames. The horizontal line at the bottom of the image represents activity in the stomach and

only appears after a few frames. The vertical lines between the two horizontal lines are the swallows, each line corresponding to a single swallow. These lines are nearly vertical as you would expect in a patient with rapid transit of activity through the esophagus. The angle of the near vertical lines is influenced by the position of the child and the frame rate. The angle between the vertical line and the line showing the passage of activity down the esophagus is wider if the child is supine or the frame rate is increased. Impression: Normal pattern of esophageal transit

Case 6.5. Impaired Initiation of Swallowing (Fig. 6.6)

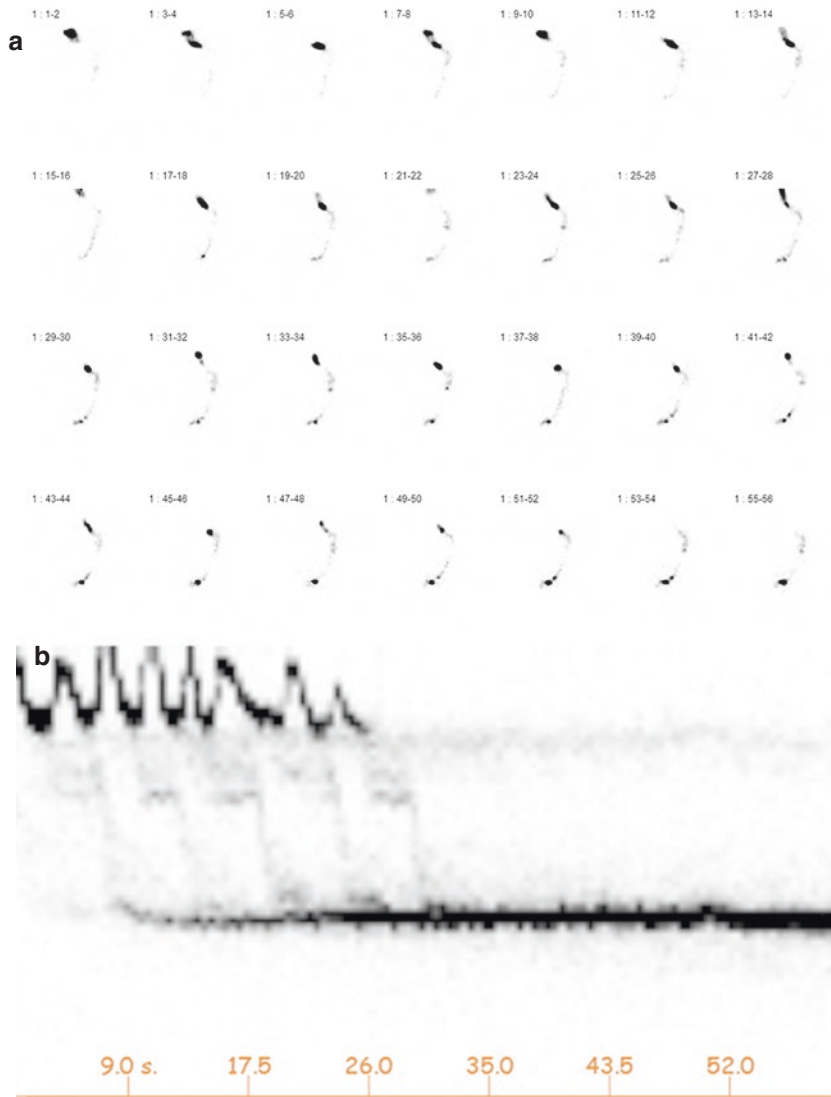


Fig. 6.6 History: A 16-month-old boy presented with feeding difficulties and symptoms of GER following an intraventricular bleed. Study report: There is a hold-up in the proximal third of the esophagus in several swallows (a). During the 1-min transit study 10 swallows were observed. In condensed image (b), the swallows have a repeat pattern of occurring in pairs, with the first swallow

of each pair showing prolonged hold-up in the proximal third of the esophagus. The hold-up persists at this level until the second swallow reaches this level, the activity then moves as a bolus to the distal esophagus. Impresison: This pattern suggests impaired initiation of swallowing seen in patients with neurological abnormalities

6.4 Salivagram

Clinical Indications

- Detection of saliva aspiration in:
 - Children with neurological impairment, recurrent lung infections, and suspected pulmonary aspiration.
 - Children with normal neurological development presenting with recurrent lung infections or unexplained chronic lung disease.

Study Protocol for Radionuclide Salivagram [9, 10]

Patient Preparation:

There is no special patient preparation for this test. Ideally, the test should be done between feeds.

Radiopharmaceutical, Administered Activity, Mode of Delivery

Radiopharmaceutical:

- [^{99m}Tc]Sn-colloid or [^{99m}Tc]sulfur colloid.

Activity:

- 10–15 MBq (0.25–0.4 mCi) in small, approx. 0.1 ml, volume.

Refer to the pediatric dosage card and to the North American consensus guidelines on radiopharmaceutical administration in children in the respective EANM and SNMMI and image gently web sites.

Reference to national regulation guidelines, if available, should be considered.

Delivery:

- The radiotracer is placed under the patient's tongue.

Study Protocol:

- Collimator: low energy all purpose.
- Position: supine, posterior view images (standard).
 - On dual head camera: optional simultaneous posterior and lateral acquisitions (detectors in “L” shape).

- If the patient is neurologically impaired with ongoing salivation it is useful to place linen savers under the head and over the chest. They can be replaced during the study if contamination occurs.

Acquisition Parameters:

- Dynamic study: 5–30 s/frame for 60 mins, matrix 128 × 128, size-appropriate zoom.
- Static images at the end of the dynamic study: anterior, posterior, lateral views, 2–5 mins/view, matrix 256 × 256, appropriate zoom.
- Markers and/or transmission images may improve localization of activity.
- If there is residual activity in the mouth at the end of the dynamic acquisition a late static image at 2 h from the beginning of the study is recommended.

Study Interpretation [11]

- Tracer visualizing the tracheobronchial tree or in the lung should be interpreted as aspiration.

Correlative Imaging

- Barium esophagogram study may show incidental aspiration.
- Modified Barium swallow can be performed in the presence of a speech or occupational therapist and videotaped, using multiple food types and consistencies and various delivery methods depending on age (e.g., different nipple types for infant feeding, feeding by cup, spoon, and straw), can detect and/or document aspiration and swallowing triggers.

Red Flags

- It is essential that the activity is given in a small bolus since it mimics native saliva transit.
- Dynamic images can be stopped earlier than 60 mins if all activity has cleared from the mouth or if clear aspiration is seen.

- If there is no clearance of buccal activity after 15 mins a small amount of water (about 0.25 ml) can be placed under the tongue.
- A normal study shows prompt clearance of activity from the mouth to the stomach and no activity in the lungs.

Take Home Messages

- Salivagram is currently the only imaging study to directly demonstrate saliva aspiration.

Representative Case Examples

Case 6.6. Normal Salivagram (Fig. 6.7)

Case 6.7. Tracheobronchial Aspiration (Fig. 6.8)

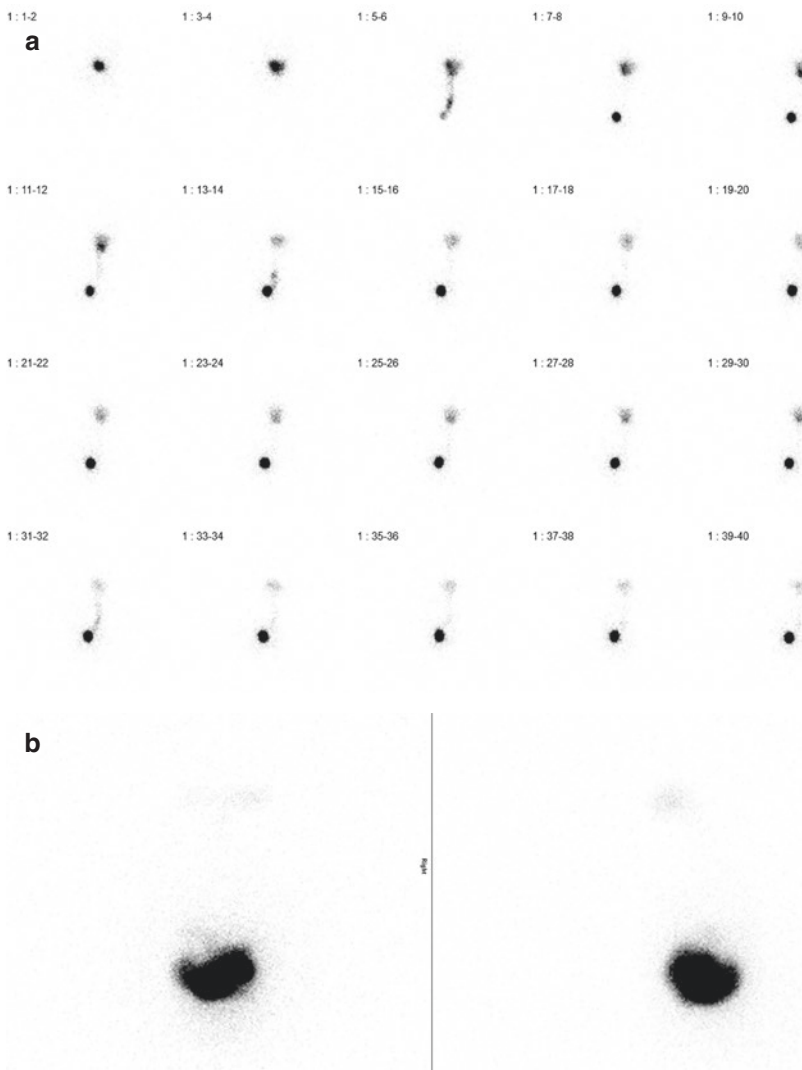


Fig. 6.7 History: A 6-month-old girl born prematurely developed nosocomial infections early during hospitalization. She had been admitted to the intensive care unit on four occasions with pneumonia and developed cystic lung disease. Study report: Early posterior images summed for

display at 10 s/frame (a) demonstrate prompt clearance of activity from the mouth to the stomach. No aspiration is detected. Planar images obtained after 1 h (b) show no evidence of tracer activity in the lungs. Impression: Normal salivagram. No evidence of pulmonary aspiration

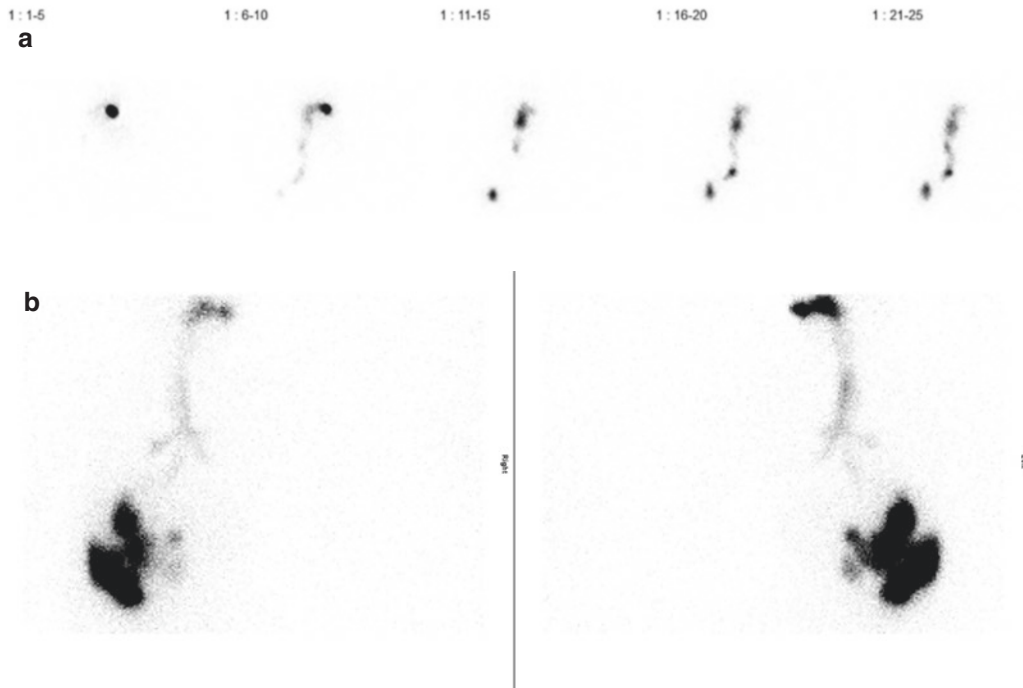


Fig. 6.8 History: A 13-year-old spastic quadriplegic patient with cerebral palsy presented with recurrent pneumonias. Study report: Early posterior images summed at 30 s/frame for display (a) show tracer activity entering the

trachea and stomach. Planar images obtained after 1 h (b) show tracer activity in the bronchi, bilaterally. Impression: Tracheobronchial aspiration

6.5 Gastrointestinal Bleeding

Ectopic Gastric Mucosa (Meckel's Diverticulum Scan)

Clinical Indications [12, 13]

- Detection of ectopic gastric mucosa in a Meckel's diverticulum or, rarely, in a duplication cyst as a source of painless lower GIB.
- Detection of a Meckel's diverticulum in rare cases of abdominal pain, due to diverticulitis, or, less common, due to recurrent intussusception.

tis, or, less common, due to recurrent intussusception.

- Unexplained anemia.

Pre-Exam Information

- Number and timing of bleeding episodes. Performing the study during active bleeding may reduce its sensitivity.
- Was premedication taken as instructed?
- Is a Barium study planned within 3 days prior to the Meckel's scan?

Study Protocol for Meckel's Scan [13, 14]

Patient Preparation:

- Fast: 3–4 h, can improve the sensitivity for detection of ectopic gastric mucosa.
- Premedication options to increase the study sensitivity for detection of ectopic gastric mucosa:
 - Histamine H₂ receptor antagonists reduce tracer release from the gastric mucosal cells. These drugs are most commonly used due to their availability, low cost, and infrequent side effects.
 - Cimetidine.
 - Orally (PO) for 1–3 days: 20 mg/kg/day. In neonates 10–20 mg/kg/day.
 - Intravenous (IV) 1 h before the scanning procedure: 300 mg in 100 mL of 5% dextrose over 20 min.
 - Famotidine.
 - PO: 0.5 mg/kg/day.
 - IV 1 h before the scanning procedure: 0.25 mg/kg.
 - Recently, proton pump inhibitors have been used to control acid secretion in children and some institutions may use this drug as a premedication. Currently, there are no fixed recommendations for the dose or the duration of this premedication.

Radiopharmaceutical, Administered Activity, Mode of Delivery

Radiopharmaceutical:

- [^{99m}Tc]pertechnetate (Pertechnetate).

Activity:

- 1.85 MBq/Kg (0.05 mCi/Kg), minimum dose 9.25 MBq (0.25 mCi).
 - Refer to the pediatric dosage card and to the North American consensus

guidelines on radiopharmaceutical administration in children in the respective EANM and SNMMI and image gently web sites.

Reference to national regulation guidelines, if available, should be considered.

Acquisition Protocol [15]:

- Collimator: low energy, high- or ultra-high resolution collimator.
- Position: tracer is injected with the patient lying supine.
- FOV: entire abdomen and pelvis to ensure the entire bladder is in the field of view.

Acquisition Parameters:

- Step 1: Dynamic study for 60 s: 1–5 s/frame, matrix 128 × 128. Aiming to look for vascular blush from arteriovenous (AV) malformation or to localize a site of rapid bleeding.
- Anterior and posterior dynamic study step 2 for 30–60 mins: 30–60 s/frame, matrix 128 × 128.
- Static images of the abdomen (upon completion of the dynamic part): anterior, RAO, and/or right lateral; 300 Kcounts, matrix 256 × 256, appropriate zoom.
 - Post-void images are mandatory when there is significant bladder activity that can obscure focal uptake from an adjacent diverticulum.
 - Posterior and lateral views can help delineate renal uptake.
 - Standing/sitting views may be needed to differentiate normal tracer transit in the duodenum from uptake in ectopic gastric mucosa.
 - Additional views after diuretic administration may also be required.

- SPECT (if performed, should be done after the dynamic phase): 60–120 projections, 10–20 s/projection, matrix 128 × 128.
- SPECT/CT including a pediatric low-dose CT with a FOV limited to the abdomen and pelvis (when available).

Study Interpretation [16]

Interpretation criteria for ectopic gastric mucosa:

- Focal tracer uptake appears at the same time as the activity in the normal gastric mucosa, and persists or increases in intensity over time.
- Typical location: right lower quadrant.
 - Other abdominal locations are occasionally seen.
 - The location of the focus may change during the study due to peristalsis.

False positives: physiologic abdominal tracer biodistribution.

- Focal tracer activity in the urinary tract:
 - Renal or extra-renal pelvis, dilated ureter, bladder diverticulum, vesicoureteral reflux (VUR), ectopic kidney. Urinary tract activity is occasionally seen but it clears during the dynamic acquisition, unlike focal uptake in a Meckel's diverticulum.
- Physiologic tracer transit in the small bowel:
 - Diffuse, usually in the left upper quadrant, or focal, commonly in the duodenal bulb.
 - Appears later in the study than uptake in ectopic gastric mucosa.
 - Cinematic display can identify normal tracer movement from the stomach to the duodenum and small bowel loops.
- Uterine blush.
- Hemangioma or AV malformation. The latter is usually prominent during the initial angiographic phase of the study.
- Ectopic gastric mucosa present in enteric duplication cysts.

False negatives:

- Barium fluoroscopy a few days prior to scintigraphy. Barium can attenuate faint activity in ectopic gastric mucosa.
- Perchlorate administration inhibits Pertechnetate uptake by gastric mucosa.
- Physiologic low Pertechnetate uptake in neonates.
- Scarring, necrosis, or ischemia within the diverticulum.
- A very small focus on ectopic mucosa.

Correlative Imaging

- Upper GI and follow-through contrast examination to detect duplication cyst.
- Contrast enema to detect duplication cyst.
- US of the abdomen may incidentally identify a cystic structure.
- Cross-sectional CT or MRI imaging may identify a mass or cyst in the bowel.

Red Flags

- The study cannot demonstrate Meckel's diverticula that do not contain ectopic gastric mucosa. It will only detect diverticula containing ectopic gastric mucosa (20–50% of cases).
- Potential pitfalls can include:
 - Very small lesions that may first appear a bit later than the stomach.
 - Uptake suspected to be in the excretory system. In doubtful cases, upright, post-void, or repeat images after administration of furosemide may clear the urinary tract activity.
 - In patients who have acute GI bleeding with a significant drop in hemoglobin, the study may be falsely negative due to failure to deliver the tracer to the ectopic mucosa. This may necessitate a repeat scan 10–14 days later.
 - Active bleeding during imaging can dilute and shift tracer activity away from the diverticulum.
- A Meckel's scan should not be performed within several days after a bleeding study that

employed in vivo labelling of red blood cells (RBCs). Small amounts of persisting circulating Sn-pyrophosphate from the prior study, will cause Pertechnetate, injected for the Meckel's scan, to label RBCs and thus no uptake will be found in the gastric mucosa. This is not the case if in vitro labelling of the RBCs; then a Meckel's scan can be performed without interference.

Take Home Messages

- Interpreting physicians should be familiar with the characteristic pattern of uptake in ectopic gastric mucosa, with conditions that can potentially result in erroneous interpretations and with the various techniques that can be used to increase the diagnostic certainty in doubtful cases.
- Pertechnetate is taken up by the mucin-producing cells of the gastric mucosa and excreted later on into the gut lumen. This feature makes a Meckel's scan the study of choice for the detection of ectopic gastric mucosa.
- Pertechnetate scintigraphy is the only direct study to demonstrate the presence of ectopic gastric mucosa within a Meckel's diverticulum. When adequately performed, it is reported to have a sensitivity of 94%, and a specificity of 97%.
- This examination is seldom of value in children with no history of rectal bleeding.
- SPECT/CT increases the diagnostic confidence:
 - In small diverticula with low uptake.
 - For precise preoperative localization.
 - To identify ectopic gastric mucosa foci obscured by the bladder.
- When studies are negative or equivocal and the clinical suspicion is high, repeat studies should be considered as they may present with more definite findings and help in establishing or refuting the diagnosis.
- Ectopic gastric mucosa present in symptomatic enteric duplication cysts often require surgical resection similar to symptomatic Meckel's diverticula.
- US of the abdomen should not be used as a screening test.

Representative Case Examples

Case 6.8. Meckel's Diverticulum (Fig. 6.9)

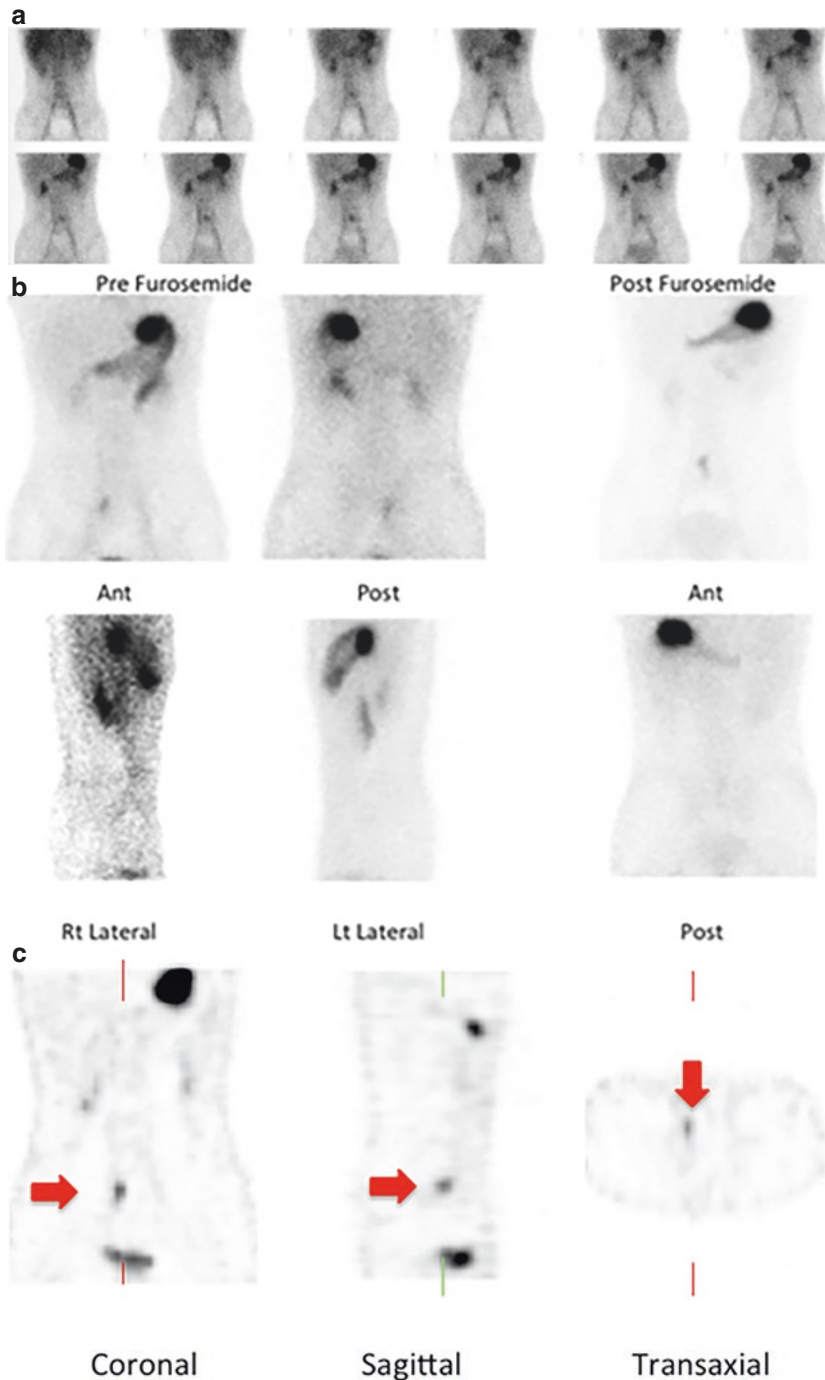


Fig. 6.9 History: A 12-year-old boy presented with significant painless melena and a drop in hemoglobin. Study report: Following oral premedication with H2 blocker 6 h previously, Pertechnetate was injected, and dynamic flow images were obtained over 2 mins (not shown), followed by 15 mins of dynamic imaging of the abdomen and pelvis (a) Subsequently, static images were obtained at 20 mins (b). There is some activity in right and left kidney

areas seen on the initial dynamic and static imaging that drained after the administration of 20 mg furosemide IV. There is a focal area of increased activity in the lower abdomen. SPECT of the abdomen and pelvis (c) identifies a focus of activity in the lower mid-abdomen (arrows). Impression: The findings are consistent with an area of ectopic gastric mucosa in a Meckel's diverticulum

Case 6.9. Meckel's Diverticulum (Fig. 6.10)

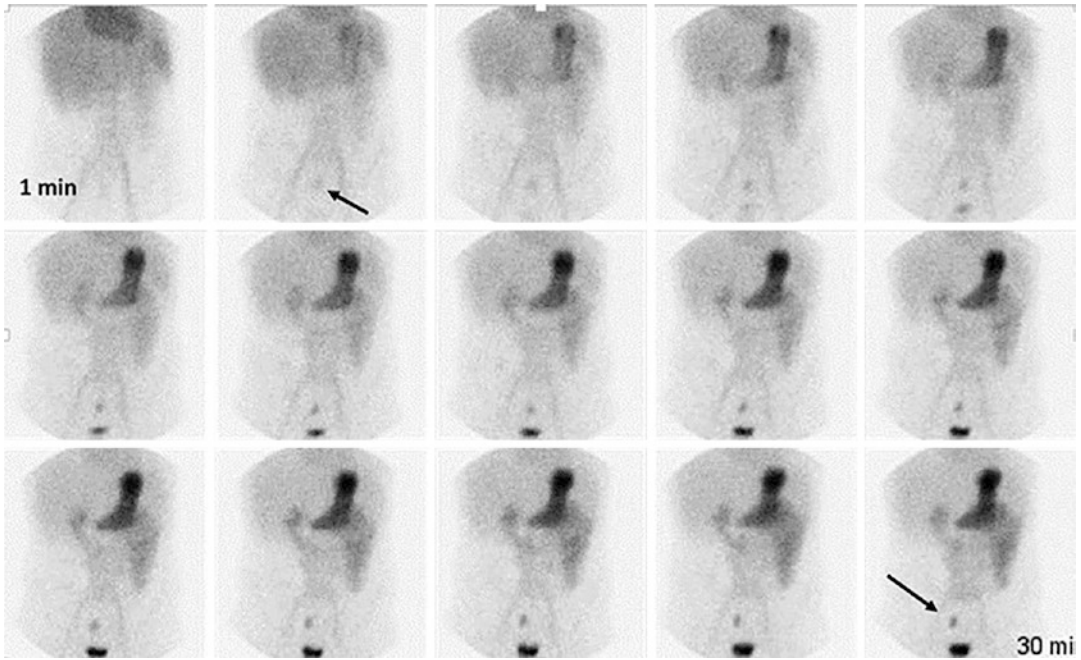


Fig. 6.10 History: An 11-year-old boy presented with recurrent abdominal pain and anemia. The study was requested in search of a possible Meckel's diverticulum with ectopic gastric mucosa as a cause of diverticulitis and was performed after premedication with ranitidine. Study report: Dynamic images obtained for 30 mins after administration of Perchnetate show a focal uptake (arrow) in the lower pelvis, above the urinary bladder. This focus appeared simultaneously with the physiological uptake in the gastric mucosa and increased in intensity over time. Impression: The findings are consistent with the diagnosis

of ectopic gastric mucosa. On surgery an inflamed Meckel's diverticulum located proximal to the ileo-caecal valve was resected. Typically, a Meckel's diverticulum manifests as painless rectal bleeding in a young child, in most cases under 2 years of age. This case illustrates that occasionally less common presentations may be encountered, especially in older children, like in the present case in whom the child suffered from "Meckel's diverticulitis" with recurrent abdominal pain and chronic blood loss

Blood Pool Scintigraphy

Clinical Indications

- Detection of GIB.

Pre-Exam Information

- Are there signs of active bleeding just prior to the study?
- Hemoglobin levels and administration of blood transfusions should be known.
- Hemodynamic status of the patient and the need for supportive therapy and monitoring.

Study Protocol for GI Bleeding Scan [14, 17]

Patient Preparation:

- No preparation is required.

Radiopharmaceutical, Administered Activity, Mode of Delivery

Radiopharmaceutical:

- [^{99m}Tc]Tc-RBCs [18] In vitro labelling is the method of choice and should be employed when an adequate facility and proper radiopharmacy practices are available 1–3 ml of the patient's blood are drawn anticoagulated with heparin or acid citrate dextrose (ACD).
- RBC are labelled with a commercially available preparation according to the manufacturer's instructions.
- In vivo labelling:
 - ¹²⁵I pyrophosphate is injected in appropriate, weight-based amounts obtained from the package insert of the commercial cold kit.
 - Administration of Pertechnetate follows 20 mins later.

Activity (Pertechnetate):

- 74 MBq/Kg (2 mCi/Kg), minimum dose 74 MBq (2 mCi).
Refer to the EANM pediatric dosage card and to the North American consensus

guidelines on radiopharmaceutical administration in children in the respective European Association of Nuclear Medicine (EANM) and Society of Nuclear Medicine and Molecular Imaging (SNMMI) and image gently web sites.

Reference to national regulation guidelines, if available, should be considered.

Delivery:

- For in vitro labelled RBCs: the labelled blood should be slowly reinjected IV into the patient from whom it was drawn.

Acquisition Protocol:

- Collimator: low energy, general purpose, or high resolution.
- Position: supine, anterior view.
- FOV: entire abdomen.

Acquisition Parameters:

- Dynamic study, Step 1: immediately following tracer injection, 60 × 1–5 s/frame, matrix 128 × 128, size-appropriate zoom.
- Dynamic study Step 2: immediately following step 1, with 30 s/frame for 60–90 mins.
- Additional delayed sequences of dynamic imaging can be performed up to 24 h if no bleeding is noted.
- SPECT or SPECT/CT, when available, can be used to clarify foci of uncertain origin.

Study Interpretation

- A new, focal tracer accumulation in the abdomen or pelvis should be considered to represent a bleeding site.
- This focus typically increases in intensity and travels through the bowel lumen from the original bleeding site in an antegrade or retrograde fashion.

- Focal or diffuse sites of tracer accumulation that do not change their location throughout the study are unlikely to represent bleeding sites.
- Bleeding is often intermittent. Abnormal uptake first detected on late images indicates that bleeding has occurred in the time that elapsed from the prior imaging sequence but does not necessarily reveal the original bleeding site because of the movement of labelled blood in the intestinal lumen due to peristalsis.
- Physiologic tracer activity accumulation can be seen in:
 - The blood pool of the kidneys or occasionally in the renal pelvis or ureter and in the bladder.
 - In the blood pool of the large abdominal blood vessels and the liver and spleen.
 - Uptake in the thyroid gland and gastric mucosa is due to free circulating Pertechnetate and suggests inadequate RBC labelling.
- Referring physicians should be advised when ordering a GIB study that this investigation can only detect active bleeding that occurs at the time of imaging and grossly localize the bleeding source to one of the four abdominal quadrants.
- Distinctions between small and large bowel bleeding can sometimes be made. The etiology of bleeding such as ectopic gastric mucosa, erosion, AV malformation, and tumor cannot be determined.
- When there is a high clinical suspicion for a Meckel's diverticulum as the bleeding site, a Meckel's scan should be performed instead of a labelled RBC bleeding study.
- Uptake in organs and sites suggesting free Pertechnetate is more commonly encountered with in vivo labelling which is not advised for GIB investigations.

Correlative Imaging

- Angiography can be used both for detection of the GIB as well as for therapeutic purposes but requires larger bleeding volumes than scintigraphy.

Red Flags

- General blood manipulation and handling precautions have to be always implemented.
- Injection of in vitro labelled blood requires extreme caution to ensure that the blood is injected into the patient from whom it was drawn. To reduce the chance of misadministration it is advised to avoid booking more than one in vitro labelled RBC study per session.

Take Home Messages

- RBC scintigraphy is a sensitive and specific study for the detection of GIB. The long scanning duration increases the likelihood of detecting intermittent bleeding episodes.
- The study can detect smaller bleeding volumes than angiography, 0.1–0.4 ml/min.
- In vitro RBC labelling is the method of choice because of significantly higher labelling efficiency and a lower likelihood of artifacts related to free Pertechnetate.
- The migration of the focus of abnormal activity both ante- and retrograde occurs because blood irritates the bowel mucosa and induces peristalsis. When sufficient labelled blood accumulates in the lumen the outline of the bowels may be recognized allowing distinction between the small and large intestines.



Fig. 6.11 History: A 3-year-old girl undergoing chemotherapy for leukemia experienced repeat episodes of melena and bright red blood rectal bleeding. Angiography failed to detect the bleeding source. Study report: Following reinjection of autologous Tc-labelled RBCs dynamic images of the abdomen acquired in the anterior

view show abnormal tracer accumulation in the upper left quadrant (arrow). The uptake increases in intensity and changes in shape and location over time. Impression: These findings suggest active gastrointestinal bleeding, most probably from the small intestines in the left upper quadrant

Representative Case Examples

Case 6.10. Left Upper Quadrant Gastrointestinal Bleeding (Fig. 6.11)

References

1. Bar-Sever Z. Gastroesophageal reflux, gastric emptying, esophageal transit, and pulmonary aspiration. In: Treves ST, editor. Pediatric nuclear medicine and molecular imaging. New York: Springer; 2014. p. 203–34.
2. Onyeador N, Paul SP, Sandhu BK. Paediatric gastroesophageal reflux clinical practice guidelines. Arch Dis Child Educ Pract Ed. 2014;99(5):190–3.
3. Bar-Sever Z. Scintigraphic evaluation of gastroesophageal reflux and pulmonary aspiration in children. Semin Nucl Med. 2017;47(3):275–85.
4. Abell TL, et al. Consensus recommendations for gastric emptying scintigraphy: a joint report of the American Neurogastroenterology and motility society and the Society of Nuclear Medicine. J Nucl Med Technol. 2008;36(1):44–54.
5. Drubach LA, et al. Gastric emptying in children: what is the best acquisition method? J Pediatr Gastroenterol Nutr. 2012;55(2):191–3.
6. Drubach LA, Kourmouzi V, Fahey FH. Cheese is a reliable alternative meal for solid-phase gastric emptying study. Nucl Med Commun. 2010;31(5):430–3.
7. Ng TSC, et al. Pediatric solid gastric emptying scintigraphy: normative value guidelines and non-standard meal alternatives. Am J Gastroenterol. 2020;115(11):1830–9.
8. Kwatra NS, et al. Gastric emptying of milk in infants and children up to 5 years of age: normative data and influencing factors. Pediatr Radiol. 2020;50(5):689–97.

9. Somasundaram VH, Subramanyam P, Palaniswamy S. Salivagram revisited: justifying its routine use for the evaluation of persistent/recurrent lower respiratory tract infections in developmentally normal children. *Ann Nucl Med*. 2012;26(7):578–85.
10. Drubach LA, et al. Utility of salivagram in pulmonary aspiration in pediatric patients: comparison of salivagram and chest radiography. *AJR Am J Roentgenol*. 2013;200(2):437–41.
11. Wu H, Zhao R. Image characteristics and classification of salivagram in the diagnosis of pulmonary aspiration in children. *Nucl Med Commun*. 2017;38(7):617–22.
12. Grady E. Gastrointestinal Bleeding scintigraphy in the early 21st century. *J Nucl Med*. 2016;57(2):252–9.
13. Sinha CK, et al. Meckel's scan in children: a review of 183 cases referred to two paediatric surgery specialist centres over 18 years. *Pediatr Surg Int*. 2013;29(5):511–7.
14. Treves, S.T. and M. Manfredi, Gastrointestinal Bleeding, in *Pediatric nuclear medicine and molecular imaging*, S.T. Treves 2014, Springer New York: . p. 265–282.
15. Spottswood SE, et al. SNMMI and EANM practice guideline for Meckel diverticulum scintigraphy 2.0. *J Nucl Med Technol*. 2014;42(3):163.
16. Irvine I, Doherty A, Hayes R. Bleeding meckel's diverticulum: a study of the accuracy of pertechnetate scintigraphy as a diagnostic tool. *Eur J Radiol*. 2017;96:27–30.
17. Lee J, et al. Red blood cell scintigraphy in children with acute massive gastrointestinal bleeding. *Pediatr Int*. 2008;50(2):199–203.
18. Radiolabelled Autologous Cells. Methods and standardization for clinical use. Vienna: International Atomic Energy Agency; 2015.

The opinions expressed in this chapter are those of the author(s) and do not necessarily reflect the views of the IAEA: International Atomic Energy Agency, its Board of Directors, or the countries they represent.

Open Access This chapter is licensed under the terms of the Creative Commons Attribution 3.0 IGO license (<http://creativecommons.org/licenses/by/3.0/igo/>), which permits use, sharing, adaptation, distribution and reproduction in any medium or format, as long as you give appropriate credit to the IAEA: International Atomic Energy Agency, provide a link to the Creative Commons license and indicate if changes were made.

Any dispute related to the use of the works of the IAEA: International Atomic Energy Agency that cannot be settled amicably shall be submitted to arbitration pursuant to the UNCITRAL rules. The use of the IAEA: International Atomic Energy Agency's name for any purpose other than for attribution, and the use of the IAEA: International Atomic Energy Agency's logo, shall be subject to a separate written license agreement between the IAEA: International Atomic Energy Agency and the user and is not authorized as part of this CC-IGO license. Note that the link provided above includes additional terms and conditions of the license.

The images or other third party material in this chapter are included in the chapter's Creative Commons license, unless indicated otherwise in a credit line to the material. If material is not included in the chapter's Creative Commons license and your intended use is not permitted by statutory regulation or exceeds the permitted use, you will need to obtain permission directly from the copyright holder.



Anita Brink, Zvi Bar-Sever, and Lorenzo Biassoni

7.1 Hepatobiliary Scintigraphy

Clinical Indications [1, 2]

- Differential diagnosis between biliary atresia and other causes of neonatal jaundice such as neonatal hepatitis.
- Evaluation of cystic masses such as choledochal cysts.
- Diagnosis of cholecystitis.
- Evaluation of liver transplants.
- Evaluation of bile leaks following surgery or trauma.

A. Brink (✉)
Nuclear Medicine Department, Division of Radiation
Medicine, University of Cape Town,
Cape Town, South Africa

Nuclear Medicine and Diagnostic Imaging Section,
Division of Human Health, Department of Nuclear
Sciences and Applications, International Atomic
Energy Agency, Vienna, Austria

Z. Bar-Sever
Schneider Children's Medical Center, Tel Aviv
University, Petah Tiqva, Israel

L. Biassoni
Department of Radiology, Great Ormond Street
Hospital for Children NHS Foundation Trust,
London, UK

Pre-Exam Information

- The need for fasting or pharmacologic interventions will be determined by the age of the patient and the specific clinical indication.
- In cases of liver transplantation: anatomy of the graft (one lobe, whole liver), site and type and location of the anastomosis with the bowel, complications during surgery.

Study Protocol, Hepatobiliary Scintigraphy [3–5]

Patient Preparation:

Fast: 4–6 h when the study is performed to investigate gallbladder pathology.

- Fasting is not required for the evaluation of biliary atresia, liver transplant, and biliary leaks.
- Premedication (in infants with suspected biliary atresia):
 - Preferred: ursodeoxycholic acid (UDCA), administered orally (PO) 20 mg/Kg every 12 h for 2–3 days prior to the study.
 - Alternative: Phenobarbital 5 mg/kg/day, administered orally in two equal doses for 5 days prior to the study.

Radiopharmaceutical, Administered Activity, Mode of Delivery

Radiopharmaceutical:

- [^{99m}Tc]labelled iminodiacetic acid (IDA) derivatives.
- Preferred: [^{99m}Tc]mebrofenin (preferred, when available) and ^{99m}Tc-disofenin.

Activity:

- 1.85 MBq/Kg (0.05 mCi/Kg), minimum dose 20 MBq (0.54 mCi).
 - Refer to the EANM pediatric dosage card and to the North American consensus guidelines on radiopharmaceutical administration in children in the respective EANM and SNMMI and image gently web sites.
 - Reference to national regulation guidelines, if available, should be considered.

Acquisition Protocol:

- Collimator: low-energy high-resolution parallel hole.
- Field-of-view (FOV): entire abdomen, anterior view.

Acquisition protocol depends on the study indication; can be customized according to interim findings.

- In general, it starts with a dynamic acquisition of 30–60 seconds/frame for a total of 60 mins, matrix 128 × 128.
- Serial static images at 1 and 4 h (for an acquisition duration of 3–5 min) follow after the completion of the dynamic study, and if needed at 24 h (for a duration of 15 min), matrix 256 × 256.
- Size-appropriate zoom.
- SPECT/CT (when available) will improve the diagnostic accuracy.

Suspected biliary atresia:

- The study can be discontinued at earlier time points if there is clear evidence of tracer accumulation in the bowel.

Suspected acalculous cholecystitis—includes a pharmacological intervention to stimulate gallbladder contraction:

- When there is clear tracer accumulation in the gallbladder at 60 mins post-injection imaging, a cholecystokinin (CCK) analogue such as Sincalide (Kinevac, Sincalide, Bracco Diagnostics, Princeton, NJ) is administered IV.
 - Dose: 0.02 microgram/Kg diluted with saline to 30 ml.
 - Delivery: infusion pump at a rate of 1 ml/min for 30 mins.
- If CCK is unavailable it can be substituted by a standardized fatty meal or by high-fat containing dairy products (milkshake, half-and-half, whipped cream).
- A second sequence of dynamic images is obtained for 30 mins.

Study Processing:

- Quantitative analysis of tracer uptake and excretion is not routinely performed in clinical practice.
- Gallbladder ejection fraction (EF) can be obtained by drawing a region-of-interest (ROI) over the gallbladder, recording pre- and 30-min post-stimulation counts.
- The EF is calculated as the difference between the pre- and post-stimulation counts divided by the pre-stimulation counts. An EF below 35% is considered abnormal.

Study Interpretation

Suspicion of Biliary Atresia [2, 6, 7]

- Initial hepatic uptake and timing of the first bowel loops appearance should be recorded.
- Increased tracer activity in the background and alternative excretion by the kidneys should be noted.
- The diagnosis is ruled out when a tracer is identified in bowel loops at any time point during the study.
- Tracer retention in the liver and lack of excretion up to 24 h post-injection may suggest biliary atresia but is not specific.
- Differential diagnosis:
 - Severe neonatal hepatitis.
 - Other entities: bile plug syndrome in patients with cystic fibrosis, Alagille syndrome, dehydration, sepsis, and occasionally total parenteral nutrition may produce similar scintigraphic findings.

Acalculous Cholecystitis:

- Scintigraphy will typically show a prominent gallbladder with little or no emptying following stimulation by pharmacologic intervention or a fatty meal.
- The gallbladder EF is typically less than 35%.

Choledochal Cysts:

- Scintigraphy will show drainage from the liver and gradual tracer accumulation in the region of the porta hepatis.
- Bowel activity can be seen when the cyst is not obstructive.
- Occasionally, early hepatic images will show a photopenic area corresponding to the cyst that gradually fills up as the rest of the liver drains.
- SPECT/CT may be helpful in selected cases to clarify the scintigraphic findings.

Liver Transplant:[8–10]

- Tracer distribution in the liver parenchyma during the early phases of the study is important.
- Areas with decreased uptake may suggest ischemia or necrosis.

- Tracer transit into the bowel is important to rule out obstructions. Transient tracer accumulation at the site of the anastomosis with the bowel is a common feature.
- Bile leaks should be suspected when there is tracer activity in fluids collected from surgical drains.
 - Contained bile leaks may be seen as ectopic sites of tracer accumulation usually close to the liver margins.
 - Free bile leaks typically manifest as ectopic tracer localization in the gutters or pelvic floor.

Correlative Imaging [11–13]

- US and cross-sectional imaging may show the presence of a cystic mass suspected to represent a choledochal cyst or non-visualization of the gallbladder that may be associated with biliary atresia.
- Choledochal cysts are usually first identified with US or CT, but these modalities cannot ascertain the nature of the cyst. Magnetic resonance cholangiopancreatography (MRCP) is also being used more frequently to evaluate the biliary tree.

Red Flags [9]

- In cases of suspected biliary atresia, it is essential to verify that pre-scan medication was taken as required. Repeat scintigraphy can be considered when the first study did not clearly demonstrate tracer localization in the bowel, prior to more invasive diagnostic measures.
- Phenobarbital blood levels prior to HBS should be within the therapeutic range. It is recommended to check drug levels prior to performing the scan. If they are still low, treatment should be continued and the test postponed.
- When no gastrointestinal (GI) excretion is visualized up to 24-h imaging, biliary atresia cannot be ruled out and must be confirmed by biopsy and other clinical tests. The report should also not conclude that the scan is consistent with biliary atresia.

- Alternative tracer excretion through the kidneys is commonly seen in infants with neonatal jaundice. Distinction between renal and bowel activity may be difficult in the late, count poor images. Posterior view images may be helpful as well as SPECT or SPECT/CT.
 - Distinction between normal uptake in the gallbladder vs. activity in a choledochal cyst can be difficult. Administration of a fatty meal can be helpful. A normal gallbladder will empty following a fatty meal stimulation unlike a choledochal cyst.
 - The location of anastomosis between bile ducts and bowel is essential for the interpretation of liver transplant studies. Tracers tend to transiently accumulate at the site of the surgical anastomosis and could erroneously be interpreted as indicating a contained bile leak. Later images should show tracer clearance from the anastomotic site.
- such as fluid collections and abdominal cysts.
 - Enhances the study sensitivity for detection of small amounts of tracer in bowel loops.
 - HBS has a high negative predictive value for biliary atresia and thus its value is in excluding biliary atresia.
 - The definite diagnosis of biliary atresia requires percutaneous or intraoperative transhepatic cholangiography and liver biopsy. Biliary atresia requires a Kasai hepatoporto-enterostomy surgery, an initial measure to enable bile drainage from the liver. Liver transplantation is usually performed later.
 - In neonatal hepatitis, the hepatocellular damage impairs tracer uptake by the liver and results in increased background activity. This characteristic is usually not seen in biliary atresia when the diagnosis is made early prior to hepatocellular damage.
 - Congenital cystic dilatations of the extrahepatic bile ducts may cause biliary obstruction. The most common type is the cystic dilatation of the common bile duct. Abdominal pain and occasionally jaundice are common clinical signs. Scintigraphy is required to prove the biliary origin of the cyst which accumulates the tracer.
 - Bile leaks following liver transplantation, other abdominal surgery, or trauma can be identified and distinguished from other fluid collections.

Take Home Messages

- IDA derivatives differ in their extraction rate from the blood and the rate of clearance from the liver parenchyma into the bowel.
- Phenobarbital increases bile flow and improves the specificity of the study by ruling out biliary atresia.
- SPECT/CT can improve the diagnostic accuracy:
 - Allows direct correlation between sites of tracer accumulation and anatomic findings

Representative Case Examples

Case 7.1. Biliary Atresia (Fig. 7.1)

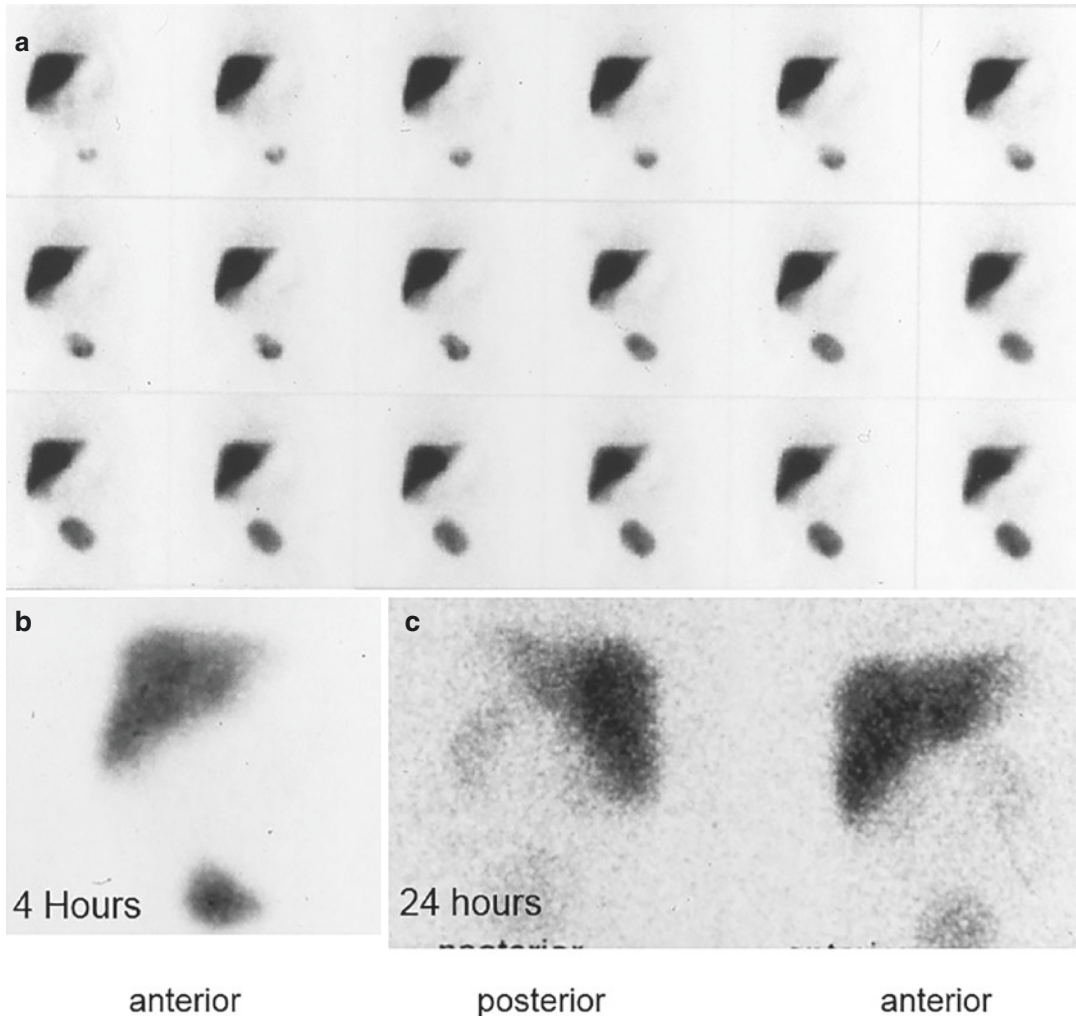


Fig. 7.1 History: A 6-week-old infant with prolonged direct hyperbilirubinemia. Biliary atresia was suspected. A hepatobiliary scan with Tc-Disofenin was performed. Study report: Dynamic images (a) obtained for 60 mins and static images obtained at 4 h (b) and 24 h after tracer administration (c) show tracer retention in the liver. There is no activity seen in the bowel. The 24-h images show

faint tracer activity in the kidneys. The liver uptake is homogenous and there is no significant background activity. Impression: These findings suggest that biliary atresia cannot be ruled out. The diagnosis was further confirmed by intraoperative transhepatic cholangiography

Case 7.2. Choledochal Cyst (Fig. 7.2)

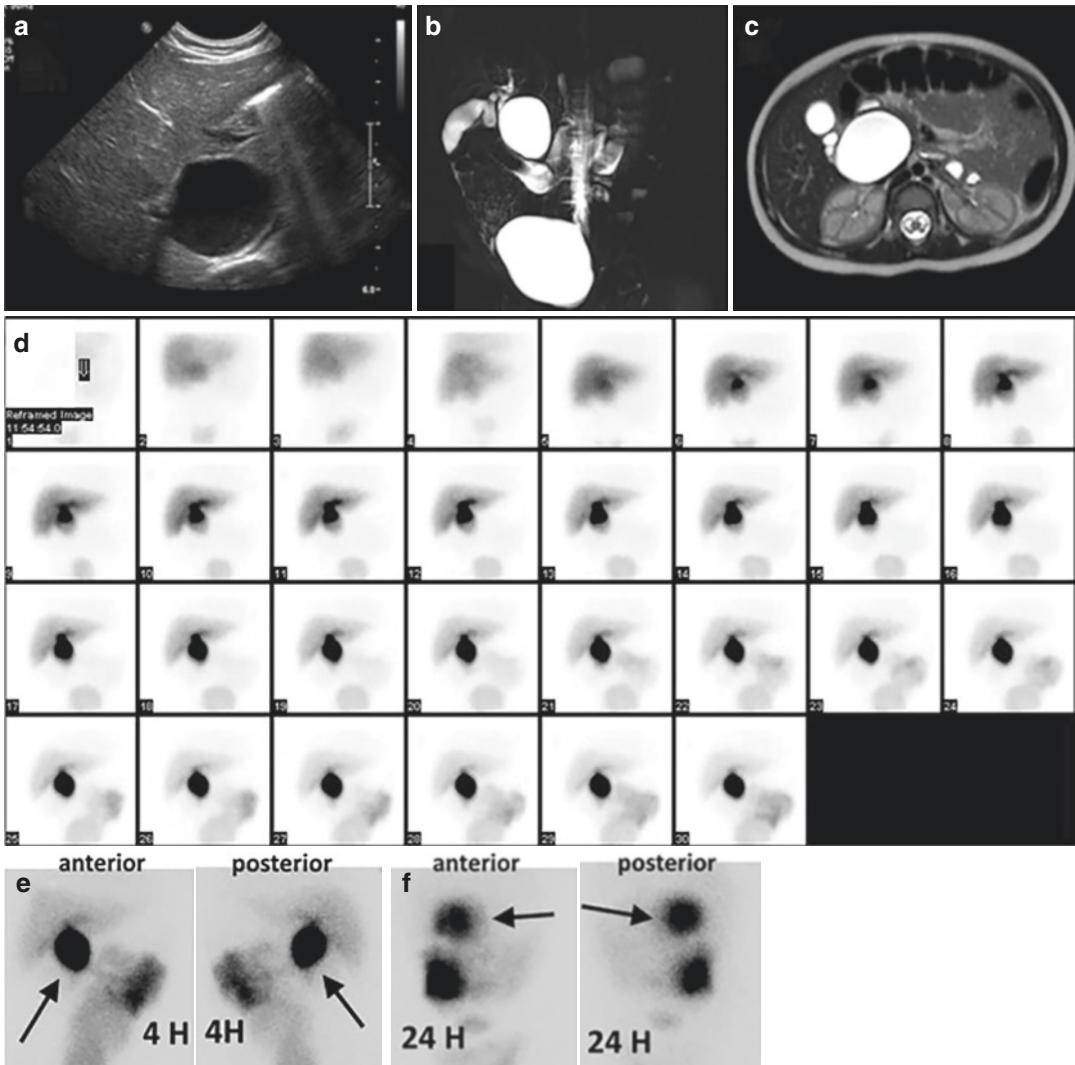


Fig. 7.2 History: An 11-month-old girl presented with a large cyst in the region of the common bile duct as shown by US (a) and MRI (b, c) suspected to be a choledochal cyst. Scintigraphy was performed to assess the relationship of the cyst to the hepatobiliary system, which could not otherwise be established. Study report: Early dynamic scintigraphy (d) shows normal liver uptake and excretion,

with gradual tracer accumulation just below the inferior liver margin, most likely in the known cyst. Tracer activity was clearly noted in bowel loops with no evidence of obstruction. Late, 4- (e) and 24-h (f) images demonstrate continuing tracer pooling in the cyst (arrows). Impression: The findings are consistent with a choledochal cyst, part of the biliary system

Case 7.3. Acalculous Cholecystitis (Fig. 7.3)

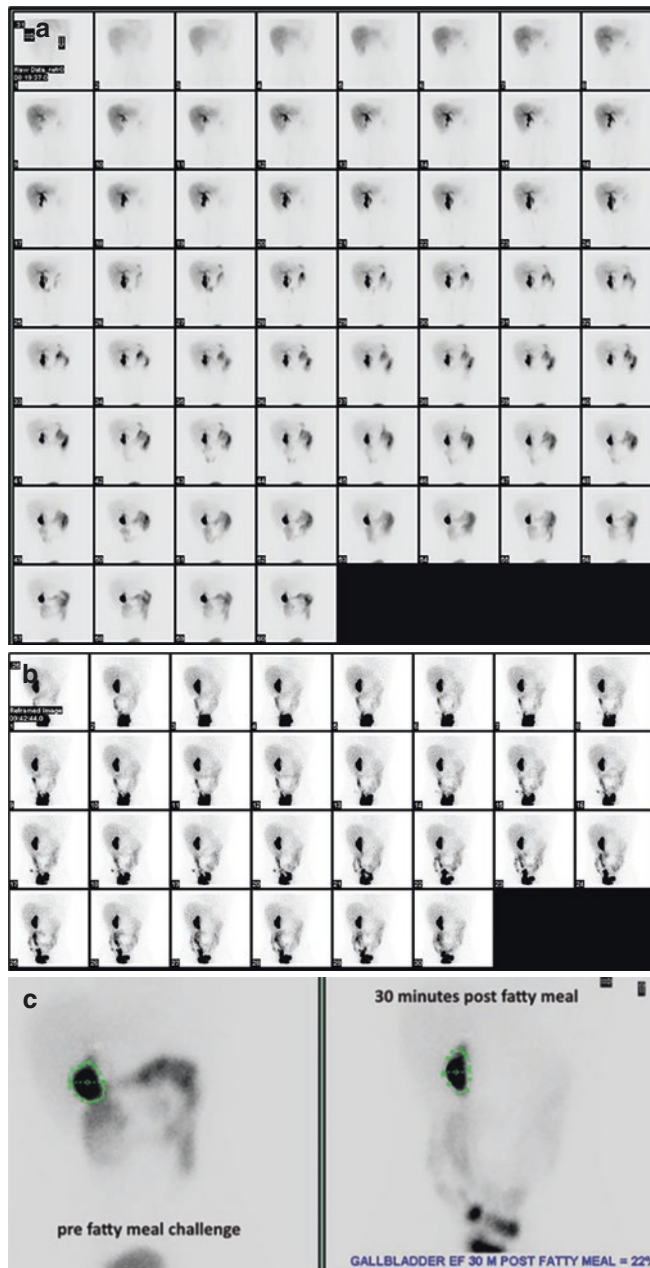


Fig. 7.3 History: A 16-year-old boy experienced repeated episodes of upper abdominal colicky pain during and after meals. Cholecystitis was suspected. The US did not show stones in the gallbladder or bile ducts. Study report: Dynamic images acquired for 60 mins following tracer injection (a) show normal uptake in and excretion from the liver. There is tracer accumulation in the gallbladder. A fatty meal was given to stimulate gallbladder

emptying, followed by only slight emptying on dynamic images acquired for additional 30 mins after ingestion of the meal (b). Gallbladder EF, calculated from static images obtained before and 30 mins after the fatty meal challenge (c) was 22% (normal values >35%). Impression: The findings suggest acalculous cholecystitis with abnormal gallbladder contraction

Case 7.4. Suspected Biliary Leak after Liver Transplant (Fig. 7.4)

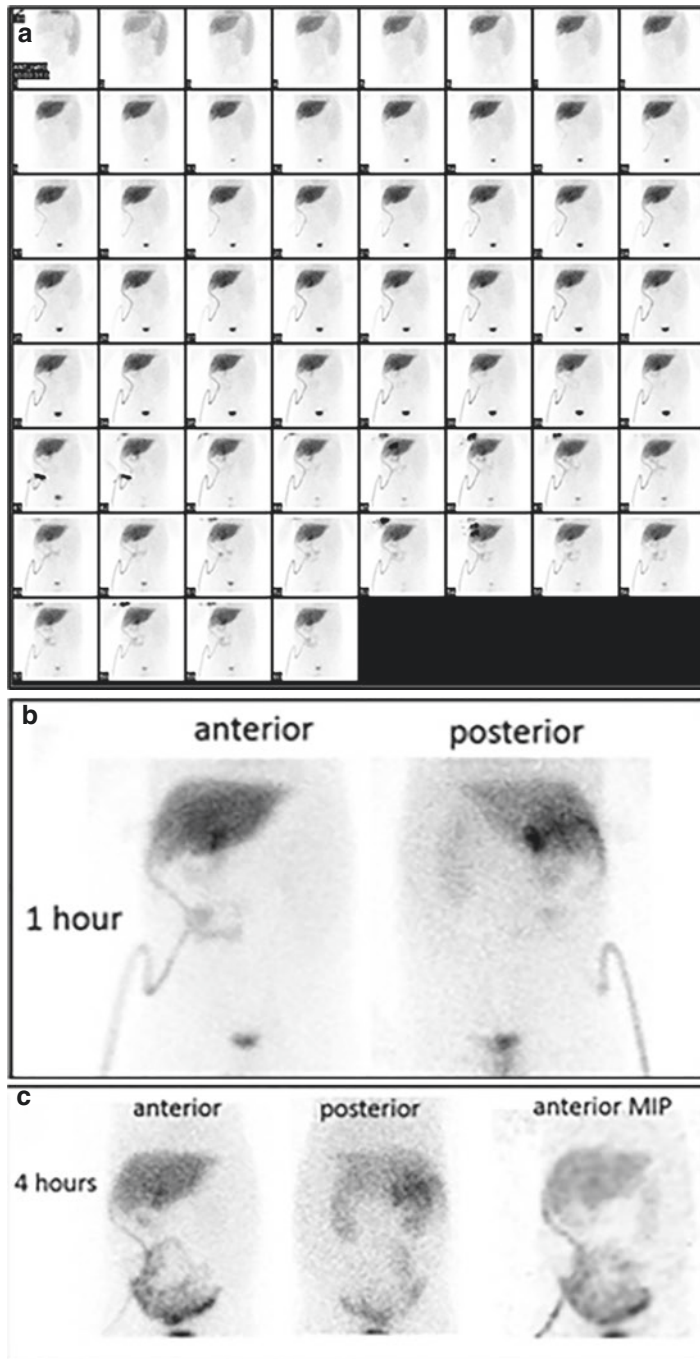


Fig. 7.4 History: An 11-year-old girl underwent liver transplantation 3 weeks prior to the current examination. During her postoperative course, she developed septicemia and ascites and a bile leak was clinically suspected. Study report: Dynamic images acquired for 60 mins after tracer injection (a) show homogenous uptake in the transplanted liver with some accumulation at the site of the anastomosis, just below the inferior margin of the liver. There is prominent tracer

activity in the tubing of the surgical drain positioned at the site of the anastomosis. No tracer transit into the bowel is noted. Static images at 1 h after tracer injection (b) show more tracer accumulation at the site of the anastomosis and a small amount in the bowel loops. At 4 h after tracer injection, anterior and posterior static images and a SPECT volume rendered image (MIP) (c) show cholestasis and tracer activity in the bowel loops. Impression: No evidence of bile leak

7.2 Liver and Spleen Reticuloendothelial System Scintigraphy

Clinical Indications [14]

At present, this study is performed quite rarely for relatively uncommon indications:

- Rarely, to assess liver and spleen involvement in metabolic diseases (e.g., Gaucher's disease and glycogen storage diseases).
- Evaluation of suspected portal hypertension.
- Evaluation of extramedullary hematopoiesis.
- Evaluation of splenic or hepatic trauma, in selective cases in conjunction with correlative imaging.
- Evaluation of the immunologic function of the spleen (functional hyposplenism).
- Presence of accessory spleens prior to or after elective splenectomy for hematologic disorders (when splenic scintigraphy with denatured RBCs cannot be performed).
- Evaluation of poly-/asplenia in cases of heterotaxy syndrome (when splenic scintigraphy with denatured RBCs cannot be performed).

Study Protocol for Liver-Spleen Scintigraphy [15]

Patient Preparation:

- No specific preparation is required.
- Check for results of correlative radiologic studies, especially in cases of heterotaxy syndrome.

Radiopharmaceutical, Administered Activity, Mode of Delivery

Radiopharmaceutical:

- [^{99m}Tc]sulfur colloid (SC).

Activity:

- 1.85 MBq/Kg (0.05 mCi/Kg), minimum dose 15 MBq (0.4 mCi).

Refer to the EANM pediatric dosage card and to the North American consensus guidelines on radiopharmaceutical administration in children in the respective EANM and SNMMI and image gently web sites.

Reference to national regulation guidelines, if available, should be considered.

Acquisition Protocol:

- Imaging can start a few minutes after tracer injection.
- Collimator: low-energy high-resolution parallel hole.
- Position: supine.
- Static images, in the anterior, posterior, RAO, LAO, and optionally right and left laterals, 2–5 min/view, matrix 256 × 256, and size-appropriate zoom.
- SPECT: 120 projections, 15 seconds/frame.
- SPECT/CT: when available can be helpful for specific indications.

Study Interpretation (Fig. 7.5)

- Normal pattern: the intensity of tracer uptake in the spleen is similar or slightly reduced compared to the liver on posterior view images.
- Size of liver and spleen: measured as maximal vertical length of the liver or vertical length of the liver at the midclavicular line (on the anterior view) and the maximal length of the spleen (on the posterior view).
- Location: abnormal ectopic foci of activity are seen in accessory spleen, polysplenia, or splenosis.
- Focal liver defects can be caused by numerous etiologies such as primary tumors, metastases, abscesses, hematoma, cirrhosis, cysts, and storage disease.
- Increased focal liver uptake is seen in focal nodular hyperplasia, regenerating nodules, and Budd-Chiari syndrome (focal increased activity in the caudate lobe).
- Focal or diffuse reduced liver uptake and increased uptake in spleen and bone marrow are found conditions causing extensive hepatocellular damage.
- Focal areas of reduced or even absent uptake of variable sizes in liver or spleen are due to trauma.
- Reduced tracer localization in a normal-appearing spleen in US suggests functional hyposplenism.

Case(s) 7.5 Patterns of liver and spleen SC uptake (Fig 7.5)

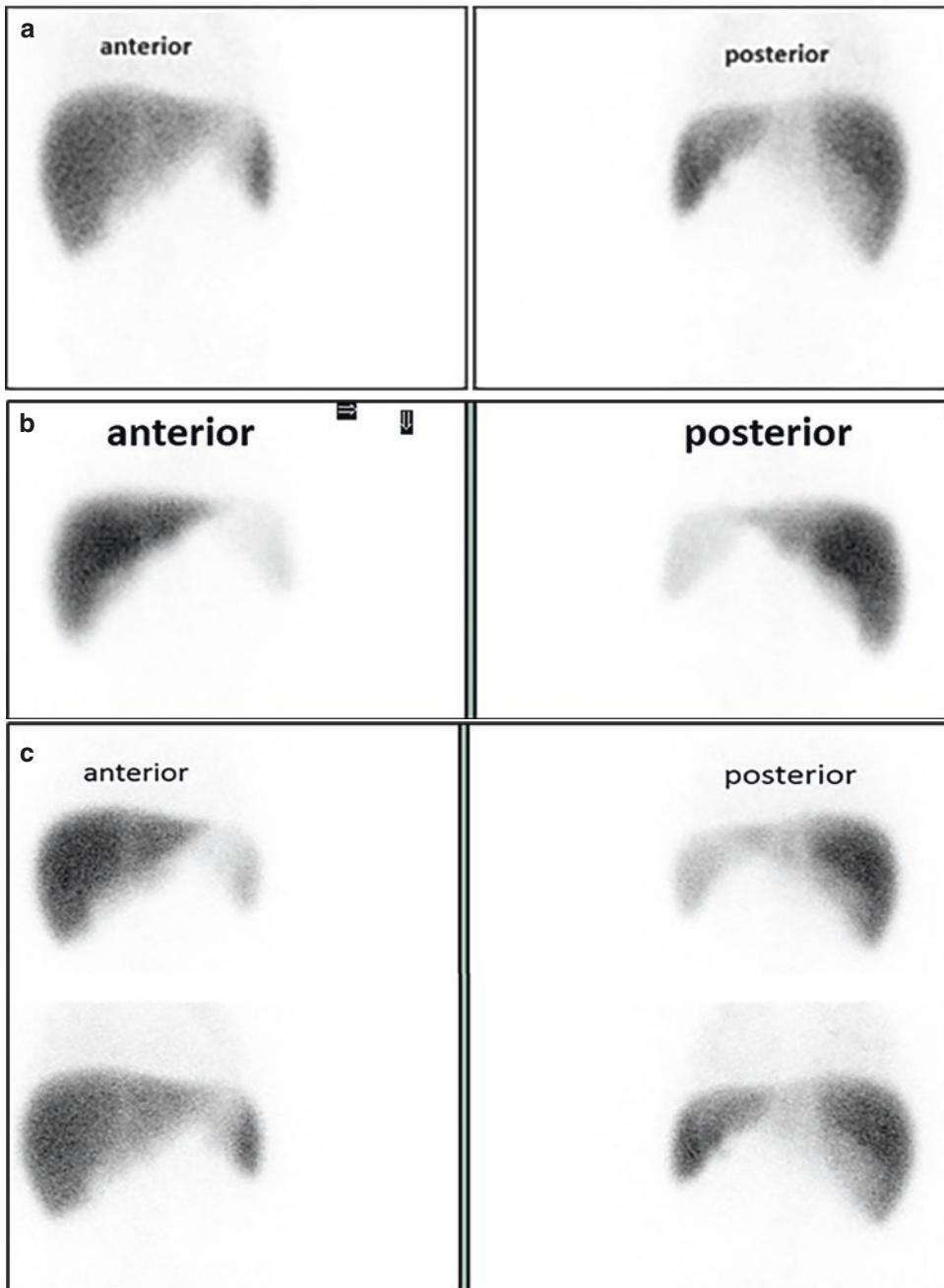


Fig. 7.5 Patterns of liver and spleen SC uptake. (a) Normal tracer uptake in liver and spleen in a 7-year-old girl with no evidence of immune deficiency. (b) Reduced uptake in an anatomically normal spleen in a 4-month-old infant evaluated for functional hyposplenism following pneumococcal meningitis and pneumonia. (c) Transiently reduced uptake in the spleen in a 5-year-old girl following

two episodes of pneumococcal meningitis who was suspected of functional hyposplenism. Reduced SC activity in the spleen supports the clinical suspicion (top row). The patient was treated with antibiotic prophylaxis. A repeat study 30 months later (bottom row) shows normalization of the tracer uptake by the spleen. Prophylaxis was discontinued

Correlative Imaging

- US and cross-sectional imaging with CT and/or MRI may show a solid mass in the liver or spleen.
- Contrast-enhanced US may be useful to characterize these solid lesions.
- MRI with specific biliary contrast agents may also help characterize lesions in the liver and biliary system.
- Correlation with US may show a normal appearing spleen in spite of low or absent radiotracer uptake.

Red Flags

- Scintigraphic findings suggesting space occupying lesions (SOL) are not specific. If clinically indicated, tissue sampling is advised following additional cross-sectional imaging.
- Improper SC labelling with subsequent appearance of dissociated free Pertechnetate in the circulation may result in the latter's focal accumulation in the renal collecting systems that may be erroneously interpreted as accessory spleens.

- Occasionally there is a significant superposition of the left liver lobe and the spleen. Planar images may suggest asplenia and a transverse lying liver. SPECT or SPECT/CT is essential to determine if there is, in fact, a superimposed functioning spleen.

Take Home Messages

- Size of the liver and spleen are age related.
- Transient enlargement of the liver and spleen is common in many pediatric diseases.
- Functional hyposplenism indicates inadequate phagocytosis of the tracer by RES macrophages in the spleen. Similar to asplenia, functional hyposplenism carries an increased risk of overwhelming, often fatal, sepsis by certain bacteria and requires prophylactic antibiotic therapy and immunizations.

Representative Case Examples

Case 7.6. Asplenia (Fig. 7.6)

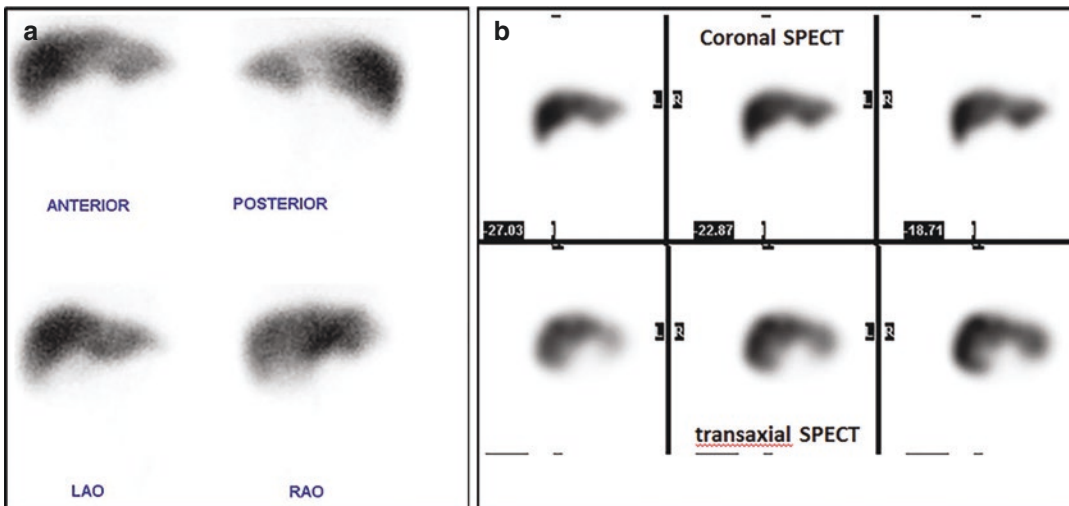


Fig. 7.6 History: A 4-month-old infant with heterotaxy syndrome that included ventricular and atrial septal defects and a right-sided stomach was evaluated for possible asplenia or polysplenia. Study report: Selected pla-

nar images (a) show a transverse lying liver and no splenic uptake, confirmed on selected SPECT slices (b). Impression: No evidence of functioning spleen tissue

Case 7.7. Splenic Infarct (Fig. 7.7)

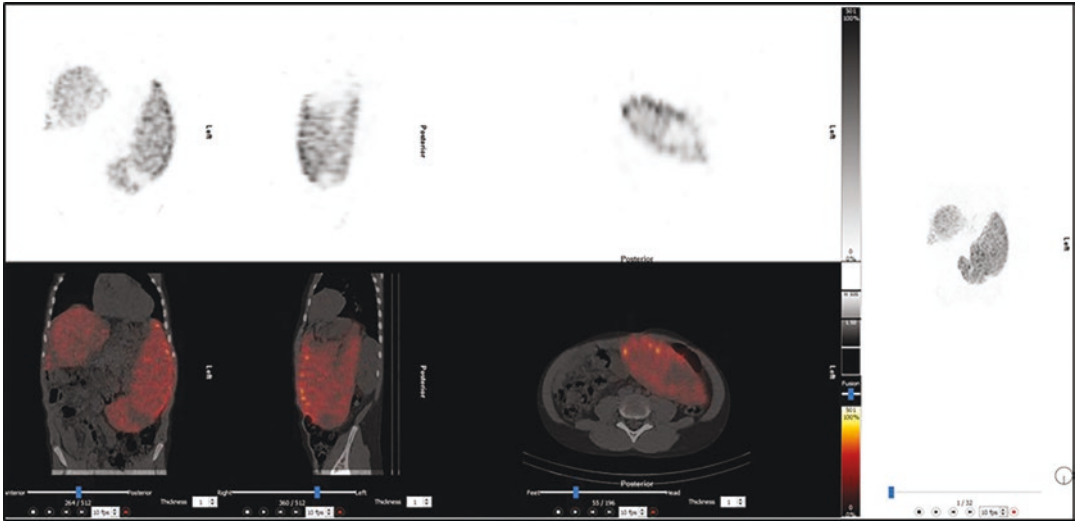


Fig. 7.7 History: This 12-year-old boy with previous biliary atresia and a functioning Kasai developed portal hypertension. He complained of recurrent sharp pain in the region of his enlarged spleen. There were concerns regarding a possible splenic infarct. Study report: The

SPECT/CT study (selected SPECT and fused coronal, sagittal and transaxial slices, left, and MIP, right) shows a wedge-shaped defect in the lower pole of the spleen. Impression: The findings are consistent with a splenic infarct in the lower pole of the spleen

7.3 Spleen Scintigraphy with Denatured (Heat Damaged) Red Blood Cells

Clinical Indications [16]

- Failure of splenectomy to relieve thrombocytopenia in idiopathic thrombocytopenic purpura (ITP) or anemia (in spherocytosis) in order to determine the presence of accessory spleen/s that was/were not resected.
- Heterotaxy syndromes, to determine the presence of polysplenia or asplenia.
- Identification of splenosis following splenectomy or abdominal trauma.
- Evaluation of abdominal or thoracic nodules suspected as ectopic, accessory, or wandering spleens.
- Evaluation of splenic torsion.

Study Protocol for DRBC Spleen Scintigraphy [17, 18]

Patient Preparation:

- No specific patient preparation is required.
- Check for results of correlative radiologic studies.

Radiopharmaceutical, Administered Activity, Mode of Delivery

Radiopharmaceutical—Preparation:

- [^{99m}Tc]heat damaged red blood cells (DRBC).
 - 1–3 ml of blood is drawn into a syringe containing heparin or acid citrate dextrose (ACD) solution for anticoagulation.
 - [^{99m}Tc] in vitro labelling of RBCs is performed.
 - Labelled RBCs are denatured by incubating the tube with the blood

in a warm water bath with a constant temperature of 49.5 °C for 15 mins.

- Allow the tube with the labelled blood to cool prior to reinjection.

Activity:

- 20–40 MBq (0.5–1 mCi).

Refer to the EANM pediatric dosage card and to the North American consensus guidelines on radiopharmaceutical administration in children in the respective EANM and SNMMI and image gently web sites.

Reference to national regulation guidelines, if available, should be considered.

Delivery:

- Slow IV reinjection.

Acquisition Protocol:

- Imaging starts 15 mins after tracer injection.
- Collimator: low-energy, high- or ultrahigh-resolution parallel hole.
- FOV: entire abdomen. The thorax should be included in suspected intrathoracic ectopic splenic tissue.
- Static anterior, posterior, 4 obliques, and 2 lateral images are acquired; 2–5 min/view, matrix 256 × 256, size-appropriate zoom.
- SPECT (or SPECT/CT if available) should follow planar scintigraphy and provides important information in particular in cases with suspected polysplenia, splenosis, and ectopic splenic tissue.

Study Interpretation

- Sites of increased tracer localization represent DRBCs trapped in splenic tissue.
- The intensity of uptake is significantly higher than the background and surrounding organs.
- The location, size, and number of these foci should be reported, as well as their relationship to the liver.
- DRBCs scintigraphy determines the presence of multiple spleens (polysplenia) or the absence of the spleen (asplenia).
- Splenosis: scattered splenic nodules (mostly in the abdomen) that appear as multiple hot spots.
- Accessory spleens: found in approximately 10–15% of autopsies in children.
- Ectopic spleen: found in a location different from the known anatomic site in the left upper abdomen can be easily identified with DRBC scans.
- Splenic torsion: the spleen is not visualized.

Correlative Imaging

- US and cross-sectional imaging with CT and or MRI may confirm the presence, position, and appearance of splenic tissue.

Red Flags

- DRBC scintigraphy is the investigation of choice when looking at anatomical localization of splenic tissue. However, it does not provide information on the function of the splenic tissue and is more cumbersome when compared to colloid scintigraphy.
- Reinjection of DRBCs should be done after proper identification of the patient and according to local regulations for blood administration.

- Scheduling no more than one RBC scan per session is a good practice to reduce the chance of labelled blood misadministration.

Take Home Messages

- The so-called wandering spleen occurs rarely, when there is abnormal mobility of the spleen that is inadequately fixed to its surroundings and can be located in a different position within the abdomen. The wandering spleen carries a risk of torsion because of the consequent occlusion of the splenic vessels.
- Splenosis is an acquired condition of splenic tissue auto-transplantation in different body compartments following trauma involving the spleen and should be distinguished from accessory spleens.
- Accessory spleens are a congenital condition of additional up to six spleens that receive their blood supply from branches of the splenic artery and are located in specific abdominal regions.
- A small ectopic spleen or multiple small spleens that are identified on DRBC scintigraphy may lack the immunological function of a normal spleen.
- SPECT/CT correlation of sites of splenic tissue with anatomic findings (e.g., nodules) is of particular value in cases with complex anatomy such as in heterotaxy syndromes.
- Intraoperative gamma-probe localization of accessory splenic tissue might be suggested.

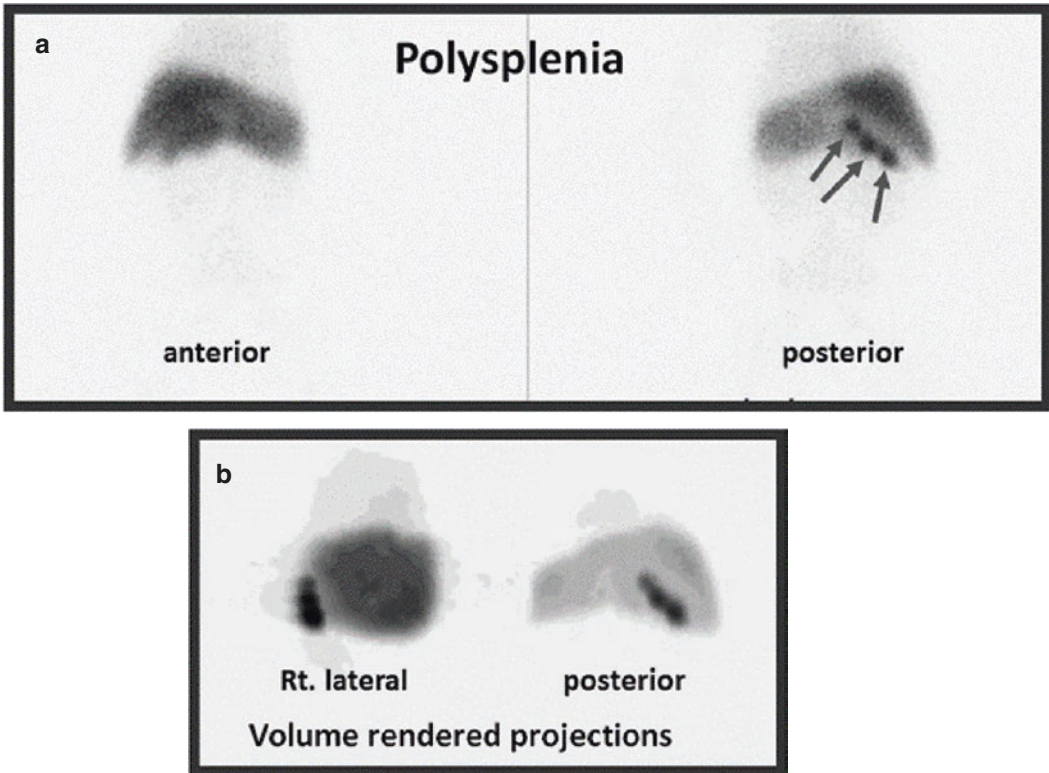


Fig. 7.8 History: A newborn baby with heterotaxy syndrome and cardiac malformations that included patent ductus arteriosus, patent foramen ovale, and interrupted inferior vena cava was evaluated. Study report: Anterior and posterior planar images (a) and volume-rendered

SPECT projections (b) show accumulation of DRBCs in three small adjacent spleens, ectopically located in the right upper abdomen (arrows). Impression: The findings are consistent with polysplenia associated with left heterotaxy isomerism

Representative Case Examples

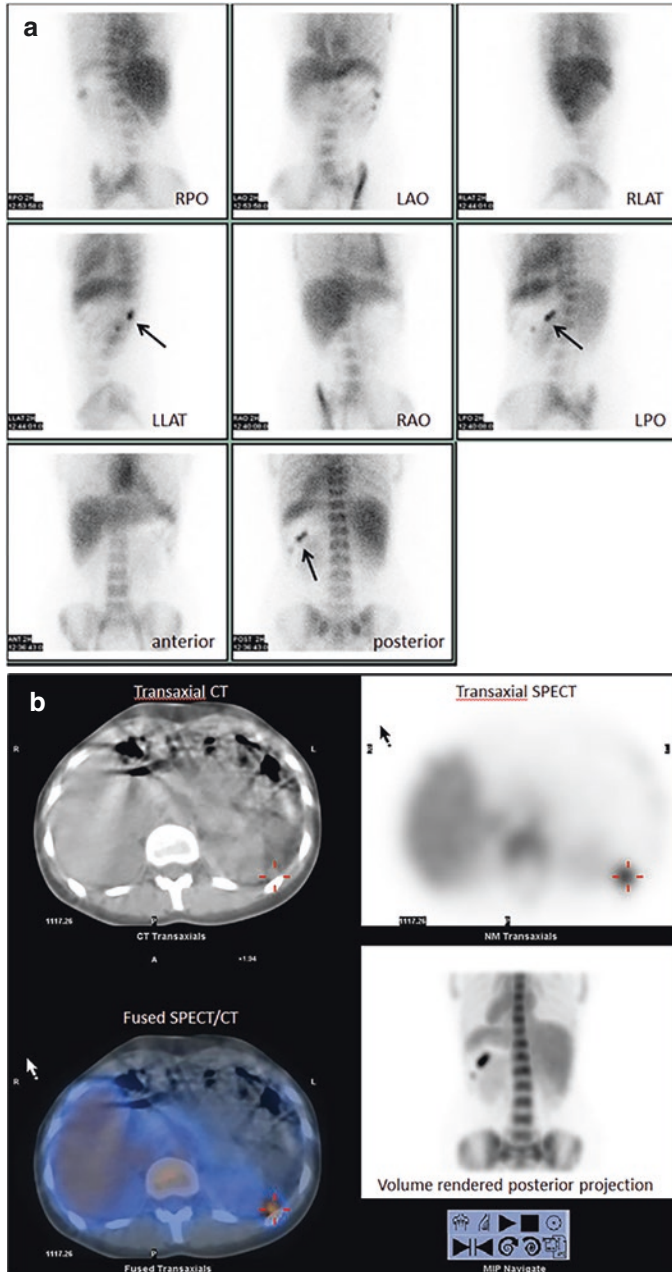


Fig. 7.9 History: An 18-year-old girl with ITP underwent elective splenectomy because of life-threatening thrombocytopenia. The thrombocytopenia persisted despite the surgical removal of the spleen. Explorative laparotomy did not reveal any residual or ectopic splenic tissue. Study report: Planar views of the abdomen and lower chest (a) show a number of foci of DRBC uptake in the posterior upper abdomen, adjacent to the left posterior

lower ribs (arrows). SPECT/CT (b) was performed to better localize the sites prior to re-exploration and showed intense uptake in one of the splenic nodules adjacent to the upper left posterior abdominal wall. Impression: Evidence for residual splenic tissue that was either not removed at previous surgery or represents splenosis due to auto-implantation of splenic tissue that occurred during operation

Case 7.8. Polysplenia (Fig. 7.8)**Case 7.9. Residual splenic tissue (Fig. 7.9)****7.4 Liver Blood Pool Scintigraphy****Clinical Indications [19]**

- Detection and evaluation of hemangiomas.

Study Protocol for RBC Scintigraphy [20]**Radiopharmaceutical, Administered Activity, Mode of Delivery***Radiopharmaceutical:*

- ^{99m}Tc RBCs [21].
 - In vitro labelling is the method of choice and should be employed when an adequate facility and proper radiopharmacy practices are available 1–3 ml of the patient's blood is drawn anticoagulated with heparin or acid citrate dextrose (ACD).
 - RBCs are labelled with a commercially available preparation according to the manufacturer's instructions.

Activity:

- Minimum dose 74 MBq (2 mCi), maximum dose 740 MBq (20 mCi).

Refer to the EANM pediatric dosage card and to the North American consensus guidelines on radiopharmaceutical administration in children in the respective EANM and SNMMI and image gently web sites.

Reference to national regulation guidelines, if available, should be considered.

Acquisition Protocol [18, 22]:

- Imaging is performed in the supine position.
- Collimator: low energy, high- or ultrahigh-resolution parallel hole.

Acquisition Parameters:

- Dynamic study: 1 second/frame x 60, matrix 128 x 128, size-appropriate zoom.
- Early blood pool static images follow the dynamic study. Multiple projections, anterior, posterior, RAO, LAO, and lateral views optional, 3–5 mins per view, matrix 256 x 256.
- Late static blood pool images 2 h after tracer injection in same projections, with same parameters.
- SPECT (or SPECT/CT when available) of the liver follows the late static images with 120 projections, 25 seconds/step, matrix 128 x 128, and appropriate zoom.
- Late whole-body images to assess for additional hemangiomas.

Study Interpretation

- Foci of increased tracer accumulation on the late blood pool planar or SPECT images are likely to represent hemangiomas.
- Large hemangiomas in the liver may appear photopenic on early blood pool images due to slow blood flow.
- SPECT/CT or software fusion of SPECT with CeCT is recommended to ascertain correspondence between anatomical and radionuclide findings.

Correlative Imaging

- Small hemangiomas are better evaluated with contrast CT or MRI.
- Contrast-enhanced US may be useful to characterize these solid lesions.
- MRI may also help to characterize these lesions.

Red Flags

- Injection of in vitro labelled RBCs requires extreme caution to ensure that the blood is injected into the patient from whom it was drawn. To reduce the chance of misadministration it is advised to avoid booking more than one in vitro labelled RBC study per session.
- Inadequate RBC labelling may result in dissociated Perchnetate with visualization of the thyroid gland and stomach.
- The ability to detect hemangiomas depends on their size and location. Lesions smaller than 1.5 cm in diameter may not be evident, especially when situated in regions with high blood pool activity.

Take Home Messages

- The study is specific for lesions with high blood pool and is useful in distinguishing them from other space occupying lesions.
- RBCs cannot distinguish between subtypes of hemangiomas or between hemangiomas and hemangiosarcomas.
- SPECT or SPECT/CT can improve the accuracy of the study and diagnostic confidence in the evaluation of lesions suspected of hemangiomas.
- Hemangiomas can be multifocal, especially in infants. It is advised to perform a whole-body late blood pool scan to screen for additional hemangiomas throughout the body.

Representative Case Examples

Case 7.10. Liver Hemangioma (Fig. 7.10)

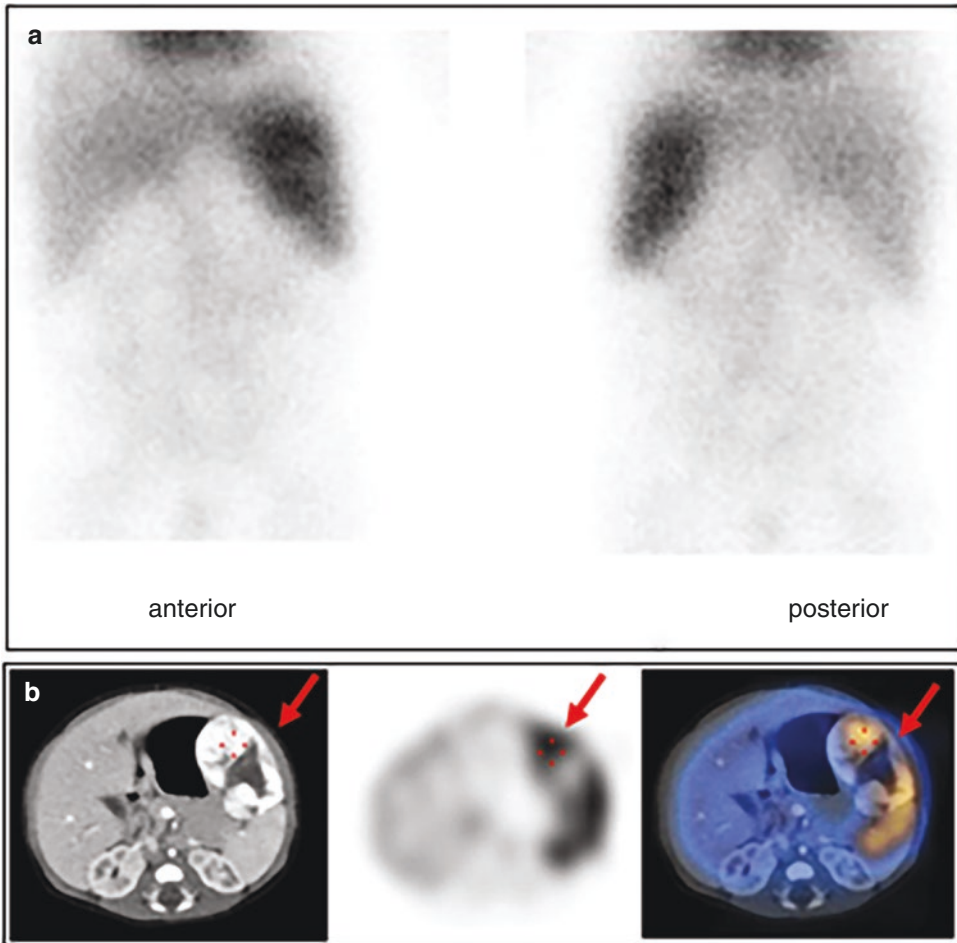


Fig. 7.10 History: A newborn in whom prenatal US detected a large mass in the left lobe of the liver confirmed on postnatal US was referred for RBCs scan since a hepatic hemangioma was included in the differential diagnosis. Study report: Late anterior and posterior planar images (a) show high physiologic activity in the splenic blood pool. A previously performed contrast-enhanced (ce) CT (b, left image) shows an enhancing mass (arrow) in the left hepatic lobe displacing the spleen posteriorly. SPECT (b, middle image) and co-registered SPECT-ceCT

(b, right image) show high blood pool with a central photopenic region in the mass (arrow). Uptake in the posterior portion of the mass is contiguous with the physiologic blood pool activity of the spleen. Impression: The findings are consistent with a large liver hemangioma. Note that planar images could not identify the hemangioma because of the superposition of blood pool activities in the liver lesion and the spleen, which could be interpreted as normal spleen activity only

References

1. Kianifar HR, et al. Accuracy of hepatobiliary scintigraphy for differentiation of neonatal hepatitis from biliary atresia: systematic review and meta-analysis of the literature. *Pediatr Radiol.* 2013;43(8):905–19.
2. Tulchinsky M, et al. SNM practice guideline for hepatobiliary scintigraphy 4.0. *J Nucl Med Technol.* 2010;38(4):210–8.
3. Nadel HR. Hepatobiliary scintigraphy in children. *Semin Nucl Med.* 1996;26(1):25–42.
4. Roca I, Ciofetta G. Hepatobiliary scintigraphy in current pediatric practice. *Q J Nucl Med.* 1998;42(2):113–8.

5. Andersen TB, Aleksyniene R, Petersen LJ. Accuracy of hepatobiliary scintigraphy and added value of SPECT/CT versus planar imaging for diagnosing biliary atresia. *Hell J Nucl Med.* 2021;24(2):108–13.
6. Ziessman HA. Hepatobiliary scintigraphy in 2014. *J Nucl Med.* 2014;55(6):967–75.
7. Barseghyan K, et al. Utility of hepatobiliary scintigraphy in diagnosing or excluding biliary atresia in premature neonates and full-term infants with conjugated hyperbilirubinemia who received parenteral nutrition. *J Matern Fetal Neonatal Med.* 2018;31(24):3249–54.
8. Shammas A, Vali R, Charron M. Pediatric nuclear medicine in acute care. *Semin Nucl Med.* 2013;43(2):139–56.
9. Low CS, Ahmed H, Notghi A. Pitfalls and limitations of radionuclide hepatobiliary and gastrointestinal system imaging. *Semin Nucl Med.* 2015;45(6):513–29.
10. Gutierrez-Villamil C, et al. Hepatobiliary scintigraphy to evaluate biliary complications of Pediatric liver transplantation: an account of an experience. *Eur J Pediatr Surg.* 2022;32(3):258–62.
11. Miller TT, et al. Choledochal cyst. Preoperative sonographic and scintigraphic assessment. *Clin Nucl Med.* 1993;18(11):1001–2.
12. Napolitano M, et al. Practical approach to imaging diagnosis of biliary atresia, part 1: prenatal ultrasound and magnetic resonance imaging, and postnatal ultrasound. *Pediatr Radiol.* 2021;51(2):314–31.
13. Napolitano M, et al. Practical approach for the diagnosis of biliary atresia on imaging, part 2: magnetic resonance cholecystopancreatography, hepatobiliary scintigraphy, percutaneous cholecysto-
- cholangiography, endoscopic retrograde cholangiopancreatography, percutaneous liver biopsy, risk scores and decisional flowchart. *Pediatr Radiol.* 2021;51(8):1545–54.
14. Treves ST, Jones AG. Liver and spleen. In: Treves ST, editor. *Pediatric nuclear medicine and molecular imaging.* New York: Springer; 2014. p. 235–63.
15. Matesan MM, et al. Assessment of functional liver reserve: old and new in 99mTc-sulfur colloid scintigraphy. *Nucl Med Commun.* 2017;38(7):577–86.
16. Scheuerman O, et al. Functional hyposplenism is an important and underdiagnosed immunodeficiency condition in children. *Acta Paediatr.* 2014;103(9):e399–403.
17. Armas RR. Clinical studies with spleen-specific radio-labeled agents. *Semin Nucl Med.* 1985;15(3):260–75.
18. Schillaci O, et al. Single-photon emission computed tomography/computed tomography in abdominal diseases. *Semin Nucl Med.* 2007;37(1):48–61.
19. Arcay A, et al. Hepatoblastoma mimicking Hemangioma in Labeled red blood cell scintigraphy. *Clin Nucl Med.* 2019;44(3):229–31.
20. Middleton ML. Scintigraphic evaluation of hepatic mass lesions: emphasis on hemangioma detection. *Semin Nucl Med.* 1996;26(1):4–15.
21. Radiolabelled Autologous Cells. Methods and standardization for clinical use. Vienna: Int Atomic Energy Agency; 2015.
22. Roy SG, et al. Importance of SPECT/CT in detecting multiple hemangiomas on 99mTc-labeled RBC blood pool scintigraphy. *Clin Nucl Med.* 2015;40(4):345–6.

The opinions expressed in this chapter are those of the author(s) and do not necessarily reflect the views of the IAEA: International Atomic Energy Agency, its Board of Directors, or the countries they represent.

Open Access This chapter is licensed under the terms of the Creative Commons Attribution 3.0 IGO license (<http://creativecommons.org/licenses/by/3.0/igo/>), which permits use, sharing, adaptation, distribution and reproduction in any medium or format, as long as you give appropriate credit to the IAEA: International Atomic Energy Agency, provide a link to the Creative Commons license and indicate if changes were made.

Any dispute related to the use of the works of the IAEA: International Atomic Energy Agency that cannot be settled amicably shall be submitted to arbitration pursuant to the UNCITRAL rules. The use of the IAEA: International Atomic Energy Agency's name for any purpose other than for attribution, and the use of the IAEA: International Atomic Energy Agency's logo, shall be subject to a separate written license agreement between the IAEA: International Atomic Energy Agency and the user and is not authorized as part of this CC-IGO license. Note that the link provided above includes additional terms and conditions of the license.

The images or other third party material in this chapter are included in the chapter's Creative Commons license, unless indicated otherwise in a credit line to the material. If material is not included in the chapter's Creative Commons license and your intended use is not permitted by statutory regulation or exceeds the permitted use, you will need to obtain permission directly from the copyright holder.



8.1 Dynamic Renal Scintigraphy

Clinical Indications [1]

- Children with a dilated urinary tract, to exclude obstruction.
- Renal transplant evaluation.
- Suspected renal arterial and venous thromboembolic disease.
- Suspected renal trauma.
- Renal length/volume asymmetry at ultrasound (US).

Pre-Exam Information

- History of a recent urinary tract infection (UTI)? If so, when was the last episode?
- Does the child have an ectopic kidney?
- Can the child void on demand? Is the patient toilet trained?
- Is this a baseline or follow-up investigation?
- What are the US results?
- Has the serum creatinine been tested? What is the value?

Study Protocol for Dynamic Renography [2]

Patient Preparation

- Oral hydration is encouraged before arrival and may be sufficient in most situations.
- Place IV line to inject the radiopharmaceutical and furosemide and intravenous (IV) fluids if required.
- IV hydration (volume expansion) is more reliable in diagnosing questionable cases of urinary obstruction.
- IV hydration in patients with no cardiovascular contraindication is suggested to reduce the incidence of false-positive results. The suggested volume is 15–20 ml/kg two-thirds of which should be given prior to furosemide administration. The slow administration of fluid is continued during the remainder of the study.
- Assess bladder status.
- Toilet-trained children should be encouraged to urinate before positioning them on the bed.

D. De Palma (✉)
Nuclear Medicine Unit, ASST Settelaghi,
Varese, Italy

T. N. Pascual
Department of Science and Technology,
Manila, Philippines

Radiopharmaceutical, Administered Activity, Mode of Delivery

Radiopharmaceutical:

- [^{99m}Tc]-mercapto-acetyl-triglycine (MAG3) or [^{99m}Tc]-ethylene dicysteine (EC) are preferred as being tubular agents.
- Alternative: [^{99m}Tc]diethylene-triamine pentaacetate (DTPA), a glomerular radiotracer.

Activity:

- MAG3: 3.7–5.55 MBq/kg (0.10–0.15 mCi/kg), with a minimum dose of 15 MBq (0.40 mCi).
- DTPA: 20–196 MBq (0.5–5.3 mCi)

Refer to the EANM pediatric dosage card and to the North American consensus guidelines on radiopharmaceutical administration in children in the respective EANM and SNMMI and image gently web sites.

Reference to national regulation guidelines, if available, should be considered.

Acquisition Protocol

Patient Positioning

- Supine with the camera in the posterior position
- Double check with a marker that the whole abdomen and pelvis (from xiphoid to symphysis pubis and lateral margins of the abdomen) are in the field-of-view (FOV) before starting the acquisition.
 - If there is a history of an ectopic kidney, ensure that it is in the FOV and acquire, whenever possible, anterior view images contemporary and in addition to posterior views and calculate the differential renal function

(DRF) from the geometric mean of anterior and posterior renal counts.

- Patients with renal transplants will be acquired in the anterior view.

Acquisition parameters

Two acquisition protocols based on the timing of furosemide (F) administration can be used:

- F-0 protocol: The radiopharmaceutical and furosemide are injected together, followed by at least 20 mins of dynamic imaging at 10–15 s/frame, matrix 128 × 128, size-appropriate zoom.
- F + 20 or F + 30 protocol: Following tracer administration, dynamic images are acquired as above for 20 or 30 mins, respectively. Furosemide is then administered, and the second set of post-furosemide dynamic images is acquired for 20–30 mins.
 - The pre- and post-furosemide dynamic images can be obtained as a single continuous acquisition or two separate acquisitions. In this second case, placing the child vertically for 5–10' may allow the kidney to empty enough, at physician's judgement, to avoid furosemide administration and shorten the scan time.
 - Whenever the pelvis is not full after 20 or 30 mins furosemide administration should be delayed until the pelvis is filling up.
- The furosemide dose across all ages is 1 mg/kg with a maximum dose of 40 mg.
- The first minute of acquisition in both protocols can be acquired with a fast frame rate of 1–2 s/frame to allow evaluation of kidney perfusion.
- A "late" image is mandatory to complete the study in both protocols if drain-

age is inadequate at the end of the post-furosemide dynamic sequence.

- It is typically acquired at least 45 mins from the start of the study.
- It should be acquired after the patient empties his bladder, unless there is a bladder catheter in place, and after he has been in a vertical position for at least 10–15 mins.
- It can be acquired as a static image or as a short sequence of dynamic images for 2 mins which will allow more straightforward incorporation of this data into the renogram if desired.
- Alternatively, a 1-min static image can be acquired at the end of the post-furosemide dynamic sequence while the patient is supine, followed by a second static image with similar acquisition parameters after the patient has been in the erect position for 10–15 mins.

Dynamic Renogram Study Processing and Interpretation [3, 5]

Study Processing

- Check for movement. DRF calculations should be interpreted with caution in the presence of motion.
- Accepted methods for DRF calculations are:
 - Integral method using the area-under-the-curve (AUC) is preferred because it is less sensitive to patient's motion.
 - the Rutland Patlak method.
- Methodology:
 - Draw renal regions-of-interest (ROIs) around the visible renal parenchyma being careful not to “cut” the kidney and not to include the collecting system. Large ROIs containing the yet unfilled pelvis are not acceptable for the DRF calculation.
 - For MAG3 studies, the ROI is constructed on the 60–120 s summed image.
 - For DTPA, the ROI is constructed on the 120–180 s summed image.

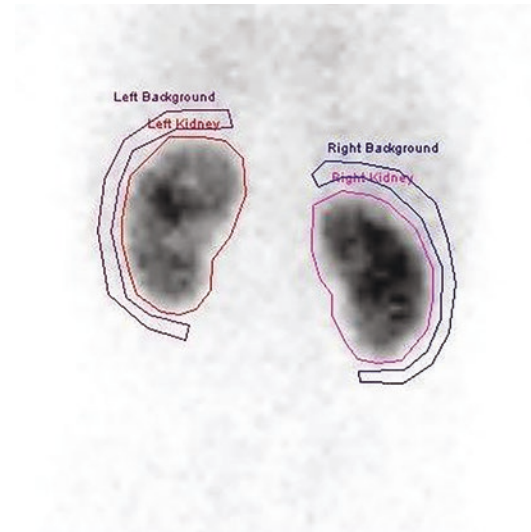


Fig. 8.1 Example of kidneys (red line for the left and pink for the right kidney) and background (purple on the left and blue on the right) ROIs

- Background ROIs should sample activity originating in the liver and spleen. The recommended background ROI has to be inside the body outline, is perirenal, semilunar, “C”-shaped, and samples activity surrounding both upper and lower poles (Fig. 8.1).
- The Rutland Patlak method requires an additional ROI drawn around the heart (blood pool), or, if the heart is not in the FOV, the spleen can be used.

Renogram Processing Quality Control

It is advised to perform the following quality assurance steps, mainly in infants and children with impaired renal function: Process the renogram more than once to check for reproducible values. (i.e., within 4%), modifying size and location of the background ROIs or the time interval selected for the calculation.

Processing the Diuretic Response

- The ROI used for the construction of the drainage curve and for analysis and calculation of semiquantitative parameters:
 - Should be positioned on the summed images showing the maximal dilatation of the collecting system.

- Should include the entire collection system. In cases of hydronephrosis, both the ureter and the pelvis should be included.
- If there is suspicion of concomitant ureteropelvic junction (UPJ) obstruction, a second ROI covering only the pelvis should be placed.
- Many centers utilize a semi-quantitation technique to measure the clearance/diuretic T1/2 of the tracer over a 20–30 min period post-diuretic administration, defined as the time at which the TAC decreases to half of its maximal activity.
- Guidelines on diuresis renography in children recommend using the normalized residual activity (NORA) index for a semiquantitative assessment of drainage calculated as the decay corrected, post-diuretic residual kidney counts divided by the 1–2 mins parenchymal counts [4].
 - This ratio normalizes the residual activity to the parenchymal function of the kidney.
 - Typical time points for NORA calculation include the end of the post-furosemide dynamic sequence and, most importantly, the late, post-micturition, post-gravity-assisted image.

Study Interpretation

- Assess the technical quality of the study as good or poor including whether there is excessive patient movement or interstitial and not IV injection of the radiopharmaceutical.
- Describe the images and renogram curves including:
 - The tracer uptake in each kidney at 1–2 mins after the beginning of the study and the appearance of the kidneys on these images.
 - With MAG3, which is a cortical agent, assesses for the presence of cortical defects, for signs of duplications of the excretory

system (see Sect. 8.2) and if there are abnormal renal positions or shapes.

- Measure DRF.
- Assess the clearance of tracer activity from each kidney, whether there is prolonged cortical transit and pooling, as well as any delay in drainage from calyces, pelvis, and ureters.
- If possible, identify the anatomic level of hold-up, i.e., the uretero-pelvic (UPJ) or uretero-vesical junction (UVJ).
- State the time that furosemide was given and the presence or absence of a diuretic response using the NORA semiquantitative drainage assessment, with a value above 1–1.5 at 60 mins being considered abnormal.
- Assess the late post-micturition and post-gravity-assisted images to determine further drainage from the kidneys.

Correlative Imaging

- US, CT, and MRI are not reliable in the assessment of renal function and in evaluation of drainage
- Correlation with the US is required when performing diuretic renography.
- At least one US should be performed prior to a renogram.
- US provides information such as uni- or bilateral disease, the size and position of the kidneys and pelvis, presence of dilated calyces or cortical thinning, very useful in deciding on the optimal time for a baseline renogram and follow-up studies.

Red Flags [6, 7]

- If the F + 0 protocol is planned and the child has an adequate oral fluid intake, a venipuncture with a 25-gauge needle and a three-way stopcock for saline flushing can be used when only very thin veins seem available.

- The indwelling venous cannula may be inserted to maintain sufficient hydration for an excellent diuretic effect and obviate repeated trauma from multiple percutaneous injections.
- The Intravenous fluid solution type used for pre-test hydration should concur with the hospital's regulations.
- In dysplastic kidneys with huge dilatation of the collecting system, when using the F+20 or + 30 protocol, the pelvis may not be filled with tracer activity at the end of the first 20–30 mins.
- The nuclear medicine technologist should stay next to the child, at least for the first 5 mins of the renogram, to ensure that movement is kept to a minimum. Parents'/caregivers' help whenever possible is also welcomed. Motion artifacts, common in pediatric studies, can introduce significant errors in half-time (T1/2) values, which should be therefore interpreted in conjunction with visual assessment.
- Accurate assessment of renal perfusion is difficult in small children because of the small administered activity.
- Bladder catheterization is an option in non-toilet-trained children. It should be performed on a selective basis keeping in mind the unpleasant nature of the procedure and the small risk of infection. Antibiotic prophylaxis for the procedure is advised. Bladder catheterization should be performed by qualified, trained personnel.
- Insufficient hydration impairs adequate drainage assessment.
- A full distended urinary bladder impairs drainage assessment, increases the likelihood of vesicoureteral reflux (VUR) and causes a "pseudo-obstruction."
- Drainage from hugely dilated systems or hydronephrotic kidneys with poor parenchymal function can be slow without any obstruction. The conclusion of obstruction should be avoided [8].
- When diuretic renography study suggests obstruction, pay attention to the cortical transit time (CTT). A prolonged CTT means that the obstructed kidney has an increased risk of losing function and thereby there is a need for surgery [9].
- MAG3 scintigraphy in children with normal renal function can identify major cortical abnormalities but can miss minor defects [10].
 - Renal immaturity in neonates makes it essential to use tubular agents such as MAG3.
 - In the presence of excessive movement during the first 1–3 mins of the study, if available, utilize a dynamic motion correction program.
 - Looking at DRF values, check the correct drawing of background ROIs in case of apparent discrepancy between values and images. This is especially important in young infants with physiologic renal immaturity and in cases of impaired renal function. It may be also difficult in some infants with huge hydronephrotic kidneys abutting the abdominal wall.
 - Acute UTI can cause a transient drop in DRF. In children presenting with signs or symptoms of UTI or fever, it may be useful to do a urinary dipstick on the day of the study to ensure that there is no ongoing infection at the time of the investigation.

Take Home Messages

- Diuretic dynamic renography provides essential information for therapeutic decisions regarding surgical or conservative management of urinary tract dilatations.
- MAG3 and EC are tubular agents characterized by higher extraction subsequently translating into images with improved kidney contrast. This is of paramount importance in young infants with physiologic renal immaturity and in patients with compromised renal function.

- DTPA is a glomerular radiotracer that can be an alternative radiopharmaceutical used only when tubular agents are unavailable.
- A fast 1-s initial acquisition step is essential for evaluating transplanted kidneys but not necessary for the evaluation of urinary tract dilatation.
- A diuretic renogram can be performed at any age. In newborns, unless an urgent surgical procedure is considered, it is best to postpone the study up to the age of 30–45 days to allow for some renal maturation.
- In selected cases (e.g., single kidney with hydronephrosis and suspected obstruction), scintigraphy is often indicated before nephrostomy tube placement, even in newborns.
- Guidelines on diuresis renography in infants and children recommend two acquisition protocols based on the timing of furosemide administration.
- If there is a history of an ectopic kidney, ensure that it is included in the FOV and acquire, whenever possible, anterior view images contemporary and in addition to posterior views using a dual-head camera to improve the accuracy of the DRF.
- It is mandatory to use the same radiopharmaceutical and acquisition protocol, the same timing of furosemide administration and the same timing of the late post-void image in follow-up studies of the same patient.
- Bladder catheterization can be helpful in cases of hydro-/ureteronephrosis, high-grade (4–5) VUR, and neurogenic bladder, as these conditions may cause false-positive results for urinary obstruction.
- Good drainage at the end of the whole study has a high positive predictive value for the absence of obstruction.
- Slow drainage following furosemide challenge might imply partial obstruction, but it is not specific.
- A $T_{1/2}$ value of less than 15 mins has a high positive predictive value in excluding obstruction.

Representative Case Examples

Case 8.1. Normal Renogram (Fig. 8.2)

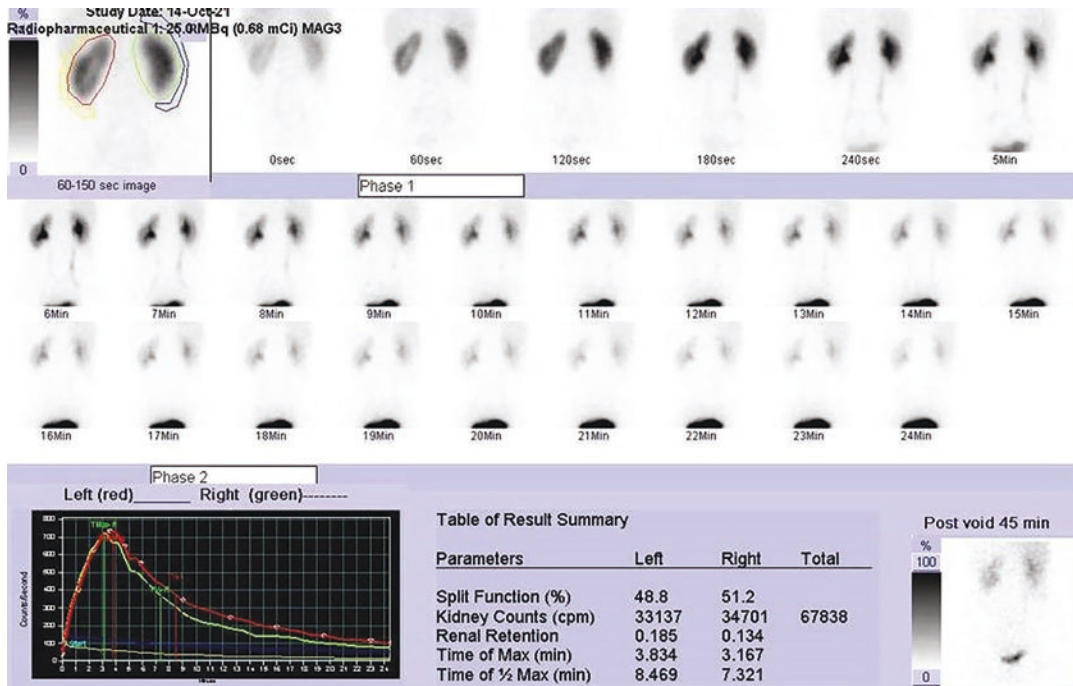


Fig. 8.2 History: A 6-year-old boy with recurrent UTIs and possible VUR performed a renogram following administration of MAG3 as a precursor for the indirect cystogram. Study report: There is good symmetrical uptake in both kidneys. No cortical defects are seen. The calyces, pelvises, and bladder are visualized 3 mins after tracer injection. There is good clearance of activity from

the kidneys to the bladder, as shown on the summed 1 min images of the renogram. The DRF is normally balanced, left kidney 49%, right kidney 51%, and the perfusion and clearance curves are normal on the 1–2.5 min clearance image with drawn ROIs. Impression: This is a normal renogram

Case 8.2. Dilated Right Excretory System with no Evidence of Obstruction (Fig. 8.3)

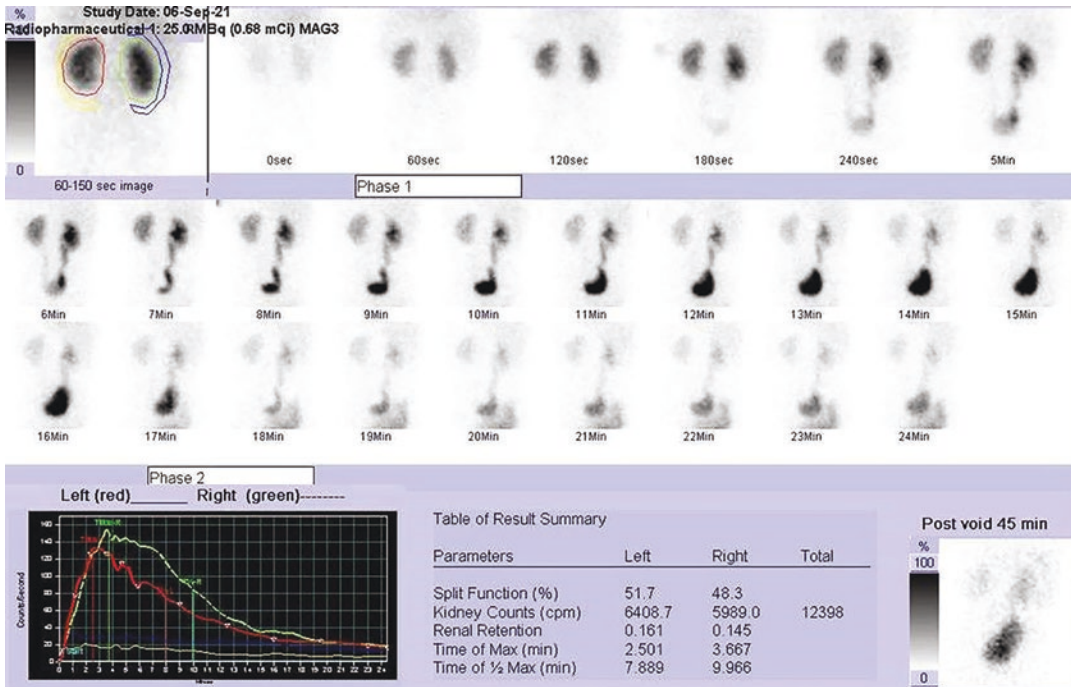


Fig. 8.3 History: A 6-month-old boy with mild-to-moderate dilatation of the right excretory system, seen on serial US examinations, performed a diuretic renal scan to exclude obstruction. The patient was orally pre-hydrated and the study was performed with the F+0 protocol, furosemide administered at a dose of 1 mg/kg. Study report: The dynamic phase over 25 mins shows mild-to-moderate dilatation of the right excretory system, with constant

visualization of the ureter that appears minimally convoluted. DRF is 52% on the left and 48% on the right. During the study acquisition there is good clearance of the tracer from both kidneys. The clearance curves confirm bilateral normal clearance, with tracer that has already cleared from the left side. Impression: There is no evidence of obstruction

Case 8.3. Hydronephrotic Kidney, Follow-Up after Pyeloplasty for UPJ (Fig. 8.4)

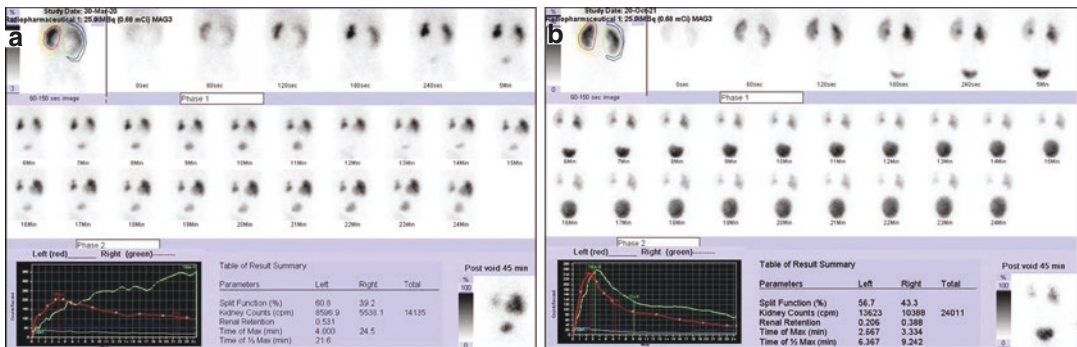


Fig. 8.4 History: A 1-month-old girl presented with severe right hydronephrosis, first detected on prenatal US, antero-posterior pelvic diameter (APD) 33 mm, further confirmed on postnatal US which showed an APD 23 mm and severe right renal parenchymal thinning. Study report: A MAG3 scan with the F+0 protocol was obtained (a), including a late post-void, gravity-assisted image at 45 mins. The right kidney is enlarged and hydronephrotic. Cortical uptake is reduced, especially in the lower pole, DRF 39%. There is prolonged CTT to the large, hydronephrotic right renal pelvis with no drainage. The left kidney shows normal parenchymal uptake, DRF 61%. The diuretic renogram curve is rising. The left kidney shows good although slow drainage. There is a significant residual activity in the right pelvis and a small residual amount in the left renal pelvis. The 45-min NORA value of the right kidney is elevated, 1.8. The findings are consistent with right hydronephrosis with reduced parenchymal function and markedly impaired drainage. The left kidney shows a normal function with tracer pooling in the pelvis

but no evidence of a significant obstruction. The patient underwent a right pyeloplasty to relieve the UPJ obstruction. Follow-up US studies showed a gradual reduction in the size of the right pelvis. A follow-up scan using the same study protocol was obtained 1 year later (b). The right kidney is normal in size with only a moderate pelvic impression. Cortical uptake has improved, DRF 43%. There is normal tracer accumulation in the right pelvis with good drainage. The left kidney shows normal parenchymal uptake, DRF 57%. The diuretic renogram curve is near normal, with good drainage. There is a small, non-significant residual activity in the right pelvis and the 45-min NORA value of the right kidney is now normal, 0.4. Impression: Following the findings of obstructive UPJ in the preoperative scan (a) and surgery to relieve the obstruction, a follow-up diuretic renogram (b) shows improved function and drainage of the right kidney with no evidence of residual obstruction. Normal left kidney with improved drainage as compared to the first study

Case 8.4. Hydronephrotic Kidney, Spontaneous Improvement (Fig. 8.5)

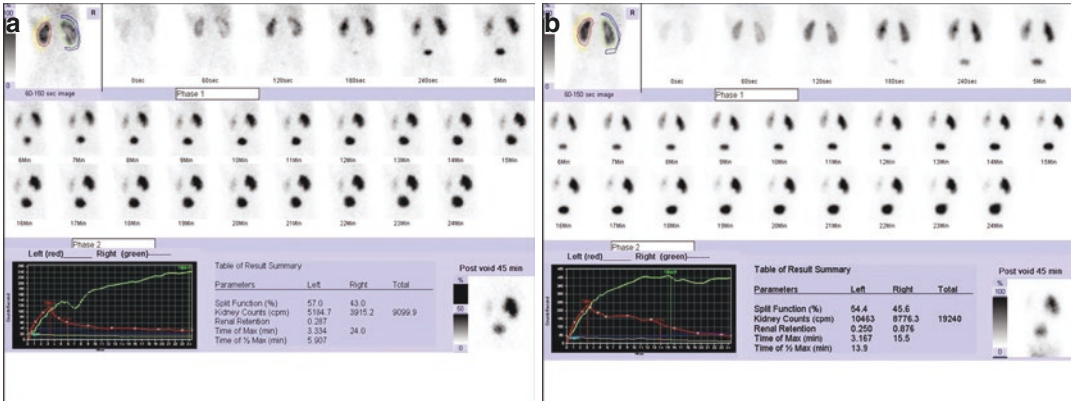


Fig. 8.5 History: A 1-month-old infant presented with right hydronephrosis, first detected on prenatal US, confirmed on postnatal examination with an APD of 20 mm, a dilated calyceal system, parenchymal thinning (4 mm) and a renal longitudinal length of 64 mm versus 49 mm of the left kidney. Study report: A MAG3 scan with the F+0 protocol was obtained, including late post-void, gravity-assisted image at 45 mins (a). During the first 3 mins of the study, the right kidney appears enlarged and hydronephrotic, with a good cortical uptake, DRF 43%. There is slow CTT to a large, hydronephrotic right pelvis. The left kidney shows normal parenchymal uptake, DRF 57%. The diuretic renogram curve is rising with progressive accumulation of tracer in a huge right renal pelvis with no drainage. In the "post-void image" (diaper was changed), there is a significant residual activity in the right renal pelvis and a small residual amount in the left renal pelvis. The 45-min NORA value of the right kidney is markedly elevated (>3). These findings suggest right hydronephrosis with preserved parenchymal function and markedly impaired drainage, worrisome for UPJ obstruction. The left kidney shows fast and complete drainage. Following these find-

ings, the infant entered a strict follow-up protocol. US performed at 3 months of age showed a decrease in the size of the right renal pelvis. The two kidneys had about the same longitudinal length, 56 vs 54 mm. A follow-up diuretic renogram using the same study protocol was obtained at the age of 4 months (b). During the first 3 mins of the study, there is improvement in the appearance of the right kidney showing a smaller renal pelvic enlargement and good cortical uptake, with an unchanged DRF of 46%. CTT to a less dilated renal pelvis is still longer than for the left kidney which shows normal parenchymal uptake, DRF 54%. The renogram curve shows progressive tracer accumulation in the right renal pelvis with partial drainage. The left kidney shows fast and complete drainage. In the "post-void image," there is a reduced but significant residual activity in the right renal pelvis. NORA of the right kidney has decreased to 1.9 but is still abnormal. Impression: Right hydronephrotic kidney with preserved parenchymal function and markedly impaired drainage, worrisome for UPJ obstruction which improves on the follow-up study performed 3 months later. Normal functioning left kidney with no evidence for significant obstruction

Case 8.5. Duplicated Left Excretory System with Obstruction of the Upper Pole (Fig. 8.6)

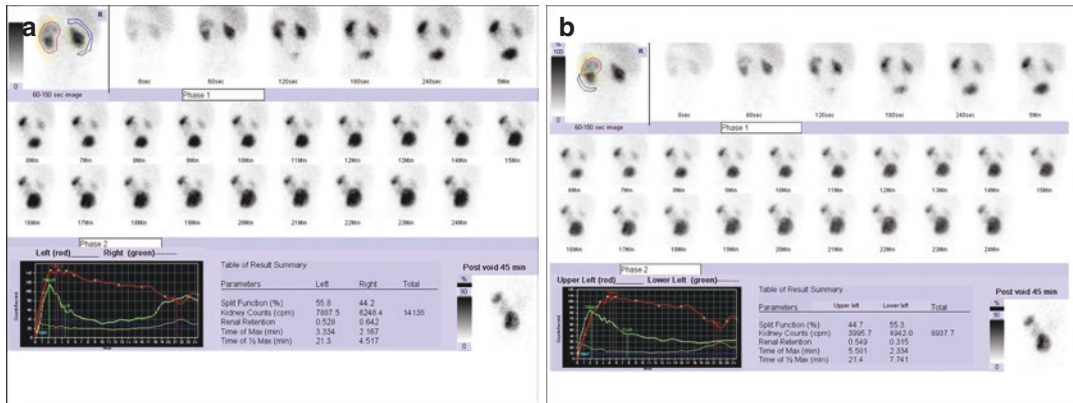


Fig. 8.6 History: A 1-month-old girl presented with US findings of complete duplication of the left excretory system and left intravesical ureterocele with dilatation of the upper pole excretory system. Diuretic renal study was requested to quantify the function of the upper pole. The patient was orally pre-hydrated. Study report: The study was performed with the F + 0 protocol, with a dose of Furosemide of 1 mg/kg. The diuretic renogram (a) shows dilatation of the upper pole of the left kidney. DRF was 56% on the left and 44% on the right. After about 8 mins there is a visualization of the left upper pole ureter that appears minimally convoluted. There is good clearance of

the tracer from the right and the lower half of the left kidney, confirmed on the clearance curves. Note an artifact due to superimposition of the very full bladder to the background ROI. A repeat second analysis was performed (b) drawing separate ROIs around the two left kidney moieties. Relative DRF was 55% for the lower and 45% for the upper pole. There is good clearance of the tracer from the lower half while the upper one does not satisfactorily empty. Impression: The findings suggest obstruction of the upper pole of the left kidney due to ureterocele, with preservation of the regional function. Ureterocele incision was then performed

8.2 Renal Cortical Scintigraphy

Clinical Indications [11–13]

- Diagnosis of acute pyelonephritis.
- Detection of renal scars after renal infection.
- Detection of renal dysplasia.
- Detection of renal ectopia and/or fusion, such as pelvic kidney, horseshoe kidney, crossed fused ectopy.
- Detection of renal infarcts.
- Confirmation of non-functioning multicystic dysplastic kidneys.
- Determination of parenchymal function:
 - DRF (one kidney relative to the other).
 - Upper vs. lower pole in cases of renal duplication.

Pre-Exam Information

- History of congenital urinary tract abnormalities.
- History of prior UTIs, clinical suspicion of acute pyelonephritis.
- Serum creatinine levels.
- History of nephrolithiasis, surgery, and trauma.
- Correlative imaging results.

Study Protocol for Renal Cortical Scintigraphy [14, 15]

Patient Preparation

- No patient preparation is required.

Radiopharmaceutical, Administered Activity, Mode of Delivery

Radiopharmaceutical:

- [^{99m}Tc]dimercaptosuccinic acid (DMSA) is the agent of choice.

Activity:

- 1.85 MBq/Kg (0.05 mCi/Kg), minimum dose 18.5 MBq (0.5 mCi).

Refer to the EANM pediatric dosage card and to the North American consensus guidelines on radiopharmaceutical administration in children in the respective EANM and SNMMI and image gently web sites.

Reference to National Regulation Guidelines, if Available, Should Be Considered.

Acquisition Protocol

- Imaging at 2–4 h post tracer injection.
- Collimator: parallel hole, low-energy, high or ultra-high resolution.
- Position: supine.
- Static images for minimum 300 Kcounts each or pre-set time of 5 mins, matrix 256 × 256 or different but allowing for a pixel size below 2 mm according to a FOV that should encompass the two kidneys (Fig. 8.7).
- Views: posterior, right posterior oblique (RPO), left posterior oblique (LPO).
- In cases of renal ectopy or malformation (e.g., horseshoe kidney), and specifically for DRF calculations, an additional anterior view of the entire abdomen and pelvis is required (Fig. 8.8).
- SPECT improves lesion detectability. Acquisition parameters: 120 projections, 15 s/frame, matrix 128 × 128. Iterative reconstruction is preferred, especially in poor count studies.
- In infants younger than 1 year of age, images acquired with a pinhole collimator (when available) can be obtained for 100–150 Kcounts or a pre-set time of 10 mins, although technically more demanding.

Study Interpretation [7, 16]

- Always based on at least a complete set of planar images (posterior, left and right posterior oblique, anterior whenever acquired) in black



Fig. 8.7 Quality control of planar DMSA scan. Good quality images must show sharp renal outline and cortico-medullary differentiation

and white, white background, with DRF clearly indicated, rounded up to the unit.

- Assess location, size, and position of kidneys.
- Identify irregularities in tracer distribution within the renal parenchyma as well as number and location of discrete cortical defects with and without associated volume loss.
- Calculate DRF, as a rule on posterior view only.

Normal variants:

- Fetal lobulations in the renal contour are normal in newborn infants.
- The lateral border of the left upper pole may appear flat due to the impression by the spleen.
- Columns of Bertin appear as areas of increased uptake. Their number and size differ from patient to patient.
- Elongated slender or pear-shaped kidneys which have different sizes of the transverse axis of the upper and lower poles.

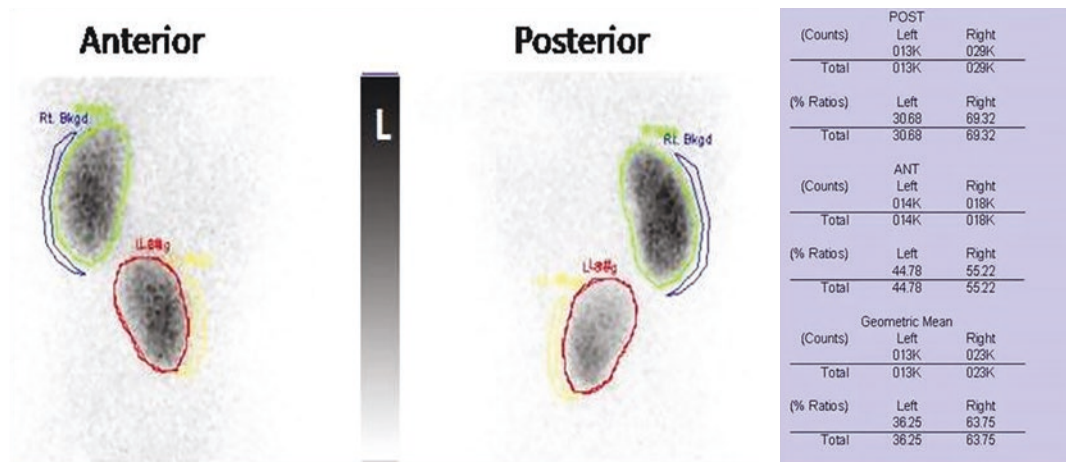


Fig. 8.8 DRF measurements in patients with renal ectopy. Calculations are based on the geometrical mean of counts measured in both anterior and posterior images

Abnormal patterns:

- One or more regions of reduced tracer uptake with a relatively preserved renal contour can suggest pyelonephritis in the appropriate clinical context.
- One or more areas of reduced or absent tracer uptake in the renal periphery interrupting the renal contour with or without associated volume loss suggest renal scar when the study is performed 6 months or more after the last UTI.
- Reduced, inhomogeneous uptake in a small kidney with a preserved outline suggests dysplasia.

Correlative Imaging [17, 18]

- Correlation with US is essential to rule out structural abnormalities (e.g., renal cysts or hydronephrosis) on the DMSA scan.
- US is not reliable in the assessment of renal acute and chronic damage.
- CT implies a higher radiation burden and MRI is more complex and less available.

Red Flags

- Air introduced into the DMSA vial may reduce renal uptake of the radiotracer and increase liver and background activities.
- Severe dilatation of the renal pelvis can result in abnormally retained activity. If significant tracer retention is noted in the renal collecting systems, additional late images up to 24 h are recommended for adequate evaluation of the cortex and in order to avoid possible inaccuracies in the assessment of split renal function.
- Reconstruction and motion artifacts, occasionally seen on SPECT, should not be confused with cortical lesions.
- Pinhole images are highly sensitive to patient motion.
- Distinction between pyelonephritis, scars, and dysplasia is not always possible based on scan findings. It should also be noted that these conditions may coexist.
- Tubular congenital abnormalities Fanconi's syndrome reduce uptake of DMSA but not of MAG3 [19].

- For diagnosis of scars, the DMSA study should be performed at least 6 months after the last documented infection to determine if the cortex has healed or was permanently damaged. Scans performed earlier than 6 months since the last UTI may be too early to identify true scarring.

Take Home Message

- DMSA binds to the proximal convoluted tubular cells. The tracer shows high parenchymal concentration and minimal excretion into the renal collecting system.
- DMSA scintigraphy is strongly integrated in evaluating children with UTI and guides management decisions. It is the best modality to determine both transient and permanent cortical damage.
- In order to diagnose acute pyelonephritis an "acute" cortical scan should be performed within 7 days of the onset of an acute febrile UTI.
- Images performed with a pinhole collimator can substitute for SPECT. They provide true optical magnification and superior spatial resolution, improving the detectability of subtle cortical lesions.
- Interpretation of DMSA studies with knowledge of US findings is strongly recommended.
- On a DMSA scan, the DRF is calculated as the ratio between the total counts inside the ROI in each kidney and the total counts in both renal ROIs after relative background subtraction.
- Duplication of the renal collecting system is not uncommon. Complications of this malformation typically include VUR to the distal collecting system with varying degrees of hydronephrosis, and possible cortical dysplasia or abnormal insertion (ectopic, ureterocele) of the upper pole ureter. The differential function of each pole can be calculated from appropriate ROIs and is useful when surgical resection is considered.
- Both MAG3 and DMSA provide equally accurate DRF [20].

Representative Case Examples

Case 8.6. Small Left Kidney with Scars (Fig. 8.9)

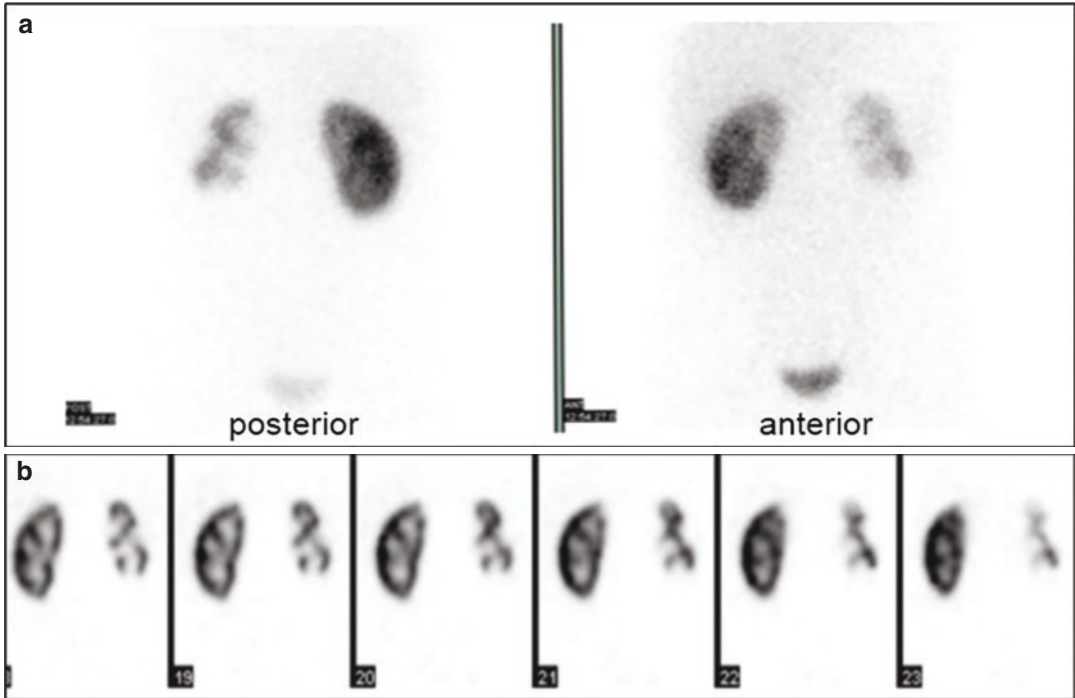


Fig. 8.9 History: A 5-year-old girl with a history of recurrent UTIs and a renal US reported as normal was referred for DMSA scintigraphy to assess for the presence of parenchymal scarring. Study report: Anterior and posterior planar images (a) show a small left kidney with an

irregular contour. There are multiple peripheral defects in the cortical outline accompanying volume loss of the left kidney, best depicted on the coronal SPECT slices (b). Impression: Small left kidney with multiple scars

Case 8.7. UTI with Progression of Bilateral Renal Scars (Fig. 8.10)

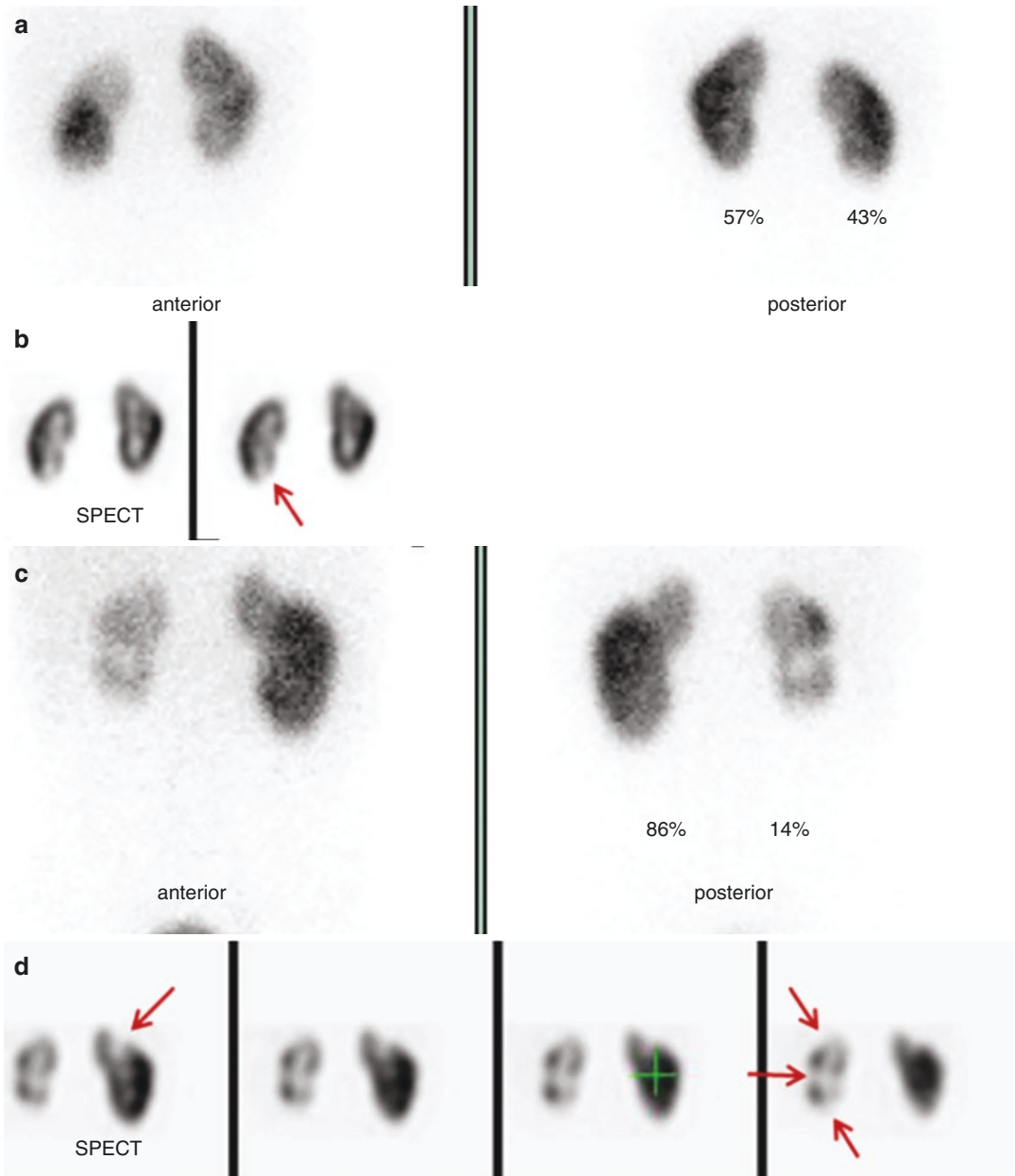


Fig. 8.10 History: A 4-year-old girl with recurrent UTIs and VUR had been lost to follow-up and returned to the clinic after 4 years with an ongoing history of infections. Study reports: the first DMSA study, anterior and posterior planar images (a) and coronal SPECT slices (b) show a small cortical defect in the lower pole of the right kidney (arrow) consistent with a small renal scar. The left kidney appears normal. The DRF of the right kidney is 43% and on the left 57%. On a follow-up DMSA study performed

4 years later planar images (c) and coronal SPECT slices (d) show decreased, inhomogeneous tracer uptake in the right kidney with multiple peripheral cortical defects (arrows). An additional cortical peripheral defect is noted in the lateral aspect of the upper pole of the left kidney (arrow). The DRF of the right kidney has dropped to 14%. Impression: Significant scarring has occurred in both kidneys in the 4-year time interval from the baseline study

Case 8.8. Acute Pyelonephritis (Fig. 8.11)

Case 8.9. Non-functioning Left Lower Renal Pole (Fig. 8.12)

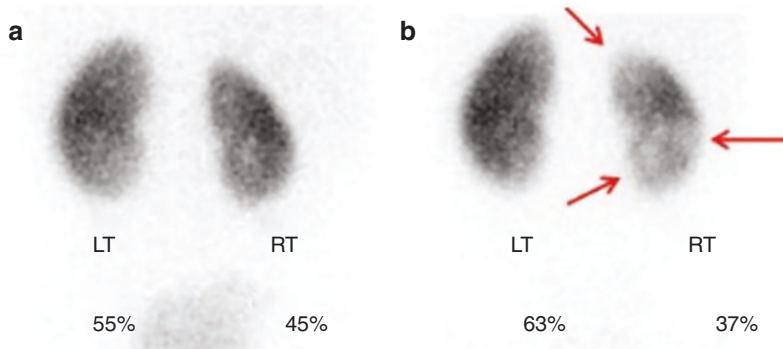


Fig. 8.11 History: A 4-year-old girl was referred for scintigraphy due to recurrent UTIs. The first DMSA scan was performed more than 6 months after the last infection. Seven months later she was hospitalized with high fever most probably due to a new UTI. An “acute” DMSA scan was performed during her hospitalization and compared to the previous study. Study reports: the first DMSA study

planar posterior view (a) demonstrates a normal DMSA uptake pattern. The second study, the “acute” DMSA scan, planar posterior view (b) shows new areas of decreased uptake (arrows) in the right kidney with preserved renal contour. The right kidney DRF has decreased from 45% to 37%. Impression: The findings on the second DMSA study are consistent with acute pyelonephritis

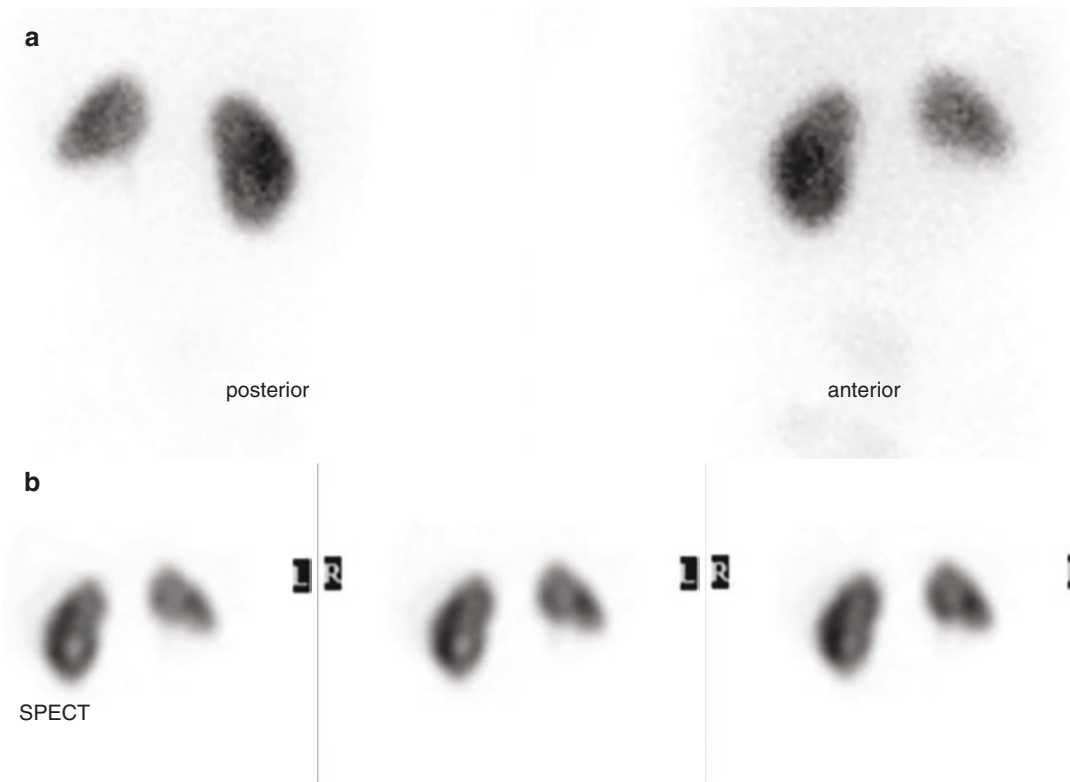


Fig. 8.12 History: A 2-year-old boy presented with left duplex collecting system. The lower collecting system was severely hydronephrotic. A DMSA scan was obtained to assess the parenchymal function of the lower pole. Study report: Anterior and posterior planar images (a) and

coronal SPECT slices (b) show a sharp demarcation between the upper and lower poles of the left kidney. The upper pole has normal cortical uptake, whereas the lower pole shows no uptake and function. Impression: Non-functioning lower pole of left kidney

8.3 Glomerular Filtration Rate Radionuclide Measurement

Clinical Indications

- Chronic renal failure prior to kidney transplant.
- Post renal transplant evaluation.
- Patients receiving nephrotoxic chemotherapy/immunosuppressive therapy.
- Bilateral renal disease.
- Solitary kidneys.

General Principles for Glomerular Filtration Rate (GFR) Measurements [21]

- GFR can be quantified by measuring the clearance rate of a substance from the plasma provided that the substance:
 - Is freely filtered in the glomerulus.
 - Does not bind to plasma proteins.
 - Is not secreted or reabsorbed by the renal tubules.
- Clearance of the substrate calculation: divide the injected dose by the area under the clearance curve.
- Simplified routine clinical calculation methods in children:
 - The “slope-intercept method”: requires two blood samples at 2 and 4 h after tracer injection.
 - The “distribution volume” method: requires a single blood sample 110–130 mins after tracer injection. This method is more practical in young children, avoiding repeated venipunctures. It is considered less accurate than the two-sample methods when GFR is expected to be <30 ml/min/1.73m².

Study Protocol for GFR Measurements [21–23]

Patient Preparation

- Avoid high-protein meals and strenuous exercise at least 12 h prior to the study.
- Adequate hydration.

- Measure height, weight, and serum creatinine.
- Explain that the test involves more than one venipuncture.
- Equipment needed:
 - A scientific scale
 - Volumetric flasks
 - A centrifuge
 - A well-counter

Radiopharmaceutical, Administered Activity, Mode of Delivery

Radiopharmaceuticals:

- [^{99m}Tc]diethylenetriaminepentaacetic acid (DTPA) is widely available.
- [⁵¹Cr]ethylenediaminetetraacetic acid (EDTA) is the best agent but has limited availability.

Activity:

- [^{99m}Tc]DTPA: Adjust the dose according to the patient body surface area (BSA) obtained from height and weight:
 - For simple GFR estimate: 30 MBq (0.8 mCi, adult dose) × (patient BSA/1.73 m²).
 - For simultaneous GFR and DTPA dynamic renal scan: 120 MBq (3.2 mCi, adult dose) × (patient BSA/1.73 m²).
- [⁵¹Cr]EDTA: 1.85 MBq (0.05 mCi).

Refer to the EANM pediatric dosage card and to the North American consensus guidelines on radiopharmaceutical administration in children in the respective EANM and SNMMI and image gently web sites.

Reference to National Regulation Guidelines, if Available, Should Be Considered.

GFR Step-by-Step: The Single Blood Sample Using the “Weight” Method

1. Check radiopharmaceutical purity, discard if <98%.
2. Draw up patient dose according to BSA and prepare a “standard” with 20 MBq.
3. Weigh full syringes (patient dose and standard), equipped with their capped needle. **Record the values.**
4. Dilute standard by expelling the syringe content into a volumetric flask containing a known, exactly measured amount of water (usually 500 ml).
5. Weigh the empty standard syringe, equipped with the same capped needle. **Record the value.**
6. Injecting the activity is the critical step! Administer the dose through a secure IV line. Flush the line carefully before injecting the activity to ensure that the line is patent and that the injection will not be an interstitial one.
7. Inject the activity into the patient *without rinsing the syringe*, taking care to inject the entire volume, flush the IV line with at least 10 ml saline.
8. **Document the time of injection.**
9. Weigh the empty patient’s syringe, equipped with the same capped needle and **Record the value.**
10. Note the site of injection—do not draw subsequent blood from this area (preferably use the opposite arm for the blood sample).
11. Draw a blood sample between 110 and 130 mins after tracer injection for children using vials with an anticoagulant (like the ones used for blood cell count). Try to get at least 5 ml of blood, allowing enough plasma for duplicates.
12. **Accurately record the time that the blood samples were taken.**

GFR Single Blood Sample Processing

- Centrifuge the blood samples at 3000 rotations/min for 5 mins to separate the plasma and blood cells.

- Count the following duplicate samples in the well counter for enough time to get at least 100 Kcounts for each sample and 500 Kcounts for each standard.
- Counting times can be different and must always be registered.
 - 1 ml of your standard solution × 2.
 - 1 ml of the plasma sample × 2.
- Always use the same volume in all the samples. The duplicates allow for an essential quality control step. If the total counts (not counts/min) in the two duplicates differ significantly, it is an alert of technical difficulties, i.e., different volumes drawn with the pipette.
- A recount of all samples is usually the first step in troubleshooting.

GFR Calculation

- Apply background corrections to all the measurements.
- Use the mean values of the two samples in the calculations.
- Standard counts are multiplied by the volume (ml) used for dilution.
- Determine injected activity. This calculation is necessary because the injected dose that was counted with an external dose calibrator needs to be calibrated to the plasma sample that was counted with a well counter.
- Use the following formula: injected activity weight divided by net standard weight × standard counts.
- Calculate the volume of distribution (VOD, ml) as:

$$\frac{\text{Counts injected (counts / min)}}{\text{Counts of the plasma sample (counts / min)}}$$

- Calculate the GFR using Ham & Piepsz’s formula $\text{GFR (ml/min)} = 2.602 * \text{VOD}(120) - 0.273$ [24].
- Whenever the blood sample is not obtained at exactly 120 mins after the injection, the counts of the sample must be corrected: $P(120) = P(t) * e^{[0.008 * (t-120)]}$, where: t = time of sampling in mins after tracer administration.

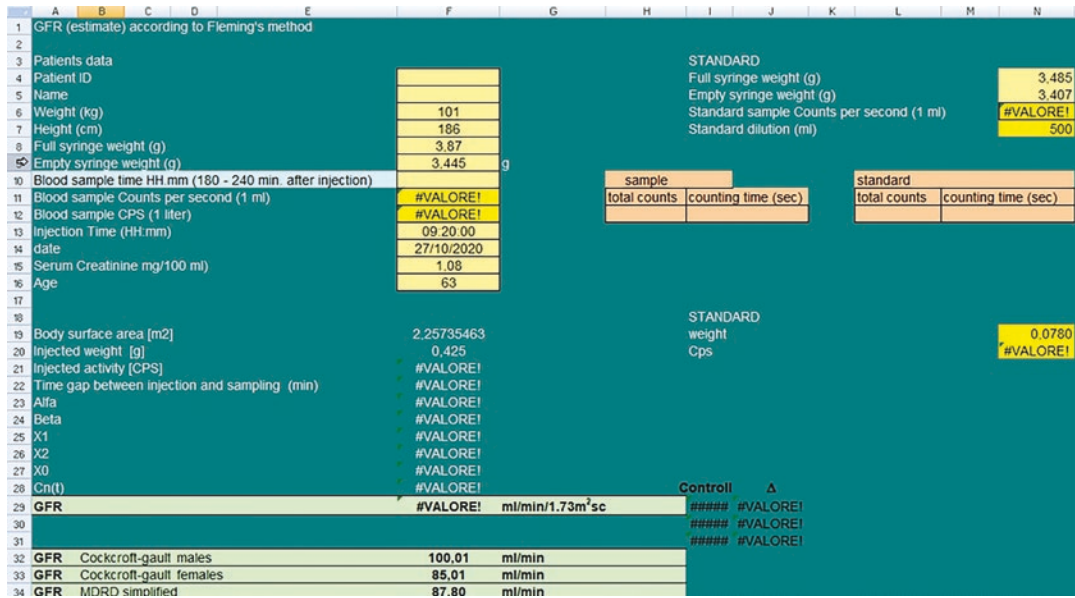


Fig. 8.13 Excel sheet including all measured parameters and calculations made with the creatinine-based method

- Normalize to 1.73 m² BSA.
- Despite the apparent complexity, data input is simple once if the math is put into an Excel sheet, where calculations made with the creatinine-based method can be also inserted and compared (Fig. 8.13).

GFR Quality Control

- Step 1: Check that the samples counted in the counter do not differ significantly. Calculate the standard error. The difference between the two samples should not exceed 3%.
- Step 2: Check the volume of distribution. It should be around 20–30% of body weight. The study should be repeated if it is less than 15% or more than 40%.

Normal Values [25]:

Normal GFR values are 104 ± 20 ml/min/1.73 m² body surface area (BSA), in the age range 2–15 years.

Below 2 years of age:

- 1–4 months 62 + 14 ml/min/1.73 m² BSA.
- 4–8 months 72 + 14 ml/min/1.73 m² BSA.

- 8–12 months 83 + 17 ml/min/1.73 m² BSA.
- 12–18 months 92 + 18 ml/min/1.73 m² BSA.
- 18–24 months 95 + 18 ml/min/1.73 m² BSA.

Red Flags

- Reproducibility of the GFR measurement should be:
 - 4.1% in patients with a GFR > 30 ml/min.
 - 11.5% in patients with a GFR < 30 ml/min².
- The precision of the calculation can be hampered in severely dehydrated or edematous patients because the radiopharmaceutical diffuses into the extracellular space.
- Recent IV fluids, e.g., fluid loading before chemotherapy, may also affect the study.
- Single sample methods are less precise when GFR is below 30 ml/min/1.73 m²BSA. On the other hand, their best use is in evaluating longitudinal loss of renal function before an overt chronic kidney failure is evident.

Take Home Message

- A detailed protocol of the two methods is available in the EANM guidelines for glomer-

ular filtration rate determination in children [26].

- Clinical GFR measurements are based mainly on serum creatinine levels, an endogenous catabolite derived from muscle protein. However, this test becomes abnormal only when about 50% of the renal function is lost. False positives occur in people with large muscle masses and false negatives in patients with muscle wasting.
- Biochemical GFR calculations based on serum and/or urinary creatinine levels are less accurate [27].
- The most accurate radionuclide GFR measurement method is based on the plasma disappearance curve after a single bolus injection of a glomerular tracer. Gamma camera methods are less reliable [22, 23].
- EDTA is the best radiotracer due to the tight binding of the two components.
- It is possible to administer EDTA together with MAG3 for dynamic renal scan; in this case count the samples after complete decay of the ^{99m}Tc . DTPA can be used (dose adjusted) for GFR measurements followed by a dynamic renal scan.

8.4 Direct Radionuclide Cystography (DRC)

Clinical Indications [28, 29]

- Detection of VUR in children after UTI.
- Follow-up of children with known VUR.
- Assessment of the results of endoscopic or surgical treatment.
- Screening of siblings of children/parents with proven VUR.

Pre-Exam Information

- Knowledge of clinical history, biochemistry, and urinalysis results, previous imaging results.
- Determine whether the patient may need sedation.
- Whether uroculture has been performed during the week before the procedure and if it is negative.

Study Protocol for Direct Radionuclide Cystography [28, 30]

Patient Preparation

Preparation prior to bladder catheterization

- Explain to the child, parents, or carers about the procedure. Continued communication, reassurance, and explanation of each step is essential for a successful study.
- A quiet, dimly lit room, watching TV, or reading a story, a calming effect can be produced, making sedation rarely necessary.
- The child may be instructed to void immediately prior to catheterization, if the residual volume is measured by catheterization rather than by computer analysis.
- Ensure the child has adequate antibiotic coverage for the procedure.
- Calculate theoretical bladder volume to avoid overdistension, mainly in children with a neurologic bladder [31].
 - Infants <1 year: Capacity (ml) = $(2.5 \times \text{age [months]}) + 38$.
 - Older children >1 year: Capacity (ml) = $(2 + \text{age [years]}) \times 30$.

Catheterization Technique

- Performed by qualified personnel.
- Catheter: usually use a feeding catheter without a balloon that will comfortably pass the meatus (6 French-gauge).
- A urine specimen can be taken for culture.

Radiopharmaceutical, Administered Activity, Mode of Delivery

Radiopharmaceutical:

- ^{99m}Tc DTPA.

Activity:

- 20 MBq (0.5 mCi) followed by 100–500 ml saline according to bladder estimate volume.

Refer to the EANM pediatric dosage card and to the North American consensus guidelines on radiopharmaceutical administration in children in the respective EANM and SNMMI and image gently web sites.

Reference to national regulation guidelines, if available, should be considered.

Delivery:

- Through the catheter at the beginning of the filling by a 3-way stopcock.
- The bottle of warm saline should be placed no higher than 80 cm above the head of the patient.
- Let the saline run at about 100 drops/min.

Acquisition Protocol

- Cover the detector with plastic and diaper to avoid contamination during micturition.
- Position: the camera is positioned posteriorly to the patient lying supine.
- Collimator: general purpose or high-sensitivity low-energy parallel hole are preferable if available.
- Filling phase: dynamic images at a rate of 5 s/frame for a total of 600 s, matrix 128 × 128.
- Voiding phase (using the same parameters as for filling phase): another 600 s. If the child is cooperative, acquire at least ten frames before the beginning of voiding and ten frames after the end.
- Non-toilet-trained children usually void without a problem with the catheter in place. In toilet-trained ones it is better to remove it for achieving more child comfort.
- Residual volume in the bladder can be calculated by a 30-s anterior pre- and post-void image using these images.
- All acquisition sequences can be repeated until the filling, or the voiding is completed.

Study Processing

- Set the image window so that a “cloud” of scatter activity is seen around the bladder during the filling phase.
- Visual assessment: if present VUR is readily seen, always evaluate the study by lowering and increasing the windowing.
- Quantitative techniques: measure the activity/ml and can evaluate the degree of VUR, bladder volumes, and voiding flow rates.
- Quantitation of post-void residual volume requires recording the volume of voided urine.

Study Interpretation

- Radionuclide classification of VUR is based on the location of the radiotracer activity:
 - Mild reflux: in the ureter.
 - Moderate reflux: in the non-dilated collecting system and ureter.
 - Severe reflux: in dilated collecting system and ureter.
- Record the volume of saline infused.
- An estimate of the residual volume can be made if the child voided just before the beginning of the study and the voided volume is recorded.

Correlative Imaging

- Fluoroscopic voiding cystourethrography (VCUG) has been the standard for detection and classification of VUR utilizing a 5-point scale. It is the best method to visualize the urethra in males and especially for detection of posterior urethral valves. It does require direct bladder catheterization and utilizes fluoroscopy to view bladder filling and presence of reflux. The bladder can be filled more than once but because of use of fluoroscopy there is

potential for a significantly increased radiation exposure to the child [32, 33].

- More recently the use of US contrast-enhanced voiding cysto-sonourethrography has been proposed as a replacement for previous techniques. It employs US without radiation exposure but still requires direct bladder catheterization. The posterior urethra can be adequately visualized when multiple cycles of bladder filling can occur. Like many US techniques, it is highly operator-dependent, and the learning curve and scanning time are longer in comparison to both X-ray and radionuclide methods [34].

Red Flags

- It is wise to have 2 or 3 radiotracer doses ready at the start of the procedure.
- Check all the tube connections to avoid spilling.
- Beware of contamination of diapers and dresses in non-toilet-trained children, especially if micturition happens at full bladder filling.
- High-resolution collimators can be used if there is no choice; modern cameras are sensitive enough to warrant a full diagnostic study.
- Quantitative techniques are not necessary for a fully diagnostic study and require a careful methodology.
- Calculation of bladder volume can be affected by bladder geometrical changes during filling/voiding.
- If a syringe, although small, is used for pushing the radionuclide into the catheter, resistance should not be forced because, although very rarely, the catheter can enter a very dilated, the so-called “golf-hole,” ureteral meatus.
- Sometimes, older non-toilet-trained children may feel such subjective pain during the first attempt to void with the catheter in situ that they will subsequently refuse to void for many hours. In this case, it is up to the caring physician to decide when to stop the scan (normally, do not wait for more than 1 h).

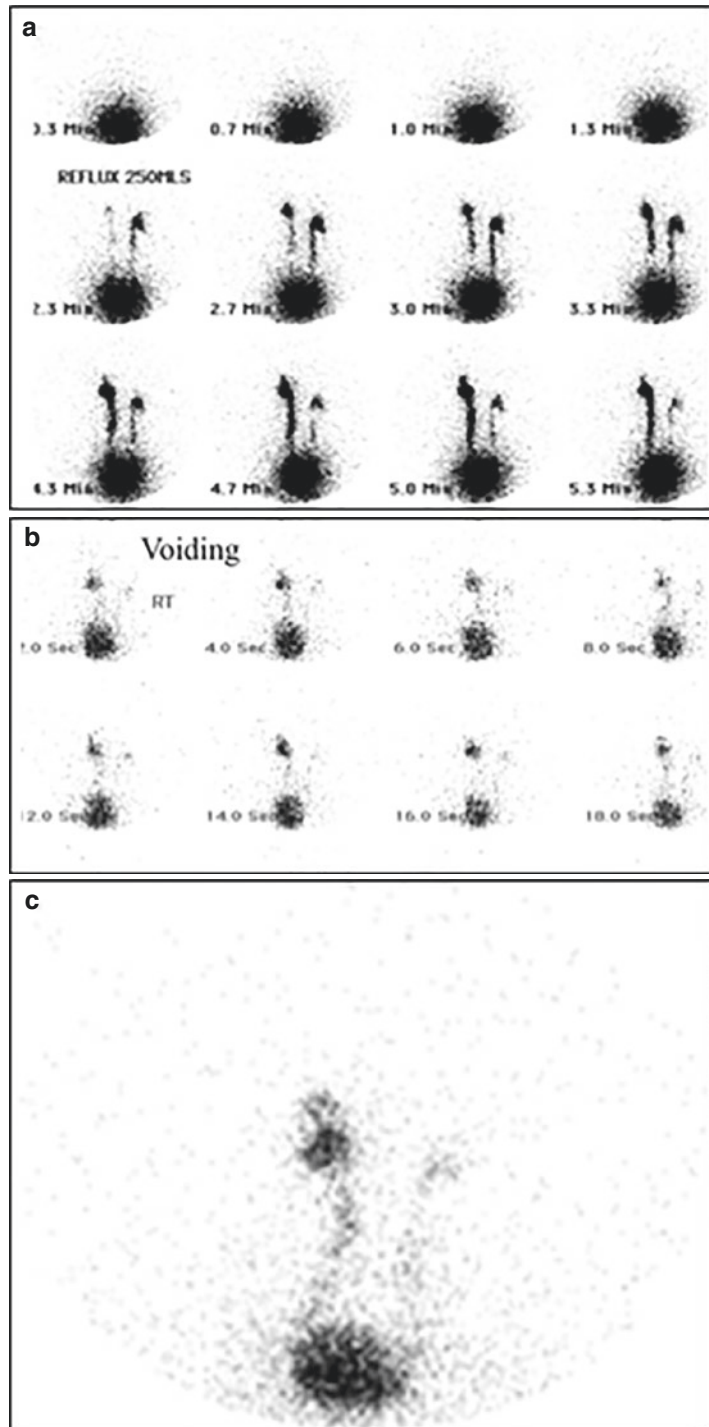
Take Home Message

- DRC is the most common nuclear medicine study to evaluate VUR. It has a low radiation dose and high sensitivity as compared to both voiding cysto-ureterogram and the indirect scintigraphic technique [35].
- VUR classification on radionuclide DRC differs from the radiographic classification.
- Do not perform DRC in children, mainly males, in whom US does not exclude anatomical bladder abnormalities.
- DRC is the preferred radionuclide procedure for assessing VUR in children who are not toilet-trained or those on whom clean intermittent catheterization (CIC) is performed.
- DRC allows for repeated cycles of bladder filling and voiding. This improves the detection of reflux in children with intermittent VUR [33].

Representative Case Examples

Case 8.10. Bilateral VUR (Fig. 8.14)

Fig. 8.14 History: A 4-year-old girl with recurrent UTI. Study report: During the filling phase (a, volume 250 ml) VUR is detected, more evident on the left side, persisting during the voiding phase (b), also seen on the post-void image (c). Impression: Bilateral moderate VUR



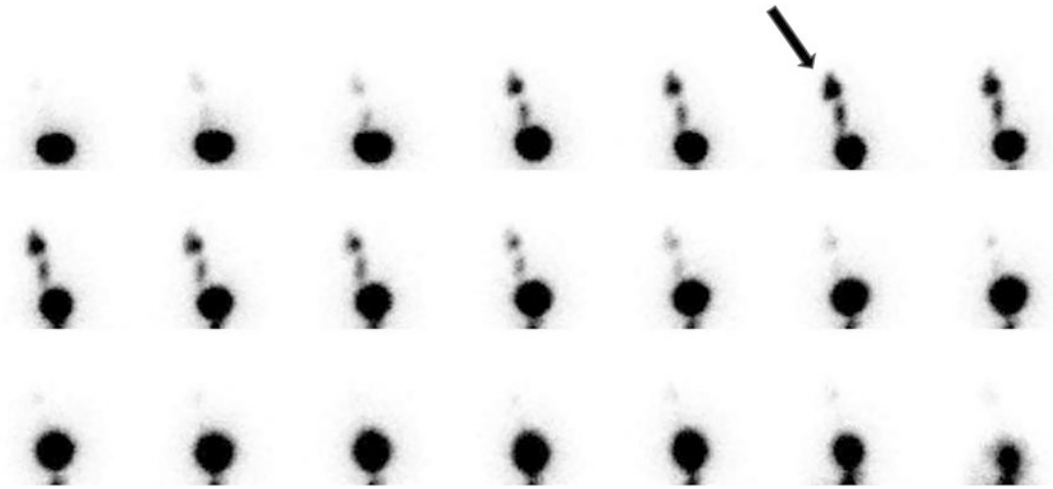
Case 8.11. High-grade unilateral VUR (Fig. 8.15)

Fig. 8.15 History: 1-year-old girl had a DRC performed one month after a febrile UTI. US had been reported as normal. Study report: After clean catheterization, the radiopharmaceutical was injected through the bladder catheter, followed by warm saline. A series of 5 s sequential frames was acquired, starting at the time of tracer administration. Selected frames show during the late fill-

ing phase, a left-side VUR which increases (arrow) during the voiding phase. The reflux activity returns to the bladder after the end of the voiding, although incomplete. A second voiding phase without a new increase of the residual intra-pelviureteric activity is visible in the last three images. Impression: Unilateral active and passive severe VUR

Case 8.12 Intermittent unilateral VUR
(Fig. 8.16)

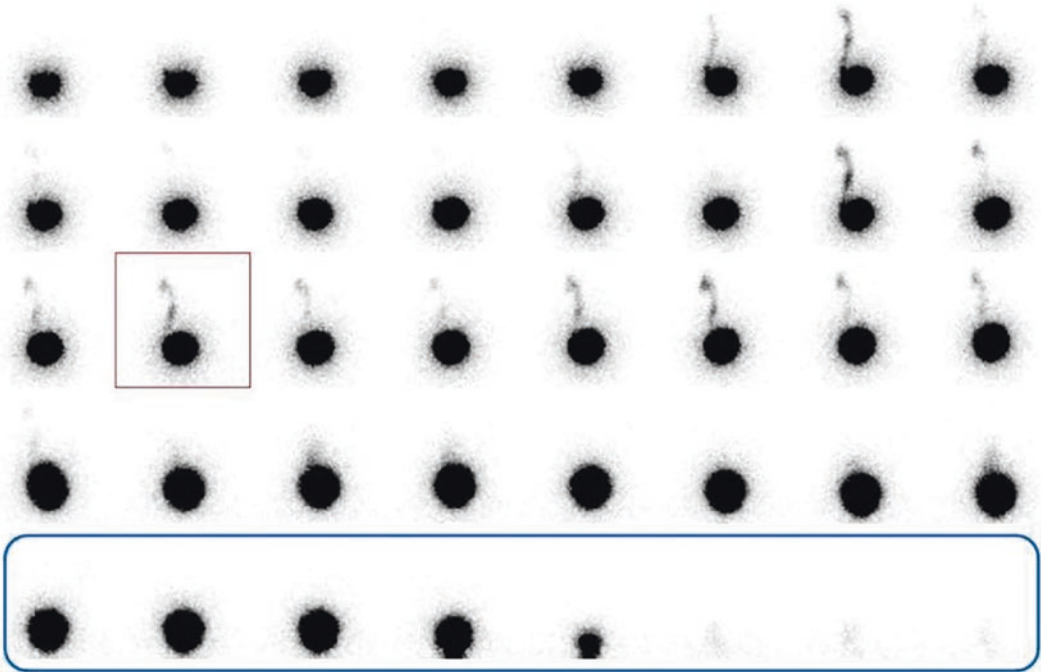


Fig. 8.16 History: Four-year-old girl. The first episode of febrile UTI 3 months prior to current study, had an early relapse after the end of the 2-weeks course of antibiotic therapy. Study description: After clean catheterization, the radiopharmaceutical was injected through the bladder catheter, followed by warm saline. A series of 5-s sequential frames were acquired, starting together with the

administration. Grouped 10-sec images are shown. In the early filling phase, a left-side VUR is detected, randomly increasing and decreasing during the bladder filling. No active reflux is visible during the voiding phase (blue box). Impression: Unilateral intermittent, passive, moderate VUR

8.5 Indirect Radionuclide Cystogram (IRC)

Clinical Indications (*in Toilet-Trained Children!*) [36–38]

- Recurrent UTIs and suspected VUR.
- Known VUR, for follow-up of disease status.

Study Protocol for Indirect Radionuclide Cystography [29, 36]

Patient Preparation

- The child should be cooperative and toilet trained.
- The child should have a relatively normal renal function.

Radiopharmaceutical, Administered Activity, Mode of Delivery

Radiopharmaceutical:

- [^{99m}Tc]MAG3.

Activity:

- 3.7–5.55 MBq/kg (0.10–0.15 mCi/kg).
Refer to the EANM pediatric dosage card and to the North American consensus guidelines on radiopharmaceutical administration in children in the respective EANM and SNMMI and image gently web sites.

Reference to National Regulation Guidelines, if Available, Should Be Considered.

Acquisition Protocol

- The study is preceded by a standard renogram.
- Collimator: the same as for the renogram.
- Detector in an upright position.

- FOV—should include the kidneys and bladder prior to starting acquisition.
- Build a makeshift toilet in front of the camera (Fig. 8.17).
 - Girls: Put a bedpan on the seat of a backless chair. A parent/caregiver can help stabilize the patient on the bedpan.
 - Boys: The patient stands and holds the urine bottle or his parent/caregiver does it for him.

To improve privacy, only one or two technologists, preferably of the same sex as the patient, are in the room with the parents and patient.

Acquisition Parameters

- Dynamic study, 1–2 s/frame until the child has finished voiding, matrix 128 × 128, using the same zoom as for the renogram.
- NB: Acquire at least 30 s of images before the start of voiding and after.
- To allow enough time, it is useful to set up the camera for 300 or even 600 s and stop the study once the urinary bladder has emptied.
- Measure the volume of the urine passed, if the RV has to be calculated.

Study Processing

Methods for accurate assessment of VUR, eliminating errors that may lead to false positives:

- Draw curves over the expected position of the kidney(s). True VUR is accompanied by a significant increase in counts in the kidney in question.
- To calculate the residual bladder activity volume (when requested) ROIs have to be drawn over the bladder on micturition images before and at the end of the void. Measure the volume of urine passed.

Example:

- Before micturition, there are 600 counts in the bladder.
- At the end of micturition 240 counts remain in the bladder.
- The child passed 50 ml of urine.
- Therefore, there were 360 counts in 50 ml and thus: 1 ml contains = 7.2 counts.
- The residual volume of bladder urine activity = $240 \text{ (counts in bladder)} / 7.2 \text{ (counts/ml)} = 33 \text{ ml}$.

- No reflux is seen on the IRC.
- Reflux of a large/small volume is seen in the left or right or both kidneys.
- The reflux starts before or at the time of micturition.
- The refluxed activity drains promptly from the kidney to the bladder or whether it persists in the affected kidney.
- Bladder emptying is complete or incomplete. If measured, note the amount of urine passed by the child and the amount that remained in the bladder at the end of micturition.

Study Interpretation

- The report of the indirect cystogram is preceded by the report of the renogram.
- Ideally, there should be little activity in the kidneys at the start of an IRC.
- Look at the renogram images because sometimes a passive reflux can be seen toward the end of the study when the bladder is filled and the kidneys empty. Assess whether:

Correlative Imaging [1]

- Same as for DRC (see Sect. 8.4).
- In doubtful cases, especially in children with renal damage, it is suggested to perform a VCUG or DRC.

Red Flags [1, 38]

- The technologist usually starts the acquisition once the patient is comfortably seated and positioned. In case of poorly cooperative chil-



Fig. 8.17 Makeshift gender-adapted toilet in front of the camera. For girls (left) there is a bedpan on the seat of a backless chair. For boys, the patient stands and holds the urine bottle (right)

dren, it may be necessary to start during patient positioning.

- To avoid missing the void the technologist instructs the child to void only after the acquisition has started and after he/she tells him to do so.
- The child should stay as still as possible during the void.
- The study is stopped once the child has finished passing urine.
- Diuresis with furosemide may decrease the sensitivity of IRC study in well-hydrated children.
- The lower target-to-background ratio with DTPA limits its use for IRC.
- In children with severe hydronephrosis or hydroureter clearance of activity from these systems may be slow and the high renal and collecting system activity can mask VUR.
- The test may be difficult to interpret if the patient has a pelvic kidney as the bladder may overlie the kidney.
- If there is still a considerable amount of bladder activity, because of poor voiding or urgency without a complete upper urinary tract clearing, a second or even third cystogram can be performed later.

Take Home Messages

- IRC is the only way to evaluate VUR without using a bladder catheter. It uniquely allows non-invasively evaluate the upper and lower urinary tract in a single session and is associated with low radiation exposure to the patient and staff. The sensitivity of IRC is lower as compared to both VCUG and DRC.
- Study processing is not mandatory, a qualitative assessment with a correct windowing is enough in the greatest majority of cases.
- If there is still a considerable amount of activity in the kidneys and the child does not need to void immediately, wait for the activity to clear from the kidneys. This improves the study outcome.
- If the child wants to void, do an indirect cystogram and repeat when the bladder refills, sometimes 2–3 cystograms can be performed following one renogram in children with incomplete voiding or discrete retention of urine into the upper excretory system.

Representative Case Examples

Case 8.13. Normal Indirect Radionuclide Cystography (Fig. 8.18)

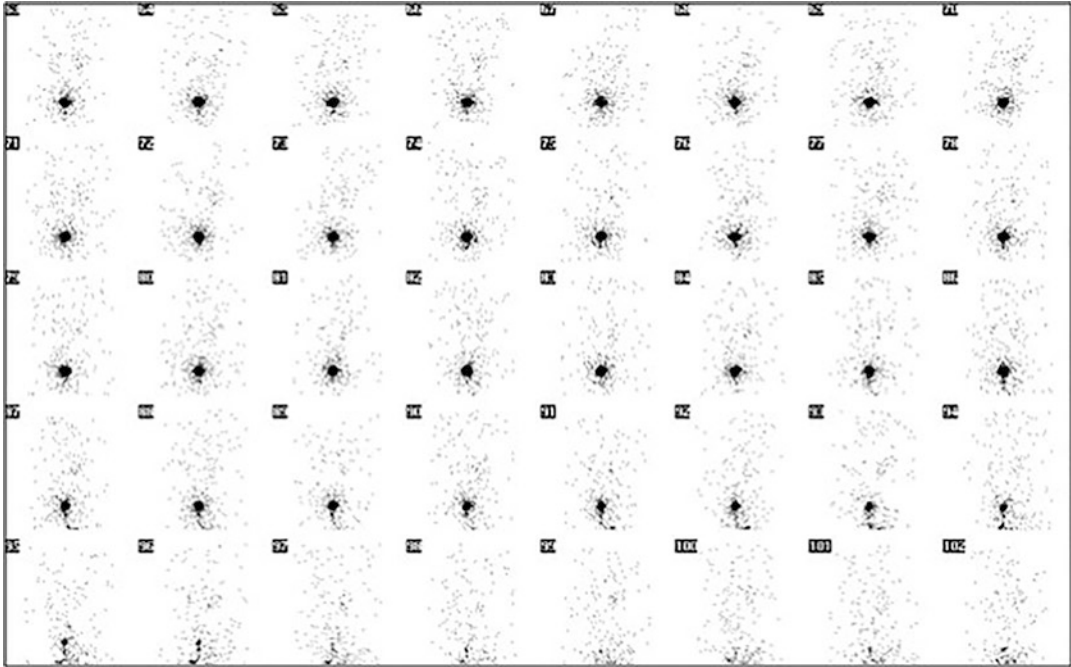


Fig. 8.18 History: A 5-year-old boy with recurrent UTIs and a family history of VUR. Study report: The posterior IRC images acquired for 1 s/frame show no evidence of reflux and complete bladder emptying. Impression: Normal study

Case 8.14. Positive Indirect Radionuclide Cystography (Fig. 8.19)

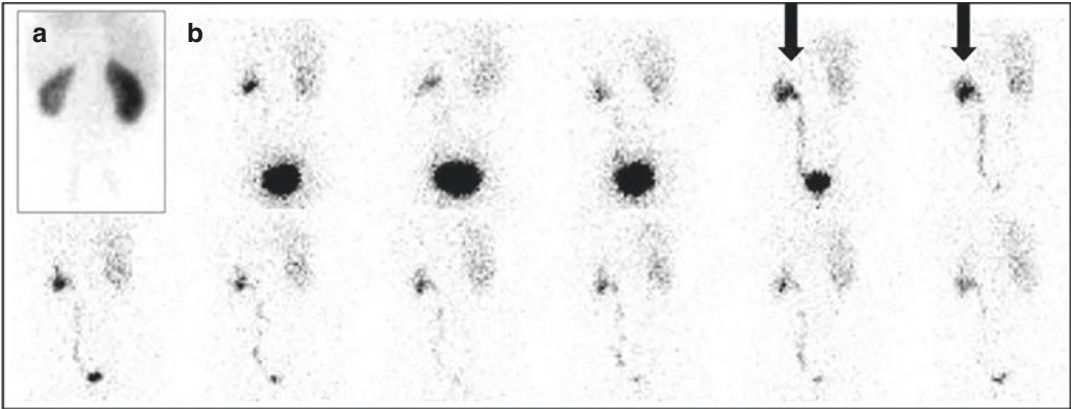


Fig. 8.19 History: An 11-year-old with bilateral VUR grade 3–4 diagnosed at 1 year of age. On US his left kidney was smaller than the right one. He was followed conservatively and remained asymptomatic for 10 years. Following a doubtful febrile UTI a renogram followed by an indirect cystogram was performed Study report: Parenchymal phase posterior images of the renogram (a)

showed a small left kidney with a DRF of 32%, and a normal right kidney with a DRF of 68%. On IRC (b) reflux into the left kidney is seen when the child starts to void (arrows). Bladder emptying is complete. Impression: Small left kidney with moderate reflux during micturition

Case 8.15. Non-functioning Left Kidney with Reflux (Fig. 8.20)

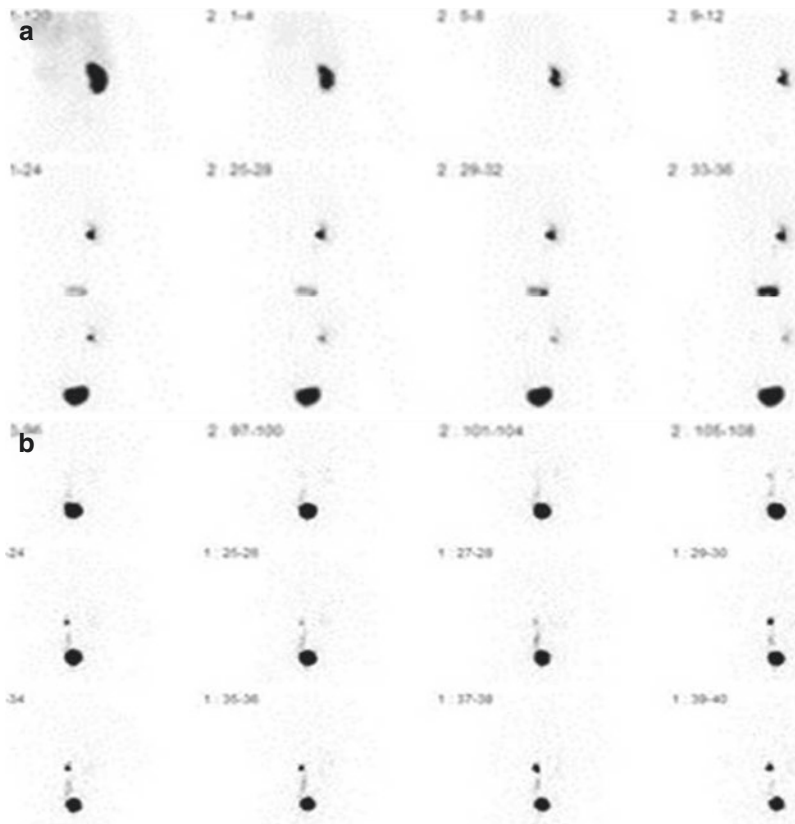


Fig. 8.20 History: A 7-year-old girl with recurrent UTIs. On US her left kidney is small and hydronephrotic. A renogram followed by an indirect cystogram was performed. Study report: On posterior images of the renogram (a) acquired for 2 s/frame, perfusion and uptake to the right kidney is normal. There is prompt drainage of activity from the kidney to the bladder. There is no functioning tissue in the expected position of the left kidney. A

small amount of activity is seen entering the left kidney after the bladder starts to fill. On IRC (b), repeated episodes of reflux into the left kidney are seen before the child starts to void and during voiding. This activity persists in the left kidney until the end of the study. Impression: Non-functioning left kidney with reflux during bladder filling and micturition. Bladder emptying is incomplete. Normal functioning right kidney

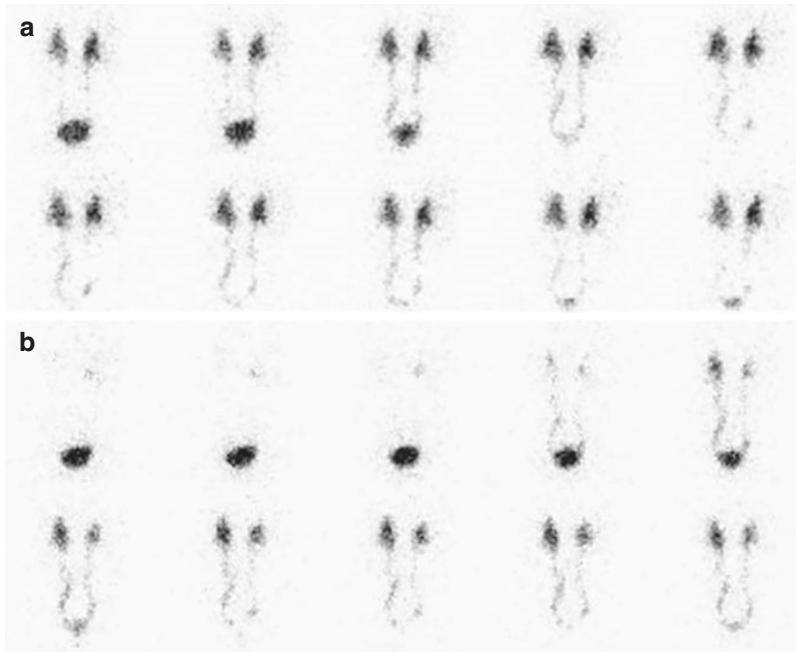
Case 8.16. Two-Voids IRC (Fig. 8.21)

Fig. 8.21 History: A 5-year-old boy with previous resection of posterior urethral valves and residual, bilateral, high-grade VUR. A renogram followed by an IRC was performed for evaluating DRF, drainage, and persistence of VUR. Study report: At the first void (a) bladder empty-

ing is complete but there is residual activity in the upper tract and the presence of VUR cannot be correctly assessed. At a second void after bladder refilling by the residual activity (b), bilateral VUR is clearly visible. Impression: Persistent bilateral VUR

References

- Piepsz A, Ham HR. Pediatric applications of renal nuclear medicine. *Semin Nucl Med.* 2006;36(1):16–35.
- Majd M, et al. The SNMMI and EANM procedural guidelines for diuresis renography in infants and children. *J Nucl Med.* 2018;59(10):1636–40.
- Piepsz A, Tondeur M, Ham H. Relative 99mTc-MAG3 renal uptake: reproducibility and accuracy. *J Nucl Med.* 1999;40(6):972–6.
- Piepsz A, Tondeur M, Ham H. NORA: a simple and reliable parameter for estimating renal output with or without frusemide challenge. *Nucl Med Commun.* 2000;21(4):317–23.
- Eskild-Jensen A, et al. Interpretation of the renogram: problems and pitfalls in hydronephrosis in children. *BJU Int.* 2004;94(6):887–92.
- Biassoni L. Pitfalls and limitations of radionuclide renal imaging in Pediatrics. *Semin Nucl Med.* 2015;45(5):411–27.
- Brink A. Pitfalls of radionuclide renal imaging in Pediatrics. *Semin Nucl Med.* 2022;52(4):432–44.
- Eskild-Jensen A, et al. Congenital unilateral hydronephrosis: a review of the impact of diuretic renography on clinical treatment. *J Urol.* 2005;173(5):1471–6.
- Schlotmann A, Clorius JH, Clorius SN. Diuretic renography in hydronephrosis: renal tissue tracer transit predicts functional course and thereby need for surgery. *Eur J Nucl Med Mol Imaging.* 2009;36(10):1665–73.
- Piepsz A, et al. Replacing 99Tcm-DMSA for renal imaging? *Nucl Med Commun.* 1992;13(7):494–6.
- Piepsz A, et al. Guidelines for 99mTc-DMSA scintigraphy in children. *Eur J Nucl Med.* 2001;28(3):Bp37–41.
- Treves ST, Packard AB, Grant FD. Kidneys. In: Treves ST, editor. *Pediatric nuclear medicine and molecular imaging.* New York: Springer; 2014. p. 283–333.
- Ammenti A, et al. Updated Italian recommendations for the diagnosis, treatment and follow-up of the first febrile urinary tract infection in young children. *Acta Paediatr.* 2020;109(2):236–47.
- Piepsz A, et al. Consensus on renal cortical scintigraphy in children with urinary tract infection. Scientific Committee of Radionuclides in Nephrourology. *Semin Nucl Med.* 1999;29(2):160–74.
- Bar-Sever Z, et al. Pediatric Nephro-urology: overview and updates in diuretic renal scans and renal cortical scintigraphy. *Semin Nucl Med.* 2022;52(4):419–31.
- Taylor AT. Radionuclides in nephrourology, part 2: pitfalls and diagnostic applications. *J Nucl Med.* 2014;55(5):786–98.
- Sinha MD, et al. Accuracy of ultrasonic detection of renal scarring in different centres using DMSA as the gold standard. *Nephrol Dial Transplant.* 2007;22(8):2213–6.
- La Scola C, et al. Different guidelines for imaging after first UTI in febrile infants: yield, cost, and radiation. *Pediatrics.* 2013;131(3):e665–71.
- Caglar M, Topaloğlu R. Reduced Tc-99m DMSA uptake in a patient with renal tubular acidosis: effect of acid-base imbalance. *Ann Nucl Med.* 2002;16(7):499–501.
- Ritchie G, Wilkinson AG, Prescott RJ. Comparison of differential renal function using technetium-99m mercaptoacetyltriglycine (MAG3) and technetium-99m dimercaptosuccinic acid (DMSA) renography in a paediatric population. *Pediatr Radiol.* 2008;38(8):857–62.
- Piepsz A, et al. Guidelines for glomerular filtration rate determination in children. *Eur J Nucl Med.* 2001;28(3):BP31–6.
- Fleming JS. An improved equation for correcting slope-intercept measurements of glomerular filtration rate for the single exponential approximation. *Nucl Med Commun.* 2007;28(4):315–20.
- Brochner-Mortensen J, Jodal L. Reassessment of a classical single injection 51Cr-EDTA clearance method for determination of renal function in children and adults. Part II: empirically determined relationships between total and one-pool clearance. *Scand J Clin Lab Invest.* 2009;69(3):314–22.
- Ham HR, Piepsz A. Estimation of glomerular filtration rate in infants and in children using a single-plasma sample method. *J Nucl Med.* 1991;32(6):1294–7.
- Piepsz A, Tondeur M, Ham H. Revisiting normal (51)Cr-ethylenediaminetetraacetic acid clearance values in children. *Eur J Nucl Med Mol Imaging.* 2006;33(12):1477–82.
- Piepsz A, et al. Guidelines for glomerular filtration rate determination in children. *Eur J Nucl Med.* 2001;28:BP31–6.
- Thapaliya S, et al. Agreement between serum estimates of glomerular filtration rate (GFR) and a reference standard of radioisotopic GFR in children with cancer. *Pediatr Radiol.* 2022;52(5):903–9.
- Fettich J, et al. Guidelines for direct radionuclide cystography in children. *Eur J Nucl Med Mol Imaging.* 2003;30(5):B39–44.
- Treves ST, Grant FD. Vesicoureteral reflux and radionuclide cystography. In: Treves ST, editor. *Pediatric Nuclear medicine and molecular imaging.* New York: Springer; 2014. p. 335–53.
- Mandell GA, et al. Procedure guideline for radionuclide cystography in children. Society of Nuclear Medicine. *J Nucl Med.* 1997;38(10):1650–4.
- Guerra LA, et al. Pediatric cystogram: are we considering age-adjusted bladder capacity? *Can Urol Assoc J.* 2018;12(12):378–81.
- Lebowitz RL, et al. International system of radiographic grading of vesicoureteric reflux. International Reflux study in children. *Pediatr Radiol.* 1985;15(2):105–9.
- Fettich JJ, Kenda RB. Cyclic direct radionuclide voiding cystography: increasing reliability in detecting vesicoureteral reflux in children. *Pediatr Radiol.* 1992;22(5):337–8.
- Ntoulia A, et al. Contrast-enhanced voiding urosonography (ceVUS) with the intravesical adminis-

- tration of the ultrasound contrast agent Optison™ for vesicoureteral reflux detection in children: a prospective clinical trial. *Pediatr Radiol.* 2018;48(2):216–26.
35. Unver T, et al. Comparison of direct radionuclide cystography and voiding cystourethrography in detecting vesicoureteral reflux. *Pediatr Int.* 2006;48(3):287–91.
 36. Gordon I, et al. Guidelines for indirect radionuclide cystography. *Eur J Nucl Med.* 2001;28(3):BP16–20.
 37. Capone V, et al. Voiding cystourethrography and (99M)TC-MAG3 renal scintigraphy in pediatric vesicoureteral reflux: what is the role of indirect cystography? *J Pediatr Urol.* 2019;15(5):514.e1–6.
 38. De Palma D. Radionuclide tools in clinical Management of Febrile UTI in children. *Semin Nucl Med.* 2020;50(1):50–5.

The opinions expressed in this chapter are those of the author(s) and do not necessarily reflect the views of the IAEA: International Atomic Energy Agency, its Board of Directors, or the countries they represent.

Open Access This chapter is licensed under the terms of the Creative Commons Attribution 3.0 IGO license (<http://creativecommons.org/licenses/by/3.0/igo/>), which permits use, sharing, adaptation, distribution and reproduction in any medium or format, as long as you give appropriate credit to the IAEA: International Atomic Energy Agency, provide a link to the Creative Commons license and indicate if changes were made.

Any dispute related to the use of the works of the IAEA: International Atomic Energy Agency that cannot be settled amicably shall be submitted to arbitration pursuant to the UNCITRAL rules. The use of the IAEA: International Atomic Energy Agency's name for any purpose other than for attribution, and the use of the IAEA: International Atomic Energy Agency's logo, shall be subject to a separate written license agreement between the IAEA: International Atomic Energy Agency and the user and is not authorized as part of this CC-IGO license. Note that the link provided above includes additional terms and conditions of the license.

The images or other third party material in this chapter are included in the chapter's Creative Commons license, unless indicated otherwise in a credit line to the material. If material is not included in the chapter's Creative Commons license and your intended use is not permitted by statutory regulation or exceeds the permitted use, you will need to obtain permission directly from the copyright holder.



Lymphoscintigraphy

9

Thomas Neil Pascual, Pietro Zucchetta,
Kevin London, and Robert Howman-Giles

9.1 Clinical Indications [1, 2]

- Sentinel lymph node (SLN) localization in malignancies, more common in children with diagnosis of melanoma and soft tissue sarcoma
Assessment of lymphedema.

9.2 Pre-exam Information

- *For SLN detection*
 - Type and location of the malignancy.
 - History or planning of the surgical resection of the tumor.
- *For lymphedema and lymphatic malformations*
 - Site of extremity edema.
 - History of surgery or trauma that could affect lymphatic drainage.
 - Suspected chyloascites or chylothorax.

T. N. Pascual (✉)
Department of Science and Technology,
Manila, Philippines

P. Zucchetta
Nuclear Medicine Unit, Department of Medicine,
Padova University Hospital, Padova, Italy

K. London · R. Howman-Giles
Nuclear Medicine Department, Children's Hospital at
Westmead, University of Sydney,
Camperdown, NSW, Australia

- Suspected developmental anomalies of the lymphatic system such as abdominal or thoracic lymphangiectasia.

Study Protocol for Lymphoscintigraphy [3]

Patient preparation

- The skin at the injection site should be cleaned with antiseptics.
- Anesthetic cream should be applied on the skin 30–60 min before injection.
- Despite the local anesthetic, the patient must be warned that temporary stinging pain might be experienced during tracer injection.

Study scheduling:

- *For SLN mapping and biopsy*
 - Number and type of injections depend on tumor type and whether it has been excised.
 - Coordination of lymphoscintigraphy and surgical excision of SLN is required.
- *For lymphedema or lymphatic malformation*

- The procedure may take several hours, depending on the speed of the lymphatic transit.
- Scheduling the study in the morning is advised, given the potential duration of the study.

Radiopharmaceutical, Administrated activity, Mode of delivery

Radiopharmaceutical

- [^{99m}Tc] labelled colloidal nanoparticles.

Activity

- 18.5–37 MBq (0.5–1.0 mCi) total dose for all ages.

Delivery

- The tracer activity is split into 2–4 separate syringes.
- The injected volume in each syringe should be limited to 0.1–0.3 ml and should contain at least 10–15 MBq (0.1 mCi).
- The tracer is injected intradermally for most indications.
- The location and number of injections depend on the study indication and involved region.

For SLN mapping and biopsy

- For soft tissue sarcomas of the limbs, this may involve peritumoral or intramuscular injections adjacent to the tumor.
- For cutaneous tumors of the extremities, the protocol requires two injections proximal to the margin of the lesion or the scar, or four injections in opposite directions around the lesion or surgical scar.

- For cutaneous tumors of the head, neck, torso, and upper thighs, 2–4 injections around the tumor or site of surgical resection are essential because lymphatic drainage from these locations is unpredictable.

For lymphedema or lymphatic malformation

- The tracer is usually injected intradermally in the interdigital web space between the first and second digits, with one injection in each foot or hand.
- Some centers employ intradermal injections in the dorsum of the feet or hands just proximal to the toes. Injections are easier to administer in these sites and may cause less discomfort to the patient.

Acquisition protocol

For SLN mapping and biopsy [4, 5]:

- Collimator: High-resolution, parallel hole.
- Acquisition begins with dynamic images, 10 seconds/frame for 2–3 min.
- Static images are acquired following the dynamic study for 3–5 min/view.
- The time interval between static images is variable and depends on the rate of tracer transit from the injection sites. Typically, the patient remains on the imaging bed and images are acquired every few minutes.
- The SLN is often visualized within 15–60 min post-injection, occasionally earlier in younger children.
- The field of view (FOV) should include the injection site and the expected lymph drainage basins where the SLN is likely to be present.
 - For tumors in the limbs and head and neck, the FOV should include the adjacent torso.

- For tumors located in the torso, the entire torso should be imaged.
- When the first lymph node (LN), the SLN, is visualized, the overlying skin should be marked with a surgical pen marker.
- Lateral or oblique views improve the localization of the sentinel node.
- SPECT/CT, when available, is the best method for accurate localization of the SLN prior to surgical excision.
- Marking the overlying skin in two planes can be useful for planning the excision of the sentinel node, providing more insight into the depth of the node.
- If images show lymph transit to more than one drainage basin, the SLN in each basin should be identified and marked.

For lymphedema or lymphatic malformations [6–9]:

- Following tracer injection, serial static images of the extremities and subsequently (as transit progresses) images of the pelvis, abdomen, and chest are obtained for up to 100 K counts.
- Continuous body sweeps for 120 seconds /bed position can be also performed. They may show a composite image of the tracer location in the body.

For lymphedema or lymphatic malformations [7, 8, 12, 13]:

- Tracer transit from the injection site proximally through the lymphatic channels of the lower or upper limbs should be symmetrical.
- The normal transit rate depends on the size of the particles and may vary from one commercial preparation to the other.
- As a general reference, tracer should be seen in:
 - Inguinal LNs within 45 min after foot injections.
 - Axillary LNs within 30 min after hand injections.
 - Liver within 4 h post-injection.
- Delayed transit of tracer is suggested when:
 - There is a delayed appearance of LNs
 - Lymphatic channels appear dilated.
 - Collateral lymphatic channels have been identified.
 - Diffuse tracer activity is seen in the superficial soft tissues (dermal backflow).
 - There is a paucity of tracer localization in inguinal and pelvic LNs.
- Diffuse tracer activity in the pleural or abdominal cavities suggests:
 - Chylous pleural effusion and/or chylous ascites.
 - Intestinal lymphangiectasia or pulmonary lymphangiomatosis.
- Findings for lymphatic insufficiency include: delay or absence of lymphatic transport from the injection site, asymmetric or absent visualization of regional lymph nodes, and the presence of radiotracer uptake in dermal lymphatics called dermal backflow.
- In cases of a postsurgical leak from the thoracic duct:
 - Tracer injection in the feet or left arm will show tracer accumulation in the pleural cavity.
 - Tracer injection in the right arm will show normal transit into the systemic circulation and normal liver accumulation.

9.3 Study Interpretation

For SLN mapping and biopsy [4, 5, 10, 11]:

- Check for the site of injections
- Identify the site of SLN and look for potentially more than one SLN

9.4 Correlative Imaging [9, 14]

- Lymphoscintigraphy has replaced lymphangiography, direct injection of contrast agents into lymphatic channels, being highly sensitive and easier to perform and carrying fewer risks of complications.
- If available correlate lymphoscintigraphy with MR lymphangiography.

9.5 Red Flags [15–17]

- Injection of the entire dose should be ensured to avoid false negative results.
- A potential second deep injection is performed selectively in some centers when superficial injection may have failed to be diagnostic.
- Despite the noninvasive nature of the study, significant pain is experienced for a short while at the injection sites.
- For SLN detection:
 - Particle size differs among various commercial preparations. This can affect the velocity of tracer transit and the time required to detect the SLN.
 - In cases with tumors of the torso transit from the injection site is less predictable and could include more than one drainage basin.
 - External radionuclide markers to outline the body surface or a superimposed ^{57}Co flood source transmission image helps localize the sites of tracer activity.
 - Care should be taken not to miss a SLN if it may be located adjacent to the injection site and therefore masked by the high tracer activity. In these cases, use SPECT/CT whenever possible.
- In cases of lymphedema:
 - The study provides functional information on lymph transit. However, it may be limited in discerning the etiology of the abnormality and associated morphological findings.
 - The injections into each limb should be performed in rapid succession to ensure

that differences in the rate of tracer transit in the limbs are not related to a delay in the timing of the second injection.

- Continuous body sweeps and the resulting composite image of the tracer location in the body are easier for orientation.
- When there is slow tracer transit from the feet, limb movement should be encouraged between the imaging sets to stimulate lymphatic transit. Furthermore, depending on the findings and clinical questions, repeated imaging may be required for several hours.
- Delayed transit may be due to obstruction of the lymphatic pathways or abnormal development of lymphatic channels.

9.6 Take Home Messages

- Lymphoscintigraphy has an important role in identifying SLNs and planning their surgical excision.
- Meticulous technique is required when performing lymphoscintigraphy and for marking the SLN.
- Initial dynamic images are important to visualize the lymphatic collectors or tracts and for the detection of the first LN visualized (the SLN).
- Good communication with surgeons is essential for the correct localization and excision of the SLN.
- Gamma probes are utilized during surgery to detect the SLN, often in conjunction with blue dye lymphatic mapping.
- Marking an SLN on the skin can help in planning surgery and therefore the patients should be in the same position as they will be during surgery. If an arm, for example, is stretched out to one side during surgery, it should be in the same position during imaging and marking.
- In cases with lymphedema, normal, and timely visualization of the liver indicates that there is normal lymph drainage into the systemic circulation via the thoracic duct or right lymphatic duct.

- Dermal backflow refers to a phenomenon in which lymphatic fluid leaks and accumulates in the skin and soft tissues by regurgitating the lymphatic flow because of increased pressure caused by occluded lymphatic vessels.

9.7 Representative Case Examples

Case 9.1 Normal Lymphatic Transit (Fig. 9.1)

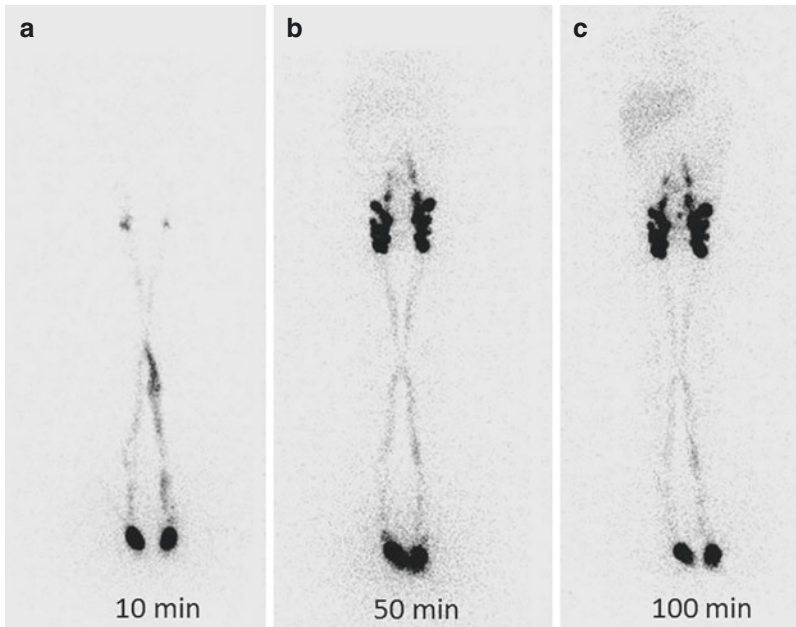


Fig. 9.1 History: An 8-year-old boy with a history of prematurity, short bowel syndrome due to necrotizing enterocolitis, and multi-organ transplantation of bowel, liver, and pancreas presented with lower limb edema. Study report: Anterior whole-body sweeps were obtained at various time points following intradermal injections of Tc-filtered sulfur colloid in the interdigital web space between the first and second digits in both feet. Rapid ascent of tracer from the injection sites is noted. At 10 min post-injection, (a) tracer is seen in the major lymphatic

channels of the lower extremities as well as initial accumulation in the inguinal nodes. At 50 min post-injection (b) there is symmetrical tracer accumulation in inguinal and iliac nodes. Faint activity is noted in the liver suggesting initial drainage of lymphatic fluid into the systemic circulation. At 100 min (c) liver uptake is more obvious. Impression: Normal symmetric tracer transit through the lymphatic system with no evidence of obstruction or abnormal development of lymphatic channels

Case 9.2 Lymphatic Obstruction (Fig. 9.2)

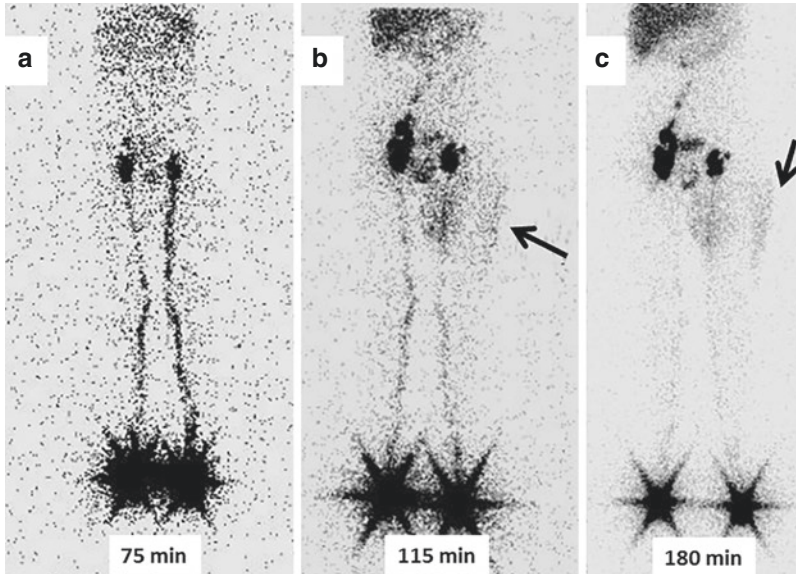


Fig. 9.2 History: A 6-year-old boy presented with lymphedema of the left thigh and buttock that developed 6 months after surgery for a left inguinal hernia. Lymphoscintigraphy was performed following two intradermal injections of Tc-filtered sulfur colloid administered in the interdigital web space between the first and second digits of the feet. Study report: Selected anterior whole-body sweeps starting at 75 min after tracer administration (**a**) show a symmetrical ascent of tracer from the injection sites through the major lymphatic channels of the lower extremities up to the groin levels. Activity is

also noted in the liver, indicating physiologic lymphatic drainage into the systemic circulation. Images obtained at 115 (**b**) and 180 min (**c**) post-injection show a relative paucity of tracer accumulation in left inguinal lymph nodes and a lack of tracer accumulation in the left iliac nodes. Diffuse tracer activity is noted in the superficial soft tissues in the lateral (arrows) and medial aspects of the proximal left thigh, suggesting “dermal backflow.” Impression: The findings suggest lymphatic obstruction at the level of the left groin

Case 9.3 Gastrointestinal Tract Lymphangiectasia (Fig. 9.3)

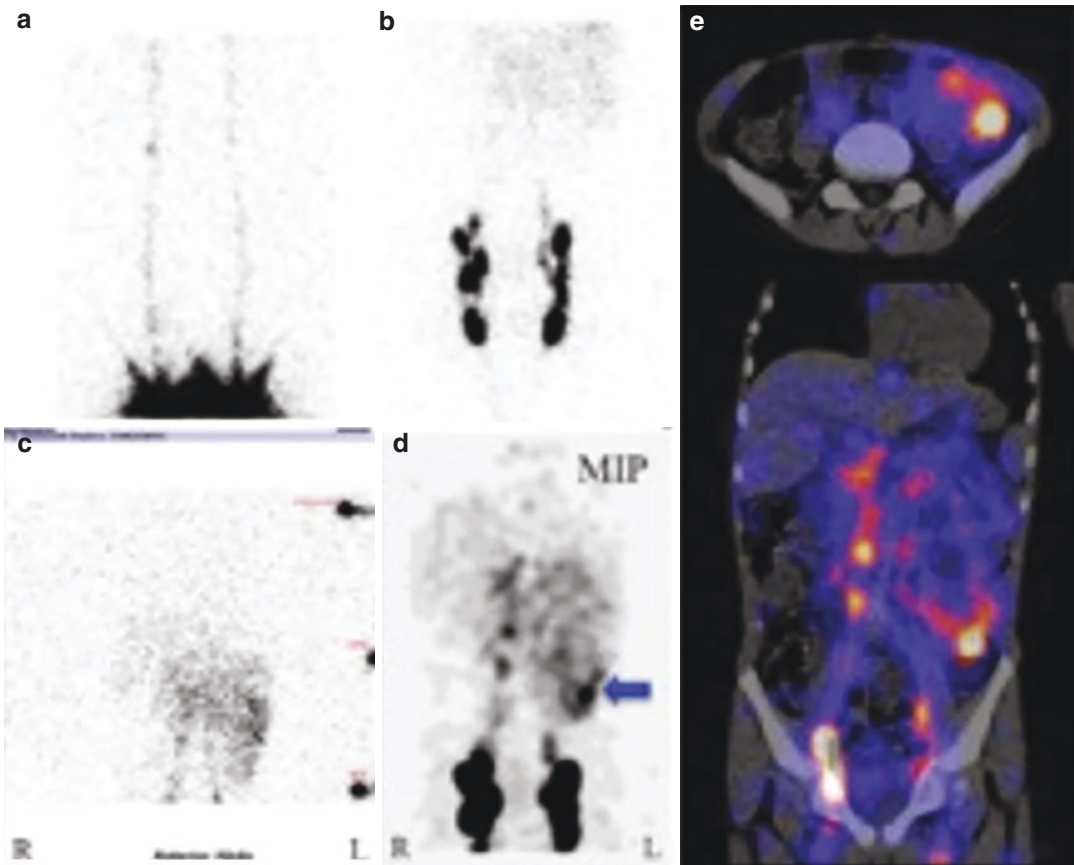
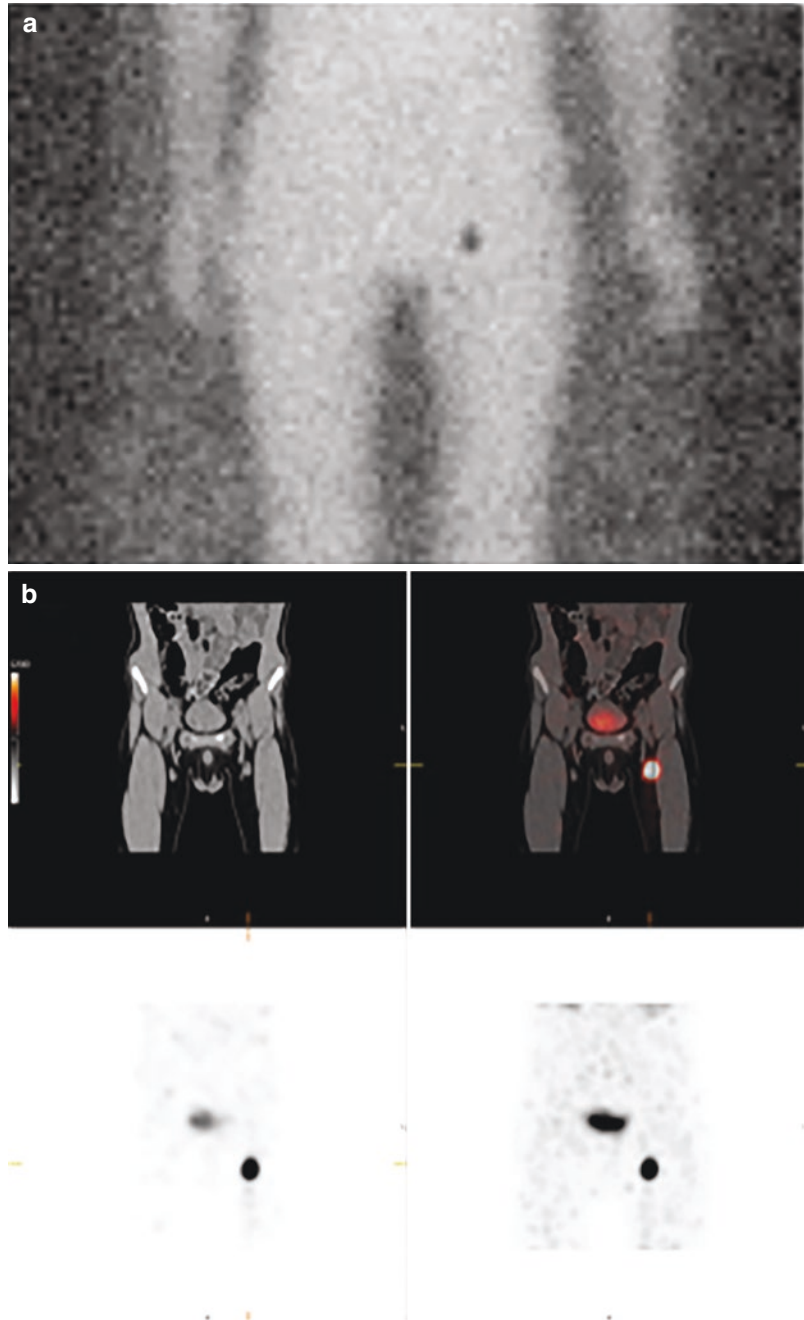


Fig. 9.3 History: An 8-year-old boy was investigated for protein-losing enteropathy with hypoalbuminemia and lymphocytopenia. Lymphoscintigraphy was performed following two dorsal pedal intradermal injections of Tc-antimony sulfide colloid. Study report: The initial dynamic images (a, b) show normal lymphatic collectors in the legs and activity in femoral and inguinal lymph nodes bilaterally. Delayed images at 1 h (c) show a diffuse increase in tracer activity in the left mid-abdomen and

only faint accumulation of tracer in the liver. Abdominopelvic SPECT MIP (d) and SPECT/CT (e, upper-transaxial, lower-coronal slices) demonstrate tracer activity in the gastrointestinal tract, specifically in a bowel loop located in the left lower abdominal quadrant. Impression: The study suggests diffuse gastrointestinal lymphangiectasia, predominantly involving the small bowel, further confirmed by capsule endoscopy

Case 9.4 Sentinel Lymph Node in a Patient with Melanoma (Fig. 9.4)

Fig. 9.4 History: A 5-year-old boy with melanoma in the left leg was evaluated prior to surgery. Study report: Planar scintigraphy of the abdominopelvic region and thighs superimposed on a ^{57}Co flood source transmission image (a) shows a focal area of uptake in the left inguinal region localized to a lymph node on SPECT and SPECT/CT coronal slices (b). Impression: The focus of uptake represents the sentinel lymph node located in the left inguinal region. At surgery, this lymph node was resected and found negative for melanoma



Case 9.5 Left Leg Swelling and Increasing Bilateral Leg Edema and Pleural Effusion (Fig. 9.5)

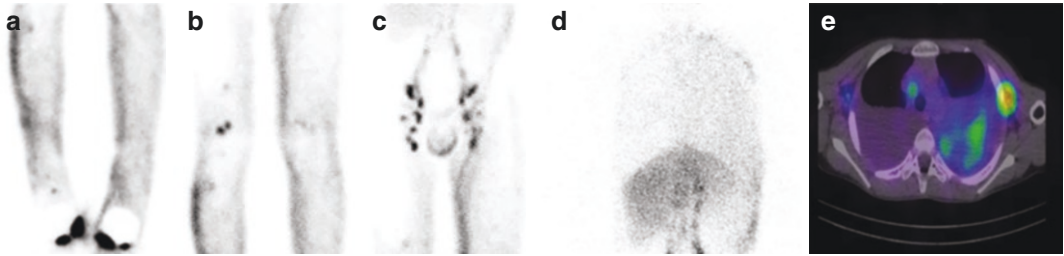


Fig. 9.5 History: A 9-year-old boy presented with left leg swelling, increasing bilateral leg edema, and pleural effusion. He had been previously treated for acute myeloblastic leukemia with total body external beam radiotherapy. Study report: Selected anterior whole-body sweeps starting at 75 min after tracer administration (**a–d**) show significant dermal backflow in the lower limbs, more pronounced on the left side (**a–c**) with adequate visualiza-

tion of bilateral inguinal lymph nodes. There is a visualization of the liver with significant abdominal dermal backflow (**d**). SPECT/CT shows axillary and mediastinal lymph nodes with a chylous leak into the left hemithorax (**e**). Impression: Collateral aberrant lymphatic drainage with abdominal wall dermal backflow, axillary and mediastinal lymph nodes, and chylous leak into the left hemithorax

References

- Grant FD, Maclellan RA, Greene AK. Lymphoscintigraphy. In: Treves ST, editor. *Pediatric nuclear medicine and molecular imaging*. New York, NY: Springer; 2014. p. 189–202.
- Greene AK, Sudduth CL, Taghinia A. Lymphedema (Seminars in pediatric surgery). *Semin Pediatr Surg*. 2020;29(5):150972.
- Howman-Giles R, Pascual T, Uren R. Lymphoscintigraphy in paediatric and adolescent patients. *Clin Transl Imaging*. 2016;4(2):103–17.
- Neville HL, et al. Lymphatic mapping with sentinel node biopsy in pediatric patients. *J Pediatr Surg*. 2000;35(6):961–4.
- Jeremiase B, et al. Value of the sentinel node procedure in pediatric extremity rhabdomyosarcoma: a systematic review and retrospective cohort study. *Ann Surg Oncol*. 2021;28(13):9048–59.
- Bellini C, et al. Lymphatic dysplasias in newborns and children: the role of lymphoscintigraphy. *J Pediatr*. 2008;152(4):587–9, 589.e1–3
- Bellini C, et al. Lymphoscintigraphy patterns in newborns and children with congenital lymphatic dysplasia. *Lymphology*. 2014;47(1):28–39.
- Baulieu F, et al. Contributions of SPECT/CT imaging to the lymphoscintigraphic investigations of the lower limb lymphedema. *Lymphology*. 2013;46(3):106–19.
- Pieper CC, et al. MR lymphangiography of lymphatic abnormalities in children and adults with Noonan syndrome. *Sci Rep*. 2022;12(1):11164.
- Toro J, et al. Sentinel lymph node biopsy in children and adolescents with malignant melanoma. *J Pediatr Surg*. 2003;38(7):1063–5.
- Bay SB, Görgün Ö, Kebudi R. Children with malignant melanoma: a single center experience from Turkey. *Turk Pediatr Ars*. 2020;55(1):39–45.
- Karaçavuş S, Yılmaz YK, Ekim H. Clinical significance of lymphoscintigraphy findings in the evaluation of lower extremity lymphedema. *Mol Imaging Radionucl Ther*. 2015;24(2):80–4.
- Kwon HR, et al. Predictive role of lymphoscintigraphy undergoing lymphovenous anastomosis in patients with lower extremity lymphedema: a preliminary study. *BMC Med Imaging*. 2021;21(1):188.
- Chavhan GB, et al. Magnetic resonance lymphangiography. *Radiol Clin North Am*. 2020;58(4):693–706.
- Yang J, Codreanu I, Zhuang H. Minimal lymphatic leakage in an infant with chylothorax detected by lymphoscintigraphy SPECT/CT. *Pediatrics*. 2014;134(2):e606–10.
- Hassanein AH, et al. Diagnostic accuracy of lymphoscintigraphy for lymphedema and analysis of false-negative tests. *Plast Reconstr Surg Glob Open*. 2017;5(7):e1396.
- Turpin S, Lambert R. Lymphoscintigraphy of chylous anomalies: chylothorax, chyloperitoneum, chylouria, and lymphangiomatosis-15-year experience in a pediatric setting and review of the literature. *J Nucl Med Technol*. 2018;46(2):123–8.

The opinions expressed in this chapter are those of the author(s) and do not necessarily reflect the views of the IAEA: International Atomic Energy Agency, its Board of Directors, or the countries they represent.

Open Access This chapter is licensed under the terms of the Creative Commons Attribution 3.0 IGO license (<http://creativecommons.org/licenses/by/3.0/igo/>), which permits use, sharing, adaptation, distribution and reproduction in any medium or format, as long as you give appropriate credit to the IAEA: International Atomic Energy Agency, provide a link to the Creative Commons license and indicate if changes were made.

Any dispute related to the use of the works of the IAEA: International Atomic Energy Agency that cannot be settled amicably shall be submitted to arbitration pursuant to the UNCITRAL rules. The use of the IAEA: International Atomic Energy Agency's name for any purpose other than for attribution, and the use of the IAEA: International Atomic Energy Agency's logo, shall be subject to a separate written license agreement between the IAEA: International Atomic Energy Agency and the user and is not authorized as part of this CC-IGO license. Note that the link provided above includes additional terms and conditions of the license.

The images or other third party material in this chapter are included in the chapter's Creative Commons license, unless indicated otherwise in a credit line to the material. If material is not included in the chapter's Creative Commons license and your intended use is not permitted by statutory regulation or exceeds the permitted use, you will need to obtain permission directly from the copyright holder.



Musculoskeletal System (Non-Oncologic Indications)

10

Gopinath Gnanasegaran, Sharjeel Usmani,
and Helen Nadel

10.1 Clinical Indications

- Assessment of alterations in bone metabolism due to trauma, infection, inflammation.
- Assessment for conditions with impaired blood flow (e.g., avascular necrosis).
- Assessment of soft tissue (ST).

10.2 Pre-exam Information

- Are symptoms focal or generalized? Duration of symptoms
- History of trauma, systemic metabolic or oncologic conditions
- History of previous interventional procedures (i.e., joint aspiration or drainage, surgery)
- History of treatment such as antibiotics or anti-inflammatory drugs, radiation therapy (including involved fields)

G. Gnanasegaran (✉)
Nuclear Medicine department, Royal Free London
NHS Foundation Trust, London, UK
e-mail: gopinath.gnanasegaran@nhs.net

S. Usmani
Department of Radiology and Nuclear Medicine,
Sultan Qaboos Comprehensive Cancer CARE and
Research Centre (SQCCRC), Muscat, Oman

H. Nadel
Lucile Packard Children's Hospital Stanford
University, Palo Alto, CA, USA

- Serum inflammatory markers available for correlation
- Relevant X-rays, ultrasound (US), CT, or MRI available for correlation?

10.3 Bone Scintigraphy

Study Protocol for ^{99m}Tc -MDP Bone Scintigraphy [1, 2]

Patient preparation

- Good hydration is important, instruct to drink at least 2 cups during the uptake time prior to delayed imaging.
- Infants should be fed prior to or immediately after tracer injection.
- Children should be encouraged to urinate frequently to reduce the exposure of the bladder.
- Sedation is usually not required, except for uncooperative neurodevelopmentally delayed children.

Radiopharmaceutical, administered activity, mode of delivery

Radiopharmaceutical:

- [^{99m}Tc]methylene diphosphonate (MDP) or similar diphosphonates.

Activity:

- 9.3 MBq/kg (0.25 mCi/Kg), minimum dose 40 MBq (1.1 mCi).

Refer to the EANM pediatric dosage card and to the North American consensus guidelines on radiopharmaceutical administration in children in the respective EANM and SNMMI and image gently web sites.

Reference to national regulation guidelines, if available, should be considered.

Delivery:

- Select intravenous (IV) injection site to avoid possible sites of pathology. For example, upper extremity lesions will require a foot injection.

Acquisition protocol: Two- or three-phase bone scan is recommended, four-phase protocol can be performed.

- Early imaging (blood flow and blood pool) to the area of concern and the adjacent region which may cause referred pain (e.g., in the presence of symptoms in a lower extremity include images from thoracic spine down).
 - Dynamic blood flow study.
 - Blood pool (regional or whole body), immediately after the completion of the dynamic study.
 - Late skeletal phase scan at 2–4 h post-injection.
 - Image total body vertex to toes in anterior and posterior projection
 - SPECT should be included in the third step in selected scenarios:
 - To areas of localized symptoms.
 - If an abnormality is detected on planar imaging.
- SPECT/CT, if available should replace SPECT

- Limit the field-of-view (FOV) of the CT to the abnormality seen on SPECT to reduce radiation exposure.
- CT can be acquired as a pediatric low-dose CT for localization and attenuation correction or as diagnostic CT. Many skeletal lesions are adequately evaluated even with low-dose CT parameters.
- A delayed 24-h scan can be performed:
 - In cases of uncertain findings on routine 3-h scintigraphy.
 - When residual bladder activity overlies the pelvis and the child refuses to urinate or when bladder emptying is incomplete.

Acquisition parameters

- Position: The child should lie supine, comfortably secured to the bed.
- Collimators.
 - High or ultrahigh low-energy collimator.
 - Pinhole collimator, if available, can improve detection of lesions in the hip joint of distal extremities.
- Blood flow images.
 - 2–5 s/frame for a total of 60 s, matrix 128 × 128, size-appropriate zoom
- Early blood pool images.
 - Recommended counts: Torso 300 Kcounts, extremities 150–200 Kcounts.
 - For lower extremity lesions the entire lower limbs pelvis and lumbar spine should be in the FOV.
- Late (skeletal) phase images.
- Whole body sweeps with bed speed adjusted to the child's age. The EANM guidelines recommend [3]:
 - 8 cm/min for ages 4–8 years
 - 10 cm/min for ages 8–12 years
 - 12 cm/min for ages 12–16 years
 - 15 cm/min above 16 years of age
- Alternative: Multiple spot views covering the entire skeleton, anterior and pos-

terior projections, start with the pelvis when the bladder is empty.

- Matrix 256 × 256.
- Recommended counts: Torso 500 Kcounts, skull 300 Kcounts, knees 100–200 Kcounts, hands and feet 50–100 Kcounts.
- Alternatively: The time to obtain 500 Kcounts for the torso should be recorded and used to time the acquisition of the other body parts.
- SPECT: 120 projections, 15–30 s/view, matrix 128 × 128.
- SPECT/CT: For the CT component use pediatric settings with dose modulation.
 - Reduce the CT field to include only the findings on the SPECT component.
 - Tube settings depend on manufacturer and the applied protocol: low-dose or fully diagnostic CT (accordingly the settings can range between 80 and 110 kVp).
 - CT slice thickness 2–2.5 mm with overlapping cuts.

- Focal activity in the ischio-pubic synchondrosis is normal in most cases and reflects asymmetric closure of bone centers.

Focally increased tracer activity:

- Osteomyelitis: Increased focal activity in the metaphysis of long bone or in the metaphyseal equivalents. There is also often increased tracer uptake in early blood flow and blood pool images.
- Arthritis: Increased blood flow and blood pool in the involved joint(s). Tracer uptake in the skeletal phase can be normal or increased in a diffuse manner.
- Multifocal tracer uptake: Multi-trauma, metastatic disease, multifocal osteomyelitis. Clinical context, labs, and correlative imaging can distinguish between the options.
- Non-accidental injury (NAI, child abuse): Bilateral, symmetrical foci in costovertebral junctions (typical for the shaken baby syndrome), multiple foci in ribs in various locations, metaphyseal fractures in the shafts of lower extremity bones in young infants who are not walking or bearing weight on their lower extremities, diffuse uptake in the calvarium that may suggest a skull fracture.

10.4 Study Interpretation [3, 4]

- Review the SPECT or SPECT/CT in orthogonal planes, MIP, and, when available, fused co-registered study.
- Review CT study on bone and soft tissue windows in addition to co-registered study.
- Patterns of tracer localization:
- Normal bone growth patterns in infants and children [5]
 - Reduced or absent activity due to physiologic delayed ossification of certain bones (e.g., navicular bone of the foot, femoral head) must be differentiated from pathologic photopenic lesion.
 - Increased activity in the orbits on the anterior view of the skull is normal in the first months of life.
- In suspected osteomyelitis, photopenic lesions are suggestive of an aggressive form known as “cold osteomyelitis.”
- In a child with an unexplained limp, photopenia in the femoral head can suggest Legg-Calve-Perthes disease.
- In children treated with high-dose steroids, multiple photopenic lesions can be due to multifocal avascular necrosis.
- Multiple photopenic lesions occur early on in cases with known hemoglobinopathies.
- Sometimes photopenic lesions, especially in the spine are due to metastatic disease (e.g., neuroblastoma, leukemia, or lymphoma)

Diffuse decreased tracer activity:

- Can be caused by prolonged limb immobilization or decreased use.
- Associated with severe pain, reduced skin temperature, and faint peripheral pulses could represent a complex regional pain syndrome (CRPS, reflex sympathetic dystrophy).

Diffuse increased tracer uptake:

- Along the cortex of the tibia and/or fibula in children and adolescents undergoing strenuous physical activities can be due to shin splints, while focal uptake can be due to a stress fracture.
- In the feet and ankles often observed in the unaffected side of limping children due to increased weight bearing on the healthy side.

Bone Scintigraphy Protocol Adjustments in Suspected Non-Accidental Injury [6, 7]

- Add routinely to standard views: lateral and oblique views of the ribs, anterior, posterior, and lateral views of the skull.
- Make sure the hands are flat, so all digits are visualized.
- Make sure the urinary bladder does not obscure pelvic structures.

10.5 Correlative Imaging [8]

- Correlation with radiographs is required when assessing skeleton.
- MRI is a sensitive modality for the evaluation of bone marrow and ST pathologies. In some centers, it is a first-line investigation for the MSK system. The examination is typically focused on the symptomatic region and can therefore miss sites of disease in cases of referred pain as well as additional sites in multifocal disease. MRI availability and cost can be limiting factors.

- Check if the child has not performed a recent CT or MRI or if one is already planned before deciding on SPECT/CT.

10.6 Red Flags [4, 6]

- When positioning patients for planar imaging, the feet should be secured with a medial (inward) tilt of the feet, thus allowing adequate visualization of the fibulae.
- Early blood pool static images should start immediately after the completion of the dynamic blood flow study as skeletal uptake begins quickly after tracer injection.
- In young children, due to high bone to ST contrast, delayed static images can be acquired as early as 2 h post-injection.
- If bladder emptying is difficult and there is no other alternative, bladder catheterization may be considered.
- All children should have delayed imaging of the entire body, performed as a whole body sweep or multiple planar static images.
- In young children recording, sets of overlapping planar static images allow for repeated selected images in case of motion with improved spatial resolution.
- Additional spot views are often necessary to improve detectability of lesions. For example, lateral, medial plantar, and dorsal views for foot and ankle pathology, lateral views for the legs, palmar, and dorsal views for the hands, oblique and lateral views for the ribs, lateral views for the skull and cervical spine.
- In older children, SPECT/CT can replace multiple spot views.
- If SPECT/CT is used attention must be paid to the additional radiation dose of the CT component.
- In general CT acquisition should be strictly limited to the body segment of interest.
- Sensitivity of bone scans is low in the detection of linear skull fractures.
- Sensitivity of bone scans in the detection of arthritis is limited.

- Suspected fractures or ischemia in weight-bearing bones should be promptly reported to the referring physician to initiate preventive measures to avoid complications.

10.7 Take Home Message

- Whole-body blood pool images are useful in suspected multifocal osteomyelitis (MFO), rheumatologic conditions, generalized pain, and NAI.
- In most cases, ST pathologies are best identified on the blood pool images and blood flow images do not provide additional information.
- When vascular compromise is suspected (e.g., limb ischemia reflex sympathetic dystrophy, avascular necrosis) blood flow images should be obtained.
- All children should have a whole-body delayed bone scintigraphy assessment.

Regional bone scans should not be performed.

- While adequate count density and optimal spatial resolution are desired, some flexibility is advised keeping in mind that long acquisition times increase the likelihood of motion artifacts that degrade image quality.
- Review correlative radiologic imaging, when possible, for findings worrisome for malignancy.
- Findings raising the possibility of NAIs should be immediately reported to the referring physician before the patient is discharged.

10.8 Representative Case Examples

Case 10.1 Osteomyelitis (Fig. 10.1)

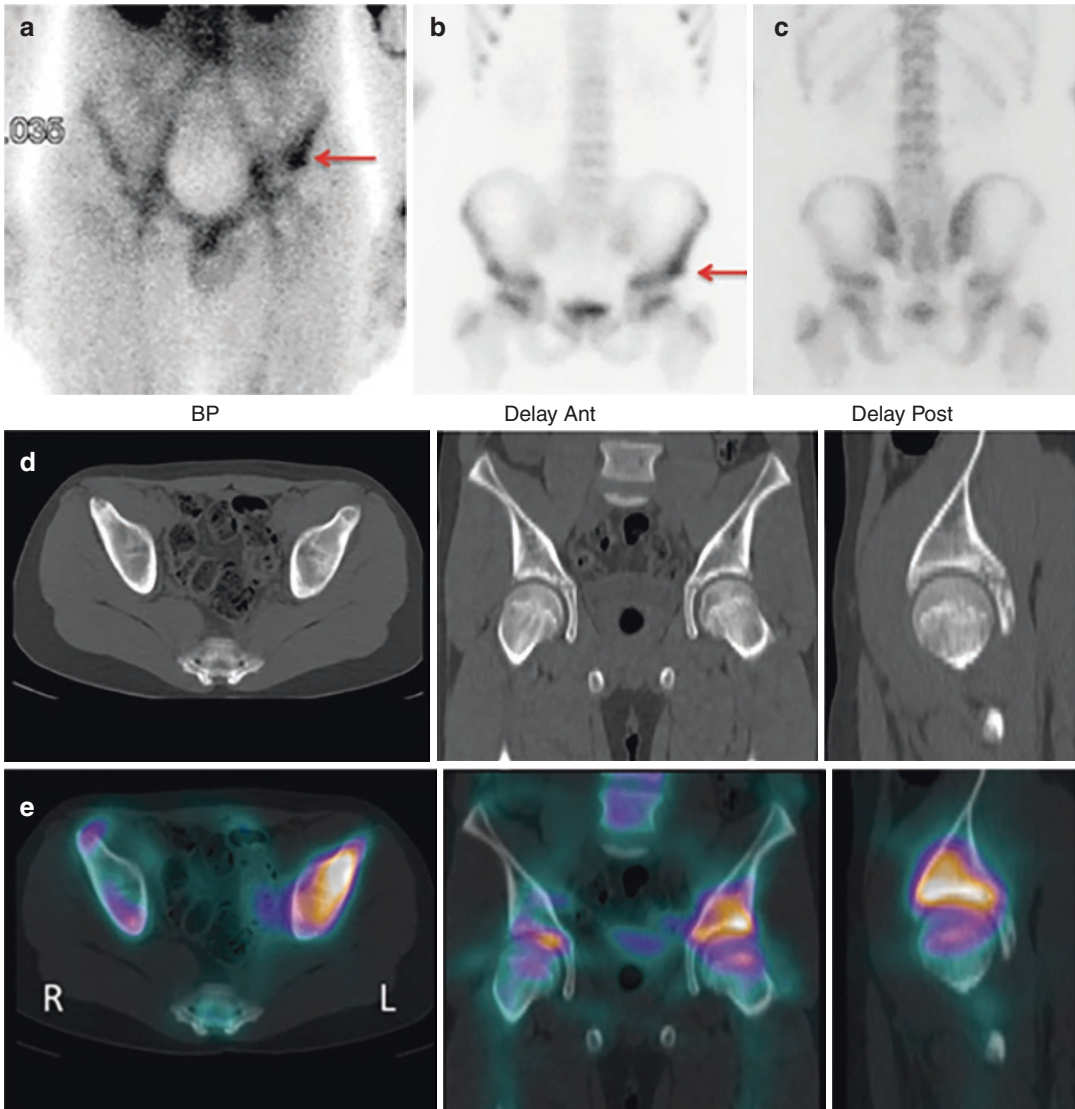


Fig. 10.1 History: An 11-year-old boy presented with a painful left hip 2 weeks after playing soccer. X-rays and US were normal. Study report: In the early blood pool study (a) there is increased tracer uptake in the left anterior inferior iliac spine (arrow). The late planar anterior (b) and posterior (c) scans show focal increased osteoblastic activity in the same area (arrow). SPECT/CT, axial, coronal, and sagittal low-dose CT slices (d) show no bone erosion around marked focal osteoblastic reaction

seen in the left iliac bone on fused images (e). Impression: The pathological uptake on bone scintigraphy, in association with the lack of abnormalities on the CT part of the SPECT/CT most likely exclude tumor. SPECT/CT cannot exclude subtle lesions such as stress fractures or enthesopathy. Acute osteomyelitis was the suggested diagnosis despite the lack of systemic fever, further confirmed by blood cultures positive for *S. aureus*

Case 10.2 Non-Accidental Bone Injuries
(Fig. 10.2)

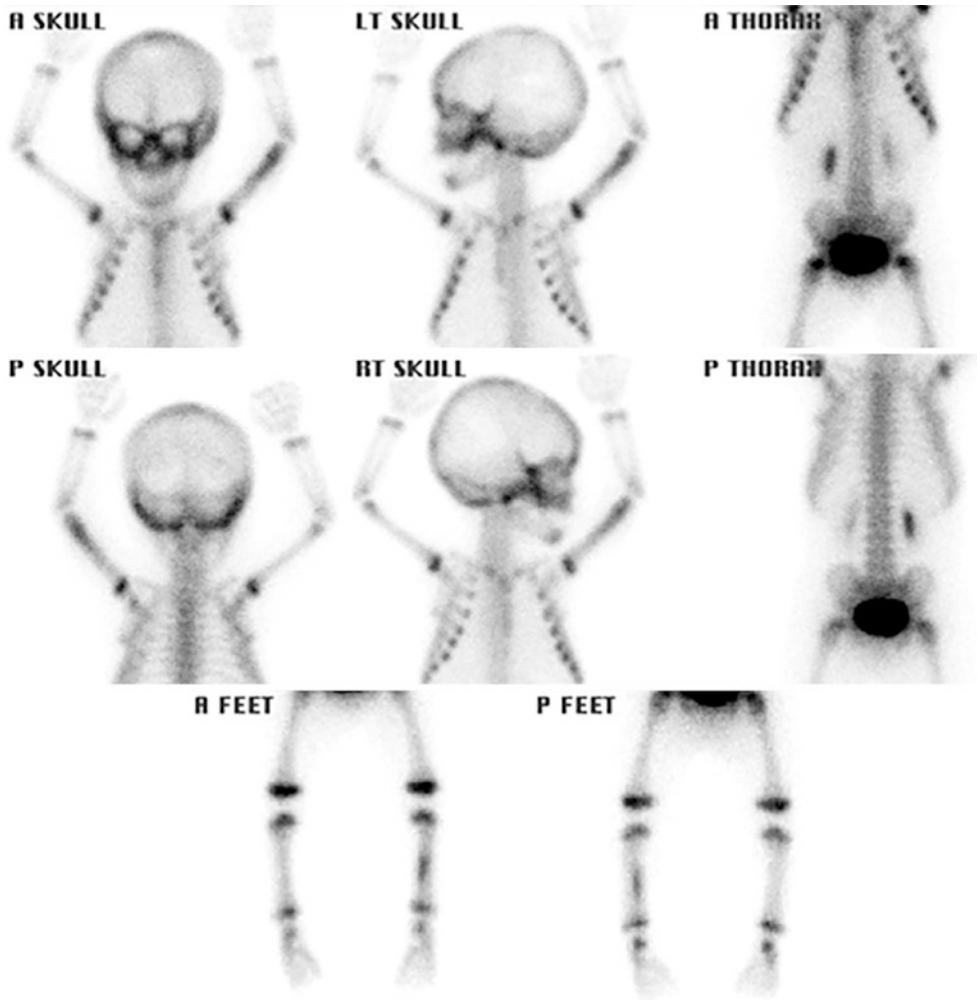


Fig. 10.2 History: A 4-month-old girl presented with a swollen left arm. X-ray showed a left humeral fracture. Study report: On early blood pool images (not shown), there is an increased blood pool in the distal left humerus and mid-left tibia. Late planar scans show foci of increased

tracer uptake in the mid-to-distal left humerus and mid-left tibia. Impression: The pattern of focal increased tracer uptake in the left humerus and left tibia are highly suggestive of non-accidental injury despite normal X-ray of the tibia

Case 10.3 Spondylolysis (Fig. 10.3)

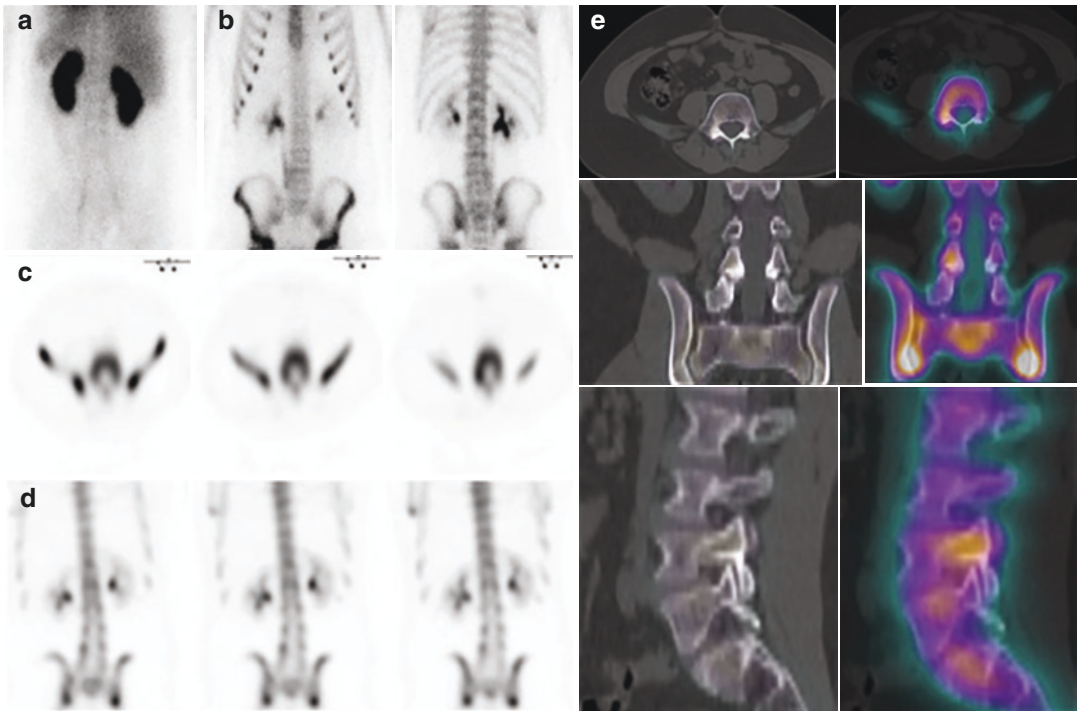


Fig. 10.3 History: An 11-year-old boy presented with a month-long low back pain after playing football. X-rays showed mild scoliosis, convex to the left, but was otherwise normal. Study report: Bone scintigraphy shows a normal blood pool (a) but mildly increased tracer uptake on the right side of the lower lumbar spine in the late planar scans (b). SPECT, transaxial (c) and coronal (d) slices,

shows focal increased uptake in the right pars interarticularis of L4 vertebra. SPECT/CT (e), transaxial, coronal and sagittal CT (left) and fused (right) images, demonstrate bilateral sclerosis, more pronounced at the site of the focal increased tracer uptake in the right pars interarticularis of L4 vertebra. Impression: The findings are consistent with an L4 spondylolytic fracture

Case 10.4. Legg-Calve-Perthes Disease (Fig. 10.4)

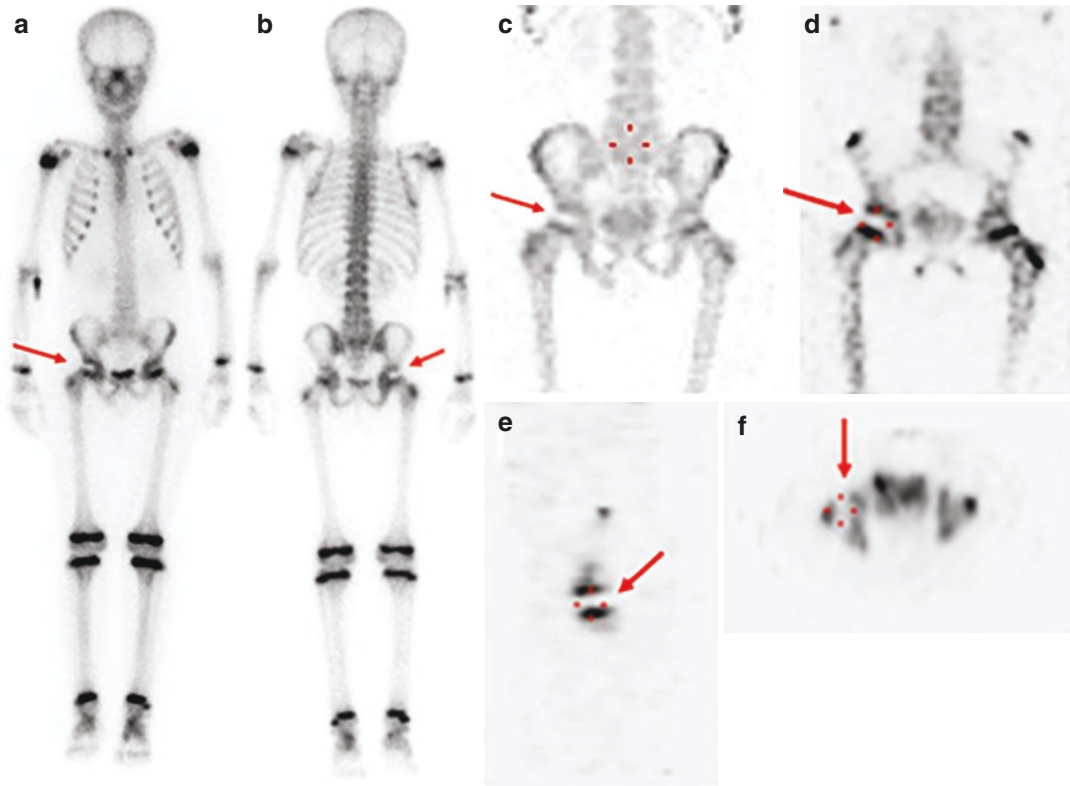


Fig. 10.4 History: An 8-year-old boy presented with complaints of right hip pain and right-sided limping for 2 weeks, without a history of fever or trauma. Study report: The early phase images (not shown) were unremarkable. Anterior and posterior late whole-body images (**a**, **b**) show reduced tracer uptake in the right femoral head

(arrows). SPECT anterior projection MIP (**c**) and coronal, sagittal, and transaxial slices (**d-f**) show a photopenic area in the right proximal femoral epiphysis (arrows) confirming the findings on the whole body sweeps. Impression: The findings suggest avascular necrosis of the right femoral head (Legg-Calve-Perthes disease)

10.9 ¹⁸F-Sodium Fluoride (NaF) Bone PET/CT

Study Protocol for NaF Bone PET/CT [1, 9–11]

Patient preparation

- Patient should be well hydrated.
- Change diaper right before imaging.
- Remove metal objects from around the patient before imaging.

Radiopharmaceutical, administered activity and mode of delivery

Radiopharmaceutical:

- [¹⁸F] Sodium Fluoride (NaF)

Activity:

- 2.22 MBq/kg (0.06 mCi/kg), range 18.5–185 MBq (0.5–5 mCi).

Refer to the EANM pediatric dosage card and to the North American consensus guidelines on radiopharmaceutical administration in children in the respective EANM and SNMMI and image gently web sites.

Reference to national regulation guidelines, if available, should be considered.

Delivery:

- Select the injection site to avoid possible sites of pathology.

Acquisition protocol

- Uptake period: 45 min after tracer administration.
- PET: 2–5 min/bed position (depending on equipment).
- FOV: varies by patient size.
- CT: Either low-dose CT (70–80 mA, 80–100 kVp) or diagnostic CT

10.10 Study Interpretation

- Review the PET MIP image, as well as fused orthogonal planes.
- Review CT with bone and soft tissue windows.
- Correlative imaging such as radiographs or other cross-sectional imaging should be reviewed at the time of reporting.

10.11 Correlative Imaging

- Correlation with radiographs is required when assessing skeleton.

10.12 Red Flags [12, 13]

- Interpreting NaF studies in children requires a learning curve. The study has a high sensitivity and there is therefore a need to identify patterns of physiologic variants and differentiate them from pathological uptake foci.

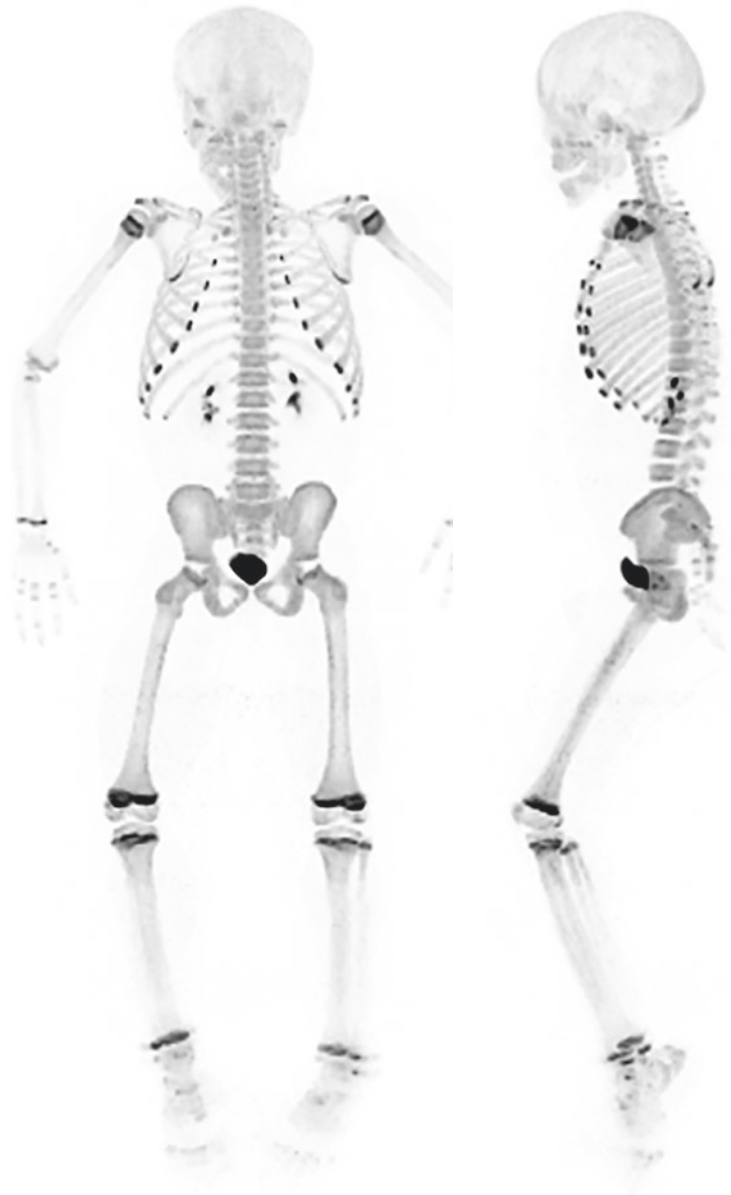
10.13 Take Home Messages [14, 15]

- NaF imaging has the advantage of shorter total study duration, higher image quality, and quantification.
- Effective dose from NaF is comparable to effective dose from Tc-MDP.
- The main current indications for NaF bone PET studies are in cancer patients for evaluation of primary and metastatic bone lesions and children with chronic recurrent multifocal osteomyelitis.

10.14 Representative Case Examples

Case 10.5 Normal NaF PET Study (Fig. 10.5)

Fig. 10.5 History: A 7-year-old boy was referred to NaF PET/CT for further evaluation of low back pain. Study report: Whole-body PET, anterior (left) and lateral (right) MIP, show increased symmetric tracer uptake in the epiphyseal plates of the long bones in the upper and lower limbs and the anterior end of the ribs, bilaterally, consistent with areas of physiologic activity in growing plates. Impression: No evidence of abnormal osteoblastic lesions in the spine



Case 10.6 Fibrous Cortical Defect (Fig. 10.6)

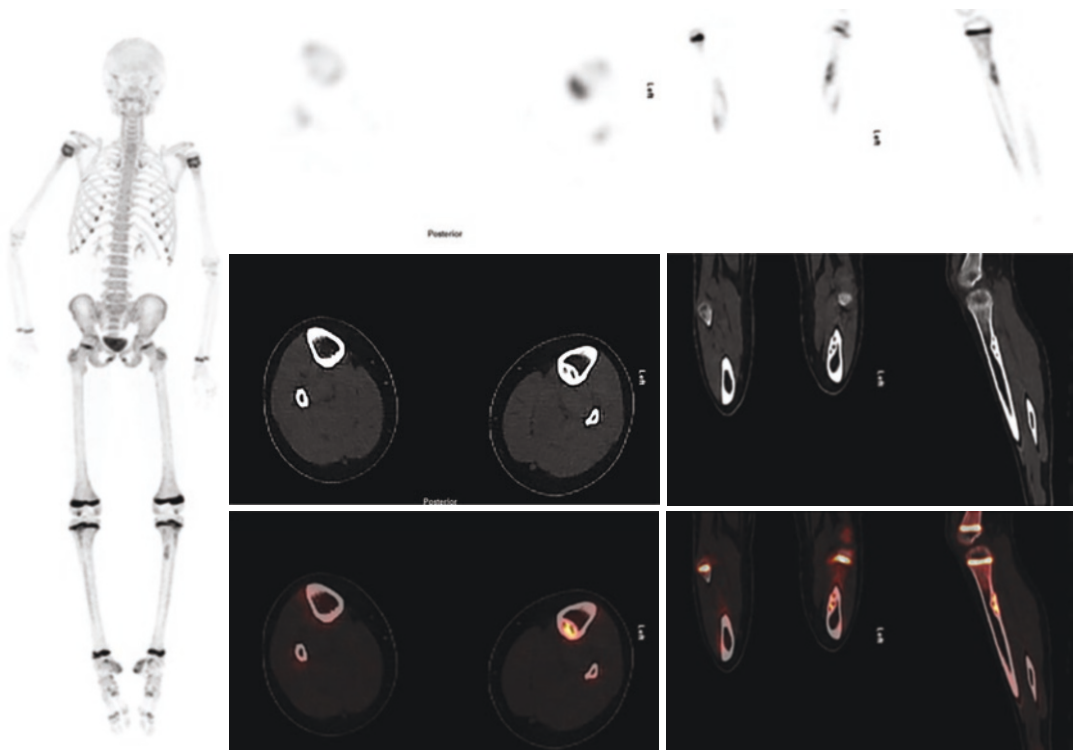


Fig. 10.6 History: A 9-year-old boy was referred to NaF PET/CT following 1-month long complaints of pain in the left leg. Study report: Whole-body MIP (left) shows a focal area of increased tracer uptake at the medial aspect of the upper shaft of left tibia. Coronal and sagittal (right) and transaxial (center) PET, CT, and fused PET/CT slices

at the level of the proximal tibia show an eccentric, well-defined lytic lesion with a rim of sclerosis, with corresponding increased tracer uptake at the posteromedial part of the left upper tibia. Impression: The findings are consistent with a fibrous cortical defect

Case 10.7 Bilateral Ischio-Pubic Synchrondrosis (Fig. 10.7)

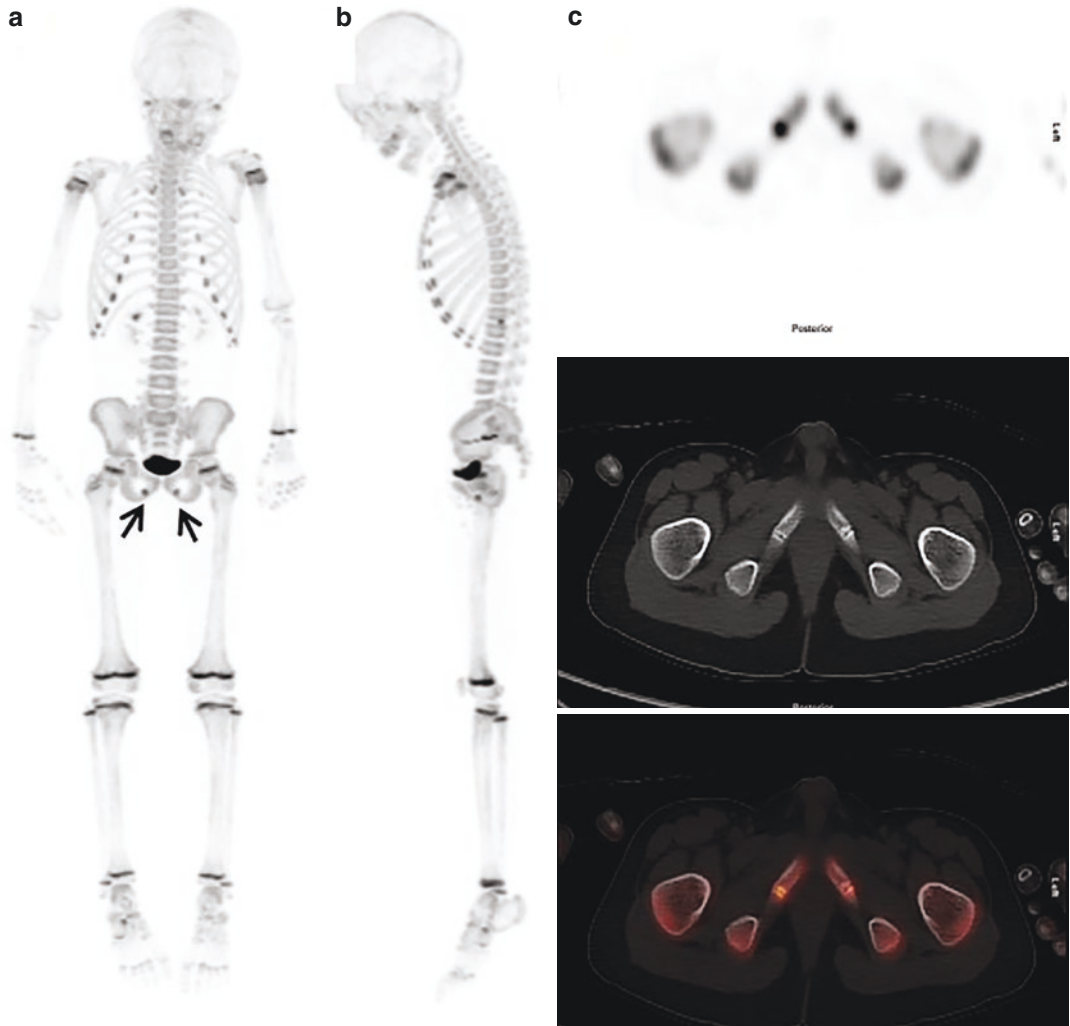


Fig. 10.7 History: A 7-year-old boy with right orbital rhabdomyosarcoma was evaluated as part of a metastatic survey. Study report: Anterior (a) and lateral MIP (b), as well as transaxial PET, CT, and fused NaF PET/CT slices at the level of the symphysis pubis (c) show physiological symmetric increase uptake at the growing ends of the bone, including costochondral junctions, and the epiphy-

seal plates of the upper and lower limbs. There is increased tracer uptake in both distal rami of the pubis (arrows). Impression: The findings demonstrate focal increased tracer uptake in sites of bilateral ischio-pubic synchrondrosis. This is a normal variant and should not be interpreted as fractures. No evidence of bone metastases

Case 10.8 Patellar Tendon Insertion Enthesopathy (Fig. 10.8)

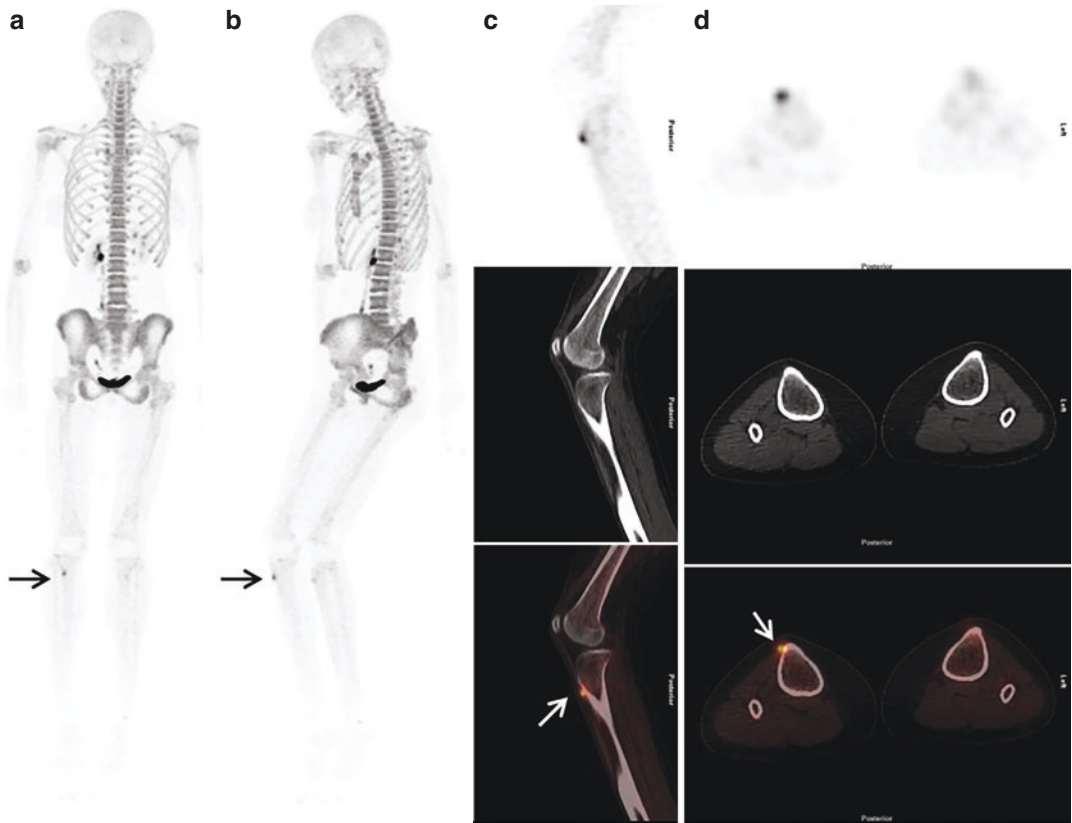


Fig. 10.8 History: A 13-year-old boy is complaining of right knee pain for 3 months. Plain X-rays were unremarkable. Study report: NaF PET/CT, anterior (a) and oblique MIP (b), as well as sagittal (c) and transaxial (d) PET, CT, and fused slices at the level of the proximal tib-

iae show focal increased tracer uptake at the cortical surface of right tibial tuberosity (arrow). Impression: The findings are consistent with patellar tendon insertion enthesopathy

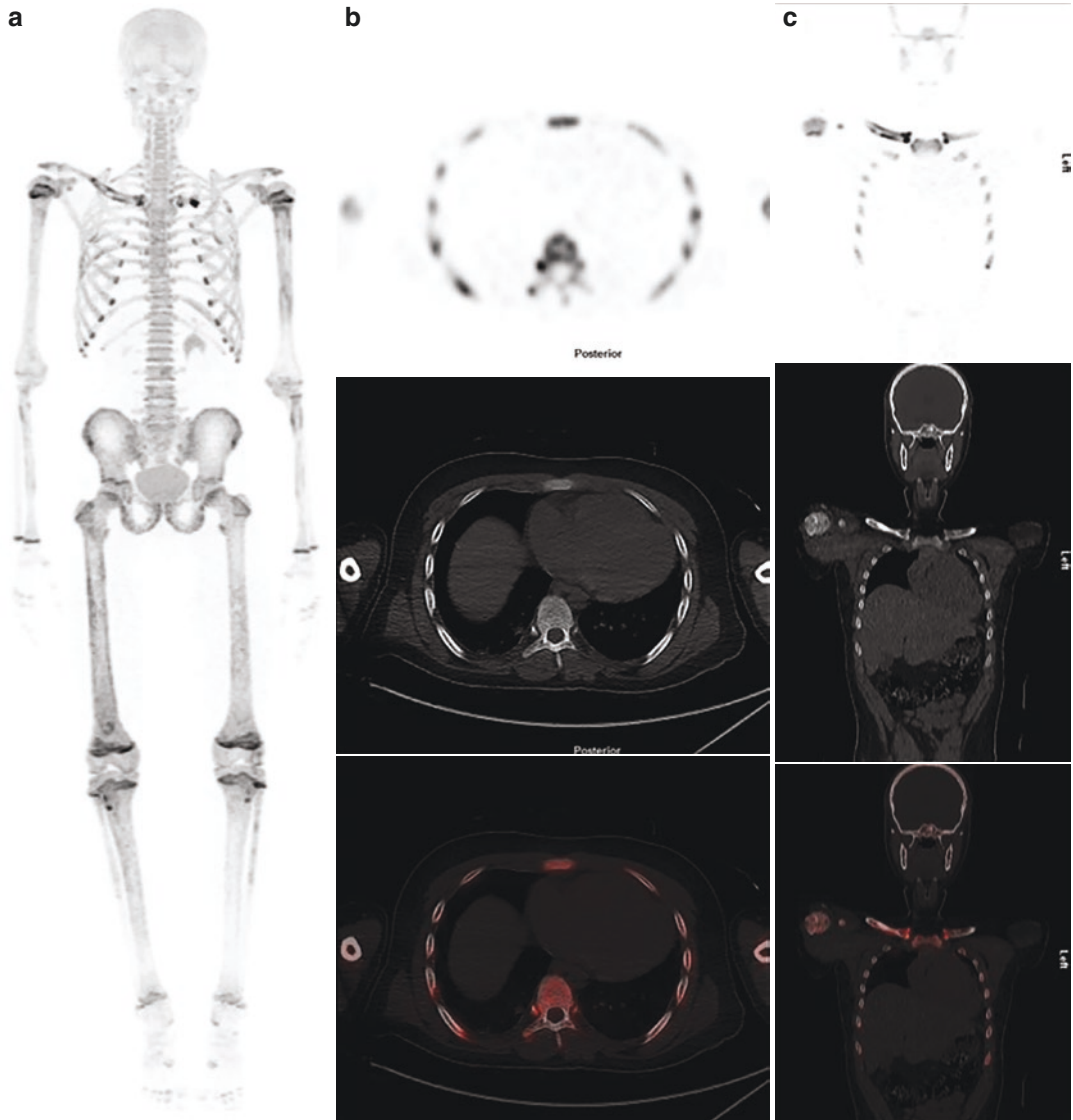
Case 10.9 Sickle Cell Anemia (Fig. 10.9)

Fig. 10.9 History: A 16-year-old boy with known sickle cell anemia presented with subacute bone pain. Study report: NaF PET MIP (a), transaxial (b) and coronal (c) PET, CT and fused images show multiple areas of

increased tracer uptake at right clavicle, bilateral ribs, the left humeral shaft, and the right trochanteric region. Impression: The osteoblastic lesions represent active bone remodeling at multiple bone infarcts

References

- Beheshti M, et al. (18)F-NaF PET/CT: EANM procedure guidelines for bone imaging. *Eur J Nucl Med Mol Imaging*. 2015;42(11):1767–77.
- Van den Wyngaert T, et al. The EANM practice guidelines for bone scintigraphy. *Eur J Nucl Med Mol Imaging*. 2016;43(9):1723–38.
- Stauss J, et al. Guidelines for paediatric bone scanning with ^{99m}Tc-labelled radiopharmaceuticals and ¹⁸F-fluoride. *Eur J Nucl Med Mol Imaging*. 2010;37(8):1621–8.
- Nadel HR. SPECT/CT in pediatric patient management. *Eur J Nucl Med Mol Imaging*. 2014;41(Suppl 1):S104–14.
- Atlas of bone scintigraphy in the developing paediatric skeleton: the normal skeleton variants and pitfalls. Vienna: International Atomic Energy Agency; 2011.
- Nadel HR. Pediatric bone scintigraphy update. *Semin Nucl Med*. 2010;40(1):31–40.
- Treves ST. Skeletal scintigraphy: general considerations. In: Treves ST, editor. *Pediatric nuclear medicine and molecular imaging*. New York: Springer; 2014. p. 365–84.
- Shammas A. Nuclear medicine imaging of the pediatric musculoskeletal system. *Semin Musculoskelet Radiol*. 2009;13(3):159–80.
- Segall G, et al. SNM practice guideline for sodium ¹⁸F-fluoride PET/CT bone scans 1.0. *J Nucl Med*. 2010;51(11):1813–20.
- Drubach LA. Pediatric bone scanning: clinical indication of (18)F NaF PET/CT. *PET Clin*. 2012;7(3):293–301.
- Fischer DR. Musculoskeletal imaging using fluoride PET. *Semin Nucl Med*. 2013;43(6):427–33.
- Drubach LA, Connolly SA, Palmer EL 3rd. Skeletal scintigraphy with ¹⁸F-NaF PET for the evaluation of bone pain in children. *AJR Am J Roentgenol*. 2011;197(3):713–9.
- Panagiotidis E, et al. Skeletal metastases and benign mimics on NaF PET/CT: a pictorial review. *AJR Am J Roentgenol*. 2018;211(1):W64–w74.
- Jadvar H, Desai B, Conti PS. Sodium ¹⁸F-fluoride PET/CT of bone, joint, and other disorders. *Semin Nucl Med*. 2015;45(1):58–65.
- Usmani S, et al. Technical feasibility, radiation dosimetry and clinical use of (18)F-sodium fluoride (NaF) in evaluation of metastatic bone disease in pediatric population. *Ann Nucl Med*. 2018;32(9):594–601.

The opinions expressed in this chapter are those of the author(s) and do not necessarily reflect the views of the IAEA: International Atomic Energy Agency, its Board of Directors, or the countries they represent.

Open Access This chapter is licensed under the terms of the Creative Commons Attribution 3.0 IGO license (<http://creativecommons.org/licenses/by/3.0/igo/>), which permits use, sharing, adaptation, distribution and reproduction in any medium or format, as long as you give appropriate credit to the IAEA: International Atomic Energy Agency, provide a link to the Creative Commons license and indicate if changes were made.

Any dispute related to the use of the works of the IAEA: International Atomic Energy Agency that cannot be settled amicably shall be submitted to arbitration pursuant to the UNCITRAL rules. The use of the IAEA: International Atomic Energy Agency's name for any purpose other than for attribution, and the use of the IAEA: International Atomic Energy Agency's logo, shall be subject to a separate written license agreement between the IAEA: International Atomic Energy Agency and the user and is not authorized as part of this CC-IGO license. Note that the link provided above includes additional terms and conditions of the license.

The images or other third party material in this chapter are included in the chapter's Creative Commons license, unless indicated otherwise in a credit line to the material. If material is not included in the chapter's Creative Commons license and your intended use is not permitted by statutory regulation or exceeds the permitted use, you will need to obtain permission directly from the copyright holder.





Infection and Inflammation Imaging

11

Ora Israel, Enrique Estrada-Lobato,
and Thomas Neil Pascual

11.1 Clinical Indications

Commonly evaluated pediatric infectious processes [1–3]:

- Musculoskeletal (MSK) infections
 - Osteomyelitis (diagnosis, differential diagnosis, single vs. multifocal disease)
 - Discitis
 - Arthritis
- Fever of unknown origin (FUO) is at present evaluated with FDG imaging as a second-line diagnostic investigations. The test has high overall performance, mainly in:
 - Immune-compromised children [4–6].
 - Febrile neutropenia (absolute neutrophil count below $500/\text{mm}^3$) in immune-suppressed and/or cancer patients [7].

Additional indications in children [8]

- Fungal infections (e.g., aspergillosis and candidiasis).
- Inflammatory bowel disease (IBD) (diagnosis, extent of disease, differential diagnosis of active disease vs. fibrosis, treatment evaluation) [9].
- Inflammatory processes
 - Vasculitis
 - Chronic granulomatous diseases (e.g., sarcoidosis)

11.2 Pre-exam Information

- Relevant clinical data:
 - Measure and record the patient height and weight.
 - Current symptoms, pertinent physical findings, duration of signs and symptoms.
 - Pre-existing conditions.
 - Previously or currently received therapy such as antibiotics, corticosteroids, chemotherapy, radiation therapy, and diphosphonates.
 - Prior orthopedic or non-orthopedic surgery, presence of orthopedic hardware.
- Relevant recent imaging studies.

O. Israel (✉)
B&R Rappaport Faculty of Medicine, Technion,
Haifa, Israel

E. Estrada-Lobato
Nuclear Medicine and Diagnostic Imaging Section,
Division of Human Health, Department of Nuclear
Sciences and Applications, International Atomic
Energy Agency, Vienna, Austria

T. N. Pascual
Department of Science and Technology,
Manila, Philippines

For the activity of all radiotracers to be administered:

Refer to the EANM pediatric dosage card and to the North American consensus guidelines on radiopharmaceutical administration in children in the respective EANM and SNMMI and image gently web sites.

Reference to national regulation guidelines, if available, should be considered.

Study Protocol for Bone Scintigraphy [2, 10]

Patient preparation:

- Good hydration, patients are instructed to drink at least 2 cups after radiotracer injection, before returning for delayed imaging.
- Infants should be fed prior or immediately after injection.
- Children should be encouraged to urinate frequently to reduce the exposure of the bladder.

Radiopharmaceutical, activity, mode of delivery

Radiopharmaceuticals:

- [^{99m}Tc]-MDP (MDP)

Activity:

- 9.3 MBq/kg (0.25 mCi/Kg), minimum dose 40 MBq (1.1 mCi).

Acquisition protocol (Figs. 11.1, 11.2, and 11.3)

- Position: Supine, with the child comfortably secured to the bed, including feet secured with an inward tilt (allows adequate visualization of the fibulae).
- Collimators: High or ultra-high low-energy collimator. Pinhole collimator, if available, can improve detection of lesions in the hip joint.
- Blood flow images: 2–5 s/frame for a total of 60 s, matrix 128 × 128, size appropriate zoom.

- Early blood pool images: torso 300 Kcounts, extremities 150–200 Kcounts.
- Late skeletal phase images are typically acquired 3 h after injection.
- Whole body sweeps: with bed speed adjusted to the child's age [11].
 - 8 cm/min for children aged 4–8 years.
 - 10 cm/min for ages 8–12 years
 - 12 cm/min for ages 12–16 years
 - 15 cm/min over 16 years of age.
- Multiple spot views (alternatively) to cover the entire skeleton in anterior and posterior projections: matrix 256 × 256, counts: torso 500 Kcounts, skull 300 Kcounts, knees 100–200 Kcounts, hands and feet 50–100 Kcounts. 2nd variant: the time to obtain 500 Kcounts for the torso should be recorded and used to time the acquisition of the other body parts.
- SPECT: 15–30 s/frame, 120 projections, matrix 128 × 128.
- SPECT/CT (when clinically indicated, if available):
 - CT component using pediatric settings with dose modulation.
 - CT field of view to the finding on SPECT, tube setting depending on whether the CT is intended to be acquired as low dose or fully diagnostic CT (range: between 80 and 110 kVp); CT slice thickness 2–2.5 mm with overlapping cuts.

11.3 Study Interpretation of Bone Scintigraphy [12]

- Osteomyelitis is based on increased local blood flow and bone turnover. The scintigraphic pattern is characterized by increased blood flow and blood pool (tissue hyperemia) and focal increased uptake in the skeletal phase (Fig. 11.1).

- Osteomyelitis involves mainly the metaphyseal portion of long bones or the metaphyseal equivalents of irregular bones.
- Less commonly, osteomyelitis presents as diffuse uptake along a segment of a long bone (probably due to periosteal irritation).
- Mandatory whole-body imaging allows the detection of at times unsuspected multifocal disease including sites related to referred pain. Multifocal osteomyelitis is more common in young infants.
- Bone scans can differentiate osteomyelitis from soft tissue infections.
 - Cellulitis presents with diffuse increased blood flow and blood pool in soft tissue adjacent to bony structures and mild diffuse increased tracer activity in the same area on the skeletal phase.
 - Arthritis presents with diffuse uptake in all bony structures of a joint, with or without accompanying findings in the blood flow and blood pool phases.
 - Discitis typically presents as increased uptake in two adjacent vertebral bodies above and below the inflamed disc.
- In most cases, an abnormal bone scan can be seen as early as 24 h from the onset of symptoms.
- Cases with long-standing osteomyelitis show increased blood pool activity surrounding photopenic defects (Fig. 11.2). On the delayed images, there are corresponding cold lesions in keeping with bony abscesses. The differential diagnosis includes infarcted bone.
- Antibiotic therapy does not affect bone scan findings of osteomyelitis in the short run.

Study Protocol for Tc-WBC Scan [8, 13]

Patient preparation:

- Patients do not need to fast and may take all their usual medications.
- The patient should be well hydrated.
- Explain to patients and parents/caregivers that the procedure is long and requires withdrawal of relatively large

amounts of blood (considering the specific pediatric population).

Radiopharmaceutical, activity, mode of delivery

Radiopharmaceutical

- [^{99m}Tc]-WBC

Activity

- 3.7–7.4 MBq/kg (0.1–0.2 mCi/Kg), minimum dose 40 MBq (1.1 mCi)

For detailed instructions regarding the WBC labelling technique, see appropriate guidelines. The blood volume required for WBC labelling has to be adjusted and reduced as much as possible in young infants [14].

Acquisition protocol (Fig 11.4)

- Collimator: low energy, high resolution, parallel hole.
- Scanning field: related to clinical indication should be either whole body or limited FOV to area of clinical complaints.
- Acquisition protocol:
 - Early images, 30 min post-injection, including of the chest and upper abdomen as well as images for in vivo quality control of WBC labelling.
 - Delayed images: 3–4 h post-injection.
 - Late images: 20–24 h post-injection.
- Acquisition parameters—static images:
 - Size appropriate zoom, matrix 256 × 256.
 - Acquisition options:
 - Time corrected for isotope decay: early images are acquired with a set number of counts or time, followed by delayed and late images corrected for the ^{99m}Tc 6-h half-life. Different images can be com-

pared with the same intensity scale avoiding operator-dependent changes in the image display.

Fixed time/image: 5–10 min/projection. Difficult to interpret because of interfering data from other organs.

- SPECT or SPECT/CT (recommended if available): Usually performed after the delayed step (3–4 h post-injection).
 - SPECT parameters if performed after delayed step: 20–30 sec/step (depending on the injected activity).
 - SPECT can be also added to the late step (20–24 h post-injection) with following parameters:
 - 30–50 sec/step (depending on the injected activity and FOV to be imaged, longer for peripheral parts, shorter for abdomen).
 - Indicated if there are new sites of pathological uptake not seen on earlier scans.
- Modified parameters for IBD: Images acquisition at 30 min and 2–3 h post-injection only (Fig. 11.5).

11.4 Study Interpretation of Tc-WBC Scan [13]

Diagnosis of infection is made by comparing delayed and late images:

- Negative: no uptake or clear decrease of intensity of uptake between delayed and late images.
- Positive: clear increase in intensity and/or size of uptake over time in lesion (Fig 11.4).
- Equivocal, cases such as:
 - Similar/slightly decreasing uptake over time.
 - Slight increase in size and/or intensity over time.

Physiologic biodistribution, pitfalls, and positivity criteria:

- WBCs show a transitory migration to the lungs, followed by accumulation in the spleen and less in the liver and bone marrow.
- Lung uptake early post-injection is physiologic, but at 4 and 24 h, it is abnormal.
- Normal bowel activity is seen in 20–30% of children at 1 h due to Tc-HMPAO excretion from the liver.
- Tc-WBCs migrate from spleen and bone marrow to infected tissues. Therefore, in cases with infection there is an increase in uptake over time in sites of disease while bone marrow and spleen activity decrease.
- The rate of Tc-WBC accumulation in infection depends on:
 - Location: earlier in cardio-vascular vs. bone and CNS infection.
 - Virulence: higher in active vs. chronic processes.
 - Pathogen: lower in fungal vs. bacterial infection.
 - Antibiotic or steroid therapy may decrease Tc-WBC uptake.

Study Protocol for [18F] -FDG [2, 6, 15, 16]

Patient preparation:

- Fast: 4 h before tracer injection and during the uptake phase is recommended in adults and adolescents. This duration should be shortened according to age in young children, toddlers, and infants.
- Good hydration with plain, unflavored water.
- Serum glucose level must be measured before radiotracer administration and should be below 200 mg/dL (11.1 mmol/L), preferably below 140 mg/dL (7.8 mmol/L) [17].

Radiopharmaceutical, activity, mode of delivery

Radiopharmaceuticals:

- [¹⁸F]-FDG (FDG)

Activity

- 3.7–5.2 MBq/kg (0.1–0.14 mCi/kg) minimum 26 MBq (0.7 mCi).

Acquisition protocol

- Uptake time: 45–60 min.
- Scanning field: related to clinical indication should be either vertex-to-feet or limited FOV to area of clinical complaints.
- Acquisition protocol: 2–4 min/bed position - these parameters will potentially change with the implementation of new PET technology (see also Chap. 10).

11.5 Study Interpretation of FDG

- Positivity criteria: focal or non-focal abnormal tracer uptake.
- False negatives: Lesion located adjacent to and masked by physiologic tracer activity.

11.6 Correlative Imaging [18]

- Plain radiographs are readily available and are associated with a low radiation burden. They are used in children with suspected pulmonary and MSK infections. In patients with a skeletal pathology, this test is used mainly for excluding fractures and bone tumors in the differential diagnosis of suspected osteomyelitis.
- US is primarily used to investigate soft tissue infections and inflammatory processes.
- CT is readily available at present. Radiation exposure can be reduced by employing specialized pediatric protocols. As a component of SPECT/CT and PET/CT, it can increase the

specificity and accuracy of nuclear medicine tests.

- MRI advantages stem from its lack of ionizing radiation. It also has higher soft tissue contrast than CT.

11.7 Red Flags [2]*Tc-MDP*

- Cannot distinguish between infectious and non-infectious arthritis.
- Cannot differentiate between infection and malignancies, such as osteosarcoma.
- Cannot detect extension of spinal infection from the disc to the adjacent soft tissues. These findings are best evaluated with MRI.
- In cases of discitis, there may be a lag of one week between the onset of symptoms and the first appearance on the bone scan.
- A negative bone scan in the presence of persistent fever does not exclude the diagnosis of arthritis and may reflect pyomyositis and needs to be further assessed.

WBC

- Children with severe neutropenia may lack sufficient leukocytes for adequate WBC labelling.
- The large quantity of blood needed for the procedure is limiting its use in neonates and young children.
- The study has lower performance indices in chronic infections and acute spinal infections.
- Visualization of liver and bowel on later images can produce false positive images in patients with suspected IBD.

FDG

- Radiotracer uptake is not specific to infection.
- Cannot differentiate between infection and (sterile) inflammation.
- Cannot differentiate between infection and malignancy.

Matching of Radiotracers Used for Specific Pediatric Infectious and Inflammatory Processes

- MSK infections
 - Osteomyelitis: Tc-MDP, WBC, FDG
 - Discitis: Tc-MDP, FDG
 - Arthritis: Tc-MDP, FDG
- FUO (including febrile neutropenia): FDG (Figs. 11.6, 11.7, 11.8 and 11.9)
- IBD: FDG, WBC
- Fungal infections: FDG
- Inflammatory processes
 - Vasculitis: FDG (Fig. 11.10)
 - Chronic granulomatous diseases: FDG

11.8 Take Home Messages

- Knowledge regarding the pre-test probability of infection is essential:
 - In low pre-test probability of infection and suspected chronic or non-bacterial processes, FDG imaging is preferred.
 - In case of high WBC counts, ESR or CRP values: Tc-WBC scan can be the first test.
 - WBC accumulation is generally more specific for infection than increased FDG uptake.
 - *For WBC studies:*
 - Images from different time points have to be displayed at the same intensity scale (Figs. 11.4 and 11.5).
 - Any adjustment of the image intensity scale must be applied to all images together to avoid operator bias.
 - Patients receiving antibiotic treatment should not be excluded from performing Tc-WBC scans.
 - *For FDG imaging:*
 - Hyperglycemia and antibiotic treatment most probably do not affect significantly the diagnostic potential of the study in suspected infection [19, 20].
 - A specific dietary regimen has to be applied in patients evaluated for the suspicion or monitoring of a cardiac infectious process.
- MSK infection* [21]:
- Three-phase bone scintigraphy, highly sensitive for diagnosing osteomyelitis in uncomplicated bones is suboptimal in patients with pre-existing fracture or orthopedic hardware. Bone scintigraphy in non-oncological indications is further discussed in detail in Chap. 10.
 - Hybrid imaging is associated with a significant improvement in specificity (Figs. 11.3 and 11.6). The SPECT/PET component detects the presence of an active process while on the CT component characteristic findings include areas of cortical destruction and adjacent soft tissue abscess or empyema.
 - Labelled WBC has been reported in only limited studies/cases of MSK infection in children. If at all, in cases of MSK pathologies this test usually follows bone scintigraphy.
 - FDG imaging shows high-performance indices even in challenging settings such as [22]:
 - Chronic and/or low-grade MSK infection (Fig 11.6).
 - In the axial skeleton, including cases with suspected spinal fusion hardware infection (superior to WBC).
 - FDG imaging can also detects extrasosseous lesions.
- FUO* [6, 16, 23, 24]
- In children with FUO, the performance indices are similar to those reported in adults.
 - Has a higher positive yield in children with fever early during the disease (less than 3 months), and in those with abnormal laboratory investigations (leukocytosis, neutrophilia, high CRP, ESR) (Figs. 11.6, 11.7, 11.8, and 11.9).
 - Can identify organs or tissues likely to contain the source of fever, thus guiding further tests including tissue sampling procedures.
 - Has a high NPV and it is thus unlikely to find a focal etiology of FUO in cases with a negative study.

11.9 Representative Case Examples

Case 11.1 Osteomyelitis, Tc-MDP (Fig. 11.1)

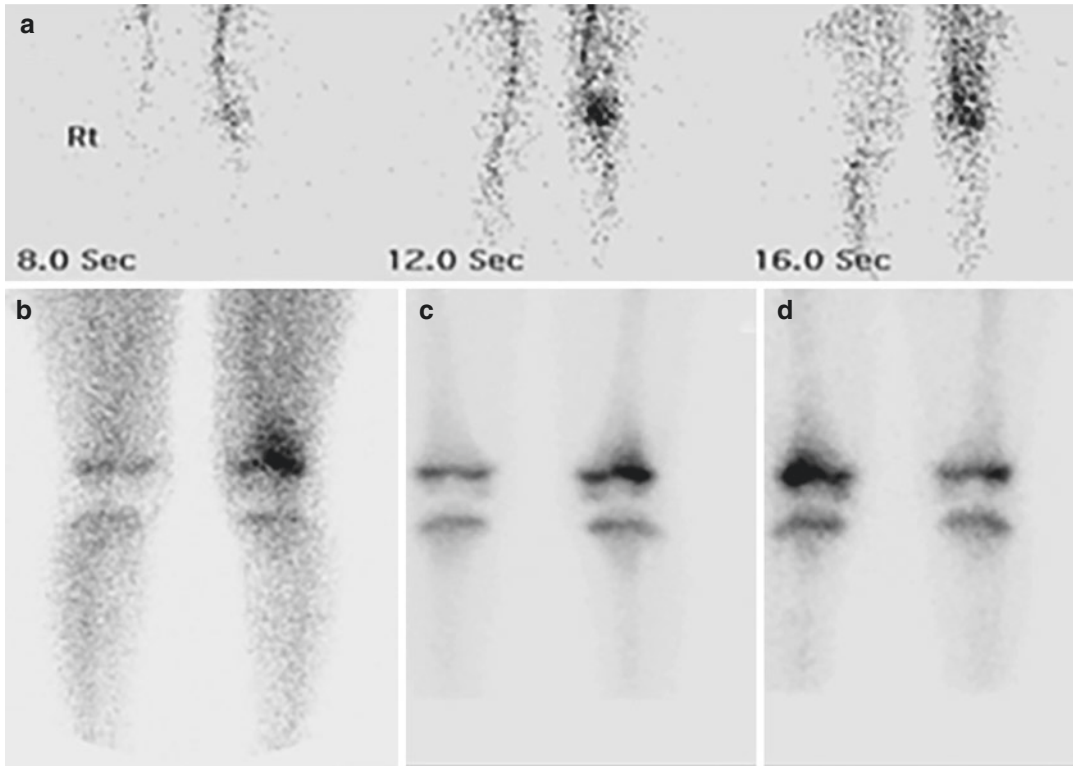


Fig. 11.1 History: A 6-year-old boy presented with a painful left knee. Radiographs were normal, and blood CRP and ESR were elevated. A whole-body bone scan was performed after injection of Tc-MDP. Study report: The dynamic (a) and blood pool (b) images show increased perfusion and hyperemia to the upper part of the left knee. Delayed planar scintigraphy of the region of the

knees (anterior view, c, and posterior view, d) shows focal increased tracer uptake in the left distal femoral metaphysis. The remainder of the whole-body scan was normal (not shown). Impression: The findings are suggestive of acute osteomyelitis. Blood cultures grew *Staphylococcus aureus*

Case 11.2 Osteomyelitis, Tc-MDP (Fig. 11.2)

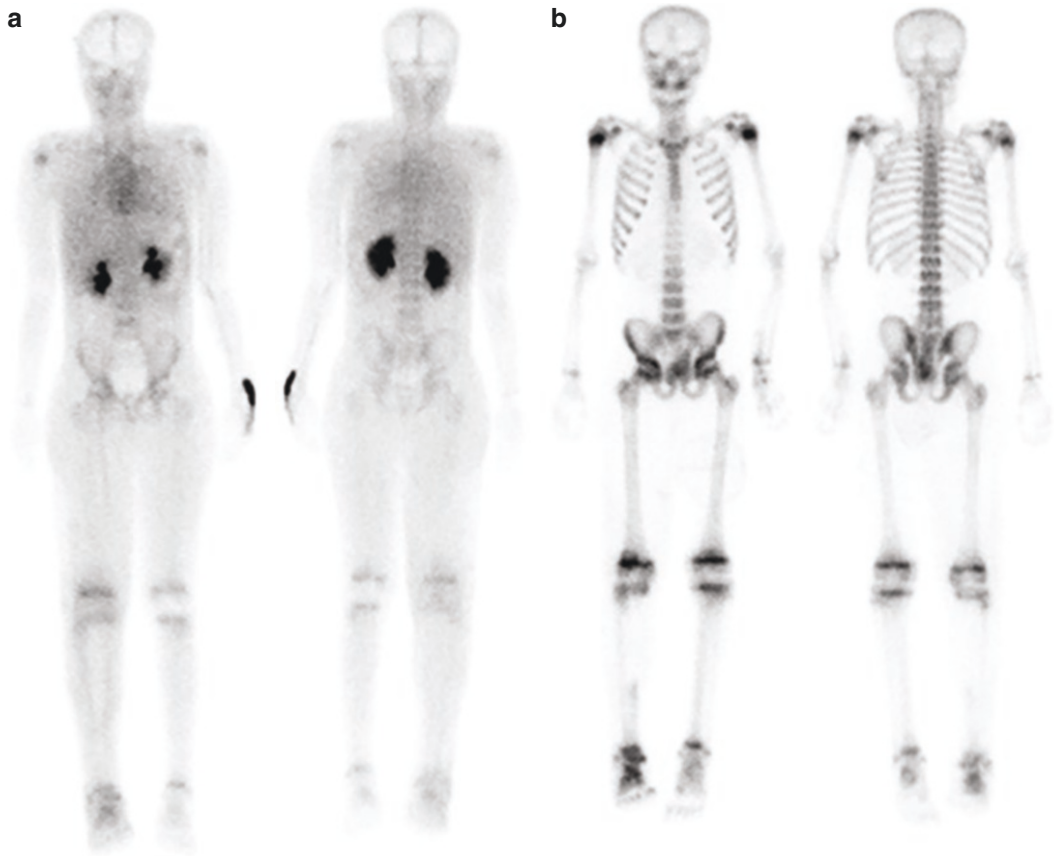


Fig. 11.2 History: A 10-year-old boy had surgery for septic arthritis of the right knee and ankle, with no significant clinical improvement. Bone scintigraphy was performed after injection of Tc-MDP for the suspicion of additional sites of infection. Study report: Early whole-body blood pool scintigraphy, anterior view (**a**, right) shows a rim of increased hyperemia surrounding an area of decreased activity in the right tibia. Increased blood pool activity is also seen in the region of the right knee

and foot. Delayed whole-body scintigraphy (**b**) shows a “cold” area of absent radiotracer uptake in the proximal two-thirds of the right tibia and decreased activity in the proximal tibial growth plate. There is also increased tracer uptake in the right knee joint and foot. Impression: The findings of a “cold bone” in this setting suggest a bony abscess or bone necrosis. The child had surgery and a large volume of pus was drained from the tibia, confirming the diagnosis of osteomyelitis

Case 11.3 Osteomyelitis in Complicated Bone, Tc-MDP (Fig. 11.3)

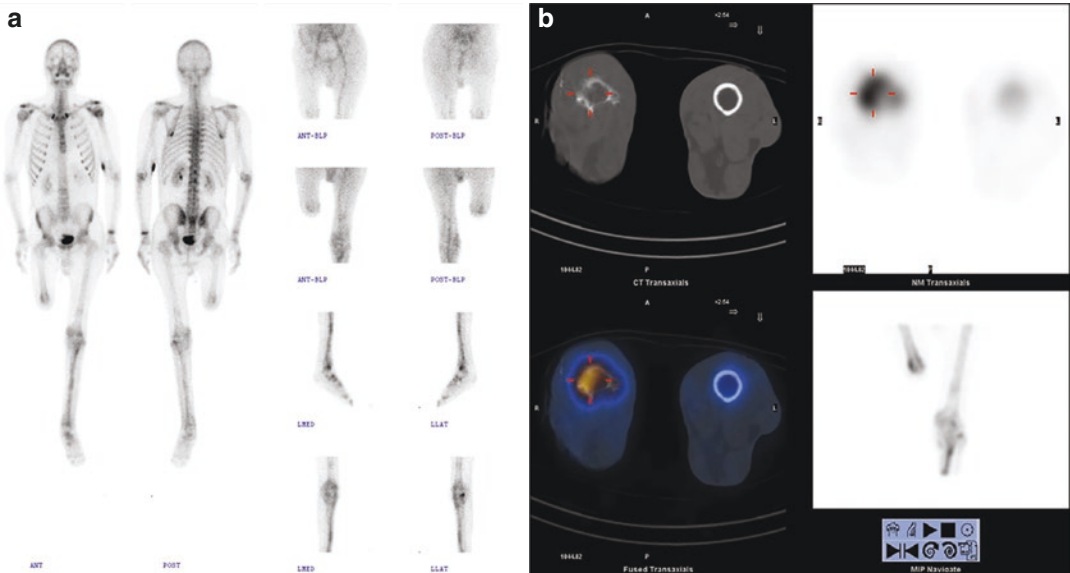


Fig. 11.3 History: An 18-year-old boy with post-traumatic right femoral amputation 18 months prior to this examination presented with a draining fistula from the right femoral stump. Osteomyelitis was suspected and a bone scan was performed after administration of Tc-MDP. Study report: Blood pool images (a, upper right quadrant) demonstrate hyperemia at the margin of the right femoral stump. On delayed planar bone scintigraphy

(a left) there is focal increased tracer activity in the right femoral stump. There is also diffuse increased uptake along the bones of the left calf and foot due to limping. SPECT/CT (b) indicates that the area of focal radiotracer uptake in the right femoral stump corresponds to signs of chronic osteomyelitis on the CT component. Impression: The findings suggest chronic osteomyelitis at the right femoral stump

Case 11.4 Infected Hematoma of the Skull, Tc-WBC (Fig. 11.4)

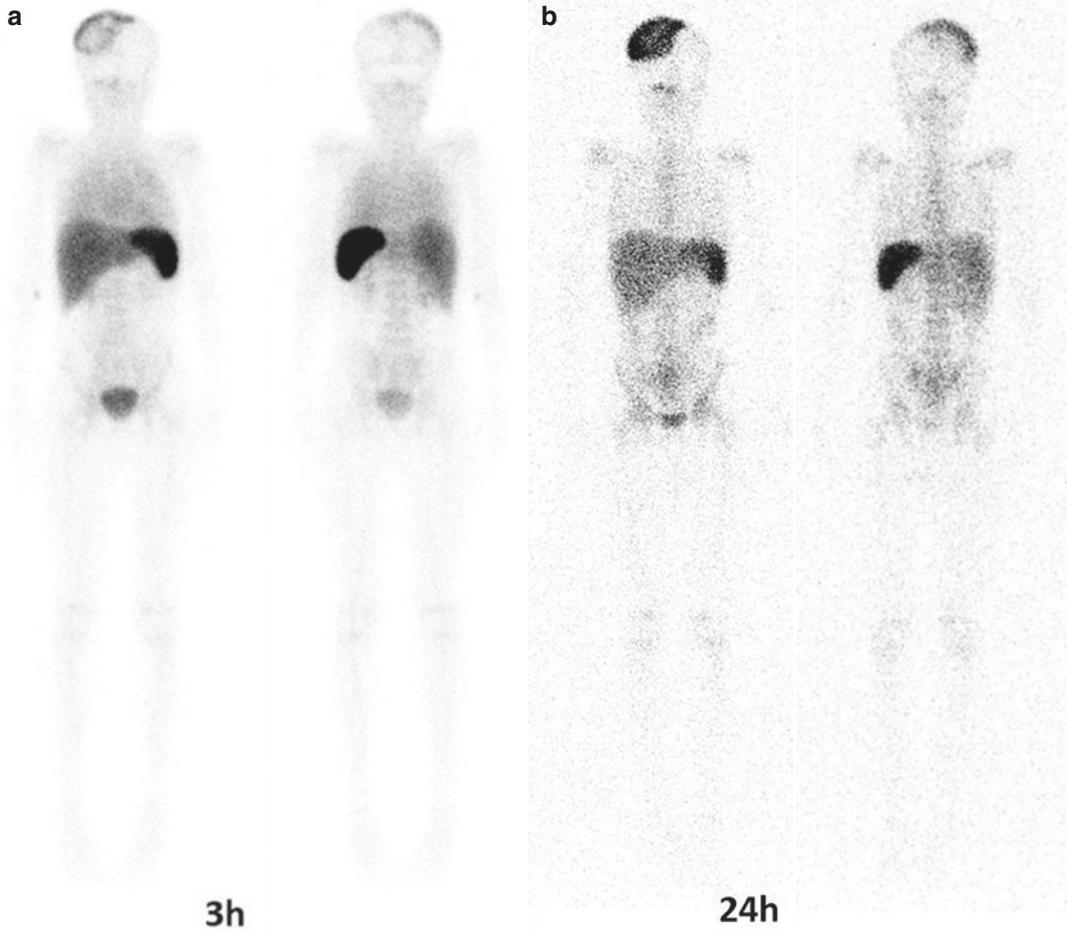


Fig. 11.4 History: A 9-year-old girl presented one day after falling and hitting the right side of her head. She subsequently developed a hematoma and periorbital swelling. She had a 1-year background history of weight loss and proptosis compatible with thyrotoxicosis and developed a thyroid storm after the initial contrast brain CT. Due to ongoing temperature spikes, a blood culture was performed and was positive for *Streptococcus constellatus*, a bacteria known to cause abscess formation. The patient

did not respond to appropriate treatment and a Tc-WBC was requested. Study report: On the 3-h whole-body scan (a) there is an abnormal accumulation of Tc-WBC in the right-sided skull hematoma, increasing in intensity on the 24-h study (b). Impression: The findings are suggestive of an infected hematoma on the right side of the skull. The patient was taken to surgery immediately after the scan and approximately 300 mL of pus was drained from the scalp lesion

Case 11.5 Inflammatory Bowel Disease, Tc-WBC (Fig. 11.5)

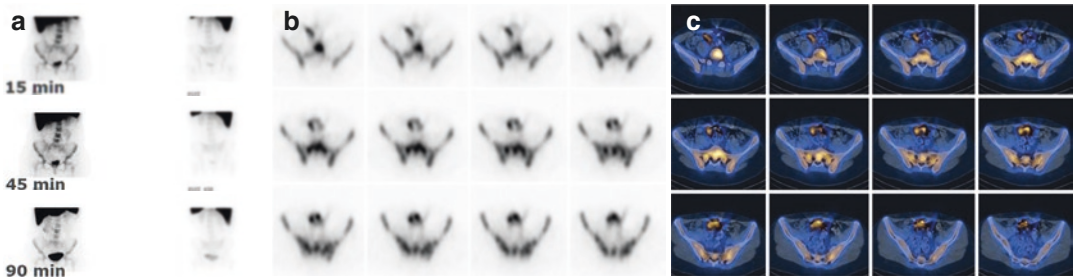


Fig. 11.5 History: An 18-year-old girl presenting with recurrent abdominal pain, fecal blood, and watery stool was evaluated with a Tc-WBC study for the clinical suspicion of inflammatory bowel disease. Study report: Planar scans at 15 and 45 min after tracer injection (**a**) show an area of abnormal tracer uptake in the right abdomen. Transaxial SPECT (**b**) and SPECT/CT (**c**) slices at the

level of the lower abdomen localize this focus of uptake to the terminal ileum. A delayed planar scan (**a**, bottom row) performed at 90 min post-injection shows the progression of the tracer activity into the ascending colon. Impression: The findings suggest terminal ileitis, further confirmed at endoscopy

Case 11.6 Chronic Recurrent Multifocal Osteomyelitis, FDG (Fig. 11.6)

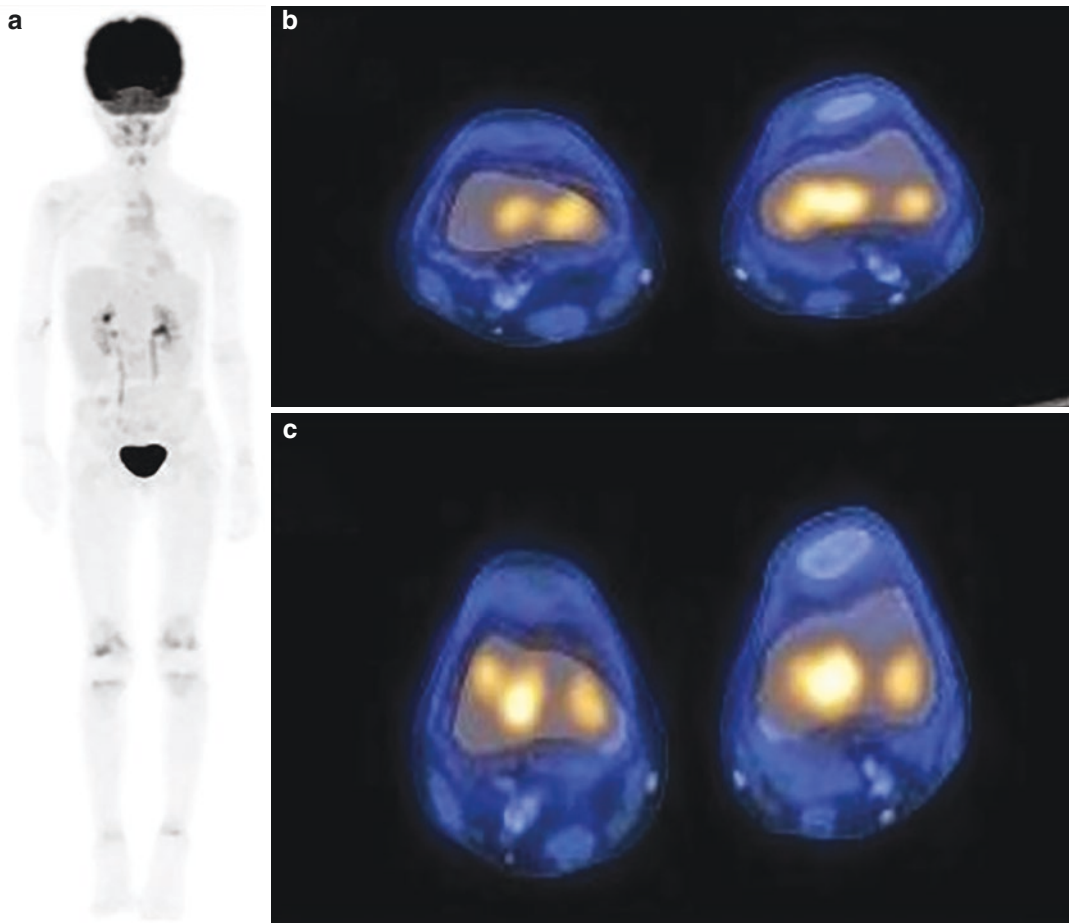


Fig. 11.6 History: A 7-year-old girl presented with joint pain, fever, and abnormal lab tests (elevated ESR, CRP, ASLO). Bone scintigraphy and abdominal US were normal and she was referred to PET/CT with FDG for further evaluation. Study report: Whole body maximum intensity projection (MIP) of the PET component (a) shows focally increased tracer uptake in both knees, involving the femoral and tibial metaphyses, also seen on transaxial PET/CT slices (b, c), as well as in both ankles, with no corresponding CT abnormalities. Impression: The findings suggest multifocal osteomyelitis, but a different etiology involving the bony structures cannot be excluded. Further evalu-

ation with MRI was suggested. MRI of the left knee (not shown) demonstrated bone marrow edema, mild periostitis, and joint effusion. The differential diagnosis included chronic recurrent multifocal osteomyelitis, leukemia infiltration, and eosinophilic granuloma. Tissue sampling was recommended. CT-guided biopsy of the left distal femur demonstrated the presence of marked fibrosis, reactive trabecular changes, and focal neutrophil infiltration, with no evidence of leukemic infiltrates. The patient was diagnosed with chronic recurrent osteomyelitis and subsequently showed a good response to treatment with methotrexate and steroids

Case 11.7 Fever of Unknown Origin (FUO), Aspergillosis, FDG (Fig. 11.7)

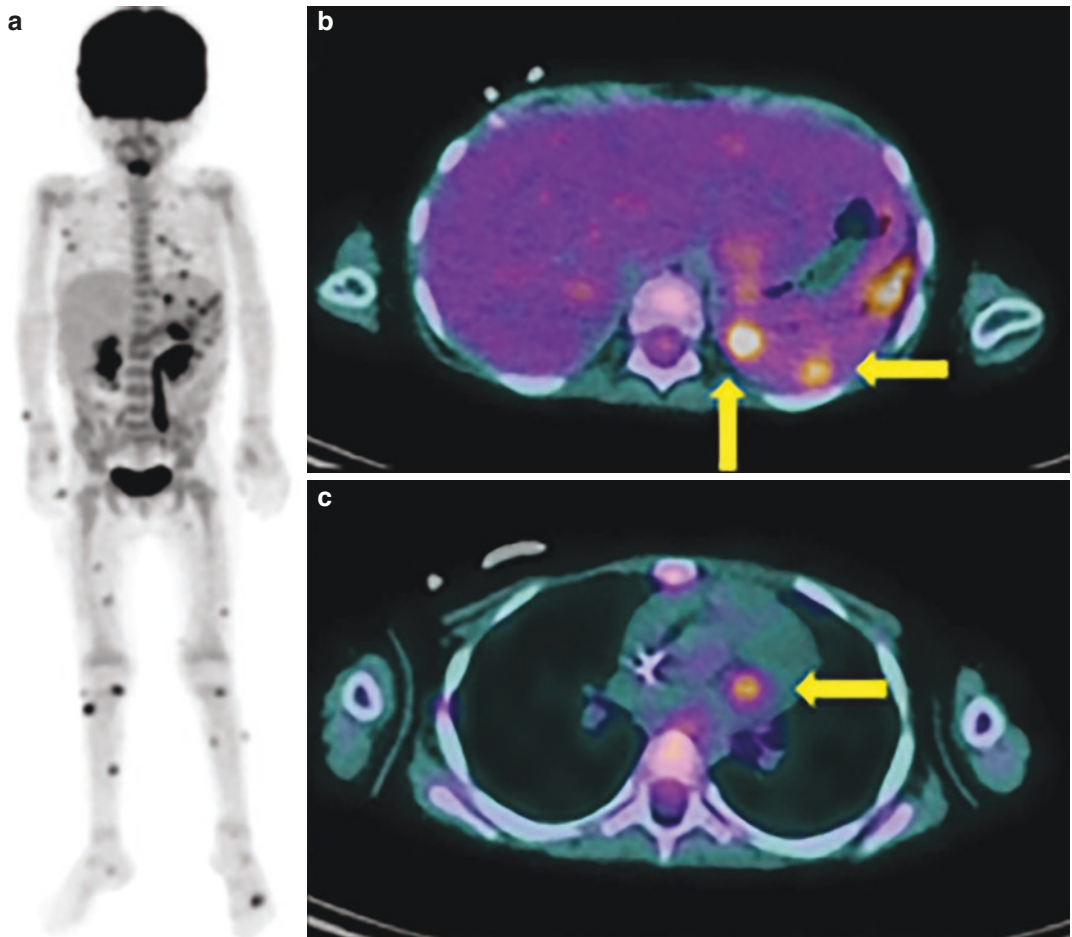


Fig. 11.7 History: A 2-year-old girl with leukemia developed pancreatitis secondary to chemotherapy followed by a persistent fever that did not respond to antibiotics. CT showed mild inflammatory changes in the lungs. A whole-body FDG PET/CT was performed to look for occult infective or inflammatory sites. Study report: FDG PET MIP image (**a**) and selected axial PET/CT slices at the level of the upper abdomen and chest (**b**, **c**) show multiple foci of abnormal tracer uptake throughout the subcutaneous and soft tissues, the lungs, pancreas, and spleen (yel-

low arrows), with a specific focal site of uptake in the heart (**c**, yellow arrow). Impression: The findings are suggestive of possible mycotic deposits. Biopsy and culture of a skin lesion revealed *Aspergillus*. Following a change of treatment to more specific antifungal agents, the patient's clinical status improved. On a repeat PET/CT study performed 2 months later (not shown), there is marked improvement with the disappearance of most tracer avid foci

Case 11.8 FUO, Septic Emboli, FDG (Fig. 11.8)

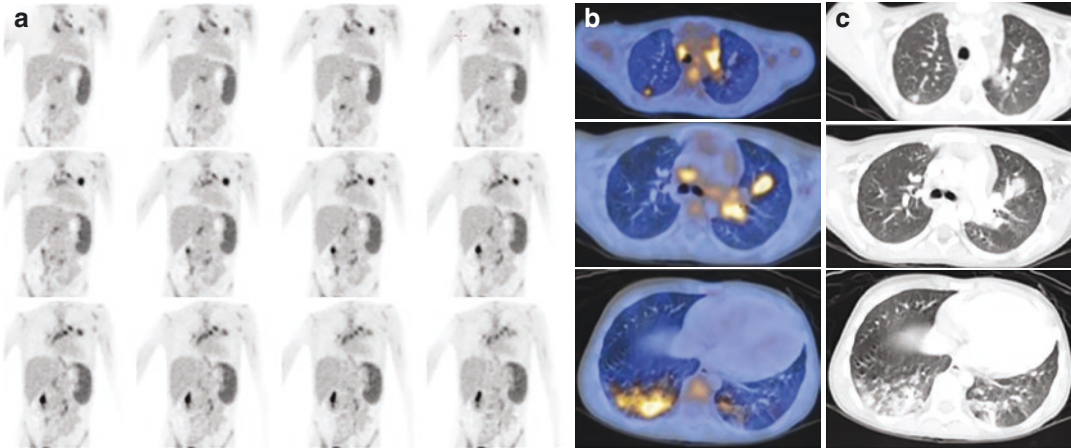


Fig. 11.8 History: A 7-year-old girl presented with fever, 39 °C, for 3 weeks. She had been previously diagnosed and treated for a urinary tract infection. She had positive blood cultures and echocardiography demonstrated the presence of endocarditis. FDG PET/CT was performed for further evaluation of potential extracardiac foci of infection. Study report: Coronal PET slices (a) show foci of increased tracer uptake in both lungs. Selected trans-

axial PET/CT (b) and CT (c) of the chest localize these sites of increased uptake to nodules and ground-glass opacities in both upper lung lobes and in a right lower lobe consolidation. Note also increased FDG uptake in an enlarged spleen. Impression: The findings are consistent with septic pulmonary emboli. Hypermetabolic splenomegaly is considered to be reactive to the infectious process

Case 11.9 FUO, Pericarditis, FDG (Fig. 11.9)

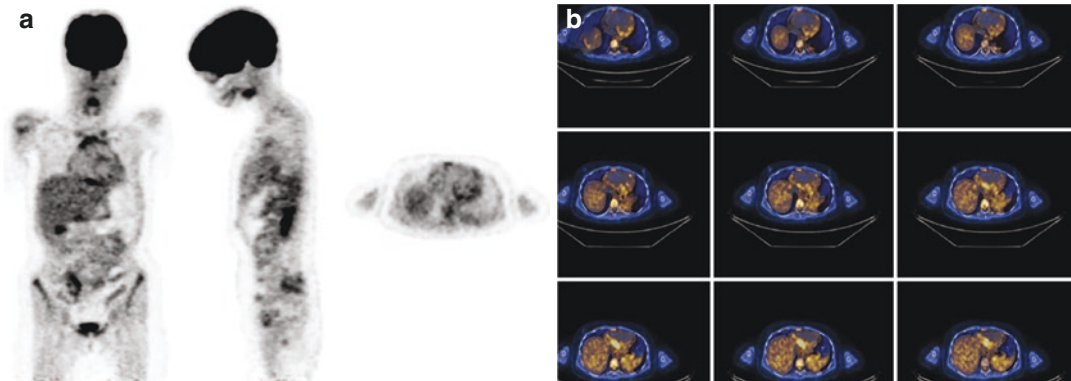


Fig. 11.9 History: An 8-year-old girl previously treated for pneumonia complained of fever (39.4 C) for three weeks. C-reactive protein was elevated. Abdominal US was normal. A whole-body FDG PET/CT was performed in search of a focal etiology that could explain the high, prolonged fever. Study report: Selected coronal, sagittal, and transaxial PET slices (a) show increased linear tracer uptake located in thickened pericardium and mild pericar-

dial effusion surrounding the heart as demonstrated on transaxial PET/CT slices of the thorax (b). In addition, note physiologic tracer uptake in the thymus. Impression: The findings suggest the presence of pericarditis. Cardiac echography showed a new pericardial effusion. The patient was diagnosed with acute pericarditis and idiopathic juvenile arthritis and showed an excellent response to treatment with NSAIDS

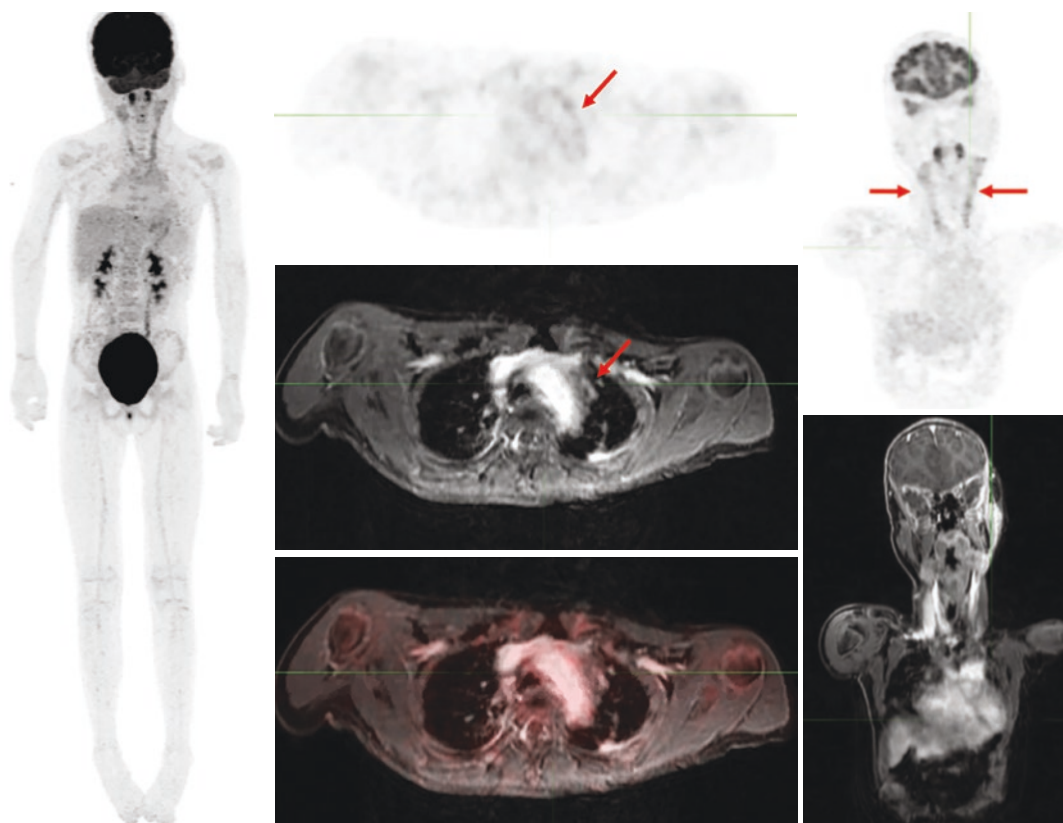
Case 11.10 Vasculitis, FDG—PET/MRI (Fig. 11.10)

Fig. 11.10 History: A 12-year-old girl presented with persistent thoracic level back pain, intermittent fever, and elevated ESR. Cross-sectional imaging showed thickening of her aortic arch and bilateral great vessels. Takayasu's arteritis was diagnosed, and the patient was referred to FDG PET/MRI. Study report: The PET/MRI study (left PET-MIP, center column selected transaxial thoracic PET, MRI, and PET/MRI slices, right selected coronal cervical PET and MRI slices) shows increased FDG uptake in wall thickening of the left common carotid artery, extending from the origin to the bifurcation, and, to a lesser extent, along the caudal aspect of the right common carotid artery near the origin (arrows). In the chest, there is increased uptake in mild wall thickening of the thoracic aorta,

involving the ascending and descending parts and the aortic arch (arrows). There is also mildly increased radiotracer uptake in the walls of the abdominal aorta, extending to the proximal iliac arteries. There is no abnormal metabolic activity or wall thickening involving the abdominal great branching arteries including the celiac axis, and the superior mesenteric and inferior mesenteric arteries. Impression: Multifocal mild wall thickening and increased metabolic activity of the left more than right common carotid arteries, thoracic and abdominal aorta, and proximal common iliac arteries. The increased metabolic activity suggests the presence of active arteritis

References

1. Signore A, et al. Nuclear medicine imaging in pediatric infection or chronic inflammatory diseases. *Semin Nucl Med.* 2017;47(3):286–303.
2. Parisi MT, et al. Radionuclide imaging of infection and inflammation in children: a review. *Semin Nucl Med.* 2018;48(2):148–65.
3. Ropers FG, et al. Evaluation of FDG-PET/CT use in children with suspected infection or inflammation. *Diagnostics (Basel).* 2020;10(9):715.
4. Sturm E, et al. Fluorodeoxyglucose positron emission tomography contributes to management of pediatric liver transplantation candidates with fever of unknown origin. *Liver Transpl.* 2006;12(11):1698–704.
5. Wang SS, et al. The clinical utility of fluorodeoxyglucose-positron emission tomography

- for investigation of fever in immunocompromised children. *J Paediatr Child Health*. 2018;54(5):487–92.
6. Pijl JP, et al. Role of FDG-PET/CT in children with fever of unknown origin. *Eur J Nucl Med Mol Imaging*. 2020;47(6):1596–604.
 7. Chang L, et al. Search of unknown fever focus using PET in critically ill children with complicated underlying diseases. *Pediatr Crit Care Med*. 2016;17(2):e58–65.
 8. Signore A, et al. Clinical indications, image acquisition and data interpretation for white blood cells and anti-granulocyte monoclonal antibody scintigraphy: an EANM procedural guideline. *Eur J Nucl Med Mol Imaging*. 2018;45(10):1816–31.
 9. Charron M. Pediatric inflammatory bowel disease imaged with Tc-99m white blood cells. *Clin Nucl Med*. 2000;25(9):708–15.
 10. Drubach LA. Nuclear medicine techniques in pediatric bone imaging. *Semin Nucl Med*. 2017;47(3):190–203.
 11. Van den Wyngaert T, et al. The EANM practice guidelines for bone scintigraphy. *Eur J Nucl Med Mol Imaging*. 2016;43(9):1723–38.
 12. Palestro CJ. Infection and inflammation. In: Treves ST, editor. *Pediatric nuclear medicine and molecular imaging*. New York: Springer; 2014. p. 541–69.
 13. Aydin F, Kın Cengiz A, Güngör F. Tc-99m labeled HMPAO white blood cell scintigraphy in pediatric patients. *Mol Imaging Radionucl Ther*. 2012;21(1):13–8.
 14. de Vries EF, et al. Guidelines for the labelling of leucocytes with (99m)Tc-HMPAO. Inflammation/Infection Task group of the European Association of Nuclear Medicine. *Eur J Nucl Med Mol Imaging*. 2010;37(4):842–8.
 15. Servaes S. Imaging infection and inflammation in children with (18)F-FDG PET and (18)F-FDG PET/CT. *J Nucl Med Technol*. 2011;39(3):179–82.
 16. Houseni M, et al. Applications of PET/CT in pediatric patients with fever of Unknown Origin. *PET Clin*. 2008;3(4):605–19.
 17. Vali R, et al. SNMMI Procedure Standard/EANM Practice Guideline on Pediatric (18)F-FDG PET/CT for Oncology 1.0. *J Nucl Med*. 2021;62(1):99–110.
 18. Dhar AV, et al. Team Approach: Pediatric Musculoskeletal Infection. *JBJS Rev*. 2020;8(3):e0121.
 19. Rabkin Z, Israel O, Keidar Z. Do hyperglycemia and diabetes affect the incidence of false-negative 18F-FDG PET/CT studies in patients evaluated for infection or inflammation and cancer? A Comparative analysis. *J Nucl Med*. 2010;51(7):1015–20.
 20. Kagna O, et al. Does Antibiotic Treatment Affect the Diagnostic Accuracy of (18)F-FDG PET/CT Studies in Patients with Suspected Infectious Processes? *J Nucl Med*. 2017;58(11):1827–30.
 21. Bagrosky BM, et al. 18F-FDG PET/CT evaluation of children and young adults with suspected spinal fusion hardware infection. *Pediatr Radiol*. 2013;43(8):991–1000.
 22. Warmann SW, et al. Follow-up of acute osteomyelitis in children: the possible role of PET/CT in selected cases. *J Pediatr Surg*. 2011;46(8):1550–6.
 23. Jasper N, et al. Diagnostic value of [(18)F]-FDG PET/CT in children with fever of unknown origin or unexplained signs of inflammation. *Eur J Nucl Med Mol Imaging*. 2010;37(1):136–45.
 24. del Rosal T, et al. ¹⁸F-FDG PET/CT in the diagnosis of occult bacterial infections in children. *Eur J Pediatr*. 2013;172(8):1111–5.

The opinions expressed in this chapter are those of the author(s) and do not necessarily reflect the views of the IAEA: International Atomic Energy Agency, its Board of Directors, or the countries they represent

Open Access This chapter is licensed under the terms of the Creative Commons Attribution 3.0 IGO license (<http://creativecommons.org/licenses/by/3.0/igo/>), which permits use, sharing, adaptation, distribution and reproduction in any medium or format, as long as you give appropriate credit to the IAEA: International Atomic Energy Agency, provide a link to the Creative Commons license and indicate if changes were made.

Any dispute related to the use of the works of the IAEA: International Atomic Energy Agency that cannot be settled amicably shall be submitted to arbitration pursuant to the UNCITRAL rules. The use of the IAEA: International Atomic Energy Agency's name for any purpose other than for attribution, and the use of the IAEA: International Atomic Energy Agency's logo, shall be subject to a separate written license agreement between the IAEA: International Atomic Energy Agency and the user and is not authorized as part of this CC-IGO license. Note that the link provided above includes additional terms and conditions of the license.

The images or other third party material in this chapter are included in the chapter's Creative Commons license, unless indicated otherwise in a credit line to the material. If material is not included in the chapter's Creative Commons license and your intended use is not permitted by statutory regulation or exceeds the permitted use, you will need to obtain permission directly from the copyright holder.



Pediatric Malignancies

12

Helen Nadel, Barry Shulkin, Zvi Bar-Sever,
and Francesco Giammarile

12.1 General Tracer-Related Parameters

Radiopharmaceutical and Administered Activity

The EANM pediatric dosage card and to the North American consensus guidelines on radiopharmaceutical administration in children in the respective EANM and SNMMI and image gently web sites should be followed [1, 2].

Reference to national regulation guidelines, if available, should be considered.

H. Nadel (✉)
Lucile Packard Children's Hospital Stanford
University, Palo Alto, CA, USA

B. Shulkin
Department of Diagnostic Imaging, St. Jude
Children's Research Hospital, Memphis, TN, USA

Z. Bar-Sever
Schneider Children's Medical Center of Israel, Tel
Aviv University, Petah Tiqva, Israel

F. Giammarile
Nuclear Medicine and Diagnostic Imaging Section,
Division of Human Health, Department of Nuclear
Sciences and Applications, International Atomic
Energy Agency, Vienna, Austria

Box 12.1 FDG Imaging Protocol [3–6]

Patient Preparation

- Fast: 4 h before tracer injection and during the uptake.
- Good hydration with plain, unflavored water is allowed and encouraged.
- Measure and record patient's height and weight on the day of the exam.
- Avoid strenuous exercise 24 h prior to scan.
- Discontinue glucose-containing IV fluids and parenteral nutrition from midnight before test or minimum of 6 h.
- Blood glucose level must be measured before radiotracer administration and should be below 200 mg/dL (11.1 mmol/L), preferably below 120 mg/dL (6.66 mmol/L).
- Date of last dose of potentially interfering medications that may cause false positive and false negative altered bio-distribution should be recorded in technologist/ study notes (see below in study interpretation).
- Brown fat reduction techniques include:
 - Early arrival (30–45 min prior to planned radiotracer injection time) to settle patient, establish IV line, and warm the patient in a temperature-controlled room with the addition of warm regular or electric blankets.

- Avoid cold and air-conditioned spaces in transportation prior to study.
- Premedication such as benzodiazepines and beta-adrenergic blockers (oral propranolol, IV fentanyl, oral diazepam in moderate dose) may be carefully used as a second option in consultation with referring physicians and pediatric anesthetists.

Radioisotope:

- [¹⁸F]-Fluorodeoxyglucose (FDG)

Activity:

- 3.7–5.2 MBq/kg (0.10–0.14 mCi/kg), minimum dose 26 MBq (0.7 mCi).

Refer to the EANM pediatric dosage card and to the North American consensus guidelines on radiopharmaceutical administration in children in the respective EANM and SNMMI and image gently web sites.

Reference to national regulation guidelines, if available, should be considered.

- FDG activity can be reduced when using modern PET technology, to 0.06–0.08 mCi/kg 2.46–2.96 MBq/kg [7].

Acquisition Protocol

- Uptake time: 60 min (±10%) between injection and scanning.
- Patients should not talk, text, play video games, chew gum, or suck candies during the uptake phase.
- Diapers should be changed in infants before the scan.
- Acquisition parameters: 2–4 min/bed position (depending on equipment).

Study Interpretation for FDG Imaging [8–10]

- Standardized elements to include in the PET/CT report can be found at the SNMMI website

http://interactive.snm.org/docs/PET_PROS/ElementsofPETCTReporting.pdf

- Abnormally increased FDG uptake should be described with respect to:
 - Intensity: mild, moderate, or severe, or compared to the blood pool and liver activity.
 - Pattern: focal, diffuse, linear.
 - Localization: based on CT or MRI.
- Physiological tracer distribution, including specific patterns in children: brain, salivary glands, lymphatic tissue of the Waldeyer's ring, muscles, brown fat, myocardium, mediastinum, thymus, liver, kidneys and bladder, gastrointestinal tract, testis, uterus, and ovaries.
- False positives, including specific patterns in children:
 - Infant mouth with feeding or sucking during the uptake phase.
 - Thymus: uptake decreases with age but may increase after chemotherapy, thymic rebound.
 - Brown fat: usually bilateral in the neck, supraclavicular regions, axillae, mediastinum, paravertebral regions, and perinephric areas. Infradiaphragmatic activity considered to be brown fat is seen, as a rule, in conjunction with supradiaphragmatic brown fat.
 - Diffuse uptake in bone marrow following hematopoietic stimulating drugs such as G-CSF.
 - Increased uptake in infectious and inflammatory processes, and in other benign entities.
 - Uptake in post-surgical scars.
 - Uptake in growth plate.
- False negatives:
 - Hyperinsulinemia and hyperglycemia.
 - Small lesions, with limited tracer avidity.
 - Low metabolic tumors are rare in children but may occur with differentiated thyroid cancer and well-differentiated NETs.
 - Tumor necrosis.
 - Recent radiation or chemotherapy.
 - Recent treatments such as high-dose corticosteroid therapy and anti-retroviral medication.

Box 12.2 Radioiodinated Meta-iodobenzylguanidine (MIBG) Imaging Protocol [11, 12]

Patient Preparation

- Administer thyroid-blocking medication.
- LUGOL solution:
 - Starting 2 days prior to and continued for 3 days after injection.
 - Dose: 0.6 mL of 5 % solution/day, single dose or split into 2 × 0.3 mL doses.
 - Delivery: diluted in any drink such as milk or juice as may cause a burn in the throat if undiluted.
- Supersaturated potassium iodide (SSKI):
 - Starting 30–60 min prior to tracer administration, on day 0 and continued for a week.
 - Dose: <1 month—one drop orally/day; 1 month—3 years: 2 drops orally/twice a day; 3–18 years of age: 3 drops orally/three times a day; ≥70 kg—adult: 6 drops orally (2 drops/3 times a day).
- Potassium iodate (in individuals sensitive to iodine and if no other thyroid blockade is available).
 - Starting 1 h prior to tracer injection, up to 5 times within the next 36 h.
 - Dose: 10 mg/kg, maximum 500 mg, minimum 50 mg.
 - Delivery: 200 mg tablet can be crushed, dissolved in 2 mL of sterile water, and administered by syringe or placed on a sugar lump.

Radiopharmaceuticals

- [¹²³I]-MIBG—the current standard SPECT tracer.
- [¹³¹I]-MIBG—should only be used if ¹²³I-MIBG or an alternative PET tracer is not available.

Activity

- ¹²³I-MIBG: North American consensus guidelines recommend a dose of 5.2 MBq/kg (0.14 mCi/kg), minimum dose of 37 MBq (1 mCi), and maximum dose of 370 MBq (10 mCi). The EANM pediatric dosage card recommends a slightly higher activity, minimum dose of 37 MBq (1 mCi), and maximum dose of 400 MBq (10.8 mCi).
- ¹³¹I-MIBG: minimum injected dose of 35 MBq (0.95 mCi) and maximum dose of 78 MBq (2.11 mCi).

Acquisition Protocols

¹²³I-MIBG:

- Time of scan: 24 h post-injection. Rare images at 48 h are added to clarify sites with low-grade uptake.
- Collimator: medium energy is preferred, reduces scatter and septal penetration of high-energy photons; low energy can be also used.
- Planar scans:
 - In older children: whole-body anterior and posterior projections, 5 cm/min, minimum 30 min, matrix 1024 × 512 or 1024 × 256.
 - In young children: multiple spot views of the entire body are preferred, matrix 256 × 256, trunk: 10 min/500 Kcounts. Limbs and skull 100 Kcounts, skull (anterior, posterior, left and right lateral views).
 - SPECT: 120 projections, 25–35 s/step, matrix 128 × 128, iterative reconstruction.
- SPECT/CT, when available, is recommended.

¹³¹I-MIBG:

- Time of scan: 48 h post-injection, possible supplements at 72 h.

- Collimator: high energy or medium energy.
- Planar scans: whole body, anterior and posterior images, scan speed 4 cm/min, or multiple spot views of the entire body (150 Kcounts/view).
- SPECT and SPECT/CT as indicated.

Study Interpretation for MIBG Imaging [11, 13, 14]

- Physiological biodistribution: myocardium, salivary and lacrimal glands, liver, lungs (blood pool on early images), bowel, renal collecting system, uterus (during menstrual period).
 - Adrenal glands: symmetric, mild (\leq to the liver), normal size on CT.
 - Brown fat.
 - Thyroid (uptake of free iodine in case of poor blockade).
- False positives:
 - Lung atelectasis, pneumonia.
 - Heterogeneous liver uptake (including focal uptake in the left lobe).
 - Kidneys and/or dilated ureters.
 - Rare-vascular malformations, accessory spleen, ectopic kidneys, foregut duplication, hemorrhagic cysts, ovarian torsion, and hernia.
- False negatives:
 - MIBG-negative neuroblastoma (10% of cases)
 - MIBG-negative metastases
 - Small lesions, below the camera resolution

Box 12.3 [¹⁸F] Fluoro-Dihydroxyphenylalanine (FDOPA) Imaging Protocol [11, 15]

Patient Preparation

- Fast: 4 h
- Adequate hydration

- Drug withdrawal (48 h prior to tracer administration): aromatic L-amino acid decarboxylase (AADC), catechol-o-methyl transferase (COMT), and monoamine oxidase (MAO) inhibitors.
- Premedication with carbidopa: if used in children a dose of 2 mg/Kg is administered 1 h before FDOPA injection.

Activity

- 3 MBq/Kg (0.08 mCi/Kg), minimum dose is 26 MBq (0.7 mCi).

Acquisition Protocol

- Uptake time: 60–90 min.
- Acquisition parameters: 3 min/bed position.

Study Interpretation for FDOPA Imaging [16, 17]

- Physiologic biodistribution:
 - High: basal ganglia, liver, adrenals, pancreas (variable).
 - Moderate: myocardium, skeletal muscles, growth plate.
 - Faint: breasts, oral cavity, esophagus, bowel.
 - Excretion: biliary (gallbladder and biliary tract) and urinary (kidneys, ureters, urinary bladder).
- False positives:
 - Physiologically intense, variable uptake in uncinate process of pancreas.
 - Stasis in small intrahepatic bile ducts and/or in the urinary system.
 - Growth plate fractures.
- False negative:
 - Lesions adjacent to sites with high physiologic uptake.
 - Small lesions.
 - Lesions with low tracer avidity.

Box 12.4 [⁶⁸Ga]-Peptides Imaging Protocol [15]

Patient Preparation

- No fasting requiring.
- Drug withdrawal: therapy with short-/long-acting somatostatin analogues (rare in children)—to avoid possible somatostatin receptor (SSTR) blockade.
- Short-acting: 1–2 days discontinuation.
- Long-acting: 4–6 weeks discontinuation.

Radiopharmaceuticals

- ⁶⁸Ga-DOTA-TATE, -TOC, -NOC.

Activity

- 2 MBq/kg (0.054 mCi/kg), minimum dose is 14 MBq (0.3 mCi).

Acquisition Protocol

- Uptake time: 60 min (range 45–90 min)
- Field-of-view (FOV): true vertex-to-toe
- Acquisition parameters: 2–4 min/bed position

Study Interpretation for ⁶⁸Ga-Peptide Imaging [18, 19]

- Physiologic biodistribution:
 - High uptake: pancreas (uncinate process), spleen, kidneys, pituitary gland.
 - Moderate uptake: liver, salivary glands, thyroid, bowel.
 - Faint uptake: adrenals, prostate, breast.
- False positives:
 - Physiologic uptake in uncinate process, accessory spleens, splenosis, epiphyseal growth plates.
 - Meningiomas.
 - Skeletal lesions such as fractures, vertebral hemangioma, fibrous dysplasia.
 - Inflammatory processes such as reactive

lymph nodes, post-radiation therapy changes.

- Urine contamination.
- False negatives:
 - Small lesions.
 - Lesions adjacent to sites with high physiologic uptake.
 - Tumors with low or variable SSTR expression.
 - Lesion dedifferentiation.

Box 12.5 Bone Imaging Protocols [20–24]

Patient Preparation

- No need to fast.
- No need for medication withdrawal.
- Good hydration.
- Frequent bladder emptying between injection and delayed imaging, and immediately before scanning.
- Change diapers immediately before scanning.

Radiopharmaceuticals

- [^{99m}Tc]Tc-methylene diphosphonate (MDP) or similar diphosphates.
- [¹⁸F]sodium fluoride (NaF)

Activity

- MDP: 9.3 MBq/kg (0.25 mCi/Kg), minimum dose 37 MBq (1.0 mCi).
- NaF 2.22 MBq/kg (0.06 mCi/kg), minimum dose 14 MBq (0.4 mCi).

Refer to the EANM pediatric dosage card and to the North American consensus guidelines on radiopharmaceutical administration in children in the respective EANM and SNMMI and image gently web sites.

Reference to national regulation guidelines, if available, should be considered.

Acquisition Protocols

Bone scintigraphy

- Position: supine, comfortably secured to the bed.
- Collimators: high- or ultrahigh low energy, parallel hole collimator.
- Time of scanning: at 2–4 h post-injection.
- Acquisition parameters:
- Whole body sweeps with bed speed adjusted to the child's age.
 - 8 cm/min for ages 4–8 years.
 - 10 cm/min for ages 8–12 years.
 - 12 cm/min for ages 12–16 years.
 - 15 cm/min over 16 years of age.
- Alternative: multiple spot views over entire skeleton, anterior and posterior projections, matrix 256 × 256, counts: torso 500 Kcounts, skull 300 Kcounts, knees 100–200 Kcounts, hands and feet 50–100 Kcounts.
- SPECT 120 projections, 15–30 s/view, matrix 128 × 128 should be included:
 - To areas of localized symptoms.
 - If an abnormality is detected on planar imaging.
- SPECT/CT, if available should replace SPECT [25].
 - For the CT component of SPECT/CT—tube setting will depend on whether the CT is intended to be low dose or fully diagnostic.
- Delayed 24-h scan can be performed:
 - In cases of uncertain findings on routine 3-h scintigraphy.
 - When residual bladder activity overlies the pelvis and the child refuses to urinate or when bladder emptying is incomplete.

Bone NaF PET/CT:

- Time of imaging: at 30–45 min after tracer injection.
- Position: supine; arms by the sides for whole-body imaging, elevated when only the axial skeleton is scanned.
- Acquisition parameters: 2–5 min /bed position, varies depending on injected amount, BMI, and camera.

Study Interpretation for Bone Imaging

- Physiologic tracer biodistribution:
 - Homogeneous throughout the entire skeleton.
 - Visualization of kidneys, ureters, bladder.
 - Increased uptake in metaphyses of children and adolescents.
- Abnormally increased skeletal uptake should be described with respect to:
 - Intensity higher or lower than in adjacent or in corresponding contralateral bone.
 - Pattern: focal or diffuse.
 - Location and number of foci.
 - Patterns of ST uptake:
 - Diffuse decreased: due to increased heterogeneous uptake in bone.
 - Diffuse increased: renal failure, short uptake time, of significant tracer extravasation at the injection site.
 - Focal increased: infection/inflammation, trauma, (calcified) ST metastasis.
- Pitfalls
 - Urinary contamination or diversion reservoirs
 - Injection artifacts
 - Patient motion
 - Faulty energy window for image acquisition

12.2 Lymphoma and Sarcoma

Clinical Indications—Imaging with FDG (see also Box 12.1) [22, 26–29]

- Staging/restaging
- Metastatic workup in sarcoma
- Response assessment
- End of therapy baseline
- Biopsy site planning
- Confirmation of equivocal or discrepant findings on other imaging studies

Specific Study Interpretation Criteria

Lymphoma [30]

- The (Deauville) five-point scale can be used in the assessment of treatment response in HL and NHL.
 - Score 1: No uptake above the background.
 - Score 2: Uptake \leq mediastinum.
 - Score 3: Uptake $>$ mediastinum but \leq liver.
 - Score 4: Uptake moderately increased compared to the liver at any site.
 - Score 5: Uptake markedly increased compared to the liver at any site.
 - Score X: New areas of uptake unlikely to be related to lymphoma.

Sarcoma [31–33]

- Reduction in standard uptake values (SUV) max from baseline of greater than 50% has been associated with overall improved progression-free survival.

Correlative Imaging [34]

- Chest radiograph may be the first examination in a child presenting with chest/ mediastinal symptoms and can identify mediastinal mass and possible tracheal compression.
- US of the abdomen and pelvis may identify lymphadenopathy but is not adequate for staging purposes. Cross-sectional imaging with contrast-enhanced CT and or MRI will be the next cross-sectional imaging study.
- PET/CT and/or PET/MRI may be performed as next cross-sectional imaging in some institutions without intermediate stand-alone CT or MRI study.
- In suspected sarcoma radiographs will be the first study in a child presenting with focal pain. Cross-sectional imaging with contrast-enhanced CT and dedicated high-resolution MRI will follow.

Red Flags

- Good hydration prior to tracer administration will accelerate and increase excretion of the excess radiotracer.
- If blood glucose levels are above 200 mg/dL (11.1 mmol/L), the study should be rescheduled, if possible. In diabetic patients, consultation with treating endocrinologist can be helpful in case of complex diabetic or insulin requirements.
- Check the quality of images and of factors that may influence the SUV before reporting.
- Study scheduling: in patients after treatment the study should be ideally scheduled at least 14 days after the last course of chemotherapy, and 2 months after surgery and 3 months after radiotherapy.
- Semiquantitative analysis, in particular, SUV measurements, should be used with caution.
- PERCIST criteria have not been validated in children.
- FDG-PET is recommended in surveillance of lymphoma only in selected cases, determined by clinical situation [30].
- Base of the skull to mid-thigh examination has been found sufficient in patients with lymphoma [35].
- Staging scans performed after the initiation of treatment may result in false-negative studies [36].

Take Home Messages

- FDG is taken up by malignant cells via glucose membrane transporters and phosphorylated by hexokinase into FDG-6-Phosphate, which does not follow further enzymatic pathways and accumulates proportionally to the glycolytic cellular rate.
- Fasting decreases serum glucose levels and maintains a low insulin level.
- The 60 min uptake time is needed for absorption and clearance of the radiotracer.

- Patients should not talk, text, play video games, chew gum, or suck candies during the uptake phase to avoid FDG uptake in tense muscles.
- PET imaging for staging in pediatric lymphoma should be given high priority for scheduling pre-therapy, especially in patients with critical condition.
- Whole-body PET studies, from vertex to toes, should be performed in sarcoma and most of the pediatric solid cancers since the

diseases can often occur distal to elbows and knees.

Representative Case Examples

Case 12.1 Diffuse Large B-cell Non-Hodgkin's Lymphoma (NHL), Staging (Fig. 12.1)

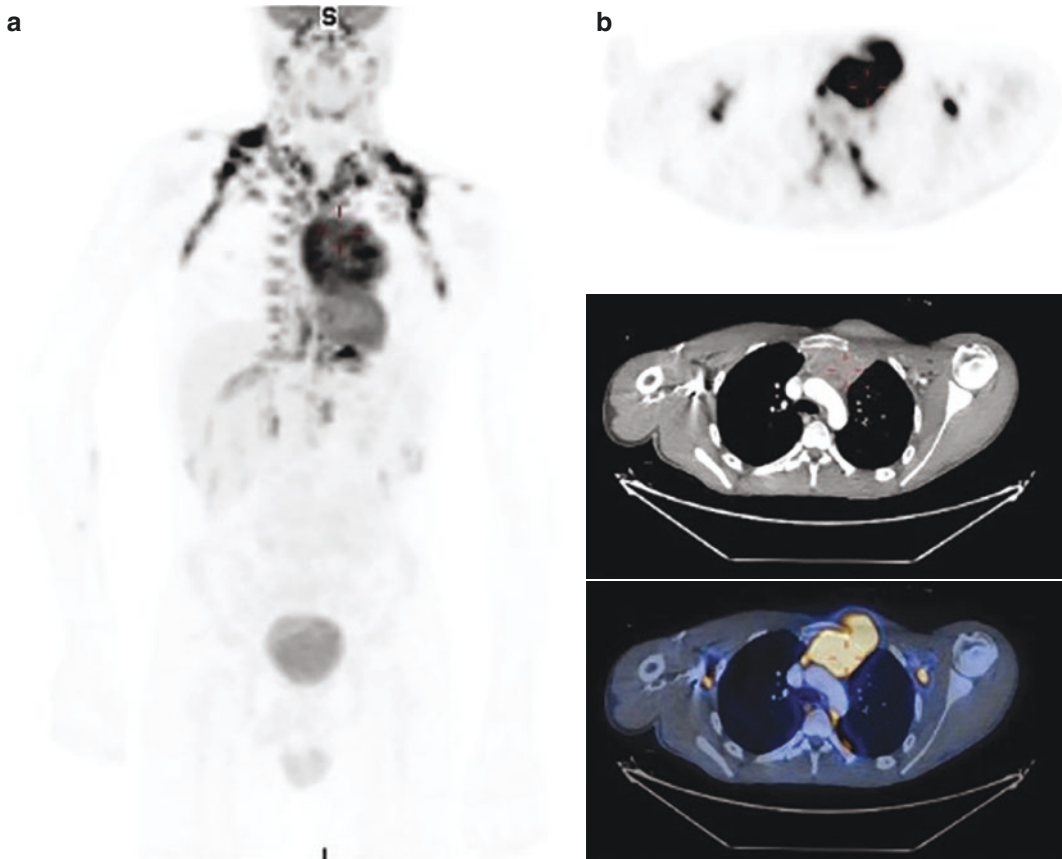


Fig. 12.1 History: An 18-year-old boy with diffuse large B-cell NHL was referred for staging. Study report: FDG-PET MIP (a) and selected PET, CT, and PET/CT transaxial slices at the level of the upper chest (b) show an area of intense, inhomogeneous, abnormal tracer uptake in a 9 × 9 cm mass in the anterior mediastinum, involving the ST and bone, specifically the left 1–4 ribs and sternum, with suspected involvement of the left lung. Note physiological cervical and axillary uptake in brown fat. There are no other sites of nodal hypermetabolism in the neck and chest, and no pulmonary nodules. There is no nodal

hypermetabolism in the retroperitoneal or pelvic lymphatic chains. The spleen is normal in size and tracer avidity. There is focal increased physiological tracer uptake in paraspinial and right suprarenal brown fat. There are no areas of abnormal uptake in the appendicular and axial skeleton. Impression: The findings are consistent with lymphoma of the mediastinum involving bony structures and possibly the left lung. The patient received four courses of chemotherapy and a repeat FDG-PET/CT study (not shown) demonstrated a complete metabolic response

Case 12.2 Burkitt's Non-Hodgkin's Lymphoma (NHL)—Staging (Fig. 12.2)

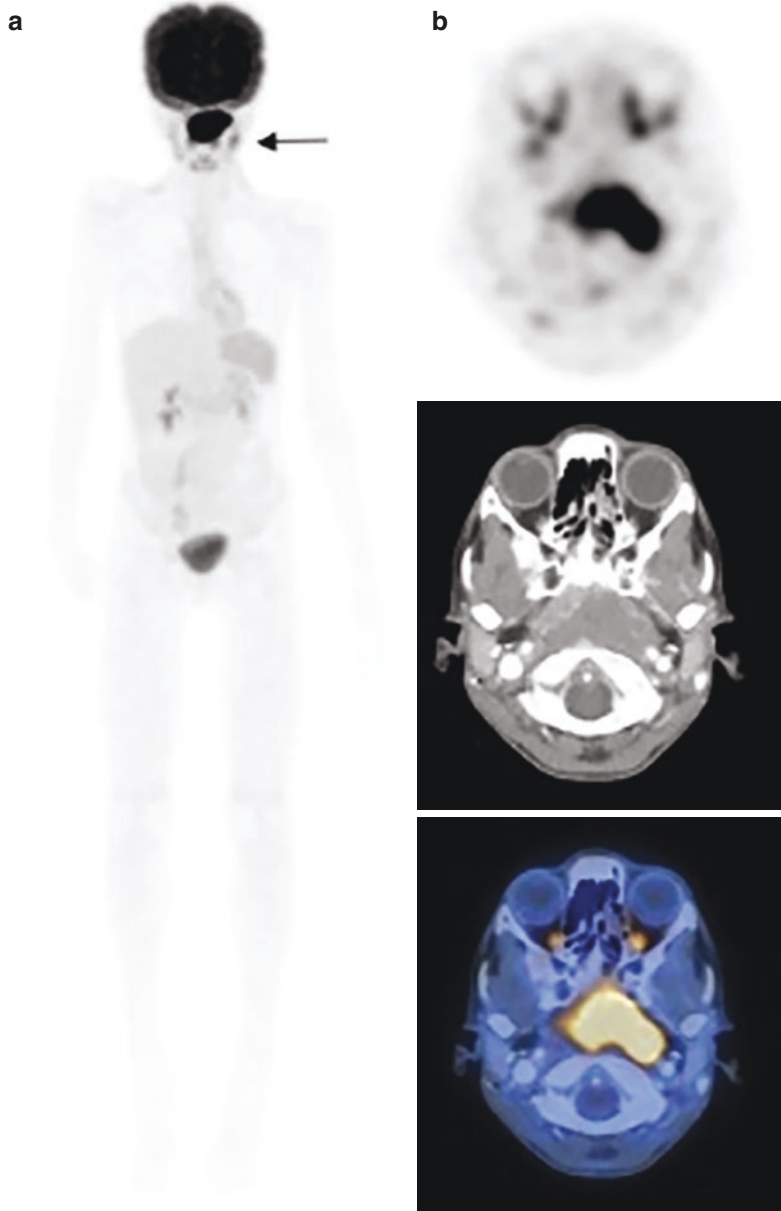


Fig. 12.2 History: A 9-year-old boy with newly diagnosed Burkitt's NHL following biopsy of the nasopharynx was referred for staging. Study report: FDG-PET MIP (a) and selected transaxial slices PET, CT, and PET/CT of the head (b) show intense pathological tracer uptake in a mass involving the nasopharynx, the oropharynx, and the base of the skull. Low-to-medium intensity uptake (SUVmax 2.24–5.51) is noted in 8 mm cervical lymph nodes, more prominent on the left. There is no nodal hypermetabolism in the chest and no pulmonary nodules. There is no nodal hypermetabolism in abdominal, retroperitoneal, or pelvic

lymphatic chains. The spleen is normal in size, with homogenous, mildly increased tracer avidity. There are no areas of abnormal uptake in the appendicular and axial skeleton. Impression: The findings are consistent with lymphoma involving the nasopharynx and possibly cervical nodes, mainly on the left side of the neck. Low-intensity activity in additional cervical lymph nodes can be related to an inflammatory reaction. Diffuse, homogenous tracer activity in the spleen, most probably due to increased hematopoiesis or an inflammatory reaction

Case 12.3 Hodgkin Lymphoma (HL), Staging, Monitoring Treatment Response and Follow-Up (Fig. 12.3)

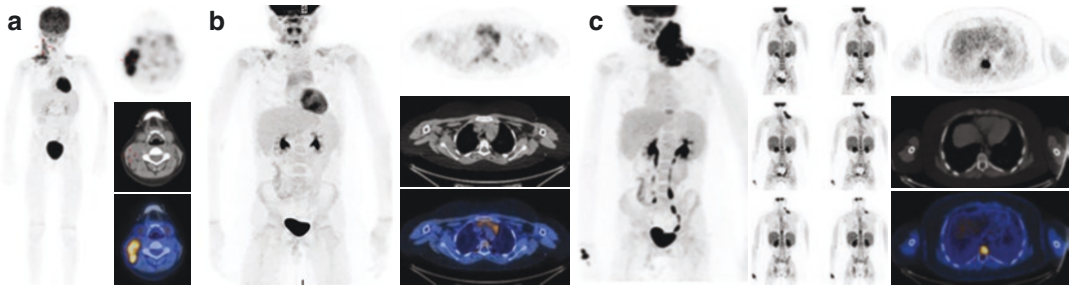


Fig. 12.3 History: A 7-year-old boy with newly diagnosed HL. Study report: At staging (a) FDG-PET MIP and selected transaxial PET, CT, and PET/CT slices at the level of the upper neck show intense abnormal tracer uptake in a nodal mass involving the neck and supra- and infra-clavicular regions on the right. Note also mild increased physiologic activity in bilateral infraclavicular sites of brown fat and in the thymus in the anterior mediastinum. There is no nodal hypermetabolism in the chest and no pulmonary nodules. There is no nodal hypermetabolism in the abdominal, retroperitoneal, or pelvic lymphatic chains. The spleen is normal in size and tracer avidity. There are no areas of abnormal uptake in the appendicular and axial skeleton. Impression: Supradiaphragmatic sites of nodal HL. The patient received treatment according to protocol and achieved a complete response. At the end of treatment (b): MIP and selected PET, CT, and transaxial PET/CT slices at the level of the upper mediastinum show that the supradiaphragmatic abnormal uptake foci in sites of HL have disappeared. There is mild-to-moderate tracer activity in an enlarged hyperplastic thymus and in sites of physiologic brown fat above the diaphragm. There is no nodal hypermetabolism in the neck and chest and in the abdominal,

retroperitoneal, or pelvic lymphatic chains. There are no pulmonary nodules. The spleen is normal in size and tracer avidity. There are no areas of abnormal uptake in the appendicular and axial skeleton. Impression: No evidence of active HL. Increased uptake in the thymus, consistent with post-treatment hyperplasia. The patient was followed up and re-evaluated 2 years later for suspicion of recurrence. At restaging (c): MIP (left), selected coronal PET slices (center) and transaxial PET, CT (with bone windows), and PET/CT slices at the level of the lower thorax (right) show new, intensely abnormal tracer uptake in significant lymphadenopathy in the left cervical, supra- and infra-clavicular regions. Note mild physiologic uptake in a hyperplastic thymus. There is no nodal hypermetabolism in the chest and in abdominal, retroperitoneal, or pelvic lymphatic chains. There is a new focal site of increased tracer uptake in the T9 vertebral body, with no corresponding lesion seen on CT. In addition, there is diffuse homogeneous increased activity throughout the skeleton. Impression: The findings are consistent with sites of nodal and skeletal recurrence of HL. Diffuse increased tracer activity in the skeleton, most probably reactive to increased hematopoiesis

**Case 12.4 Post-transplant
Lymphoproliferative Disorder (PTLD),
Transformation to Non-Hodgkin's
Lymphoma (NHL)–PET/MRI (Fig. 12.4)**



Fig. 12.4 History: A 7-year-old boy with known heterotaxy. Status after heart transplant in 2013, presented with a left neck mass. At clinical examination, he was found to have diffuse lymphadenopathy, small bowel intussusception, and kidney masses. The patient was referred with a suspicion of PTLD. PET/MRI was performed after administration of FDG and contrast for the MRI component. Study report: MIP images of FDG-PET and MRI demonstrate tracer activity in both maxillary sinuses, in a right costo-phrenic lymph node and in bilateral avid pulmonary nodules, mainly in a left apical pleural-based lesion. There is focal uptake in bowel in the right upper quadrant, due to small bowel-small bowel intussusception seen on prior CT. There is abnormal uptake in a conglomerate of left renal masses. There is no nodal hypermetabolism in the abdominal, retroperitoneal, or pelvic lymphatic chains. The spleen is absent, consistent with the history of

heterotaxy. There are multiple abnormal foci of tracer uptake in the skeleton. A soft tissue mass encompasses the left mandibular ramus. Additional foci of increased activity are seen in the mandible and maxilla bilaterally, the occiput, the left glenoid, the pelvic bones, the right femoral shaft, and the left femoral neck. Diffuse bony involvement includes multilevel vertebral bodies, some with soft tissue and epidural extension. There is increased uptake and enhancement along multiple nerve roots, such as the sacral nerves and left L2 nerve root. Impression: The findings are consistent with diffuse FDG-avid disease including bony involvement of the axial and appendicular skeleton, bilateral renal masses, lymphadenopathy above the diaphragm, bowel involvement, and lung lesions, suggesting PTLD with transformation to NHL, further confirmed by subsequent biopsy. Status after known heterotaxy and orthotopic heart transplant

Case 12.5 Osteosarcoma, Metastatic to Bone, Staging (Fig. 12.5)

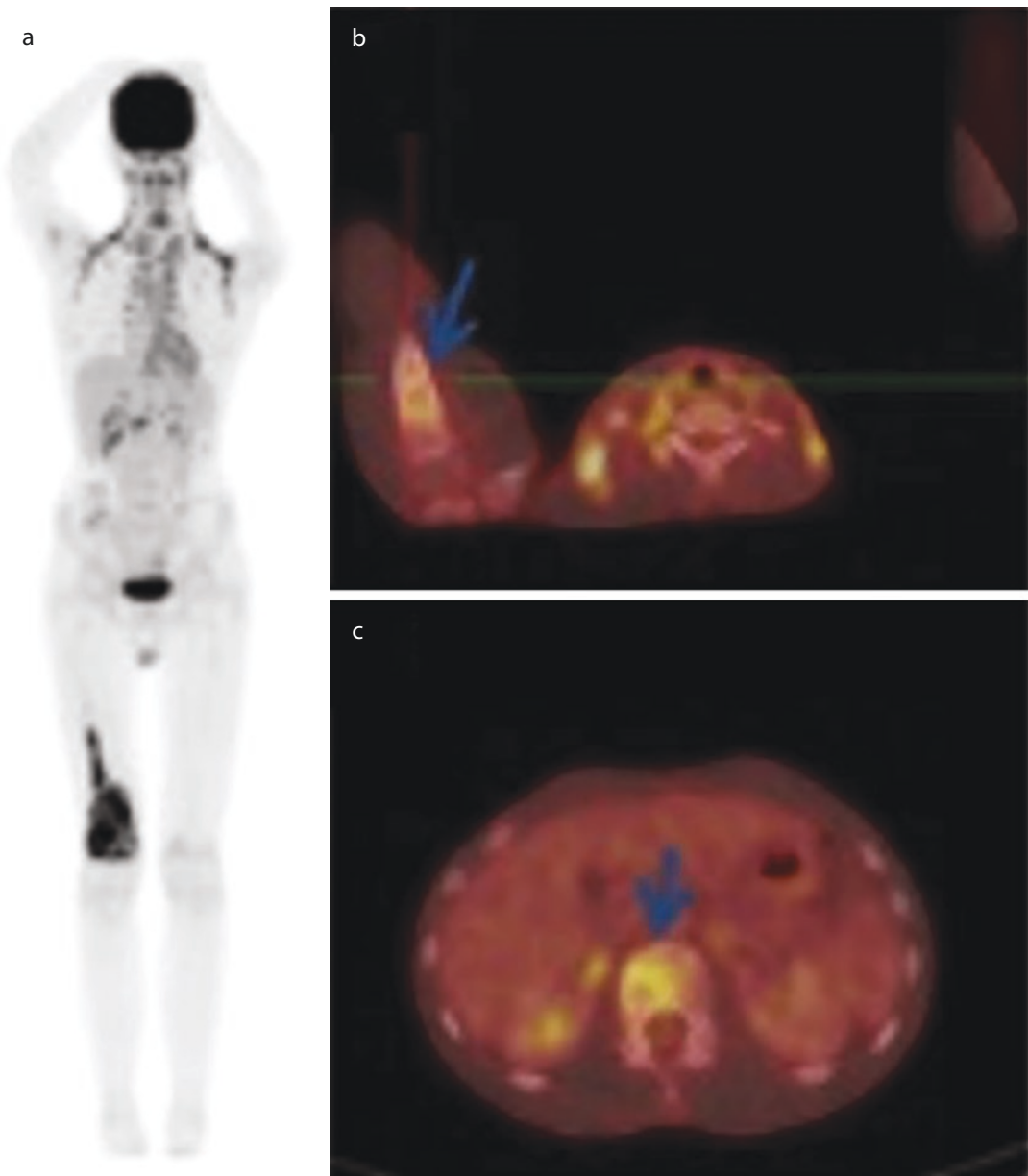


Fig. 12.5 History: A 14-year-old girl presented for evaluation of a destructive lesion in the right distal femur suggestive of a primary bone tumor. Study report: There is no nodal hypermetabolism in the head and neck. Note physiological cervical and axillary uptake in brown fat. There is no nodal hypermetabolism in the chest and no pulmonary nodules. There is no nodal hypermetabolism in abdominal, retroperitoneal, or pelvic lymphatic chains. The

spleen is normal in size and tracer avidity. There is intense tracer uptake in the known lesion in the distal right femur seen on the FDG-PET MIP image (a). Additional foci of moderately increased tracer uptake are seen in mixed, lytic-blastic bone lesions in the right proximal humerus (b, arrow) and L2 vertebral body (c, arrow). Impression: The findings are consistent with right femur osteosarcoma with skeletal metastases

Case 12.6 Metastatic Rhabdomyosarcoma (Fig. 12.6)

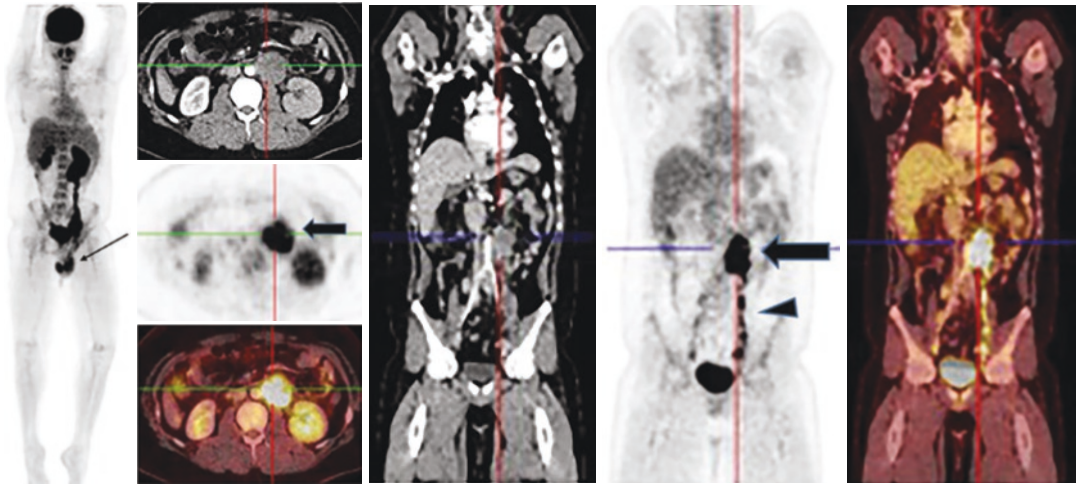


Fig. 12.6 History: A 14-year-old boy presented with a left testicular mass. FDG-PET/CT was performed for staging evaluation. Study report: MIP (left), transaxial (center) and coronal (right) CT, PET, and fused slices at the level of retroperitoneal lymphadenopathy demonstrate focal increased tracer activity in the left testicular mass (thin arrow), hypermetabolic left retroperitoneal paraaor-

tic lymphadenopathy, extending from the level of the left kidney (thick arrow and arrowhead) to just above the bladder. Impression: The findings are consistent with left testicular neoplasm with left retroperitoneal extensive metastatic lymphadenopathy. Biopsy diagnosed rhabdomyosarcoma

12.3 Neuroblastoma

Clinical Indications [11]

- Staging.
- Prognostic information based on scoring methods measuring disease extent.
- Assessment of response to treatment.
- Restaging of recurrence.
- Long-term surveillance.
- Imaging prior to treatment with radiolabelled tracers: ^{123}I -MIBG scan will determine whether a neuroblastoma is tracer-avid and treatment with ^{131}I -MIBG can be considered.

Correlative Imaging [37, 38]

- Neuroblastoma will often present as an abdominal mass and the US will be the initial imaging study. Characteristic calcification and location of disease may suggest the likelihood of neuroblastoma diagnosis.
- Bone scintigraphy is not routinely performed in a child presenting with suspected neuroblastoma since MIBG scintigraphy and PET imaging have replaced this test. However, a child presenting with bone pain or limp may have initial imaging with a bone scan.
- Bone scintigraphy in a patient with suspected neuroblastoma can show typical abnormal, often symmetrical metaphyseal activity, focal bony lesions in the axial and appendicular skeleton as well as soft tissue uptake in a, mainly abdominal, mass (see Case 12.14, and Fig. 12.15).
- Plain radiographs can show no abnormalities in cases with skeletal involvement of neuroblastoma.
- MRI is the most common study performed to evaluate a mass in the chest, abdomen, and/or pelvis, in a child with neuroblastoma. It is mandatory when epidural and intracranial disease is suspected.
- CT scans may also be used for imaging evaluation of chest, abdomen, and pelvic disease suspected to be neuroblastoma. It is not adequate as the single cross-sectional anatomic

imaging modality when epidural or intracranial disease is suspected.

MIBG Scintigraphy of Neuroblastoma

Specific Study Interpretation Criteria (See also Box 12.2—Imaging with MIBG)

- Pathological tracer uptake is found in the primary tumor and in metastases in lymph nodes, liver, bone, bone marrow, and rarely, skin, lungs, and brain.

MIBG Scoring Systems [39]

- Provides a semiquantitative assessment of initial disease burden and response to therapy.
- It is used for treatment tailoring and for prognosis.
- Two validated scoring systems are in use:
 - The Curie Score (Children’s Oncology Group—COG) divides the skeleton into 9 compartments and a 10th compartment for the soft tissues. The uptake score for each compartment ranges from 0 to 3 [40].
 - The SIOPEN score (International Society of Paediatric Oncology Europe Neuroblastoma), only scores skeletal disease. The skeleton is divided into 12 segments. The uptake score for each segment reflects the disease extent in that segment and ranges from 0 to 6 [41].

Red Flags [14]

- Careful drug history should be obtained before imaging. Numerous drugs interfere with the uptake or retention of MIBG and should be discontinued for approximately 4 biological half-lives. A detailed list of interfering drugs, most of them rarely used in children, can be found in Appendix 1 of the EANM guidelines [11]. The main drugs to be withdrawn in children are those used for symptomatic treat-

ment of asthma and of upper respiratory tract infections (decongestants), and occasional antihypertensive drugs.

- Thyroid blockage medication is required to prevent unnecessary irradiation of the thyroid gland by free radioiodine. Sedation, especially important for SPECT/CT, may be required because most children undergoing MIBG scintigraphy are young, and acquisition takes 60–90 min. In some occasions, feeding and bundling the infant prior to scan is all that is required to keep the child immobile.
- Slow administration of the tracer reduces the likelihood of adverse reactions such as hypertension, nausea, vomiting, and pallor that may occasionally occur.
- Children should be monitored during, and for a short time after, MIBG injection.
- The most appropriate collimator type for ^{123}I -MIBG imaging varies among different manufacturers and should be decided based on the equipment available in each department.
- In young children, multiple spot views should be used because of higher count density and improved spatial resolution. Multiple views obtained for the skull (anterior, posterior, left, and right lateral views) improve detection of orbital and skull base lesions.
- A full bladder can conceal pelvic lesions. Post-void images, SPECT, and/or SPECT/CT of the pelvis and less commonly, bladder catheterization can be employed.

Take Home Messages [14]

- Primary tumors most commonly originate from the adrenal gland or from the sympathetic ganglia, along the abdominal, thoracic, and rarely cervical spine.
- MIBG is an iodinated analogue of guanidine, structurally similar to norepinephrine (NE). It shares the same transport pathway as NE via the cell membrane NE transporter system. In the cytoplasmic compartment, MIBG is stored in the neurosecretory granules.
- For functional imaging assessment of neuroblastoma, ^{123}I -MIBG is considered a first-line

test. It is the current standard due to appropriate physical characteristics for the best image quality and dosimetry.

- ^{131}I -MIBG should not be used for diagnostic purposes due to poor image quality and higher radiation exposure.
- About 10% of neuroblastomas do not accumulate MIBG.
- Any MIBG uptake in the skeleton indicates metastatic disease.
- SPECT/CT is of particular value for:
- Differential diagnosis of heterogeneous hepatic tracer uptake, a known physiologic pattern vs. metastatic involvement.
- To distinguish intracranial from skull lesions. Lesions involving the calvarium are on rare occasions due to cerebral metastases.
- Distinction between cortical bone and bone marrow metastases.
- Discrepancy in MIBG uptake between the primary tumor and metastases may be due to:
 - Biological heterogeneity in populations of tumor cells can alter their MIBG avidity.
 - Changes occur during the course of the disease course.
 - MIBG avidity of relapsed disease might differ from the initial disease.
 - After treatment, uptake in residual tumor deposits may persist due to differentiation of the tumor to mature MIBG-avid ganglioneuroma.
 - MIBG imaging plays a theranostic role in the assessment of neuroblastoma.
 - Alternative imaging of neuroblastoma with PET tracers can be considered.

PET *Imaging of Neuroblastoma* (see also Box 12.1, Box 12.3, and Box 12.4)

Clinical Indications [42, 43]

- Alternative metabolic imaging in cases of MIBG-negative or weakly positive tumor.
- When radiologic imaging modalities show more disease than MIBG scintigraphy.
- Advantages of PET imaging of neuroblastoma include:

- One-day appointment
- No need for iodine blockage
- Faster scan
- Lesser need for anesthesia
- Improved lesion detectability
- Quantitation of tracer uptake

FDOPA [44–46] (*See also* Box 12.3)

- FDOPA uptake is relatively specific for NETs including neuroblastoma. When available, it is considered the preferred PET alternative to ^{123}I -MIBG.

Red Flags

- In adults, carbidopa reduces physiologic uptake in peripancreatic region and increases uptake in lesions. However, there is no consensus regarding the use of carbidopa in children.
- Avoid misinterpretations by performing late imaging after ambulation/hydration/diuretic administration.

Take Home Messages [47]

- DOPA is present in the nervous system as a precursor of dopamine and FDOPA PET imaging tracks the metabolism of catecholamines.
- Neuroblastoma FDOPA PET imaging provides a sensitive and specific assessment of the disease status. While being a relatively specific tracer for NETs other indications are also known.
- Small-scale studies comparing FDOPA with ^{123}I -MIBG in children show a higher sensitivity of the former tracer and superior detectability of small metastases in bones, soft tissues, and bone marrow.

FDG [5] (*see also* Box 12.1)

- Advantages:
 - Uptake is proportional to the degree of malignancy.

- Prognostic value with higher FDG uptake at diagnosis is associated with poorer prognosis.
- It can differentiate between residual active tumor and benign ganglioneuromas which maintain MIBG avidity but are typically FDG negative.

- Limitations:

- Lack of specificity, mainly for assessing the presence of bone marrow involvement, a very common location for neuroblastoma metastases and also a site of physiologic FDG uptake.
- Cranial vault lesions may be difficult to detect on FDG imaging due to the adjacent high brain activity.

^{68}Ga -PEPTIDES [15, 48, 49] (*see also* Box 12.4)

Clinical Indication

- ^{68}Ga -peptides target SSTR which are commonly expressed in neuroblastoma cells.
- To select suitable patients for theranostics using peptide receptor radionuclide therapy (PPRT).

Red Flags

- Poorly differentiated tumors have a low affinity for the tracer.
- Inflammatory processes such as reactive lymph nodes or post-radiotherapy changes may show some degree of tracer activity, usually of mild intensity, due to the expression of SSTRs in activated lymphocytes.
- Further validation is required prior to increasing the utilization of this modality in routine clinical practice.
- SSTR imaging to determine whether a NET is receptor positive. Peptide receptor radionuclide therapy (PRRT) such as ^{177}Lu -DOTA-octreotate is, in pediatric patients, still investigational.

Take Home Messages

- Pathological uptake in neuroblastoma is typically intense SUVs.
- Somatostatin receptor imaging of neuroblastoma is a sensitive, second-line PET alternative to ^{123}I -MIBG with a potential for theranostic application.
- All these tracers target SSTRs.

- They have rapid clearance from the blood and renal excretion. Maximum tumor activity is reached at 70 ± 20 min.

Relevant Case Examples

Case 12.7 Metastatic Neuroblastoma—MIBG Scintigraphy (Fig. 12.7)

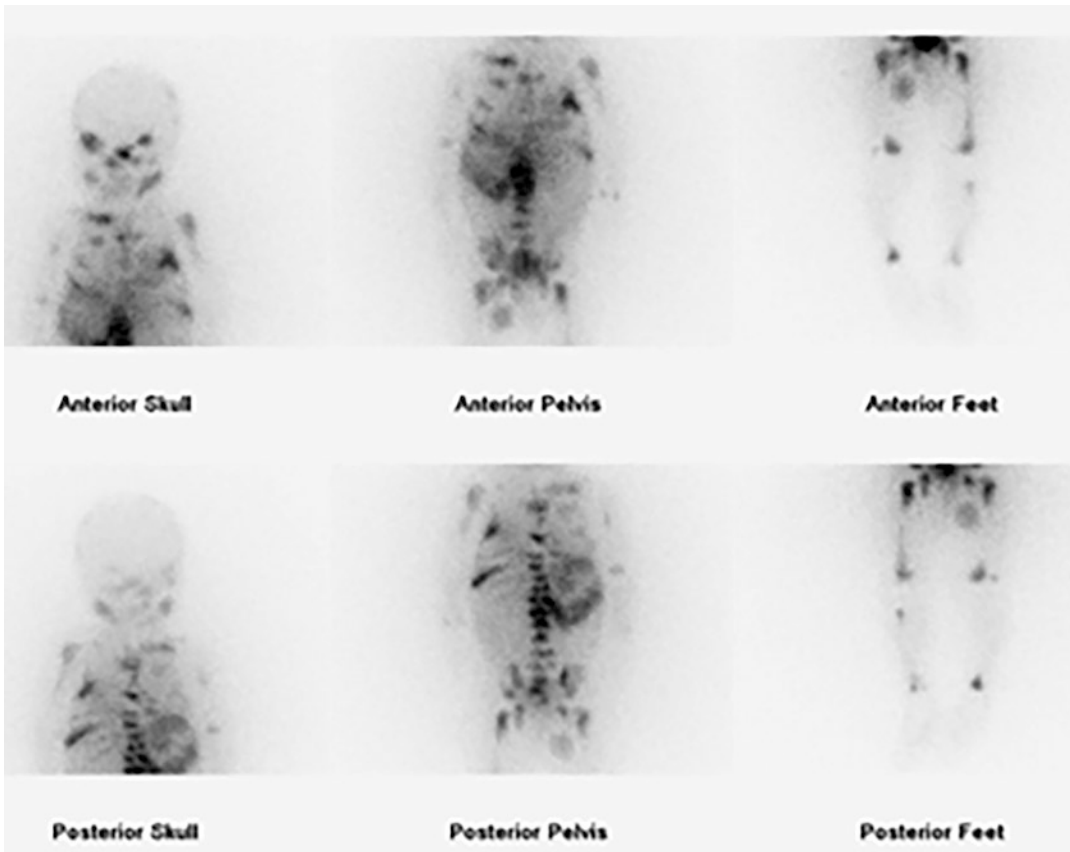


Fig. 12.7 History: A 16-month-old boy presented with multiple soft tissue masses over the right eye and the right thigh, and an additional palpable mass in the abdomen. Biopsy of the right thigh mass and of the bone marrow diagnosed neuroblastoma. Study report: MIBG scintigraphy, anterior and posterior planar spot views of the whole body, demonstrate foci of abnormally increased tracer

uptake involving the known soft tissue masses in the roof of the right orbit, in the right upper abdomen (with a cold, photopenic, central area, most probably necrosis) and the upper right thigh. There are also multiple foci of increased tracer uptake in the skeleton, in the left mandible, ribs, and vertebrae. Impression: The findings are consistent with metastatic neuroblastoma

Case 12.8 Metastatic Neuroblastoma, Response to Treatment—MIBG Scintigraphy (Figs. 12.8 and 12.9)

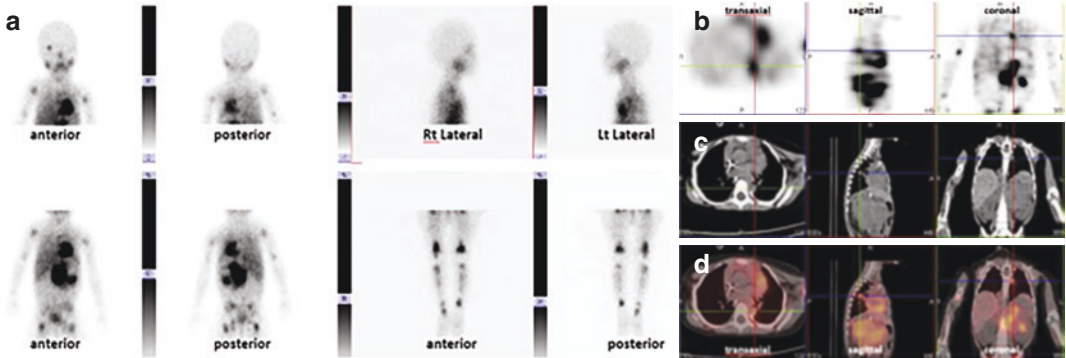


Fig. 12.8 History: An 18-month-old infant girl presented with a large abdominal mass suspected of neuroblastoma. A baseline MIBG scan was obtained for initial staging. Study report: Planar spot images of the whole body (a) show intense tracer uptake in the abdominal mass, as well as in multiple skeletal metastases in the skull, upper limbs, pelvis, and lower limbs. SPECT, low dose CT and SPECT/

CT transaxial, sagittal, and coronal slices (b–d) show a left paravertebral, metastatic mediastinal mass (cross hair) that was not evident on planar images. Impression: The findings suggest metastatic neuroblastoma, further confirmed by biopsy of the abdominal mass. The patient started induction chemotherapy

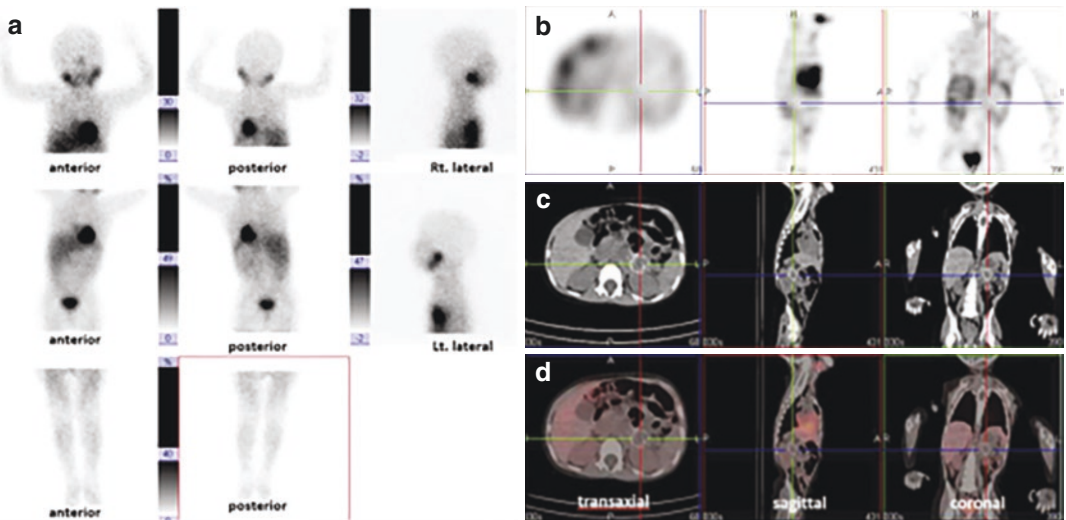
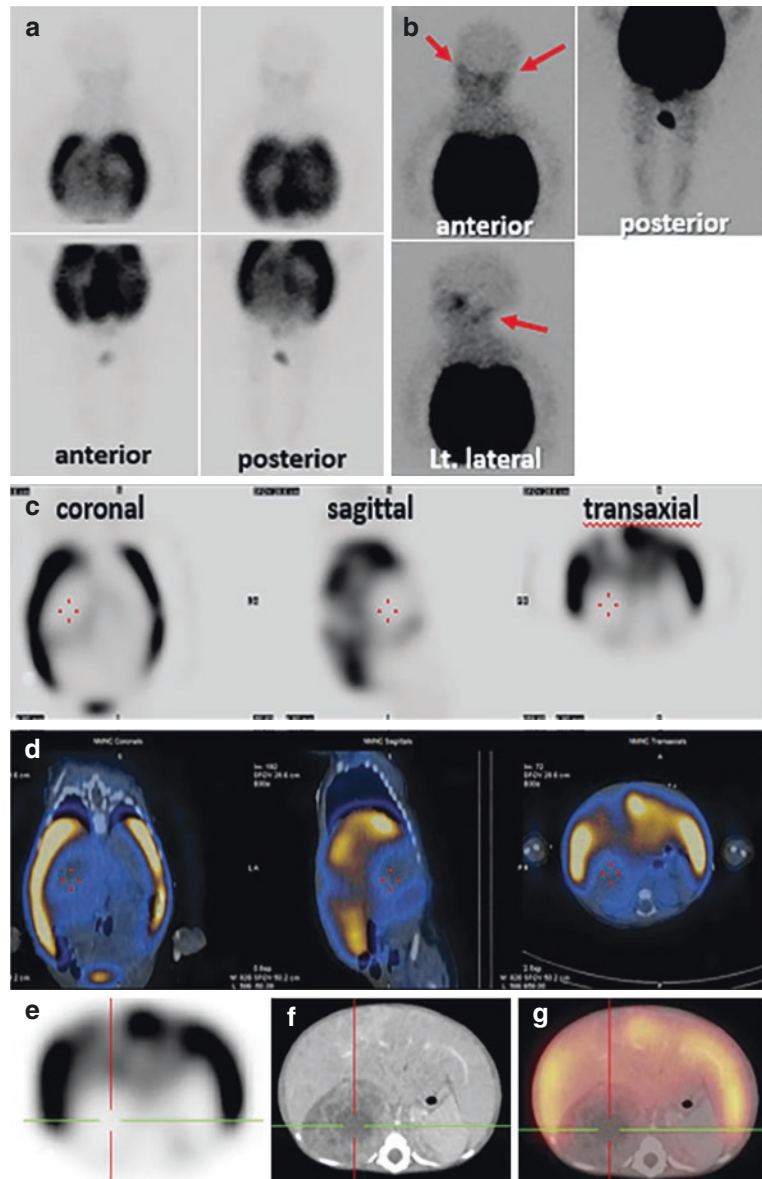


Fig. 12.9 A follow-up ¹²³I-MIBG scan was obtained 2 months after the start of treatment according to the therapy protocol. Study report: MIBG scintigraphy, anterior, and posterior planar spot views of the whole body, (a) show normal tracer distribution with a resolution of the uptake in the abdominal tumor and in the metastatic sites.

Transaxial, sagittal, and coronal SPECT, CT, and SPECT/CT slices (b–d) demonstrate that the size of the abdominal tumor has significantly decreased. The crosshair is positioned over a calcified portion of the residual tumor and shows no tracer uptake. Impression: The findings indicate a complete metabolic response

Case 12.9 Metastatic Neuroblastoma, Heterogeneous Uptake on MIBG Scintigraphy (Fig. 12.10)

Fig. 12.10 History: A 2-month-old girl presented with a large right-sided abdominal neuroblastoma and massive enlargement of the liver. MIBG SPECT/CT was obtained for initial staging. Study report: scintigraphy, anterior and posterior spot views of the whole body (a) shows intense tracer uptake in a huge liver occupying both sides of the abdomen. Tracer activity in the rest of the body is faint. Using manipulation of the image gray scale (b) physiological tracer localization is identified in the orbits, skull base (arrows), and lower limbs. Transaxial and sagittal SPECT (c) and fused SPECT/CT slices (d) show intense tracer uptake in an enlarged liver occupying both sides of the abdomen. There is no appreciable MIBG uptake in the primary tumor in the right upper abdomen (crosshair). SPECT co-registered to an external diagnostic, contrast-enhanced CT to better delineate the primary tumor (e–g) shows no MIBG uptake in a large abdominal tumor. Impression: The findings are consistent with a non-MIBG-avid abdominal neuroblastoma with MIBG-avid metastases to liver and bone marrow. The difference in MIBG avidity between the primary tumor and the distant metastases reflects the biological heterogeneity of neuroblastoma cell populations



Case 12.10 Neuroblastoma, Tumor Progression, PET/CT with FDOPA (Fig. 12.11)

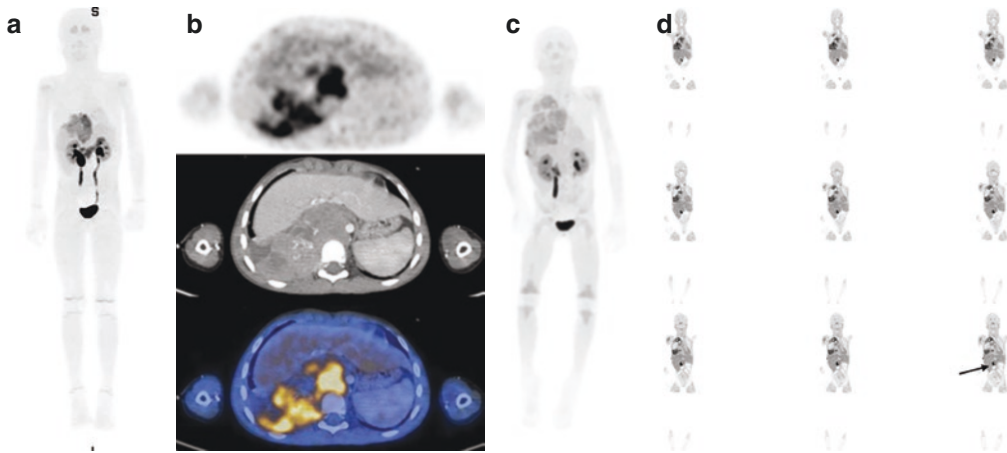
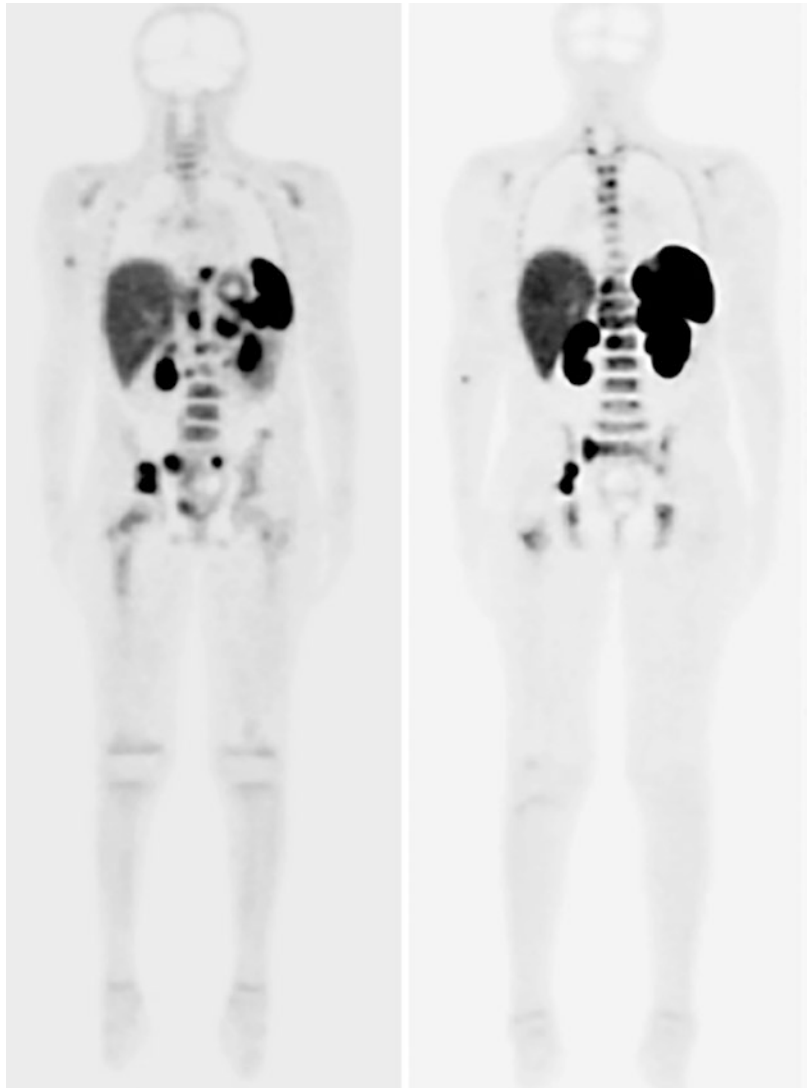


Fig. 12.11 History: A 5-year-old boy presenting with a thoracoabdominal mass was referred with the suspicion of neuroblastoma. Study report: At diagnosis MIP (a) and selected transaxial PET, CT, and PET/CT slices at the level of the lower thorax/upper abdomen (b) show an area of inhomogeneous abnormal tracer uptake (SUVmax up to 6.4) in a heterogeneous mass, $7 \times 10 \times 10$ cm in size, located right paravertebral to the lower thoracic spine, most probably involving the right foramina of T10. There is no increased activity in lymph nodes in the neck and chest and in the abdominal, retroperitoneal, or pelvic lymphatic chains. There are no pulmonary nodules. The spleen is normal in size and tracer avidity. There are no areas of abnormal uptake in the appendicular and axial skeleton. Impression: The findings suggest the diagnosis

of neuroblastoma with suspected involvement of the right foramina of T10. The diagnosis of intermediate-risk neuroblastoma was confirmed by pathology. Laminectomy of T7–T10 with partial surgical removal of the tumor was performed and protocol treatment was started. At 2 months post-surgery a 2nd FDOPA PET/CT study was performed prior to the institution of a new treatment line. MIP (c) and selected coronal PET slices (d) demonstrate intense abnormal tracer uptake in new right supraclavicular lymphadenopathy, in a conglomerate of pleural nodules in the right hemithorax that involve the mid- and lower mediastinum and the chest wall muscles and in right para-aortic lymph nodes (arrow). Impression: The findings demonstrate significant tumor progression

Case 12.11 Metastatic Neuroblastoma, PET/CT with ^{68}Ga -DOTATATE PET/CT (Fig. 12.12)

Fig. 12.12 History: An 8-year-old girl with refractory stage 4 neuroblastoma was referred to PET/CT to determine suitability for ^{177}Lu -DOTATATE therapy. Study report: PET MIP, anterior, and posterior views, show multiple areas of abnormal tracer uptake in the primary tumor in the upper abdomen and in skeletal metastases involving vertebrae, the pelvis, and proximal femuri. Impression: The findings are consistent with metastatic neuroblastoma with SSTRs, a suitable candidate to PRRT



12.4 Other Neuroendocrine Tumors

⁶⁸Ga-PEPTIDE IMAGING OF NETS (see also Box 12.4—Imaging with ⁶⁸Ga-peptides)

Clinical Indications [15]

- Localization and characterization of NETs with the expression of high density of SSTR such as succinate dehydrogenase (SDHx)-mutated NETs and head and neck PGL when ¹⁸F-FDG-PET is negative.
- Detection of occult NETs in cases of metastatic tumors with unknown primary or if high serum tumor markers are found.
- Characterization of a bronchial tumor mass.
- In the theranostic setting, when PRRT is considered.

Red Flags [50]

- Brown fat visualization is not a common problem in ⁶⁸Ga-peptide imaging in NETs.

Take Home Message

- In well-differentiated NETs, ⁶⁸Ga-peptides PET imaging has a higher detection rate as compared to FDG imaging which may play a complementary role, especially in cases of poorly differentiated tumors known to show high FDG avidity.
- ⁶⁸Ga-peptides PET may evolve as a preferred imaging modality for disease surveillance in certain cancer predisposition or premalignancy syndromes (e.g., von Hippel Lindau disease).

FDOPA IMAGING OF NETS (*See also* Box 12.3—Imaging with FDOPA)

Clinical Indications [51, 52]

- NETs with absent SSTR expression, for (re) staging and monitoring response to treatment.
- Adrenal pheochromocytoma, sporadic or related to cancer predisposition syndromes.
- Congenital hyperinsulinism, to identify focal forms in the pancreas that can be resected [53].

Red Flags

- Inflammatory processes such as reactive lymph nodes or post-radiotherapy changes may show tracer activity.
- SSTR imaging to determine whether a NET is receptor positive. Peptide receptor radionuclide therapy (PRRT) such as ¹⁷⁷Lu-DOTA-octreotate is, in pediatric patients, still investigational.

Take Home Message

- FDOPA PET imaging is more specific in cases of neuroblastoma and insulinoma as compared with FDG and ⁶⁸Ga-peptides.
- Advantages of NET PET imaging (over NET SPECT imaging):
 - Earlier and shorter acquisition time
 - Improved patient comfort
 - Improved spatial resolution
 - Less radiation exposure

Representative Case Examples

Case 12.12 Paraganglioma (PGL), ⁶⁸Ga-DOTATE PET/CT (Fig. 12.13)

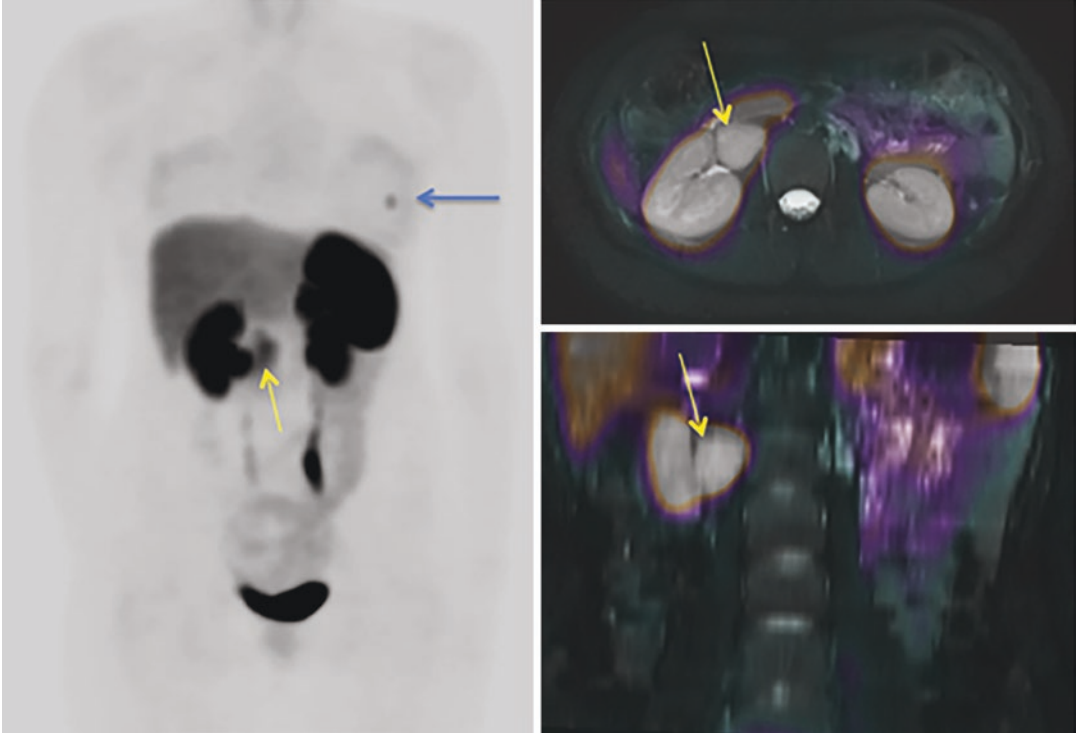


Fig. 12.13 History: A 9-year-old girl presented with hypertension and headaches and was diagnosed with a right lumbar paravertebral PGL with a SDH gene line mutation. The tumor was resected and hypertension and symptoms improved. Four years later, at the age of 13 years, the patient presented again with hypertension. MRI showed recurrence of the mass in the right paravertebral region. PET/CT was performed for restaging of the recurrence. Study report: MIP (left) and selected transaxial (right top) and coronal (right bottom) PET/CT slices at the level of the mid-abdomen show increased focal tracer

uptake in the right paravertebral mass (yellow arrow) as well as in a metastatic focus in the left 6th rib (blue arrow). There is no increased activity in lymph nodes in the neck and chest and no pulmonary nodules. There are no additional areas of abnormal uptake in the appendicular and axial skeleton. Impression: The findings are consistent with recurrent PGL metastatic to bone. Both sites were resected, however, a follow-up scan performed 6 months later showed tumor progression with multiple bone metastases. The patient was treated with ¹⁷⁷Lu- DOTATATE and remained stable for 2 years

Case 12.13 Pheochromocytoma—FDG-PET/CT (Fig. 12.14)

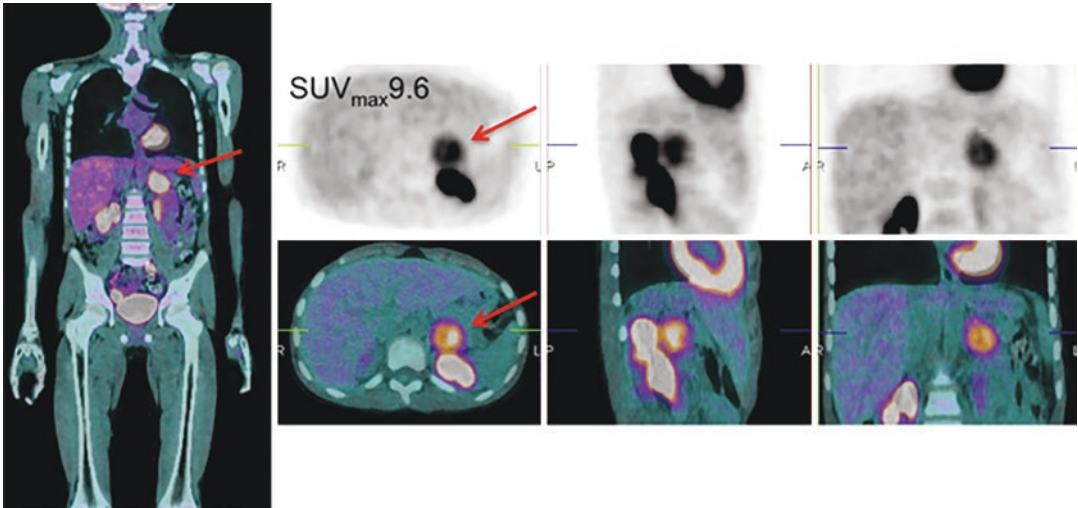


Fig. 12.14 History: An 11-year-old boy presented with hypertension. CT scan showed a left adrenal mass. ^{123}I -MIBG was negative (not shown). Study report: FDG-PET/CT shows abnormal uptake in the left adrenal mass (arrow) on transaxial, sagittal, and coronal PET (top right) and CT (bottom right) slices and coronal CT image of torso. There is no nodal hypermetabolism. There is no nodal hypermetabolism in the neck and chest and in the

abdominal, retroperitoneal, or pelvic lymphatic chains. There are no pulmonary nodules. The spleen is normal in size and tracer avidity. There are no areas of abnormal uptake in the appendicular and axial skeleton. Impression: The findings are suggestive of malignancy with no evidence of metastatic disease. Biopsy diagnosed pheochromocytoma

12.5 Musculo-Skeletal Malignancies (see also Box 12.5)

Clinical Indications [21, 23, 54–56]

- To identify and localize bone and bone marrow metastases in order to determine the extent of disease in patients with known malignancies.
- To assess primary bone and ST tumors such as osteosarcoma, Ewing sarcoma, and rhabdosarcoma.

Correlative Imaging

- In the presence of specific symptoms, plain radiographs are followed as a rule by MRI, the first choice investigation in most children with bone tumors.

Red Flags

- If MRI is not readily available or the child needs sedation or general anesthesia, bone scintigraphy and, recently in some centers, bone PET/CT are the next choice.
- For multiple spot views of the whole body start with the pelvis when the bladder is empty.
- It is still debated whether SPECT should be routinely performed even if planar scan is unremarkable or only for better characterization of an abnormality detected on planar imaging.
- When performing SPECT/CT the FOV of the CT should be shortened to include only the

region of the abnormality seen on SPECT to reduce radiation exposure.

- The CT component of a bone SPECT/CT can be acquired as a pediatric low-dose CT for localization and attenuation correction or as a diagnostic CT. Many skeletal lesions are adequately evaluated even with low-dose CT parameters.

Take Home Messages

- Increased tracer uptake, due to locally increased blood flow or calcium depositions, indicates an alteration in bone metabolism caused by increased new bone formation (osteoid) due to higher availability of binding sites, but also related to local or regional hyperemia.
- Bone marrow lesions tend to have a more diffuse pattern along a portion of a bone whereas cortical bone lesions are typically focal.
- With the dissemination of FDG-PET imaging which is the method of choice in oncology, most centers use this modality as the main scintigraphic study for malignancies even when they are limited to bone. Skeletal scintigraphy is used only occasionally and thus the significant decrease in its use in children with cancer.
- NaF PET imaging is becoming the preferred alternative for imaging of the skeleton due to the tracer's rapid localization and rapid clearance from the blood.

Representative Case Examples

Case 12.14 Metastatic Neuroblastoma, Bone Scintigraphy

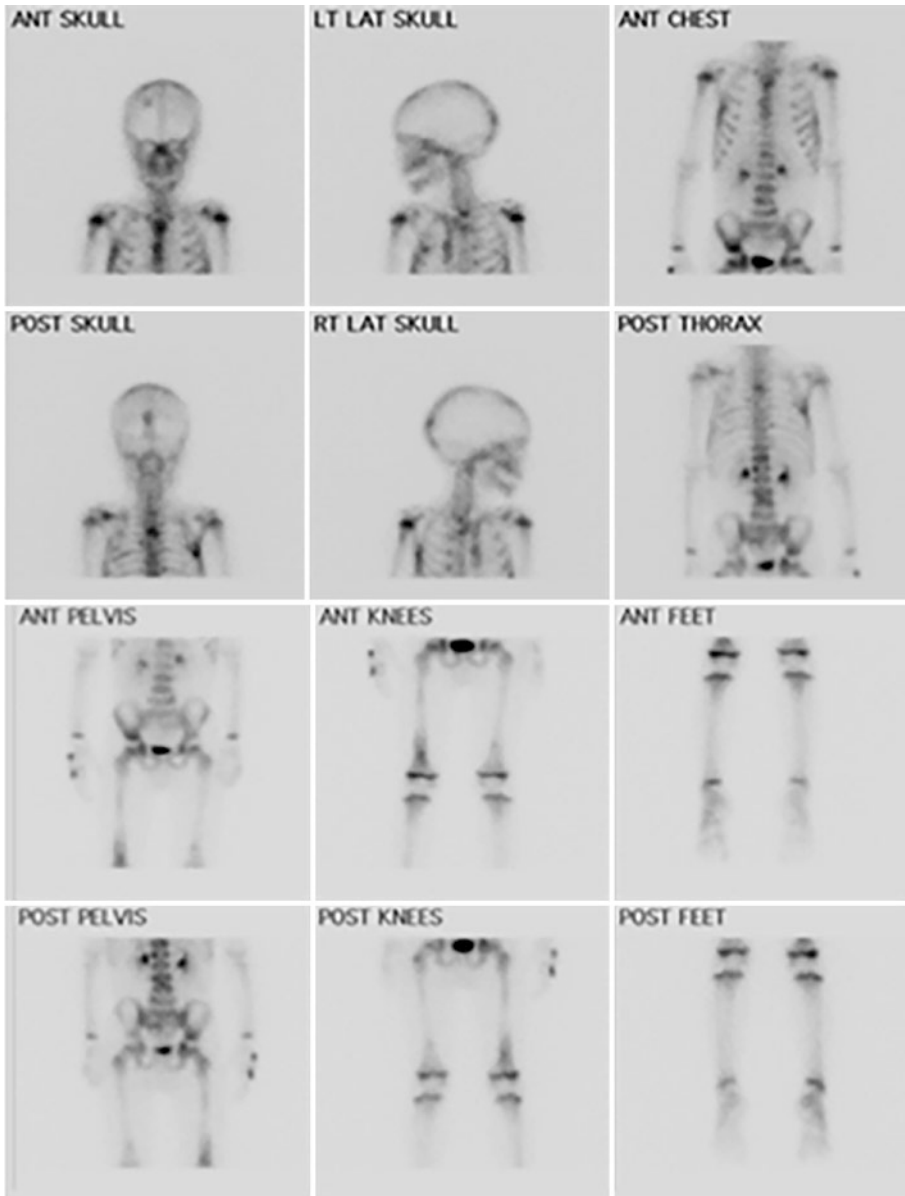


Fig. 12.15 History: A 5-year-old boy presented with right-sided limp. Clinical examination was normal. Plain radiographs of his pelvis and lower limbs were normal. Lab tests including ESR and CRP were mildly elevated. Study report: Bone scintigraphy, anterior and posterior planar spot views of the whole body, demonstrate multiple focal areas of increased tracer uptake in the skull, right proximal humerus, both scapulae, upper and lower tho-

racic and lumbar vertebrae, right acetabulum and distal femora (right more than left). Note asymmetrical metaphyseal activity specifically in the distal femora. Impression: The findings are consistent with neuroblastoma metastatic to bone. Abdominal US revealed a mass in the right adrenal. Tissue sampling diagnosis was stage IV neuroblastoma. Total body MIBG scintigraphy showed tracer uptake in the primary tumor and metastatic bone lesions

Case 12.15 Ewing Sarcoma, Staging, Bone Scintigraphy (Fig. 12.16)

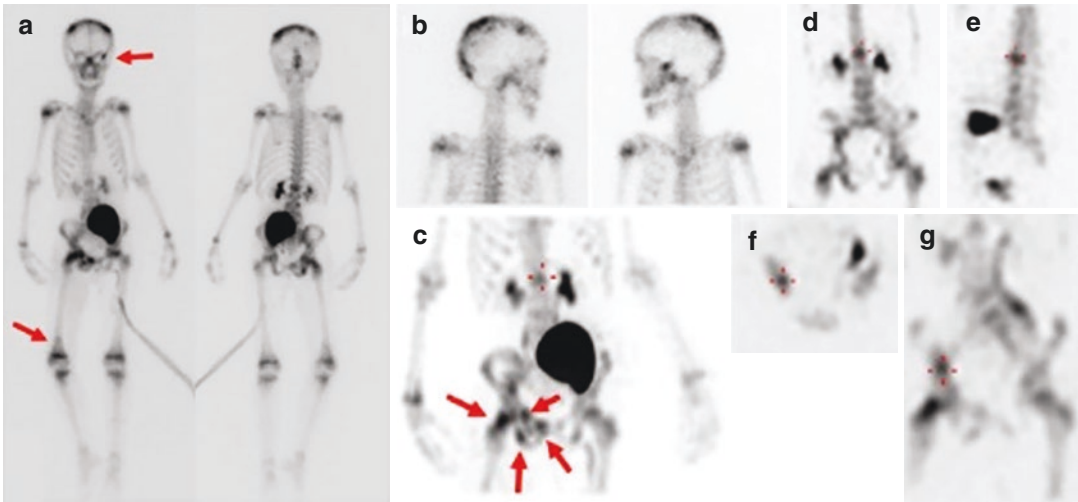


Fig. 12.16 History: An 8-year-old boy presented with a large pelvic mass. Histopathology diagnosed Ewing's sarcoma. Bone scintigraphy was performed for staging. Study report: Anterior and posterior whole body (a) and lateral spot views of the skull (b) show marked displacement of the urinary bladder to the left upper pelvis due to the known large tumor. Activity is noted in a urinary catheter to the left side of the body. Skeletal lesions are noted in the parietal and occipital skull, left orbit (arrow), L1,

acetabulum, the right pelvis involving the superior pubic ramus, ischium, and ilium, as well as in the proximal and distal (arrow) left femur. Coronal (d) and sagittal (e) SPECT slices show the L1 lesion (crosshairs). Transaxial (f) and coronal (g) slices show a lesion in the internal pelvic rim. MIP image (c) provides an overview of the pelvic and lumbar lesions (arrows). Impression: The findings suggest stage 4 pelvic Ewing's sarcoma with multiple skeletal metastases

Case 12.16 Metastatic Osteosarcoma, Bone Scintigraphy (Fig. 12.17)

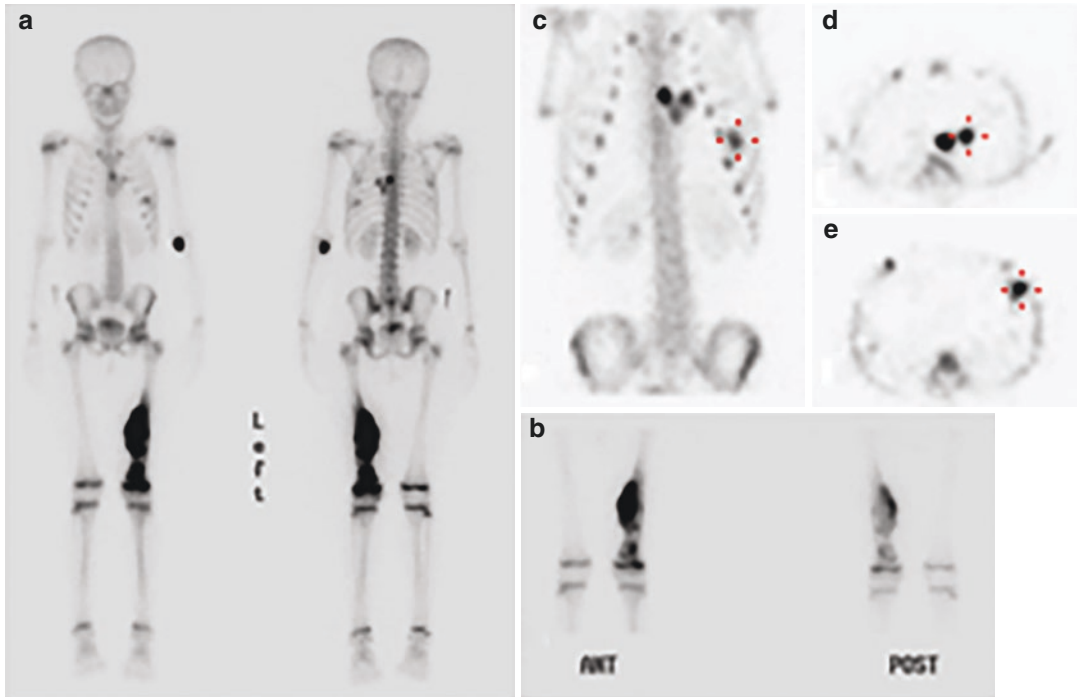


Fig. 12.17 History: An 8-year-old girl with left femoral osteosarcoma underwent bone scintigraphy for staging. Study report: Anterior and posterior whole body (a) and spot views (b) of the thighs show intense tracer uptake in the known primary tumor in the left mid-thigh. A “skip” lesion is seen in the distal left femur, better appreciated on the spot views (b). MIP (c) and transaxial slices (d, e)

from the SPECT of the thorax show several lesions in the left chest, localized to the posterior mediastinum and lung parenchyma. Impression: The findings are consistent with metastatic stage 4 osteosarcoma of the left femur with a skip lesion in the distal left femur and additional bone-forming metastases in the ST of the left hemithorax

Case 12.17 Osteosarcoma, NaF PET/CT
(Fig. 12.18)

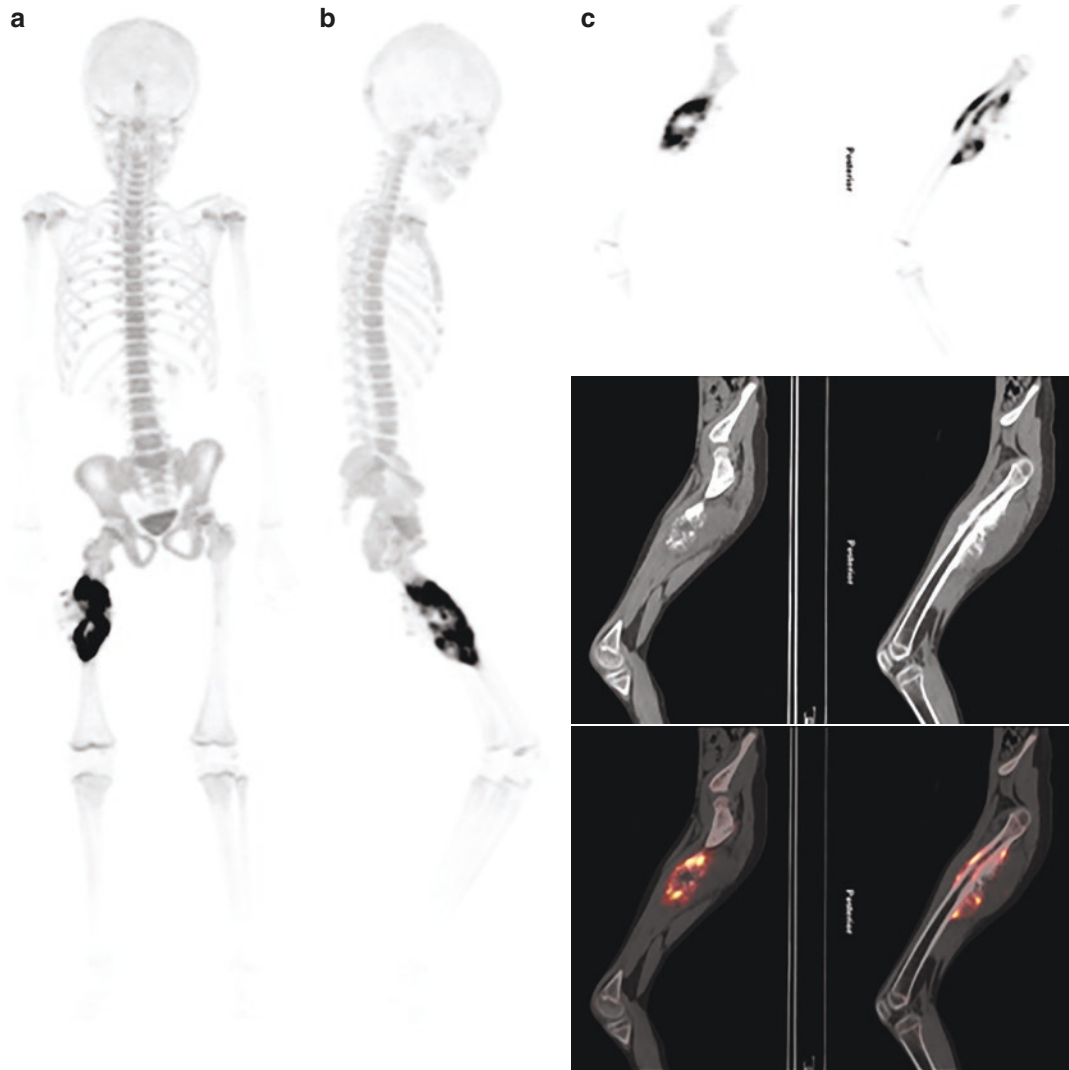


Fig. 12.18 History: An 8-year-old girl with chondroblastic osteosarcoma of the right femur performed NaF PET/CT for staging. Study report: Anterior (a) and lateral (b) MIP projections and sagittal PET, CT, and PET/CT slices at the level of the thigh (c) show inhomogeneous increase

tracer uptake in a destructive lesion in the mid-shaft of the right femur. No other skeletal lesions are seen. Impression: The findings demonstrate the primary osteosarcoma in the right femur with no evidence of metastatic spread

Case 12.18 Langerhans Cell Histiocytosis, NaF PET/CT (Fig. 12.19)

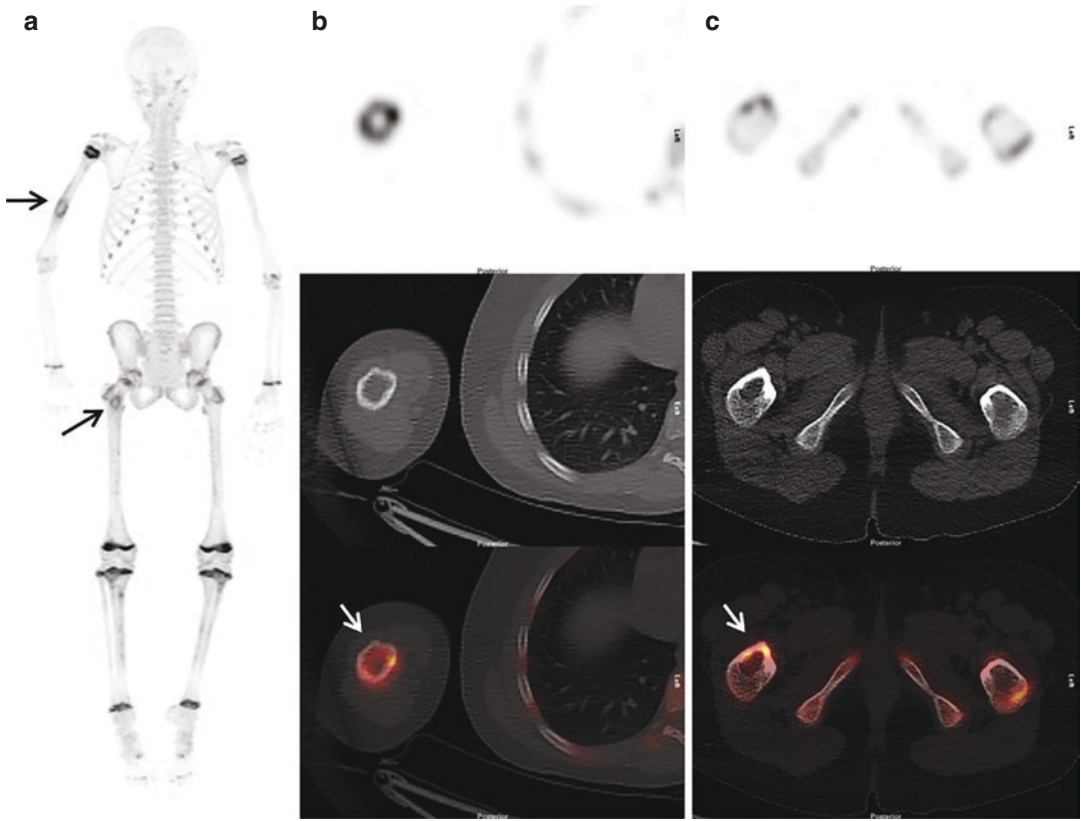


Fig. 12.19 History: A 11-year-old girl complains of right hip pain for 2 months and was referred to NaF PET/CT for further evaluation. Study report: Anterior MIP (a) and selected transaxial PET, CT, and PET/CT slices at the level of the mid-thorax (b) and lower pelvis (c) show two foci of inhomogeneous increased tracer activity localized

at the distal one-third of the right humeral shaft and the trochanteric region of the right femur, with corresponding lytic lesions on CT images (arrows). Impression: The findings are consistent with aggressive osteoblastic bone lesions in the right humerus and proximal right femur. Biopsy diagnosed Langerhans cell histiocytosis

References

1. Treves ST, et al. 2016 update of the North American consensus guidelines for pediatric administered radiopharmaceutical activities. *J Nucl Med.* 2016;57(12):15N–8N.
2. Lassmann M, Treves ST. Paediatric radiopharmaceutical administration: harmonization of the 2007 EANM paediatric dosage card (version 1.5.2008) and the 2010 North American consensus guidelines. *Eur J Nucl Med Mol Imaging.* 2014;41(5):1036–41.
3. Alessio AM, et al. Weight-based, low-dose pediatric whole-body PET/CT protocols. *J Nucl Med.* 2009;50(10):1570–7.
4. Uslu L, et al. Value of 18F-FDG PET and PET/CT for evaluation of pediatric malignancies. *J Nucl Med.* 2015;56(2):274–86.
5. Vali R, et al. SNMMI procedure standard/EANM practice guideline on pediatric (18)F-FDG PET/CT for oncology 1.0. *J Nucl Med.* 2021;62(1):99–110.
6. Bicakci N, Elli M. (18)Fluorine-fluorodeoxyglucose PET/CT imaging in childhood malignancies. *Mol Imaging Radionucl Ther.* 2021;30(1):18–27.
7. Daube-Witherspoon ME, Cherry SR. Scanner design considerations for long axial field-of-view PET systems. *PET Clin.* 2021;16(1):25–39.
8. Shammas A, Lim R, Charron M. Pediatric FDG PET/CT: physiologic uptake, normal variants, and benign conditions. *Radiographics.* 2009;29(5):1467–86.
9. Bestic JM, Peterson JJ, Bancroft LW. Pediatric FDG PET/CT: physiologic uptake, normal variants, and benign conditions [corrected]. *Radiographics.* 2009;29(5):1487–500.
10. Agrawal A, et al. PET/CT normal variants and pitfalls in pediatric disorders. *Semin Nucl Med.* 2021;51(6):572–83.
11. Bar-Sever Z, et al. Guidelines on nuclear medicine imaging in neuroblastoma. *Eur J Nucl Med Mol Imaging.* 2018;45(11):2009–24.
12. Rafael MS, et al. Theranostics in neuroblastoma. *PET Clin.* 2021;16(3):419–27.
13. Matthay KK, et al. Criteria for evaluation of disease extent by (123)I-metaiodobenzylguanidine scans in neuroblastoma: a report for the International Neuroblastoma Risk Group (INRG) task force. *Br J Cancer.* 2010;102(9):1319–26.
14. Sharp SE, et al. MIBG in neuroblastoma diagnostic imaging and therapy. *Radiographics.* 2016;36(1):258–78.
15. Bozkurt MF, et al. Guideline for PET/CT imaging of neuroendocrine neoplasms with (68)Ga-DOTA-conjugated somatostatin receptor targeting peptides and (18)F-DOPA. *Eur J Nucl Med Mol Imaging.* 2017;44(9):1588–601.
16. Chondrogiannis S, et al. Normal biodistribution pattern and physiologic variants of 18F-DOPA PET imaging. *Nucl Med Commun.* 2013;34(12):1141–9.
17. Calabria FF, et al. 18F-DOPA PET/CT physiological distribution and pitfalls: experience in 215 patients. *Clin Nucl Med.* 2016;41(10):753–60.
18. Hofman MS, Lau WF, Hicks RJ. Somatostatin receptor imaging with 68Ga DOTATATE PET/CT: clinical utility, normal patterns, pearls, and pitfalls in interpretation. *Radiographics.* 2015;35(2):500–16.
19. Sanli Y, et al. Neuroendocrine tumor diagnosis and management: (68)Ga-DOTATATE PET/CT. *AJR Am J Roentgenol.* 2018;211(2):267–77.
20. Stauss J, et al. Guidelines for paediatric bone scanning with 99mTc-labelled radiopharmaceuticals and 18F-fluoride. *Eur J Nucl Med Mol Imaging.* 2010;37(8):1621–8.
21. Segall G, et al. SNM practice guideline for sodium 18F-fluoride PET/CT bone scans 1.0. *J Nucl Med.* 2010;51(11):1813–20.
22. Eary JF, Conrad EU. Imaging in sarcoma. *J Nucl Med.* 2011;52(12):1903–13.
23. Beheshti M, et al. (18)F-NaF PET/CT: EANM procedure guidelines for bone imaging. *Eur J Nucl Med Mol Imaging.* 2015;42(11):1767–77.
24. Van den Wyngaert T, et al. The EANM practice guidelines for bone scintigraphy. *Eur J Nucl Med Mol Imaging.* 2016;43(9):1723–38.
25. Nadel HR. SPECT/CT in pediatric patient management. *Eur J Nucl Med Mol Imaging.* 2014;41(Suppl 1):S104–14.
26. Miller E, et al. Role of 18F-FDG PET/CT in staging and follow-up of lymphoma in pediatric and young adult patients. *J Comput Assist Tomogr.* 2006;30(4):689–94.
27. Howman-Giles R, London K, Uren RF. Solid tumors in childhood. In: Treves ST, editor. *Pediatric nuclear medicine and molecular imaging.* New York: Springer; 2014. p. 513–40.
28. Ferrari C, et al. Pediatric Hodgkin lymphoma: predictive value of interim 18F-FDG PET/CT in therapy response assessment. *Medicine (Baltimore).* 2017;96(5):e5973.
29. Kim K, Kim SJ. Diagnostic performance of F-18 FDG PET/CT in the detection of bone marrow involvement in paediatric Hodgkin lymphoma: a meta-analysis. *Leuk Res.* 2021;102:106525.
30. Barrington SF, Kluge R. FDG PET for therapy monitoring in Hodgkin and non-Hodgkin lymphomas. *Eur J Nucl Med Mol Imaging.* 2017;44(Suppl 1):97–110.
31. Hawkins DS, et al. [18F]Fluorodeoxyglucose positron emission tomography predicts outcome for Ewing sarcoma family of tumors. *J Clin Oncol.* 2005;23(34):8828–34.
32. Kubo T, et al. Prognostic significance of (18)F-FDG PET at diagnosis in patients with soft tissue sarcoma and bone sarcoma; systematic review and meta-analysis. *Eur J Cancer.* 2016;58:104–11.
33. Harrison DJ, Parisi MT, Shulkin BL. The role of (18)F-FDG-PET/CT in pediatric sarcoma. *Semin Nucl Med.* 2017;47(3):229–41.

34. London K, et al. 18F-FDG PET/CT in paediatric lymphoma: comparison with conventional imaging. *Eur J Nucl Med Mol Imaging*. 2011;38(2):274–84.
35. Cerci JJ, et al. Is true whole-body (18)F-FDG PET/CT required in pediatric lymphoma? An IAEA multicenter prospective study. *J Nucl Med*. 2019;60(8):1087–93.
36. Benz MR, Crompton JG, Harder D. PET/CT variants and pitfalls in bone and soft tissue sarcoma. *Semin Nucl Med*. 2021;51(6):584–92.
37. Swift CC, et al. Updates in diagnosis, management, and treatment of neuroblastoma. *Radiographics*. 2018;38(2):566–80.
38. Körber F, Schäfer JF. [Radiological imaging of neuroblastoma]. *Radiologe*. 2021;61(7):639–48.
39. Yanik GA, et al. Semiquantitative mIBG scoring as a prognostic indicator in patients with stage 4 neuroblastoma: a report from the Children's oncology group. *J Nucl Med*. 2013;54(4):541–8.
40. Yanik GA, et al. Validation of postinduction curie scores in high-risk neuroblastoma: A Children's Oncology Group and SIOPEX Group Report on SIOPEX/HR-NBL1. *J Nucl Med*. 2018;59(3):502–8.
41. Ladenstein R, et al. Validation of the mIBG skeletal SIOPEX scoring method in two independent high-risk neuroblastoma populations: the SIOPEX/HR-NBL1 and COG-A3973 trials. *Eur J Nucl Med Mol Imaging*. 2018;45(2):292–305.
42. Pai Panandiker AS, Coleman J, Shulkin B. Whole-body pediatric neuroblastoma imaging: 123I-mIBG and beyond. *Clin Nucl Med*. 2015;40(9):737–9.
43. Sharp SE, et al. Functional-metabolic imaging of neuroblastoma. *Q J Nucl Med Mol Imaging*. 2013;57(1):6–20.
44. Masselli G, et al. Clinical application of (18)F-DOPA PET/TC in pediatric patients. *Am J Nucl Med Mol Imaging*. 2021;11(2):64–76.
45. Pfluger T, Piccardo A. Neuroblastoma: MIBG imaging and new tracers. *Semin Nucl Med*. 2017;47(2):143–57.
46. Piccardo A, et al. Diagnosis, treatment response, and prognosis: the role of (18)F-DOPA PET/CT in children affected by neuroblastoma in comparison with (123)I-mIBG scan: the first prospective study. *J Nucl Med*. 2020;61(3):367–74.
47. Lopci E, et al. 18F-DOPA PET/CT in neuroblastoma: comparison of conventional imaging with CT/MR. *Clin Nucl Med*. 2012;37(4):e73–8.
48. Kong G, et al. Initial experience with Gallium-68 DOTA-octreotate PET/CT and peptide receptor radionuclide therapy for pediatric patients with refractory metastatic neuroblastoma. *J Pediatr Hematol Oncol*. 2016;38(2):87–96.
49. Maaz AUR, O'Doherty J, Djekidel M. (68) Ga-DOTATATE PET/CT for neuroblastoma staging: utility for clinical use. *J Nucl Med Technol*. 2021;49(3):265–8.
50. Imperiale A, et al. Variants and pitfalls of PET/CT in neuroendocrine tumors. *Semin Nucl Med*. 2021;51(5):519–28.
51. Chondrogiannis S, Marzola MC, Rubello D. ¹⁸F-DOPA PET/computed tomography imaging. *PET Clin*. 2014;9(3):307–21.
52. Piccardo A, et al. Head-to-head comparison between (18) F-DOPA PET/CT and (68) Ga-DOTA peptides PET/CT in detecting intestinal neuroendocrine tumours: a systematic review and meta-analysis. *Clin Endocrinol (Oxf)*. 2021;95(4):595–605.
53. Adzick NS, et al. Surgical treatment of congenital hyperinsulinism: results from 500 pancreatectomies in neonates and children. *J Pediatr Surg*. 2019;54(1):27–32.
54. Bartel TB, et al. SNMMI procedure standard for bone scintigraphy 4.0. *J Nucl Med Technol*. 2018;46(4):398–404.
55. Usmani S, et al. Technical feasibility, radiation dosimetry and clinical use of (18)F-sodium fluoride (NaF) in evaluation of metastatic bone disease in pediatric population. *Ann Nucl Med*. 2018;32(9):594–601.
56. Vaz S, et al. Molecular imaging of bone metastases using bone targeted tracers. *Q J Nucl Med Mol Imaging*. 2019;63(2):112–28.

The opinions expressed in this chapter are those of the author(s) and do not necessarily reflect the views of the IAEA: International Atomic Energy Agency, its Board of Directors, or the countries they represent.

Open Access This chapter is licensed under the terms of the Creative Commons Attribution 3.0 IGO license (<http://creativecommons.org/licenses/by/3.0/igo/>), which permits use, sharing, adaptation, distribution and reproduction in any medium or format, as long as you give appropriate credit to the IAEA: International Atomic Energy Agency, provide a link to the Creative Commons license and indicate if changes were made.

Any dispute related to the use of the works of the IAEA: International Atomic Energy Agency that cannot be settled amicably shall be submitted to arbitration pursuant to the UNCITRAL rules. The use of the IAEA: International Atomic Energy Agency's name for any purpose other than for attribution, and the use of the IAEA: International Atomic Energy Agency's logo, shall be subject to a separate written license agreement between the IAEA: International Atomic Energy Agency and the user and is not authorized as part of this CC-IGO license. Note that the link provided above includes additional terms and conditions of the license.

The images or other third party material in this chapter are included in the chapter's Creative Commons license, unless indicated otherwise in a credit line to the material. If material is not included in the chapter's Creative Commons license and your intended use is not permitted by statutory regulation or exceeds the permitted use, you will need to obtain permission directly from the copyright holder.

